UNIVERSITY OF SOUTHAMPTON

FACULTY OF ENGINEERING, SCIENCE AND MATHEMATICS

School of Chemistry

Anion Recognition, Assembly and Transport Properties of Amidopyrrole Derivatives

by

Korakot Navakhun

Thesis for the degree of Doctor of Philosophy

November 2004

UNIVERSITY OF SOUTHAMPTON

ABSTRACT

FACULTY OF ENGINEERING, SCIENCE AND MATHEMATIC

Doctor of Philosophy

ANION RECOGNITION, ASSEMBLY AND TRANSPROT PROPERTIES OF AMIDOPYRROLE DERIVATIVES

by Korakot Navakhun

This thesis describes the synthesis and study of the anion recognition, assembly and transport properties of new functionalised amidopyrrole compounds. In the first topic, the series of simple amidopyrrole cleft receptors containing amine, ammonioum and amide as the functional groups at their pendent arms has been synthesised. These receptors have been investigated their simple anion coordination properties. It has been found the amine functionalised amidopyrrole has had a high recognition with protonated oxo-anions as hydrogensulfate and dihydrogenphosphate even in high polar solutions like DMSO/water; however, the rest of receptors in this series have not shown any high selective anion binding.

Secondly, synthesises of new prodigiosin mimics consisting with imidazolium amidopyrrole and their analogues have been achieved in order to investigate their HCl tranport across the membranes abilities. One of them has been improved its chloride binding when has been protonated in the solution. The solid-state studies support the compounds in protonated forms could form the chloride complexes. Chloride and proton transport studies results also confirm that imidazolium amidopyrrole derives could used as the HCl symporters.

In the next topic, the library of amidopyrrole derives 'tweezer' receptors proposed to selectively bind with carboxylate anion, red dye-spacer-L-Leu-L-Asn-L-Phe, which represents to C-termini of HIV-1 protease has been prepared. The sequencing of the highly carboxylate bound receptors have been identified from screening experiments and Edman sequencing analysis.

Finally, The dimers and trimers composed of amidopyrrole and two chlorine atoms at 3- and 4- position of the pyrrole rings have been synthesised. Two dimers, which have directly attached phenyl groups on both sides of the pyrrole shows their anion-anion self-assembly properties in solid-state when the NH pyrrole have been deprotonated by basic anions as fluoride and/or hydroxide.

Contents

Appendix 3: *HCl transport assay*

Acknowledgments

At first, I would like to thank Dr. Philip A. Gale, my supervisor, for his kind suggestions and encouragement during my time in Southampton. I also would like to thank Prof. Jeremy D. Kilburn for his supervision as co-supervisor of work in chapter 4.

Next, I would like to thank my sponsors who support me along three years. They are the Universities UK, University of Southampton and Ramkhamhaeng University, Thailand.

Additionally, I would like to thank the EPSRC National Crystallographic Service for supporting the X-ray crystallography instruments. Especially, Prof. Mike Hursthouse, Dr. Simon Coles and Dr. Mark Light who solved the solid-state structures reported in this thesis.

I must also thank to Prof. Bradley D. Smith and Ms. Beth McNally at the University of Notre Dame, Illinois, for the HCl symport studies reported in chapter 3. Thanks also to Ms. Kathy E. Whitefield at the school of bio-medical science for analysis of the compounds by Edman sequencing reported in chapter 4. Many thanks to NMR and MS services at the school of chemistry for their support during the last couple years.

Thanks also to the members of the Gale group past and present. Salvo who looked after me in my first year, Colin, Josep, Ismael, Louise, Simon and Somchai for their help and friendship. Many thanks to Sandra, Nittaya, Andrea and Jon in Jeremy's group for their help with synthesis techniques. Thanks also to all the project students who worked with me. They are Gemma, Kate, Alan and Michael.

Thanks also go to all my Thai friends in UK and aboard who help and cheer me up along the period time here. Among them are p'Keng, p'Ek, p'Ying, p'Nut, p'Bodin, p'Rose, Pla, Rung, Pam, Te, Jo, Korn and lots of people who have not been named here.

Finally, I would like to thank my parents and my family who wish me carried out my Ph.D. study and back to Thailand.

Abbreviations

Ac	Acetyl
Ar	Aryl
Boc	*tert*-Butyloxycarbonyl
br	Broad resonance (NMR)
^{t}Bu	*tert*-Butyl
Bu	Butyl
Calc.	Calculated
cat	Catalyst
d	Doublet (NMR)
DCM	Dichloromethane
DDPE	2-Phenylacetyldimedone
decom.	Decomposed
DIC	*N,N'*-Diisopropylcarbodiimide
DIPEA	Diisopropylethylamine
DMAP	4-Dimethylaminopyridine
DMF	*N,N*-Dimethylformamide
DMSO	Dimethyl Sulfoxide
equiv.	Equivalent (s)
Et	Ethyl
ES	Electrospray
Fmoc	9-Fluorenyloxycarbonyl
g	Gram (s)
h	Hour (s)
HOBt	1-Hydroxybenzotriazole hydrate
HRMS	High resolution mass spectrometry
Hz	Hertz
i.e.	*Id est* (Latin : that is)
J	Coupling constant (NMR)
LD	Laser desorption (Mass spectroscopy)
min	Minute (s)
m	Multiplet (NMR)

M	Molarity
Me	Methyl
mol	Mole (s)
m.p.	Melting point
m/z	Mass to charge ratio (Mass spectrometry)
NMR	Nuclear magnetic resonance
Ph	Phenyl
ppm	Parts per million
PyBOP	Benzotriazol-1-yloxytripyrrolidinophosphonium hexafluorophosphate
q	Quartet (NMR)
R_f	Retention factor
ROESY	Rotational nuclear Overhauser Effect Spectroscopy
s	Singlet (NMR)
t	Triplet (NMR)
TEA	Triethylamine
TBA	Tetrabutylammonium
TFA	Trifluoroacetic acid
TOF	Time of flight (Mass spectroscopy)

Amino acids

Ala	Alanine (A)	Arg	Arginine (R)
Asn	Asparagine (N)	Asp	Aspartic acid (D)
Cys	Cysteine (C)	Gln	Glutamine (Q)
Glu	Glutamic acid (E)	Gly	Glycine (G)
His	Histidine (H)	Ile	Isoleucine (I)
Leu	Leucine (L)	Lys	Lysine (K)
Met	Methionine (M)	Phe	Phenylalanine (F)
Pro	Proline (P)	Ser	Serine (S)
Thr	Threonine (T)	Trp	Tyrosine (W)
Tyr	Tyrosine (Y)	Val	Valine (V)

1. *Introduction*

1.1. Supramolecular chemistry

Supramolecular chemistry is a multidisciplinary field. The concept and the term of supramolecular chemistry were introduced in 1978 as a development and generalization of earlier work.[1-3] The field of supramolecular chemistry has been defined in words 'Just as there is a field of *molecular chemistry* based on the covalent bond, there is a field of *supramolecular chemistry*, the chemistry of molecular assemblies and of the intermolecular bond' also as 'chemistry beyond the molecule' by Jean-Marie Lehn (Figure 1.1).[4,5]

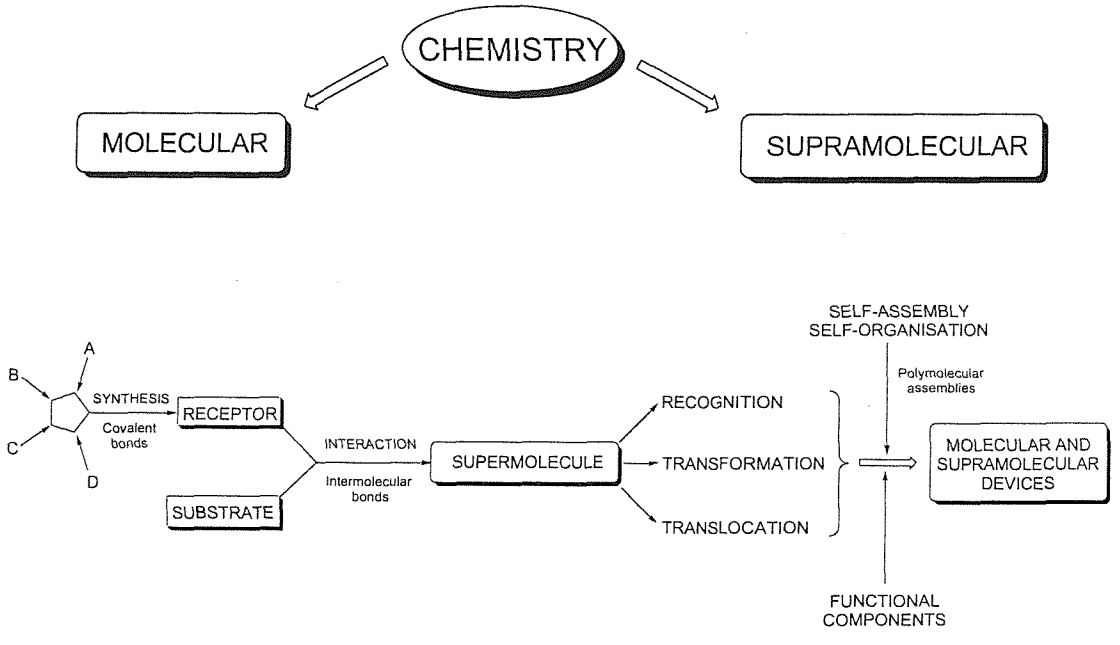

Figure 1.1: From molecular to supramolecular chemistry: molecules, supermolecules, molecular and supramolecular devices.

This field involves investigating new molecular systems in which the most important feature is that the compounds are held together reversibly by intermolecular forces, not by covalent bonds. These non-covalent interactions include:[6]

I) Electrostatic interactions (ion-ion, ion-dipole and dipole-dipole) which are based on the Coulombic attraction between opposite charges (Figure 1.2). Bond energy are in the ranges 100-350 kJ mol^{-1}, 50-200 kJ mol^{-1} and 5-50 kJ mol^{-1} for ion-ion, ion-dipole and dipole-dipole interactions respectively.

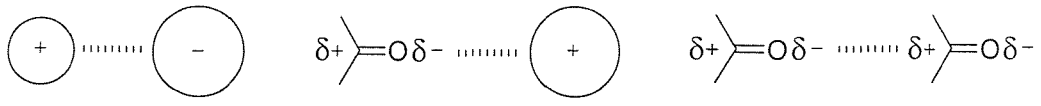

Ion-Ion Ion-Dipole Dipole-Dipole

Figure 1.2: Electrostatic interactions.

II) Hydrogen bonds (4-120 kJ mol^{-1}) which may be regarded as a particular kind of dipole-dipole interaction in which hydrogen atom attached to an electronegative atom (or electron withdrawing group) interacts with a neighbouring dipole on an adjacent molecule or functional group. Because of its relatively strong and highly directional nature, hydrogen bonding has been described as the 'masterkey interaction in supramolecular chemistry'.[7] Some general parameters of the hydrogen bond interaction are shown in Table 1.1.

	Strong	Moderate	Weak
A-H···B interaction	Mainly covalent	Mainly electrostatic	Electrostatic
Bond energy (kJ.mol^{-1})	60-120	16-60	<12
Bond lengths (Å)			
H···B	1.2-1.5	1.5-2.2	2.2-3.2
A···B	2.2-2.5	2.5-3.2	3.2-4.0
Bond angles (°)	175-180	130-180	90-150
Relative IR vibration shift (stretching sym-metrical mode, cm^{-1})	25%	10-25%	<10%
^{1}H NMR chemical shift downfield (ppm)	14-22	<14	?
Example	Gas phase dimers with strong acid/bases	Acids	O-H···π hydrogen bonds
	HF complexes	Biological molecules	C-H hydrogen bonds

Table 1.1: Properties of hydrogen bonded interactions.

III) π-π Stacking interactions (0-50 kJ mol^{-1}) occur between aromatic rings, often in situations where one is relatively electron rich and one is electron poor. There are two general types of π-stacking: face-to-face and edge-to-face (Figure 1.3), although a wide variety of intermediate geometries are known.

Face-to-face Edge-to-face

Figure 1.3: π-π Stacking interactions.

IV) Dispersion and induction forces (van der Waals forces) occur from the polarisation of an electron cloud by the proximity of an adjacent nucleus, resulting in a weak electrostatic attraction (<5 kJ mol^{-1}).

V) Hydrophobic (or solvatophobic) effects are the specific driving force for the association of non-polar hosts and guests in aqueous solution and may be divided into two energetic components: enthalpic and entropic. The enthalpic hydrophobic effect involves the stabilisation of water molecules that are driven from a host cavity upon guest binding. Because the host's cavities are often hydrophobic, intracavity water does not interact strongly with the cavity wall and is therefore of high energy. Upon release into the bulk solvent, it is stabilised by interactions with other water molecules. The entropic hydrophobic effect arises from the fact that presence of two (often organic) molecules in solution (host and guest) creates two 'holes' in the structure of bulk water. Combining host and guest to form a complex results in less disruption to the solvent structure and increasing an entropic (resulting in a lowering of overall free energy) as shown in Figure 1.4.[8]

These forces from above can be used individually, but they normally are used in concert to maximize the selectivity and tunability of the new receptor and also increase the strength of the complex formed.

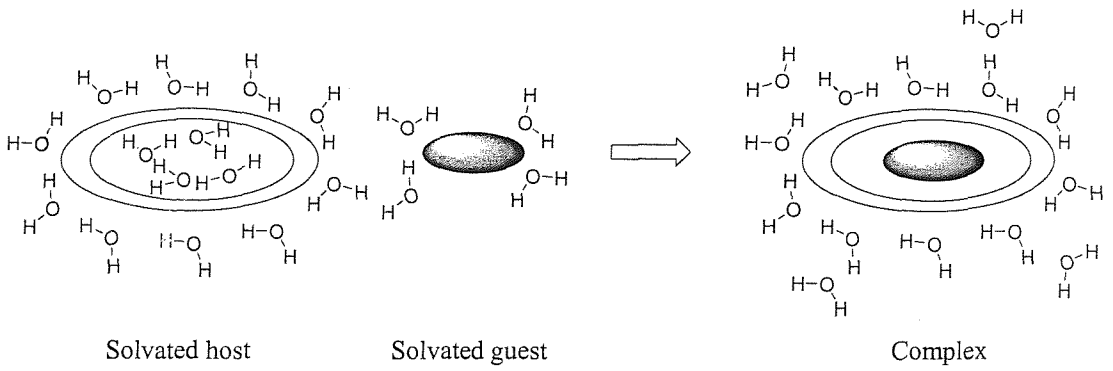

Figure 1.4: Hydrophobic binding of organic guests in aqueous solution.

1.2 Anion coordination

Anion coordination is classified is a sub-set supramolecular chemistry. The design of anion receptors is a particularly challenging.[9] There are a number of reasons for this. Anions are relatively large and therefore have lower charge densities than isoelectronic cations. For example, F^- is larger than Na^+ (Table 1.2).[10] Hence electrostatic interactions are weaker.

Anion	Radius (Å)	Cation	Radius (Å)
F^-	1.33	Li^+	0.69
Cl^-	1.81	Na^+	1.02
Br^-	1.95	K^+	1.38
I^-	2.16	Cs^+	1.70
SO_4^{2-}	2.30	Ca^{2+}	1.00
PO_4^{3-}	2.38	Zn^{2+}	0.75
$H_2PO_4^-$	2.00	Al^{3+}	0.53
Na^-	2.2	La^{3+}	1.05
Cs^-	3.5	NH_4^+	1.48

Table 1.2: Comparison of the radius (Å) of anions and cations.

Anions may be sensitive to pH (becoming protonated at low pH and so losing their negative charge). Thus receptors must function within the optimum pH range of their target anion. Anions exhibit a wide range of geometries such as spherical (halides),

linear (N_3^-, CN^-, SCN^-, OH^-), trigonal planar (CO_3^{2-}, NO_3^-), tetrahedral (PO_4^{3-}, VO_4^{3-}, SO_4^{2-}, MnO_4^{2-}, SeO_4^{2-}, MnO_4^-), octahedral $[Fe(CN)_6]^{3-}$, $[Co(CN)_6]^{3-}$) as well as more complex shapes as in the case of biologically important anions. Therefore, a higher degree of design may be required to make receptors complementary to their anionic guest. Solvation is another factor to consider. Electrostatic interactions generally dominate in anion solvation, and hydroxylic solvents in particular can form strong hydrogen bonds with anions. A potential anion receptor must therefore effectively compete with the solvent environment in which the anion-recognition event takes place. The Hofmeister series,[11] which orders anions by their hydrophobicity, shows that hydrophobic anions are generally bound more strongly in hydrophobic binding sites.

By contrast with supramolecular cation coordination chemistry which was first realised through the pioneering work of Pedersen[12] on crown ethers and work of Lehn[13] on cryptands, three-dimensional cation receptors, in the late 1960s, the coordination chemistry of anions has historically received little attention (with a few notable exceptions) after Park and Simmons reported the first synthetic organic ligands of the bicyclic diammonium type **1**, named 'katapinate', displaying halide complexation.[14]

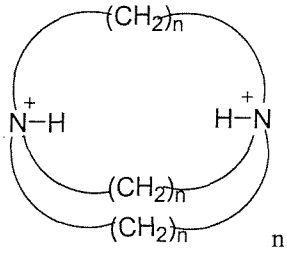

1

It has only been in the last twenty five years that sustained effort has been applied to the problems inherent in binding anions.[15] However, recent developments in the area of anion coordination have produced a variety of new selective complexation agents for anionic guests.[16-18] The great variety of anionic species and their importance in several areas such as biology,[19,20] the environment,[21-23] catalysis[24] and in potential medical applications[25] is responsible for the fact that interest in anion coordination has becoming more widespread.

In environment, the large amount of anions like nitrate and phosphate can be the cause of severe problems. These anions are commonly attributed to anthropogenic activities such as atmospheric emissions, livestock feeding, agricultural runoff, timber harvesting practices and domestic/industrial effluent discharge. They can contribute to surface water eutrophication, may cause infant methaemoglobinaemia ('blue baby' syndrome) and have been implicated in certain cancers.[22,23] The production of pertechnetate during the reprocessing of nuclear fuel (and its subsequent discharge into the seas and oceans) is also a matter of environmental concern.

Anions are ubiquitous throughout biological systems. The deoxyribonucleic acid[26] (DNA) double helix perhaps is the most important example in the living cell. The individual monomers, called nucleotides, are comprised of a phosphoric acid (phosphate) group, a five carbons sugar (deoxyribose) and an organic purine or pyrimidine base. The DNA double helix combines two anti-parallel strands that are held together by complementary hydrogen bonds between pairs of bases, adenine (A) with thymine (T) and cytosine (C) with guanine (G) (Figure 1.5).

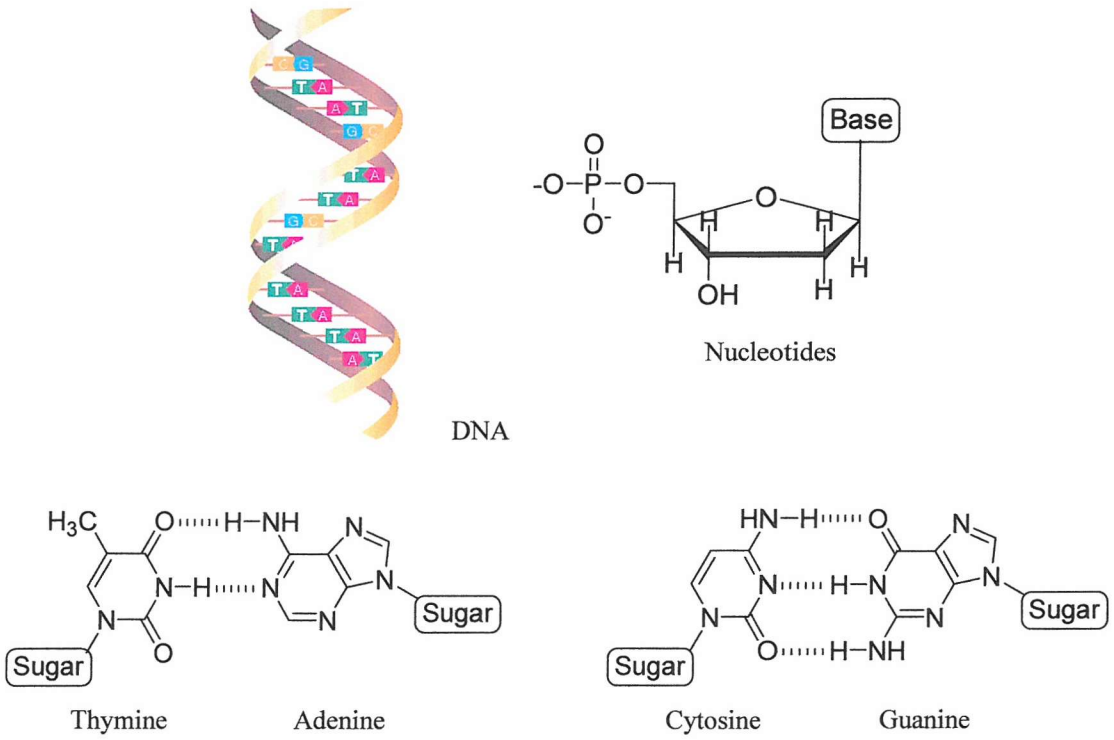

Figure 1.5: DNA double helix, nucleotides monomer and hydrogen bonded complementary A-T and G-C base pairs in DNA.

Between 70 and 75 per cent of enzyme substrates and cofactors are anions. A well known example is carboxypeptidase A,[27,28] an enzyme that coordinates to the C-terminal carboxylate group of polypeptides by the formation of an arginine-asparate salt bridge, and catalyses the hydrolysis of this residue (Figure 1.6). The salt-bridge binding motif is also observed in zinc finger/DNA complexes[29] and RNA stem loop-protein interactions.[30]

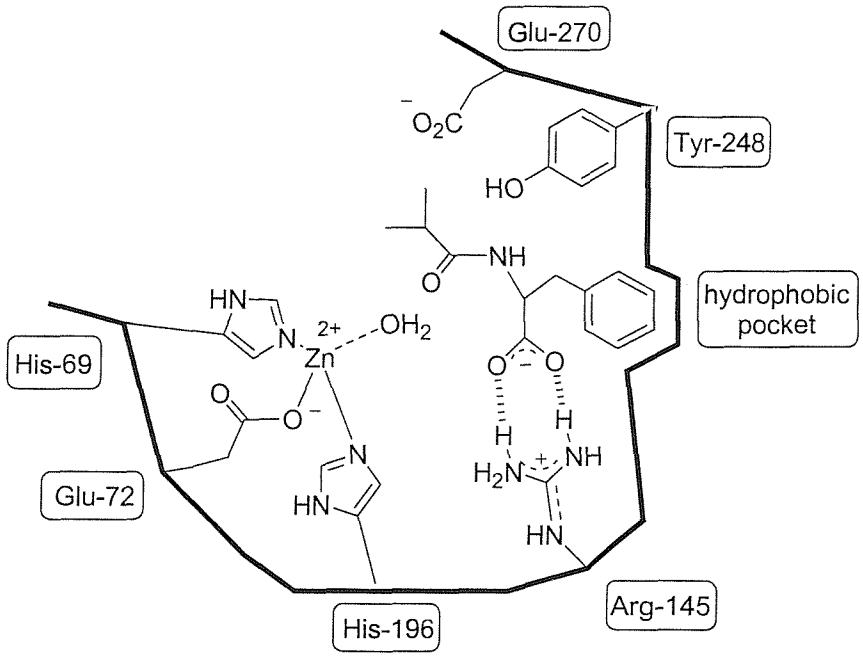

Figure 1.6: The active site of carboxypeptidase-A with a bound peptide chain.

Examples of small inorganic anion recognition by proteins have been recently provided by crystal structures of several complexes for example the phosphate binding protein (PBP)[31] and sulfate binding protein (SBP)[32] (Figure 1.7). They have been developed by the members of a family of bacterial periplasmic proteins. These proteins, which have the specificity of the phosphate and sulfate recognition characters are used for the transport of small molecules like sugars and oligopeptides. Their function is to bind the anion tightly once it has passively diffused across the cell outer membrane.[33-34]

Selective ion transport is crucial for a range of cellular processes and ion channels are the proteins that carry out this vital role. Ion channels must be selective for certain types of ions and transport them with a high rate rather than necessarily

bind them with high affinity.[35] In recently structures of two chloride channels from *E. coli* and *S. tryphimurium* have been determined.[36] These high sequence channels are homodimers. Their structures are homologies and each subunit has its own ion-conducting pore. The narrowest part of the pore of the anion channel consists highly conserved amino acids acting as the selectivity filter. Chloride in this filter is coordinated by backbone amide groups and side chain hydroxyl groups, all located at the N-termini of α-helices (Figure 1.8). Charge-dipole binding interaction in this type facilitates fast complexation and decomplexation rates and thus fast anion transport through membranes. As in PBP and SBP, hydrogen bonds play critical roles in the formation of a well-ordered binding domain that leads to selective recognition of chloride.

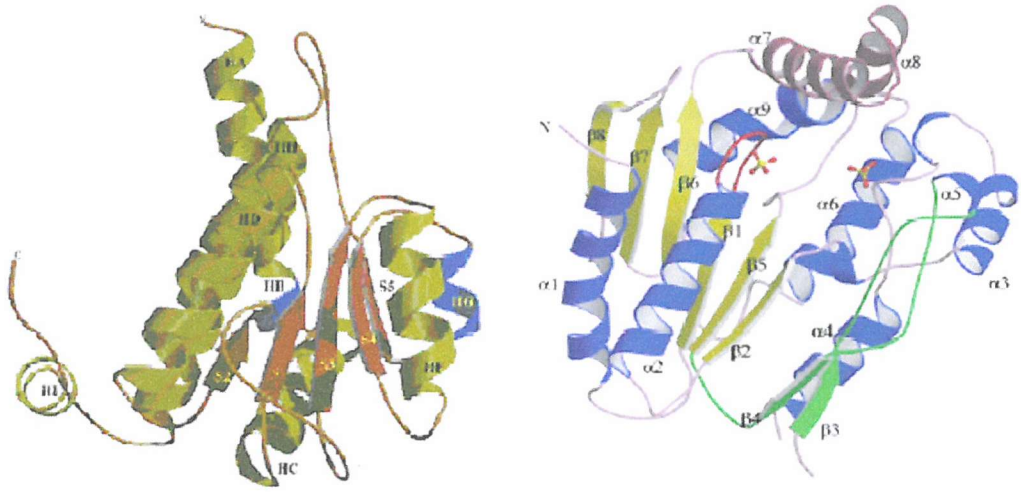

Figure 1.7: Crystal structures of the phosphate binding protein, PBP (left) and sulfate binding protein, SPB (right) .

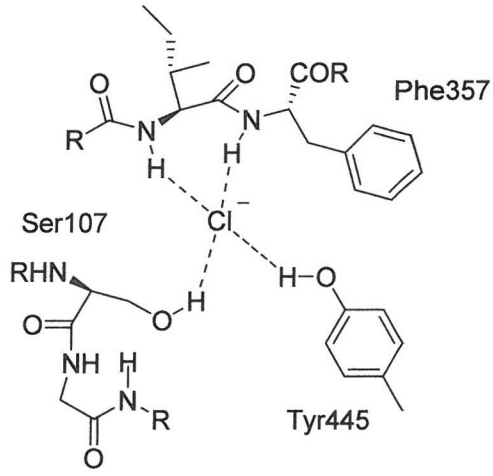

Figure 1.8: The Cl^- binding active site of chloride channel.

Anions also play roles in disease. Cystic fibrosis (CF), a genetically inherited disease, is caused by misregulation of chloride channels (Figure 1.9).[37] These channels are constituted by the cystic fibrosis transmembrane regulator or CFTR protein.[38] The misregulation leads to a thick build up of mucous deposits in the lungs and to a higher than normal susceptibility towards fatal pulmonary infections. It is these infections, often of the *Pseudomonas aeruginosa* type, that are generally the causative agents of cystic fibrosis related death. Unfortunately, currently treatment methods including chloride analysis as well as treating with appropriate antibiotics or adjusting diet have not succeeded in prolonging the median lift expectancy of cystic fibrosis patients past the age of 25.[39] Thus, the existence of a chloride-selective carrier could be of prime clinical utility in terms of treating a major public health problem.

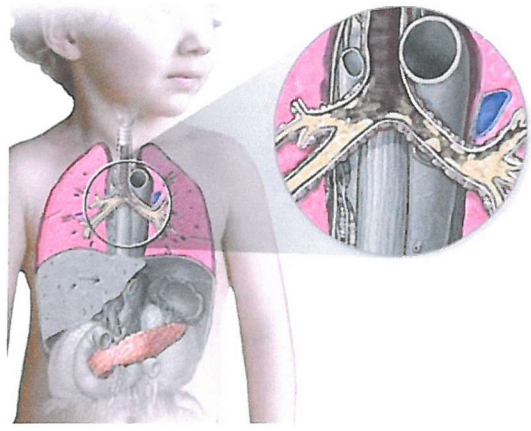

Figure 1.9: Cystic fibrosis (CF). A hereditary disorder characterized by lung congestion and infection and malabsorption of nutrients by the pancreas.

Frankel and co-workers have reported an example of anion recognition with the synthesis of short peptides containing nine arginines which mimic the basic region of the HIV-1 Tat protein that forms a specific network of hydrogen bonds with adjacent pairs of phosphate at the RNA bulge with a recognition motif called 'the arginine fork'.[40] These arrangements were likely to occur near RNA loops and bulges and not within double-stranded A-form RNA.

Catalysis by abiotic receptors is a rapidly developing field in supramolecular chemistry, and systems have been developed that mimic enzyme properties. For example, Mandolini and co-workers have reported that salophen-uranyl complexes are effective catalysts of 1,4-thiol additions with high turnover efficiency and low product inhibition.[41] Crabtree and co-workers have synthesised cleft-type disulfonamide receptors that catalyse imine formation from aldehydes and amines, by apparently binding the transition state for the rate-determining nucleophilic attack of the amine on the aldehyde.[42]

Nucleotide polyphosphates are important anions in biology particularly adenosine mono- (AMP), di- (ADP), and triphosphate (ATP) which are basic components in the bioenergetics of all living organisms.[43]

The ditopic macrocyclic hexamine [24]N_6O_2 **2** when protonated was found to bind nucleotide polyphosphates strongly.[44] The hydrolysis of ATP in the presence of **2**+nH^+ is probably a true catalytic process. Based on detailed kinetics and mechanistic studies, at neutral pH, the catalytic cycle shown in Figure 1.10 is proposed for ATP hydrolysis catalysed by 2+nH^+.[45]

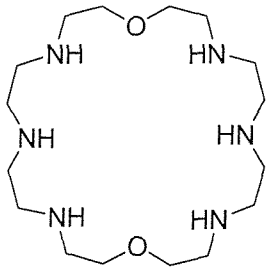

2

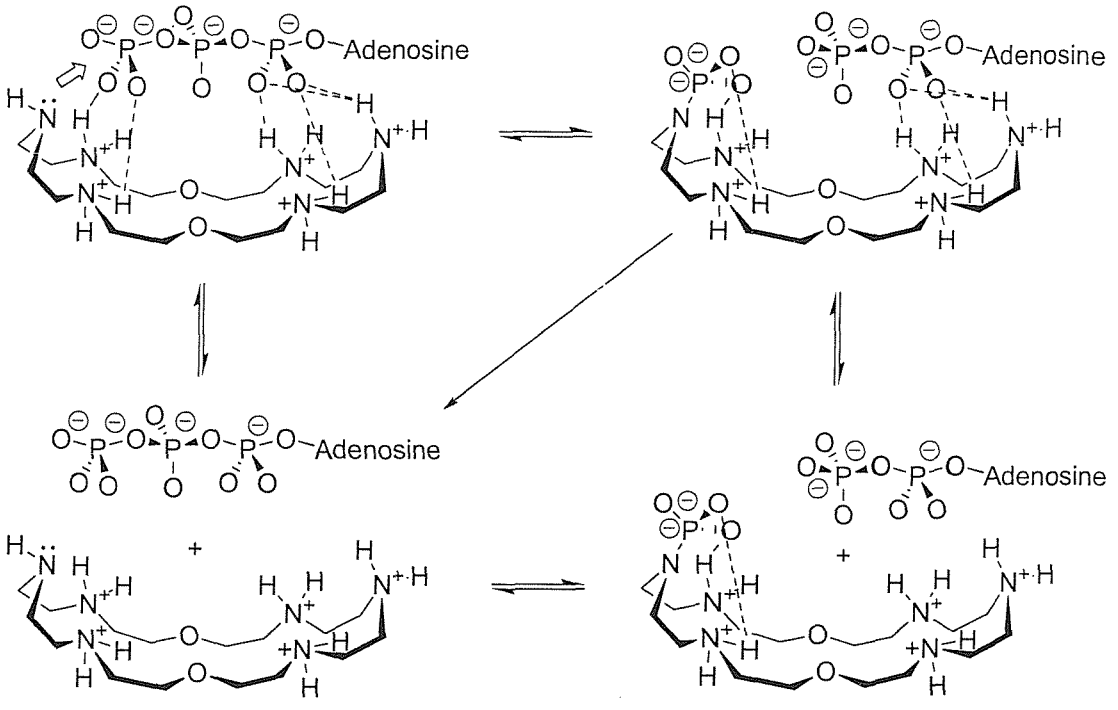

Figure 1.10: Catalytic cycle for ATP hydrolysis in the presence of **2**.

1.3 Synthetic anion receptors

To design an artificial anion host molecule, there are some fundamental points of host-guest relationships which must be considered:[46]

I) Which guests are to be selected by binding to the molecular host? The mutual recognition pattern of host and guest must be defined with the aim of maximizing discrimination of similar guest species.

II) In which solvent is the host-guest complexation to take place? The solvent will affect complex stability even to the extent that the association constant may vary by orders of magnitude depending on the identity and properties of the solvent.

A variety of functional groups have been used in host molecules to interact with anions through hydrogen bonding and/or electrostatic interactions. Amide groups have been employed to produce a wide range of receptors capable of coordinating

anions.[47] Crabtree and co-workers have shown that very simple amides such as the isophthalic acid derivatives, **3** and **4**, can bind anions with hydrogen bonds between the two amidic NH groups and the halide anions.[48] Receptor **4** forms complexes with exclusively 1:1 anion:receptor stoichiometry in solution of dichloromethane-d_2.

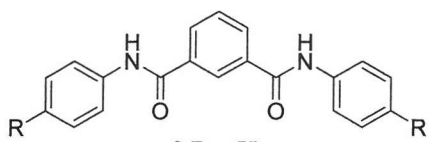

3 R = H
4 R = n-Bu

The crystal structure of the bromide complex of receptor **3** shown the bromide anion is coordinated to the amide NH group with H-Br = 2.39 and 2.68 Å. In addition this bromide ion was not coordinated to any other groups on the receptor.

More recently Szumma and Jurczak synthesised pyridinium macrocycle **5** and the open-chain analog **6**.[49] The macrocycle selectively bound acetate (K_a = 2640 $\pm$ 270 M^{-1}). In solution the 1:1 receptor:anion complex were formed exclusively; however, the crystal structure of the tetrabutylammonium acetate complex of **5** reveals the formation of a 2:1 receptor:anion complex in the solid state (Figure 1.11).

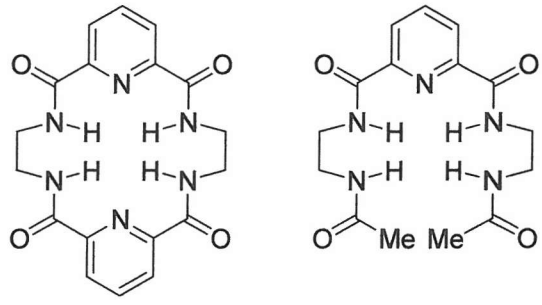

5 **6**

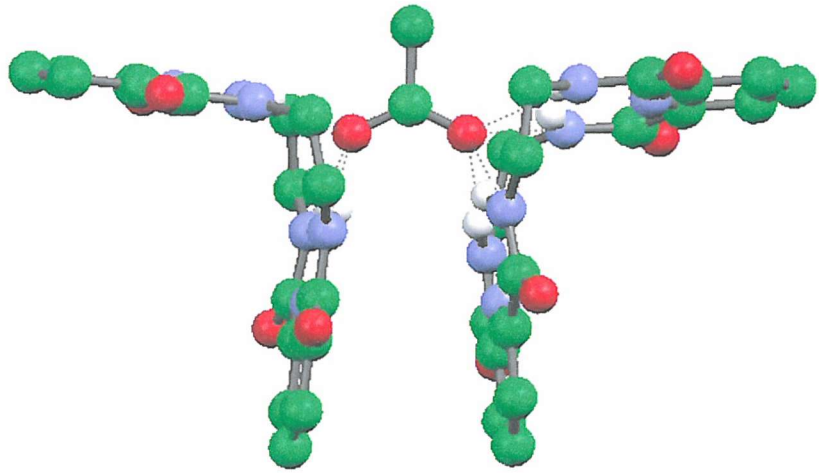

Figure 1.11: Crystal structure of the **5**/tetrabutyl ammonium acetate complex.

Hamilton and co-workers have synthesised macrocyclic tri-amide anion receptors with C_3 symmetry **7**.[50] NMR evidence suggests that this receptor binds iodide in a sandwich fashion at low I^- concentrations. The complexes switched to a 1:1 binding mode at higher concentrations of the halide supported by an initial up-field of the NH resonances in the ^{1}H-NMR of **7** upon addition of I^- followed by a downfield shift after approximately 0.5 equivalents I^-. The receptor is selective for oxo-anions such as tosylate (K = 2.1x10^5 M^{-1} in 2% DMSO-d_6/$CDCl_3$ at 296 K). Fluorescent sensors such as **8** based on the same macrocyclic skeleton have also been developed employing a 'dual channel' mechanism based upon proton transfer from the fluorophore in the excited state.[51]

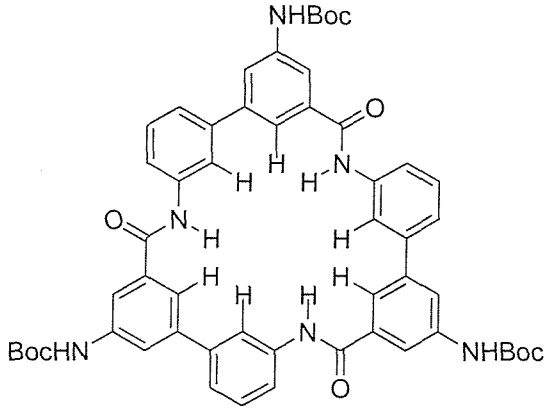

7

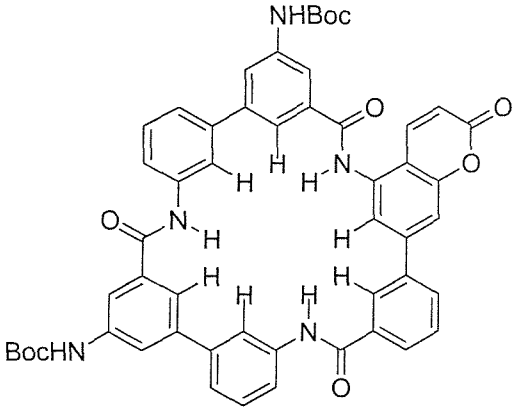

8

A variety of peptide based anion receptors have recently been reported. Kubik *et al.* reported that the cyclic hexapeptide **9** has been used to complex a variety of anions in 80% D_2O/CD_3OD.[52] In solid state, the crystal structure of the iodide complex of the macrocycle contributing with L-proline and 6-aminopicolinic acid shows the halide guest bound in a sandwich fashion between two macrocycles by a total of six hydrogen bonds.

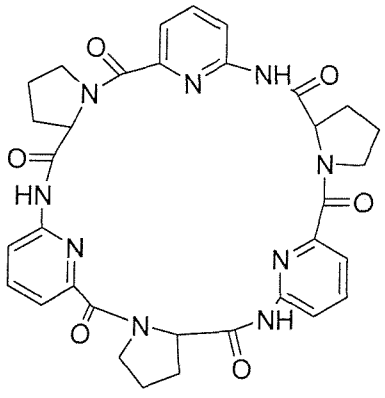

9

The same group have also investigated the anion receptor properties of cyclic peptides containing alternating natural amino acids and 3-aminobenzoic acids[53] whilst Spichiger and co-workers have identified linear polypeptides that interact with oxo-anions.[54] Kemp and co-workers have studied the stabilization effect of chaotropic anions on the helicity of short uncharged *N*-capped peptides.[55]

The Diederich group is focusing in mimicking biological receptors such as the natural antibiotic vancomycin.[56] Natural systems were of interest because of their ability to bind guests in aqueous solution. Receptor **10** has shown its ability to bind organic anions such as dansyl and benzenesulfonate with association constants of 45 M^{-1} in D_2O and 0.5 M KCl/DCl to a pD of 2 as a buffer. However, the complex precipitated at the high concentration.

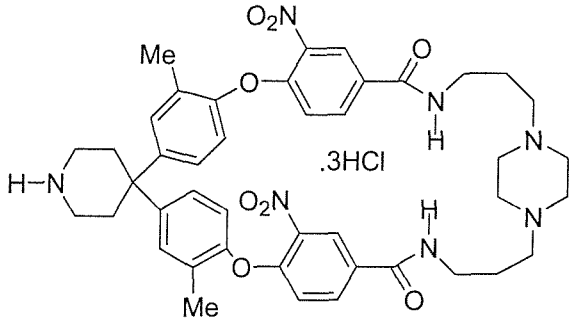

10

Davis developed a steroid-based cryptand **11** that recognized halide anions.[57] The system was comprised of a macrodilactam derived from the steroid cholic acid. The macrocycle formed a small, rigid cavity with four hydroxyl groups and two amide N-H groups directed inside the cavity.

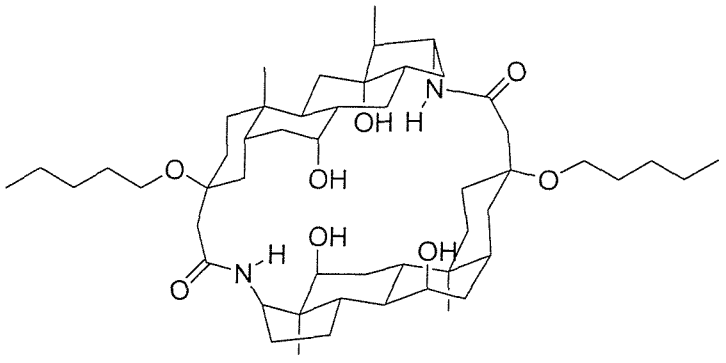

11

^{1}H NMR titrations in $CDCl_3$ showed a downfield shift for N-H proton and 1:1 binding constants at 3220, 990 and 250 M^{-1} for F^-, Cl^- and Br^- respectively. When compared with the acyclic version the preorganized macrocycle proved to be a much better host.

Ungaro and co-workers have attached C-linked peptide chains to the upper rim calix[4]arene and shown these species act as receptors for oxo-anions and chloride.[58] The calix[4]arene based receptor **12** binds acetate in DMSO-d_6 with an association constant of 33 M^{-1} at 300 K.

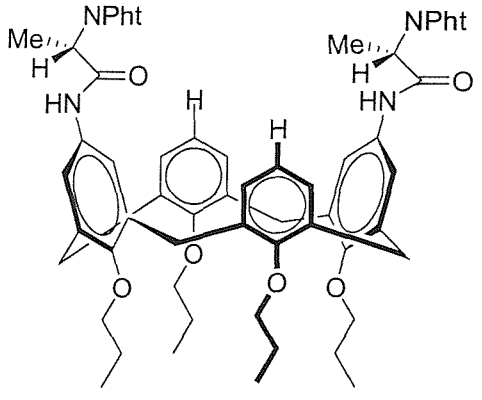

12

Urea and thiourea are particularly good hydrogen-bond donors and are excellent receptor for Y-shaped anions such as carboxylate through the formation of two hydrogen bonds. Kim and co-workers reported that the simple urea-based receptor **13** showed increasingly stable complexes with more highly charged and more basic bidentate anions.[59]

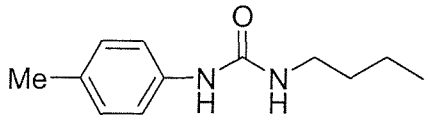

13

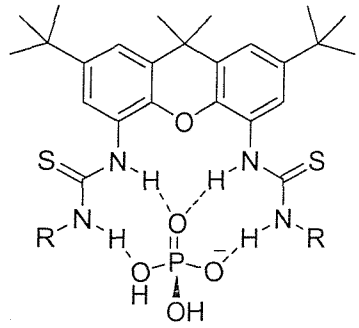

14 R = nBu

15 R = Ph

Umezawa and co-workers reported that the highly preorganized bis-thiourea receptors based on a xanthene spacer, **14** and **15**, selectively bound dihydrogen phosphate ($H_2PO_4^-$>CH_3COO^->Cl^-) in DMSO-d_6 via multitopic hydrogen bonding.[60] The stability constants of these $H_2PO_4^-$ complexes were 55000 M^{-1} for receptor **14** and up to 195000 M^{-1} for receptor **15**. The selectivity for $H_2PO_4^-$ ions can be attributed to the complementary hydrogen-bonding array present in these clefts that can form four hydrogen bonds to each $H_2PO_4^-$.

Kilburn and co-workers have synthesised a series of acyclic thiourea receptors for binding the carboxylate group of amino acid species.[61] For example, compound **16** was found to be selective for a variety of amino acid derivatives revealing, for example, a 30:1 selectivity for *N*-Ac-L-Trp-CO_2^- over *N*-Ac-L-Ser-CO_2^- in $CDCl_3$. Additionally, moderate enantioselectivity was observed with slight preference for L-amino acids.

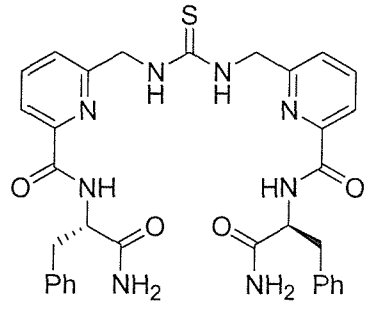

16

Other functional groups that can be exploited in the anion binding are the guandinium and the amidinium groups. Like ureas or thioureas, the positively charged guanidinium moiety can form two hydrogen bonds to anions such as carboxylate and phosphate. The combination of hydrogen bonding and electrostatic

interactions leads to the formation of strong complexes, even in very competitive hydrogen bond accepting and donating solvents such as water.[62] Schmidtchen and co-workers incorporated the guanidinium group into a bicyclic ring to form compound **17** – **19**. These receptors consisted hydrogen-bonding arrays similar to those present in ureas. Receptor **17** formed a very stable complex (K_a = 1.4 x 10^5 M^{-1}) with *p*-nitrobenzoate in chloroform.[63]

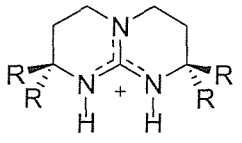

17 R = 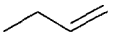

18 R = 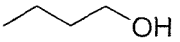

19 R = H

de Mendoza and co-workers synthesised the chiral receptor **20** that showed a preference for extracting *tert*-butoxycarbonyl (Boc)-protected L-tryptophane into chloroform from a racemic mixture in water.[64] In this case, the guanidinium–carboxylate interaction is further enhanced by π–π stacking. Later, another derivative of this scaffold was synthesised which contained one naphthoyl as well as one uracil derived substituent appended to the bicyclic core **21**.[65] The nucleotide derivative was attached in order to effect a base pairing interaction for the binding of guests containing an adenine moiety. The host formed a complex with 3'-AMP, while showing little interaction with 3',5'-cAMP.

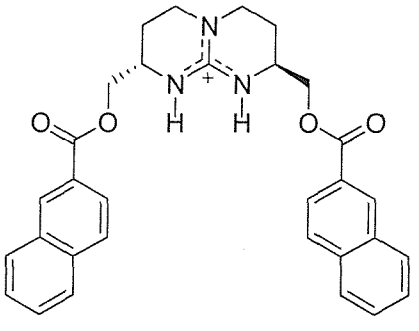

20

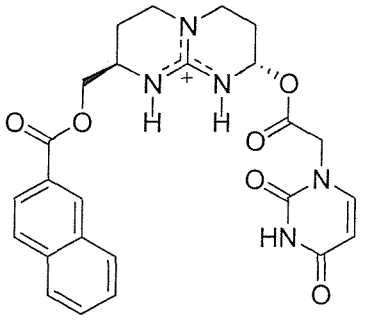

21

Davis and co-workers reported the synthesis of a variety of steroidal guanidines by functionalisation of cholic acid.[66]

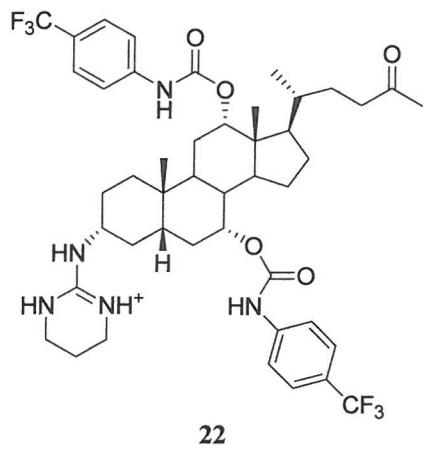

22

Extraction experiments from an aqueous solution to chloroform revealed that these compounds could coordinate amino acid derivatives. In certain cases chiral discrimination was observed. For example, receptor **22** was used to extract *N*-acetyl-α-amino acids from a racemic mixture with the extraction efficiency between 41 and 90%. It proved possible to enantioselectively extract the L and D isomers of the *N*-acetyl-alanine in a ration of 10:1.

Pyrrolic NH groups can be used to produce receptors that have an extremely high affinity for anions via electrostatic interactions. Recently, Gale and co-workers highlighted pyrrole's coordinating ability by crystallizing tetramethylammonium chloride from pyrrole (Figure 1.12).[67] The crystal structure reveals the complexation of one chloride anion by two molecules of pyrrole (N···Cl = 3.241 Å). However, in solution, pyrrole binds anions very weakly and therefore it must be functionalised with complementary groups to enhance its affinity toward anions.[68]

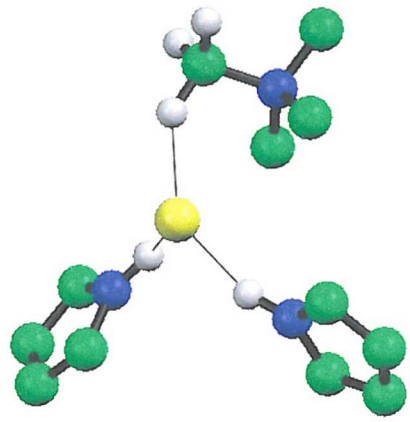

Figure 1.12: Crystal structure of the pyrrole/tetramethyl ammonium chloride complex.

Sessler and co-workers demonstrated that sapphyrins were capable of coordinating to anions. The core of sapphyrin macrocycle **23** can be doubly protonated to form a receptor with a positive charge and array of five NH hydrogen-

bonding groups. Solution-phase experiments have indicated that fluoride ions bound over 10^3 times more strongly to diprotonated sapphyrin than either bromide or chloride ions.[69,70] X-ray crystallographic analysis revealed that the fluoride ion was held in the plane of the sapphyrin ring by five N–H ··· F^- hydrogen bonds.[71]

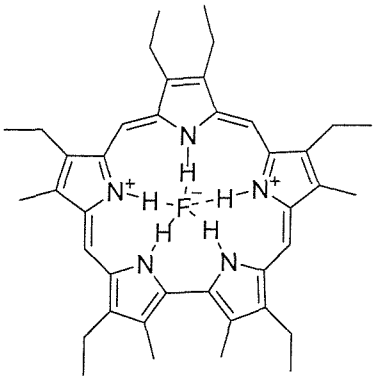

23·F^-

Sessler and co-workers also reported dipyrrolequinoxaline systems consisted of the unsubstituted system **24** and its mono-nitro derivative **25**.[72] The electronic influence of the functional groups present in the receptors play a crucial role in their recognition and sensing abilities investigated by UV-Vis and fluorescence titration experiments. It was found that compound **25** has a higher affinity for fluoride in dichloromethane ($1.2x10^5$ M^{-1}), than compound **24** ($2x10^4$ M^{-1}). In fact, solutions of compound **25** undergo a dramatic yellow to purple colour change in the presence of fluoride. Both systems also display fluorescence emission spectra that are quenched in the presence of fluoride.

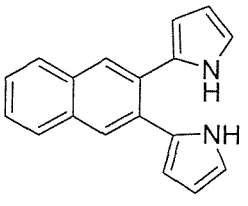

24

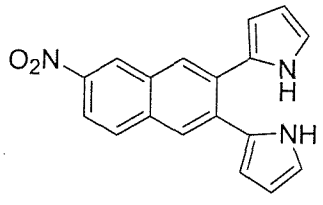

25

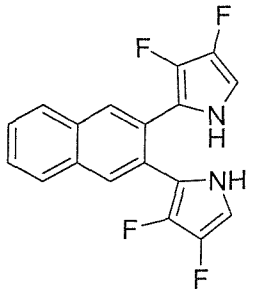

26

Moreover, the tetrafluoro derivative **26** displayed an increased affinity for anions studied in the case of **24** as well as a higher dihydrogenphosphate:chloride selectivity ratio (96 vs. 1.2 in the case of **26** and **24**, respectively).[73] These quantitative findings

were highlighted by the fact that **26** was observed to undergo a naked-eye-detectable yellow-to-orange colour change when exposed to 100 molar equivalents of either TBA fluoride or TBA dihydrogenphosphate in dichloromethane solution, while failing to undergo a discernable colour change when exposed to an equivalent concentration of chloride anion.

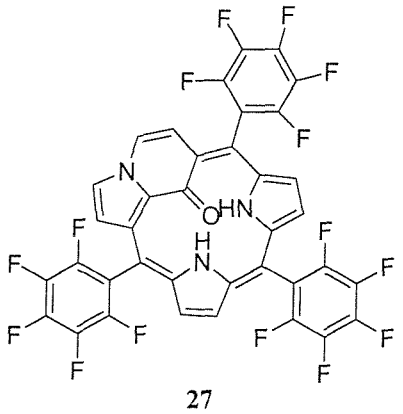

27

Furuta *et al.* have used the derivative of a doubly *N*-confused porphyrin as an anion receptor.[74] Compound **27** proved capable of binding anions with association constants comparable to those of typical, unsubstituted calix[4]pyrrole (e.g. $K_a \sim 10^4$ M^{-1} for fluoride anion in dichloromethane-d_2)

Anion receptors containing both pyrrole and amide groups have been shown to be effective and selective in their complexation properties. Gale and co-workers have recently shown that simple amide substituted 2,5-diamidopyrroles, **28** and **29**, could be used as receptors for binding a variety anionic guest species with selectivity for oxo-anions as benzoate and dihydrogen phosphate anions in CD_3CN and DMSO-d_6-0.5% H_2O solution.[75]

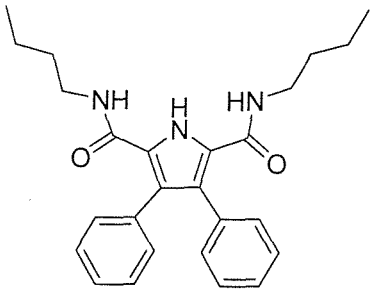

28

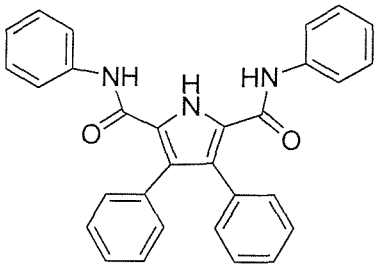

29

Modification by appending ferrocene groups to the 2,5-diamido pyrrole skeleton, Gale and co-workers have shown that these compounds may also be used as electrochemical sensors for anions.[76] Compound **30** and **31** each contain two ferrocene moieties linked directly to the amide group in compound **30** or via a methylene carbon in compound **31**. Both compounds crystallise as dimers linked via NH-OC hydrogen bonds.[77] The crystal structure of compound **30** also shows this

binding motif and in addition a CH-O interaction from the substituted ferrocene cyclopentadienyl ring to an amide oxygen atom.

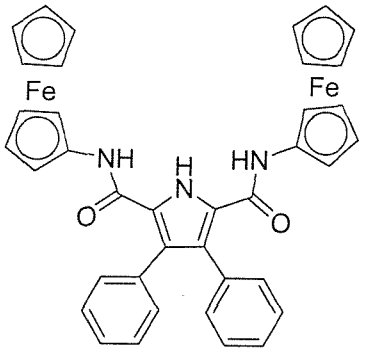

30

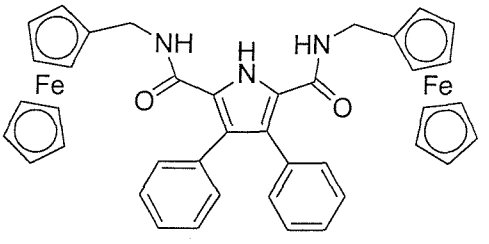

31

The electrochemical behaviour of these compounds was investigated by cyclic voltammetry. Significant shifts of the ferrocene-ferrocenium redox couple were observed upon addition of a variety of anions to solutions of the receptor; however, in a number of cases, the voltammetric wave was found to be seriously distorted as the product of the electrochemical reaction passivated the electrode.

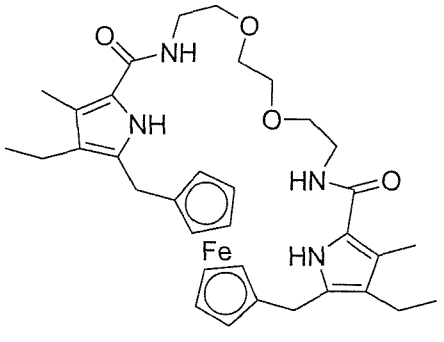

32

Sessler and co-workers have recently reported the synthesis of a bridged dipyrrole *ansa*-ferrocene **32**.[78] This receptor acted as an effective redox-based sensor for fluoride and dihydrogen phosphate anions. The electrochemical measurements revealed that the cathodic shift in the ferrocene-ferrocenium redox couple of compound **32** showed a greater response in the presence of fluoride (80 mV) and dihydrogen phosphate (136 mV).

Schmuck has studied on the anion-complexation and self-assembly properties of guandinium functionlised pyrrole including a study of 2-(guanidiniocarbonyl)-pyrrole-4-carboxylate **33** in DMSO solution.[79] The formation of guanidinium-carboxylate salt bridges in solution to form non-covalently linked oligomers of **33** was found to be an entropy driven process. The dimerisation of compound **34** which as the chloride or hexafluorophosphate salt has also been studied in DMSO solution.[80]

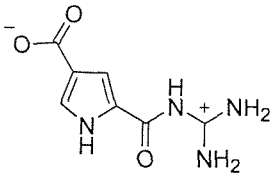

33

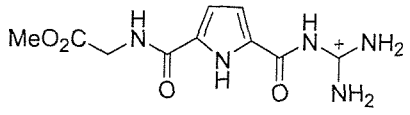

34

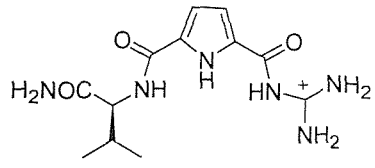

35

The molecule forms discrete dimers via the formation of guanidinium-ester hydrogen bonds together with a contribution from a pyrrole-pyrrole π-stacking interaction. The addition of picrate anions breaks up the dimers and the receptor forms a picrate complex (Figure 1.13). Meanwhile, Schmuck has shown that the chiral receptor **35** is capable of discriminating between enantiometric carboxylates in 40% water/DMSO-d_6 solution (e.g. Ac-L-AlaO$^-$: K_a = 1610 M^{-1}; Ac-D-AlaO$^-$: K_a = 930 M^{-1}).[81]

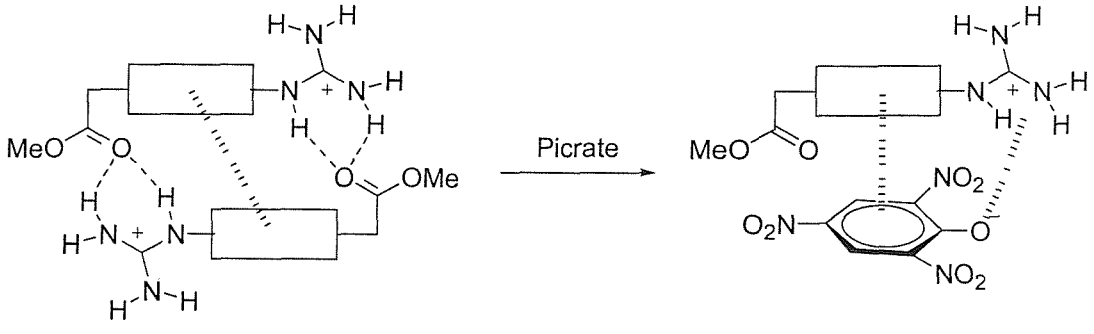

Figure 1.13: Dimerisation of Schmuck's system is disrupted by picrate.

1.4 Self-assembly

Self-assembly allows access to new molecular architectures that are inaccessible (or accessible in only very small yields) via traditional multi-step covalent bond making and bond breaking techniques. The new molecular architectures are produced by combining appropriately designed sub-units, which can be quite simple, and yet after the assembly process produce quite complex architectures.[6]

In biological systems, viruses represent some of the best natural examples of self-assembly. A well-known example is the tobacco mosaic virus[82] (TMV). This virus contains 2130 identical protein subunits, therefore minimising the amount of genetic information required to encode the final helical structure assembled around a single strand of RNA. The TMV self-assembly required all of the information contained within the constituent parts of the virus. No additional factors are needed. Although all of the protein subunits are bound to each other in the same manner and creating the symmetrical helical structure, the assembly process is by no means as straightforward as it might first appear (Figure 1.14).[83]

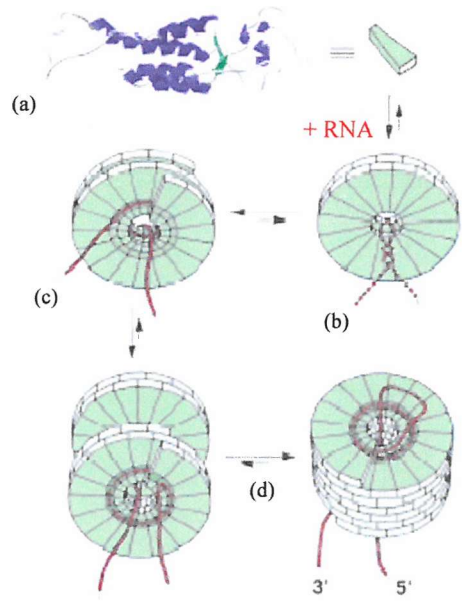

Figure 1.14: The assembly of the tobacco mosaic virus. (a) Protein sub-units. (b) Associate with viral RNA to form a double disk structure. (c) Conformational change results in the formation of a slipped double disk and (d) initiates viral assembly.

The self-assembling double-helical structure of DNA has provided the inspiration for a further area of supramolecular chemistry. Use of metal ions to template the assembly of organic threads into multiple-helical structures has been explored by a number of research groups. For example, interaction of the helicand **36** which is preorganised helically by virtue of steric repulsions between the methyl group with Cu(I) rapidly produces the binuclear [4+4] helicate $[Cu_2(\mathbf{36})_2]^{2+}$.[84]

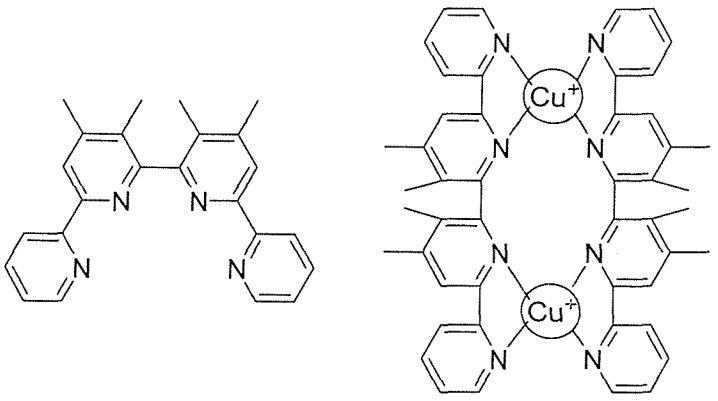

36 $[Cu_2(\mathbf{36})_2]^{2+}$

Examples include n x n grid-like polynuclear complexes that could be synthesised by the controlled arrangement of ions into specific arrays and patterns. Lehn, Youinou and co-workers have shown that ligands **37** and **38** form 2 x 2 grids with four Cu(I) ions[85] and a 3 x 3 grid-like array with nine silver ions[86] respectively (Figure 1.15).

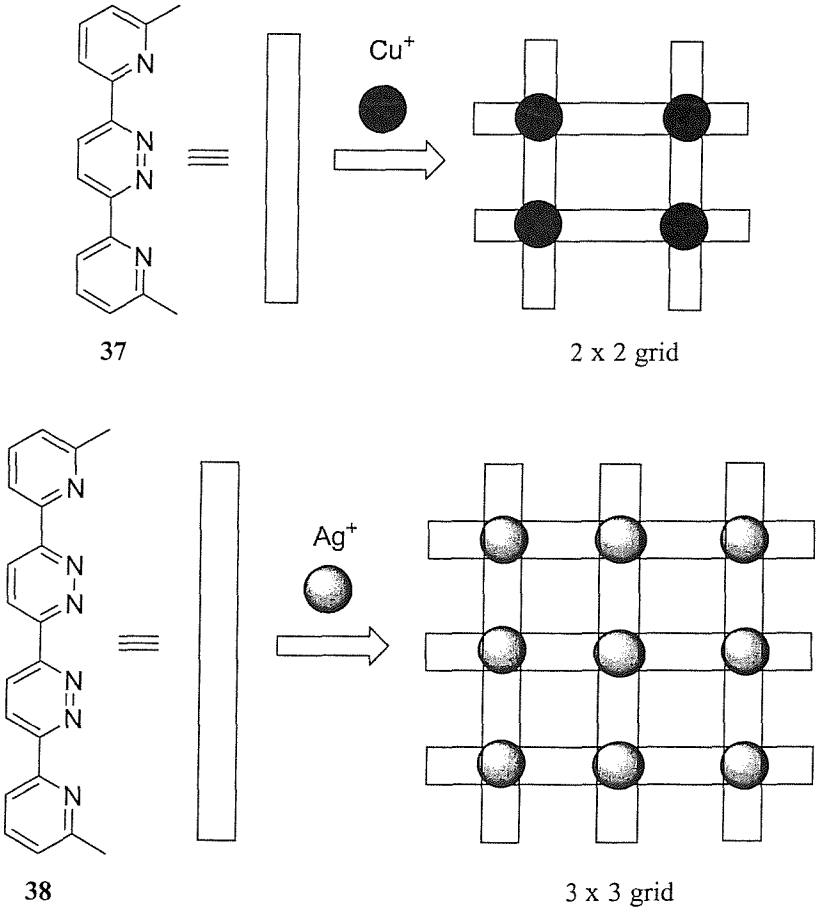

37 2 x 2 grid

38 3 x 3 grid

Figure 1.15: Self-assembly of 2 x 2 grid from **37** with Cu^+ and 3 x 3 grid array from **38** with Ag^+.

Until a few years ago, examples of anions directing the formation of molecule architectures were difficult to find. However, this situation has now changed, and reports of the templating influence of anions are now becoming widespread. de Mendoza and co-workers have synthesised a tetraguanidinium strand **39** that self-assembles around sulfate anions to form a double helix.[87] Evidence for the anion directed helical structure was provided by ROESY NMR spectroscopy. The complexation behaviour of this and other tetraguanidinium reagents with α-helical peptides containing negatively charged aspartate residues has recently been reported by Hamilton and de Mendoza.[88]

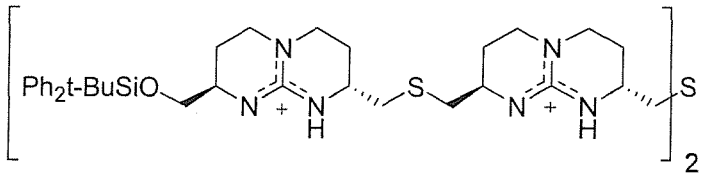

39

Vögtle and co-workers have employed anion coordination in a high yielding rotaxane synthesis. They discovered that phenolates, thiophenolates and sulfonamide anions when bound to tetralactam macrocycles are capable of reacting as a nucleophile and therefore may be used in rotaxane synthesis. Rotaxane **40** was synthesised in an excellent 95% yield.[89,90]

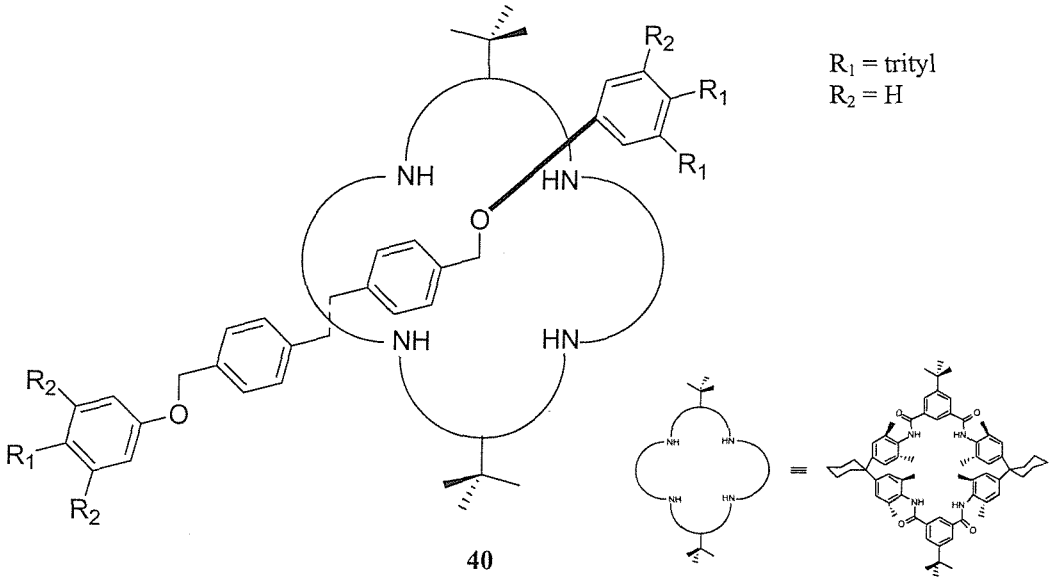

40

An anion-directed pseudo-rotaxane has been reported by Beer and co-workers.[91] Mixing the zwitterions **41** with macrocycle **42** results in the formation of a pseudo-rotaxane **43** in acetone-d_6 with an association constant of 2400 M^{-1} (Figure 1.16). The pseudo-rotaxane is stabilised by chloride-HN hydrogen bonds, π-π stacking interaction and CH-O hydrogen bonds. Analogues of **41** containing other counter anions such as bromide, iodide or hexafluorophosphate assemble with **42** with lower association constants than chloride complex (700, 65 and 35 M^{-1} respectively).

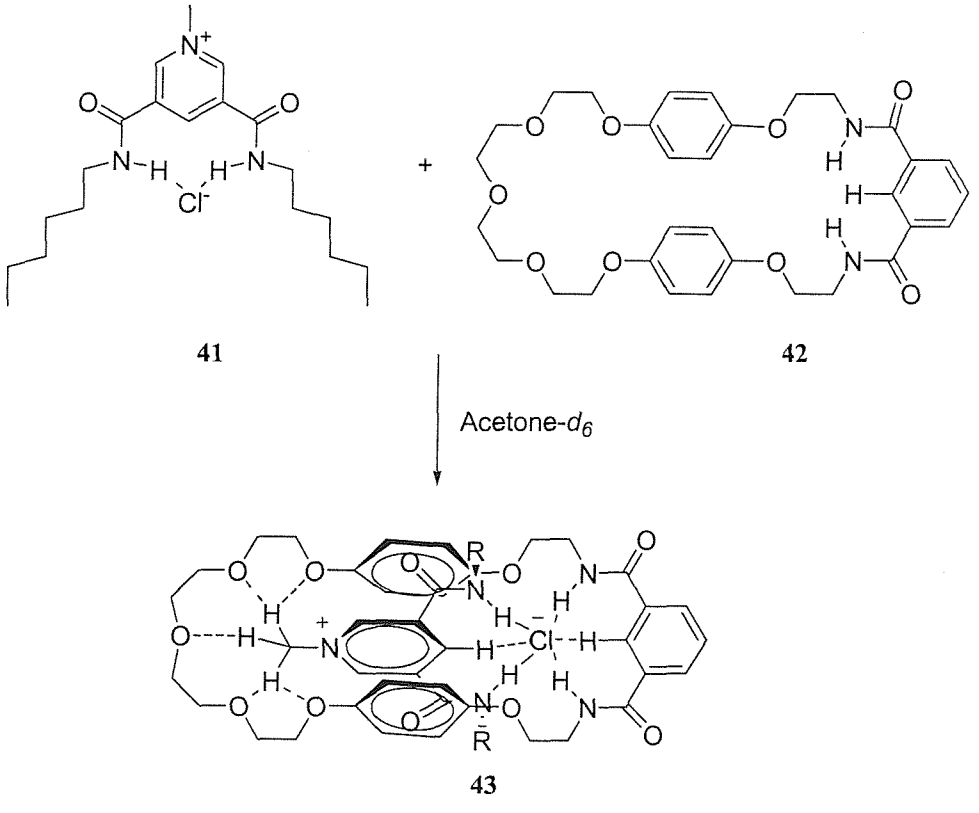

Figure 1.16: Chloride direct assembly of pseudo-rotaxane **43**.

1.5 Aim of the project

The information and examples shown throughout the chapter, provide a wide variety of anion receptors that utilise coordinating groups such as amide, urea, thiourea, guanidinium, pyrrole and other functional groups as well as the important of anions in several fields. Selectivity fowards an anionic substrate represents the main target of many research groups and is difficult to achieve. For these reasons, anion coordination chemistry is a field continuous growth, and challenges researchers to employ considerable effort in designing, synthesising and investigating new and more selective anion receptors.

In this thesis, new amidopyrroles, and their anion recognition, anion transportation and also anion assembly properties are reported.

Specifically:

- Functionalization of pyrrole with amide groups in the 2- and 5- positions in order to investigate whether simple pyrrolic clefts can behave as efficient anion receptors designed to bind oxo-anions via multiple hydrogen bonds.
- Prodigiosin mimics containing imidazolium amidopyrrole and their analogues and the study their anion binding properties especially their HCl symport properties in vesicles (in collaboration with Bradley Smith and co-workers at the University of Notre Dame).
- Synthesis of pyrrole-derived 'tweezer' receptor libraries by solid phase synthesis and use of screening experiments to investigate their anion recognition with the tri-peptide guest tetrabutylammonium salt of red dye-spacer-L-Leu-L-Asn-L-Phe.
- Anion-anion self-assembly of interlocking pyrrole materials dimers and trimers contained 3-,4-dichloro amidopyrrole.

2. *Anion recognition: Pendant arm amidopyrrole compounds*

2.1 Introduction

Anion receptors containing both pyrrole and amide groups have been shown to be effective and selective in their complexation properties.[76,92] These types of receptors can bind anion molecules using hydrogen bonds via both the NH-amide and the NH-pyrrole (Figure 2.1).

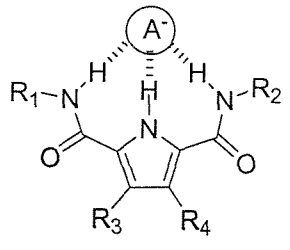

Figure 2.1: Pyrrolic amide receptor for anion molecule.

For example, bis-amido cleft species such as **28** have been shown to coordinate to the benzoate ion with a stability constant of 2500 M^{-1} in acetonitrile-d_3 (0.03% water) solution. Compound **29** was found to bind dihydrogenphosphate selectively with a stability constant of 1450 M^{-1} in DMSO (0.5% water) solution.[75] However, the mono-amido cleft species **44** and **45**, did not show highly selective binding to oxo-anions as seen with the bis amido pyrrolic compounds.[93] The solid state structure of the **28**/benzoate complex confirmed that the three NH donors in the compound formed hydrogen bonds to the benzoate anion (Figure 2.2).[94]

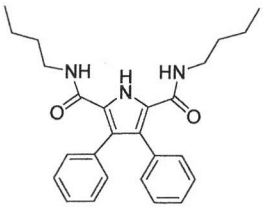

28

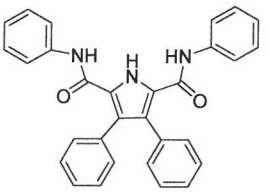

29

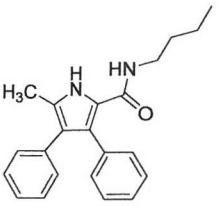

44

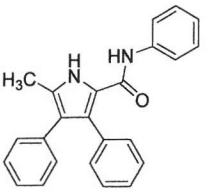

45

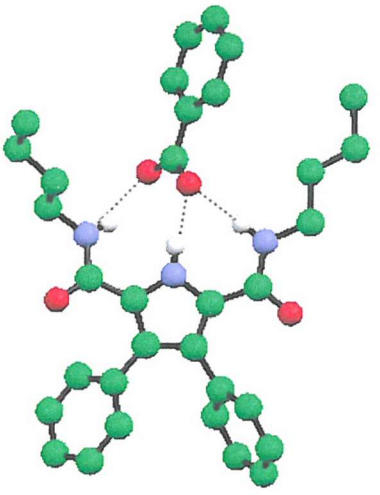

Figure 2.2: Crystal structure of the benzoate complex of **28** (tetrabutylammonium counter cation omitted and hydrogen atoms not involved in hydrogen bonding interactions have been removed for clarity).

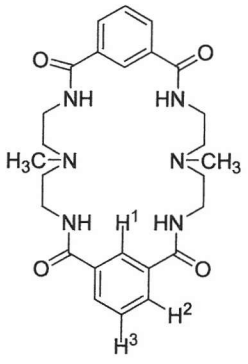

46

These receptors offer a number of possible avenues for modulating the anion affinity of the bis-amido pyrrole unit. Bowman-James *et al.* have found that macrocycles containing mixed amides and amines e.g. **46** show a marked selectivity for protonated oxo-anions such as $H_2PO_4^-$ and HSO_4^-, binding these species strongly due to a proton transfer from the anion to the receptor causing the formation of a more highly charged anion and receptor pair.[95]

For these reasons, the synthesis of pendant arm bis-amido pyrrole cleft receptors for protonated oxo-anions has been performed. A variety of compounds have been synthesised by introducing amido groups at the 2- and 5- position of pyrrole, and the anion binding properties of these receptors have been investigated by the use of ^{1}H NMR titration techniques.

2.2 Synthesis and characterization

Three new pyrrole amide clefts 3,4-diphenyl-1H-pyrrole-2,5-dicarboxylic acid bis-[(2-amino-ethyl)-amide] **47**, the hexafluophosphate salt of 3,4-diphenyl-1H-pyrrole-2,5-dicarboxylic acid bis-[(2-amino-ethyl)-amide] **48** and 3,4-diphenyl-1H-pyrrole-2,5-dicarboxylic acid bis-[(2-acetylamino-ethyl)-amide] **49** have been synthesized in an analogous fashion to the simple pyrrole based amide cleft species[96] (Scheme 2.1).

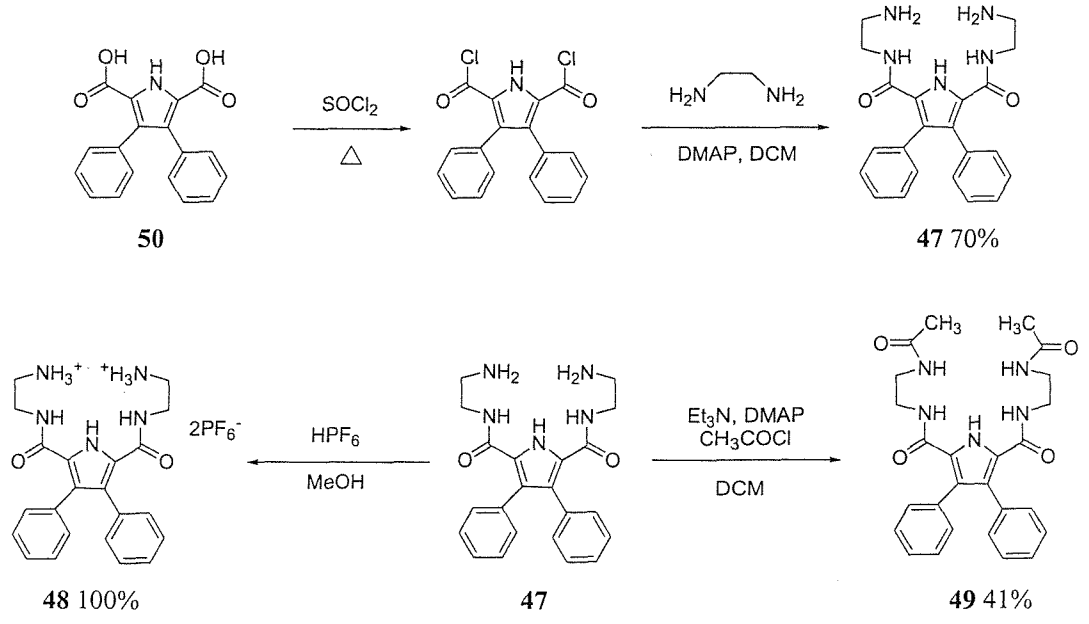

50 **47** 70%

48 100% **47** **49** 41%

Scheme 2.1: The preparation methods of compound **47**, **48** and **49**.

Hexafluorophosphate salts of the ethylenediamine substituted pyrrole were used, since the PF_6^- anion is relatively 'innocent' and does not significantly interact with hydrogen bond donating moieties. 2,5-Dicarboxy-3,4-diphenyl pyrrole **50** was prepared following literature procedures[97] and was refluxed with an excess of thionyl chloride overnight in order to obtain the bis-acid chloride.[75,93] This compound was reacted directly with ethylenediamine in dichloromethane in the presence of a catalytic quantity of DMAP. Removal of the solvent and subsequent purification by column chromatography on silica gel (eluting with dichloromethane-methanol 10:3 v/v) afforded the bis-amine **47** in 70% yield. This receptor was protonated by the addition of hexafluorophosphoric acid to the solution. After stirring for 5 minutes the solvent was removed, affording receptor **48**. Receptor **49** was prepared by reaction of compound **47** with 2.5 equivalents of acetyl chloride in dichloromethane in the presence of triethylamine and a catalytic quantity of DMAP. After purification by column chromatography on silica gel (eluting with dichloromethane-methanol 10:1 (*v/v*) the product was obtained in 41% yield.

Crystals of the mono-hexafluorophosphate salt of compound **47** were obtained by dissolving compound **47** in methanol and adding 2 equivalents of HPF_6. Stirring the solution for 3 h resulted in the formation of a white precipitate, which was collected by filtration. This material was crystallised from MeOH-water affording X-ray quality crystals from which the structure could be elucidated (Figure 2.2).

The asymmetric unit contains $C_{22}H_{26}O_2^+PF_6^-2H_2O$. The hydrogens on the oxygen and nitrogen atoms were located from the difference map and fully refined. Although it was possible to refine three hydrogen atoms on N5, the temperature factors where consistently higher than for those on N1 and therefore this group was modelled as a disordered NH_2 with each hydrogen having an occupancy of 2/3. This is consistent with having two water molecules and one PF_6^-. The structure consists of hydrogen bonded dimers interlinked in to a three-dimensional array by further extensive hydrogen bonding interactions involving PF_6^-, and H_2O. The hydrogen bond distance between the pyrrolic nitrogen and the carbonyl group (N3-H3···O1) is 2.911(5) Å whereas the length of the ammonium nitrogen-carbonyl hydrogen bond (N1-H1C···O2) is 2.806(5) Å.

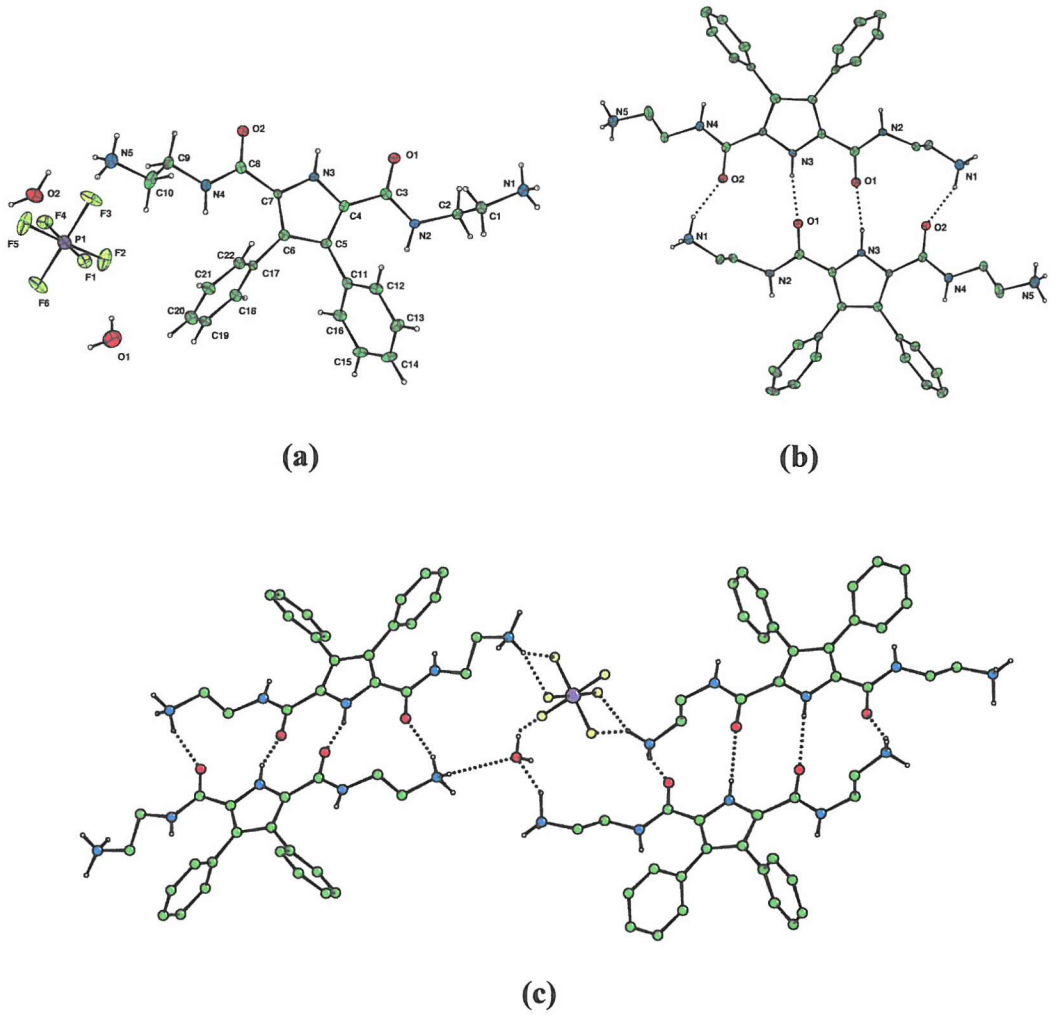

Figure 2.3: (a) Crystal structure of mono-PF_6^- with compound **47** and $2H_2O$. (b) Dimers molecules. (c) Network showing the formation of dimers and their linking via bridging PF_6^- and H_2O groups. Selected hydrogen atoms have been omitted for clarity.

2.3 Binding studies

The anion receptor properties of compounds **47**, **48** and **49** were studied using ^{1}H NMR titration techniques and the EQNMR computer program[98] to determine the stability constants of the complexes. Anions were added as their tetrabutylammonium salts. The results of these titrations in DMSO-d_6-0.5% water (except where noted) are shown in Table 2.1. Several NH proton resonances were

followed during the NMR titration with stability constants being calculated for each. The protons can be identified by the numbers shown which correspond to the labels present in Figure 2.3.

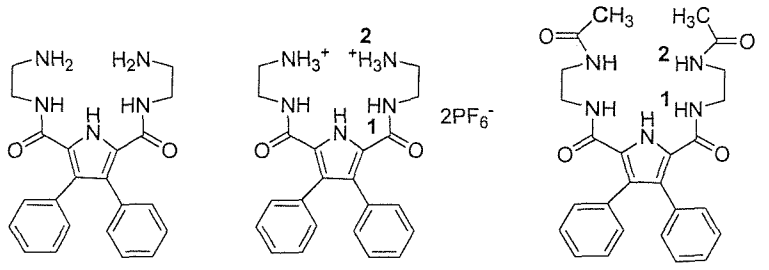

Figure 2.4: Binding sites of compound **47**, **48** and **49**.

When binding was observed with chloride, bromide, benzoate or hydrogensulfate the data fitted a 1:1 receptor:anion binding model well. The bis-amine receptor **47** is a weak chloride receptor and does not appear to interact with bromide under these conditions. In addition, in this case the association with benzoate is weak in contrast to the other 2,5-diamidopyrrole clefts such as **28** and **29**.[75] Dihydrogenphosphate was found to bind strongly to this receptor, however large errors were present in the least squares non-linear fit of the titration curve. Therefore, DMSO-d_6-5% water solution was used in the titration to weaken the interaction. Under these competitive conditions a stability constant of 2050 M^{-1} was found, however this value should be treated with caution, as the systematic errors in this set were non-random.

Compound	Anion[a]	K_a/M^{-1}
47	Chloride	<20
47	Bromide	[b]
47	Dihydrogenphosphate	2050[c]
47	Benzoate	47.6
47	Hydrogensulfate	$>10^4$
48	Chloride	(1) 110, (2) 39, (3) 140
48	Bromide	35
48	Dihydrogenphosphate	44
48	Benzoate	125
48	Hydrogensulfate	(1,2) <20
49	Chloride	<20
49	Bromide	[b]
49	Dihydrogenphosphate	(1) 525 (2) 190
49	Benzoate	(1) 152 (2) 19.5
49	Hydrogensulfate	[b]

[a] Anions added as tetrabutylammonium salts. Error < 15% except where noted.
[b] No binding observed. [c] NMR experiments carried out in DMSO-d_6-5% water (error 29%).

Table 2.1: Association constant of receptors **47**, **48** and **49** (M^{-1}) with various anionic guest species following protons (1), (2) and (3) at 25°C in DMSO-d_6-0.5% water (excepted were noted).

In the presence of 0.5% water in DMSO-d_6, a very strong complex was formed between **47** and HSO_4^- ($K_a > 10^4$ M^{-1}). It is likely that these strong interactions are due to protonation of the receptor by the anion, as observed by Bowman-James and co-workers,[95] in amine containing macrocyclic systems, resulting in the addition of an electrostatic component to the binding interaction (and the bound anion now carrying a higher negative charge). Therefore where proton exchange is occurring the stability constant can only be regarded as apparent data as the binding process is accompanied by proton transfer. Further evidence for this mechanism comes from the data found for the bis-amide based receptor **49**. In this

case, protonation of the receptor is not possible, a fact that is reflected in the lower stability constants for dihydrogenphosphate and the failure of the receptor to interact with hydrogensulfate.

The bis-ammonium based receptor **48** shows enhanced binding of halide anions as compared to receptor **47**, reflecting the extra electrostatic component to the binding interaction. It is unlikely that hydrogensulfate is being deprotonated by this receptor, the lack of an interaction may once again reflect the absence of proton exchange (and hence no formation of SO_4^{2-}). Wherever possible, the association constants have been calculated by following a variety of protons on the receptor (in the case of **48** with chloride and **49** with dihydrogenphosphate and benzoate). In the case of **48** with chloride, the stability constants determined by the shift of the pyrrole and amide NH protons are in close agreement, whereas the stability constant determined by following the shift of the ammonium protons is considerably lower. In the case of receptor **49** and dihydrogenphosphate and benzoate, the stability constants determined by following the shift of the amide group closer to the pyrrole ring gives a higher K_a value. Presumably, the pyrrole NH and directly attached amides interact more strongly with the bound anion than the pendant hydrogen bond donors, however it is interesting that the same result is not obtained for all these protons as there can be only one stability constant for this binding event.

Proton NMR titration curves of these compounds with tetrabutylammonium dihydrogenphosphate and tetrabutylammonium hydrogensulfate are shown in Figure 2.5.

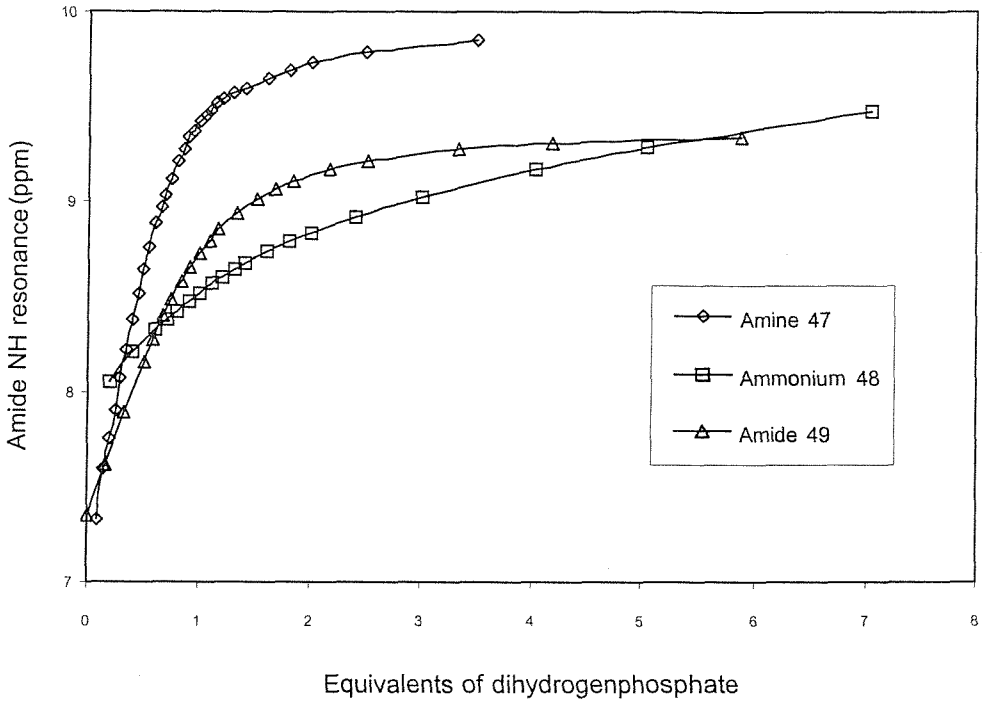

(a)

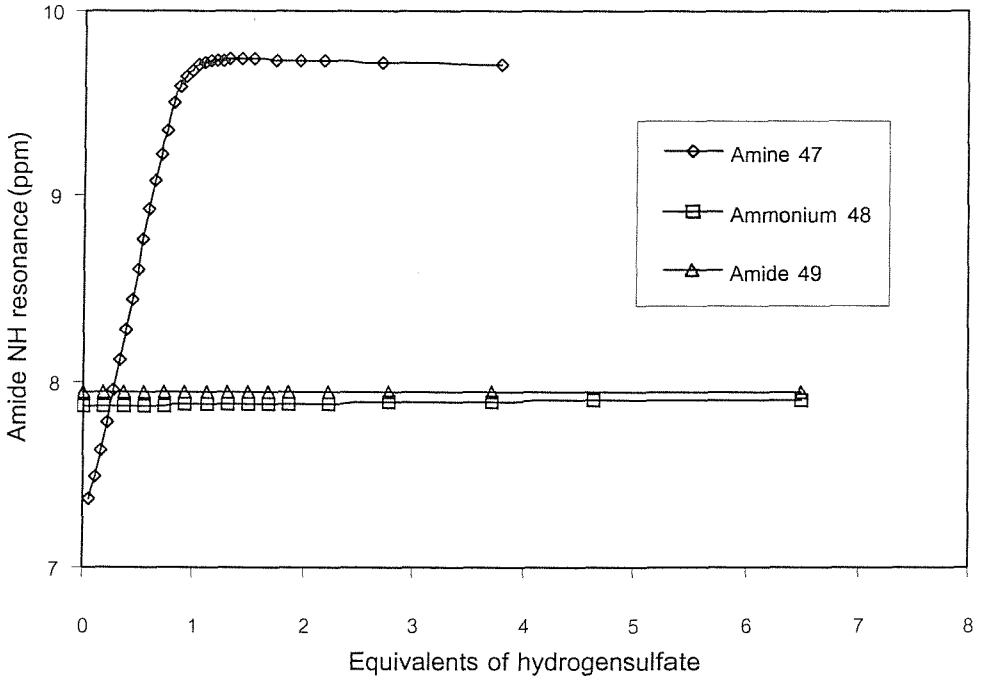

(b)

Figure 2.5: ^{1}H NMR titration curves of compounds **47**, **48** and **49** in DMSO-d_6-0.5% water at 25°C with (a) tetrabutylammonium dihydrogenphosphate (in DMSO-d_6-5% water for **47**) and (b) tetrabutylammonium hydrogensulfate.

2.4 Conclusion

Receptors **47**, **48** and **49** containing amine, ammonium and amide pendant arms were synthesised. The anion-coordination ability of these species has been determined by ^{1}H NMR titration techniques. The amine pendent arm receptor **47** forms strong complexes with protonated oxo-anions such as HSO_4^- whilst amide and ammonium pendant arm bis amide pyrroles bind these anions more weakly.

3. *Towards synthetic HCl symporters*

3.1 Introduction

The transport of anionic species across hydrophobic membranes presents a considerable challenge to the supramolecular chemist.[99] Such processes are essential in biological systems to maintain the balance of electrolytes both within and outside the cell. Chloride transport has attracted interest recently with several reports of anionophores mediating transport of this anion across membrane systems.[100,101] Indeed, chloride transporters have direct medical potential as treatments for cystic fibrosis (CF) that is caused by a loss of channel function and other diseases caused by defective channel proteins.[102]

We decided to take our inspiration from nature and design a variety of structurally simple low-molecular-weight synthetic HCl symport agents capable of transporting this ion pair across lipid bilayers and hence potentially possessing a range of biological activity ranging from proton pump inhibition to triggering apoptosis.[103]

The HCl symport mechanism is shown in Figure 3.1. A mobile carrier (M) is protonated within the membrane at the low pH (high proton concentration) side and then becomes an effective chloride receptor. The protonated mobile carrier (MH^+) binds a chloride ion so forming a neutral complex in the membrane. The complex then diffuses through the membrane to the other side where it comes into contact with the high pH environment. Deprotonation occurs and consequently loss of chloride. The free receptor may then diffuse back across the membrane.

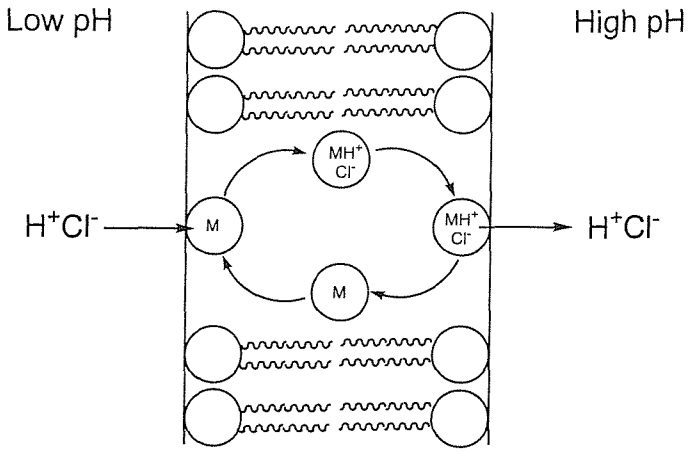

Figure 3.1: H^+/Cl^- Symport mechanism.

The symport of HCl in some biological systems such as bacteria, has been found to be regulated by a class of naturally occurring pigments known as the prodigiosins.[104] Prodigiosins are naturally occurring pyrrole alkaloids,[105] whose red pigments are produced by microorganisms such as *Streptomyces* and *Serratia*.[106,107] The naturally occurring prodigiosins may be divided into acyclic and cyclic forms as shown in Figure 3.2.

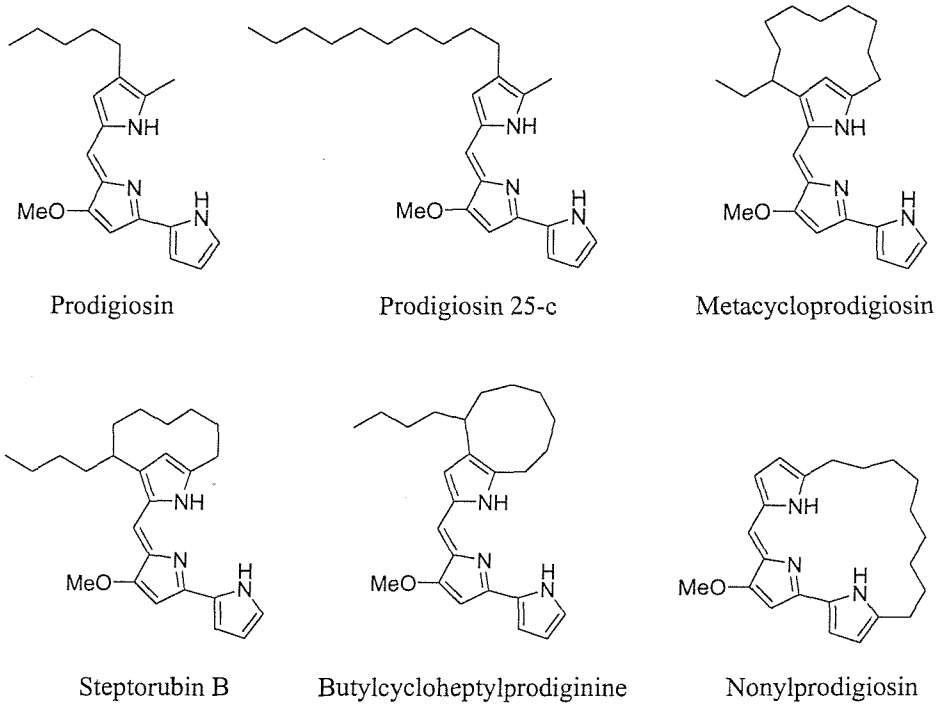

Figure 3.2: Representative members of the prodigiosin family.

All naturally occurring prodigiosins contain the 4-methoxy-2,2'-bipyrrole ring system; variation in structure is found in the C-pyrrole ring. Prodigiosin itself is acyclic and contains a 2-methyl-3-pentyl-pyrrole as the **C**-ring. Pyrrole alkaloids of this type exhibit a broad range of immuno-suppressive activity against bacteria, protozoa, and pathogenic fungi.[108,109] They have a pronounced effect on the human malaria parasite *Plasmodium falciparum* at dosages below the acute cytotoxicity thereshold (IC_{50} of metacycloprodigiosin: 5×10^{-3} μgml^{-1}).[110]

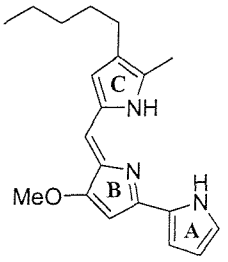

Prodigiosin

Pyrrole alkaloids are known to act as H^+/Cl^- symporters, possibly through protonation and subsequent binding of the positively charged triple hydrogen bond donor to chloride.[111,112] This activity has been ascribed to their promotion of apoptosis[113] by acidification of the intracellular pH (pHi).[114] The protonated pyrromethane chromophore of prodigiosin is thought to play a critical role in pHi regulation, and the **A**-pyrrole ring is known to be important for anticancer activity.[115,116] They show significant cytotoxicity *in vitro* againt the P388 mouse leukaemia cell (IC_{50} 3.7×10^{-4} μgml^{-1}) as well as against human melanoma and liver cancer lines.[117,118]

Ohkima *et al.* showed that prodigiosins increase lysosomal pH in cultured cells causing the inhibition of the function of vacuolar H^+-ATPase, an enzyme involved in ATP dependant proton pumps.[119] Vacuolar-type H^+-ATPase (V-AYPases) reside on the membranes of acidic organelles such as sunaptic vesicles, lysosomes and the trans-Golgi network and maintain an acidic environment by pumping H^+, using the energy of ATP hydrolysis.[120]

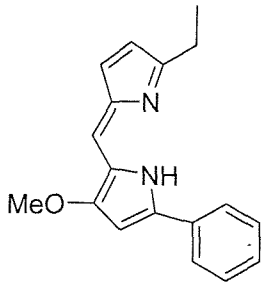

51

Melvin, Manderville and colleagues have reported that prodigiosin facilitates double-strand DNA cleavage in the presence of Cu(II) and molecular O_2.[121] Double-strand DNA cleavage is a known mechanism of apoptosis and may well provide an alternate rationale for the cytotoxic properties of prodigiosin-group natural products. They have also recently reported anion complexes of the prodigiosin-type compounds. The HCl salt of the phenyl-substituted dipyrrolylmethene derivative **51** has been

crystallographially characterised by X-ray diffraction analysis.[116] The resulting structure is shown in Figure 3.3. This structure reveals the presence of a single, chloride-pyrrole hydrogen bonding interaction in the solid state.

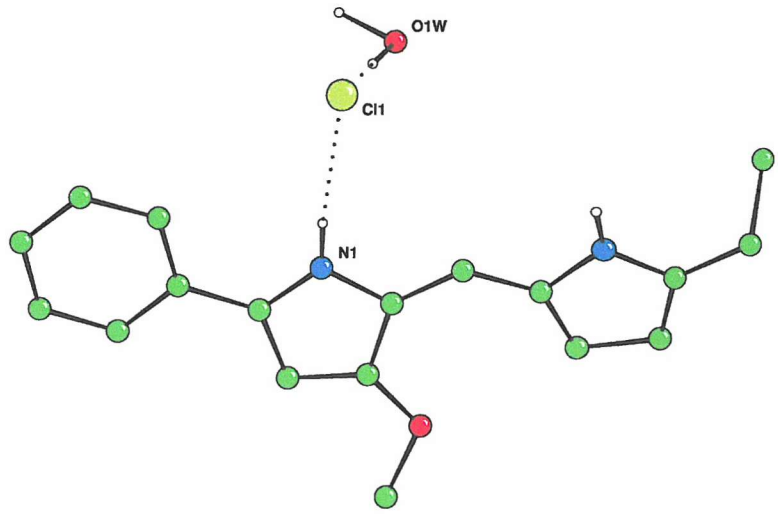

Figure 3.3: The X-ray structure of the hydrochloride salt of the pyrrolyopyrromethene prodigiosin analogue **51**.

For these reasons, the synthesis of prodigiosin mimics has been one of the central aims of this project in order to shed light on the mode of action of the prodigiosins and to provide a new series of compounds with potentially useful biological activity. The design of these compounds was based on the amidopyrrole skeleton connected to a basic group (e.g. imidazole or pyridine). The receptors were designed to bind chloride strongly only upon protonation. The anion binding properties, specifically of chloride, and also the HCl symport properties of these compounds were investigated by several different techniques.

3.2 Synthesis and characterization

Eight putative prodigiosin mimics were synthesised (Figure 3.4). The compounds contain hydrogen bond donor groups in addition to either a methylimidazole or pyridine ring which may be protonated so potentially enhancing the affinity of the receptors for chloride.

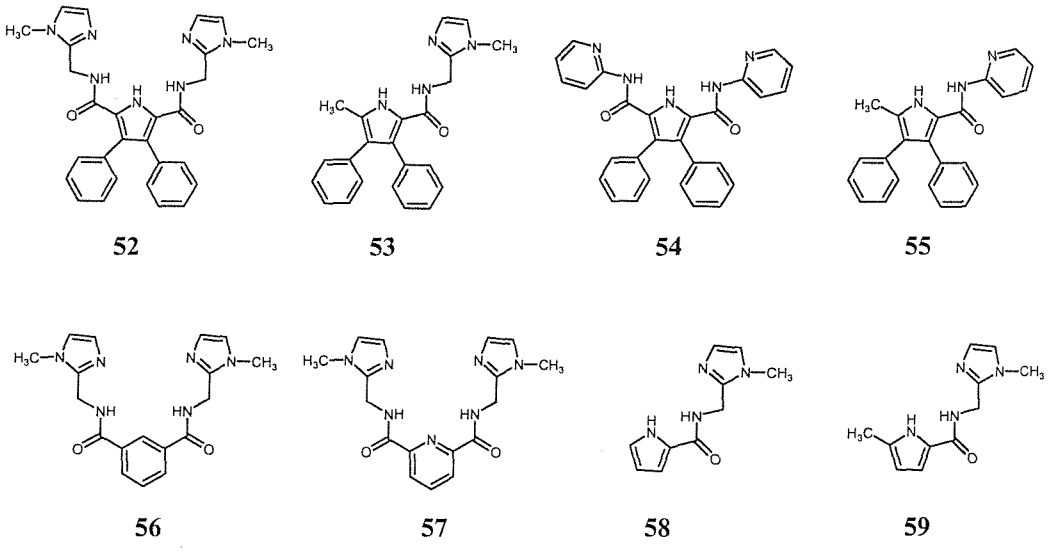

Figure 3.4: Potential prodigiosin mimics.

1-Methyl-2-aminomethylimidazole **60**, was used as a starting material, from which the imidazole-containing prodigiosin mimics were synthesised via a modification of literature methods[122,123] (Scheme 3.1).

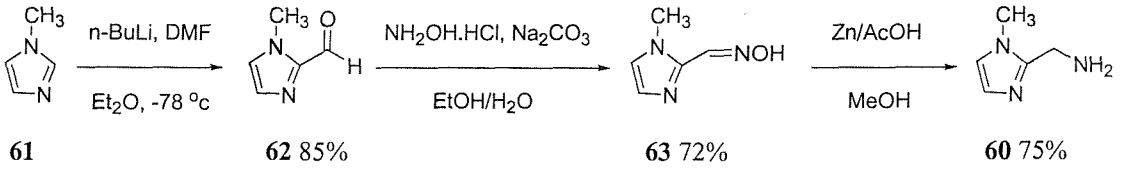

Scheme 3.1: Synthesis of compound **60**.

1-Methyl imidazole **61** was lithiated with n-BuLi and reacted with DMF to yield aldehyde **62** that was then reacted with hydroxylamine hydrochloride to obtain oxime **63**. This was reduced by zinc and acetic acid in methanol, to afford the desired aminomethyl imidazole **60** in 46% yield for overall. This compound and 2-aminopyridine were used to prepare compounds **52-59** via an acid chloride route or via reaction of the appropriate amine with a methyl ester in the presence of trimethylaluminum[124] (Scheme 3.2).

3,4-Diphenyl-1H-pyrrole-2,5-dicarboxylic acid **50** was prepared by literature methods[97], and was converted to the acid chloride by heating at reflux in thionyl chloride overnight. After removal of the thionyl chloride, the remaining acid chloride was dissolved in dichloromethane and added to the dichloromethane solution of **60** (2 equiv.) to obtain compound **52**, and to a dichloromethane solution of 2-aminopyridine (2 equiv.) to obtain compound **54**, in the presence 2.5 and 2.3 equivalents of triethylamine respectively, and 5 milligrams of DMAP. These products were crystallised from acetonitrile solution in 40 and 21% yield respectively.

5-Methyl-3,4-diphenyl-1H-pyrrole-2-carboxylic acid ethyl ester **64** was synthesized by literature methods.[125] This compound was added to the dichloromethane solution of compounds **60** (2 equiv.) and trimethylaluminium (5 equiv.) to afford compound **53** after heating at reflux for seven days in 27% yield. Compound **64** was also used to prepare compound **55** by adding **64** to the dichloromethane solution of 2-amino pyridine (10 equiv.) and trimethylaluminium (7 equiv.). Heating the reaction at reflux for five days afforded compound **55** in 13% yield.

Isophthaloyl chloride and 2,6-pyridinedicarbonyl dichloride were used to synthesise **56** and **57** respectively. These acid chlorides in dichloromethane were added directly with 2.5 equivalents of **60** in the presence of 2.5 equivalents of triethylamine and 5 milligrams of DMAP and the reaction mixtures were stirred for 24 hours to afford **56** and **57** in 87 and 76% yield respectively.

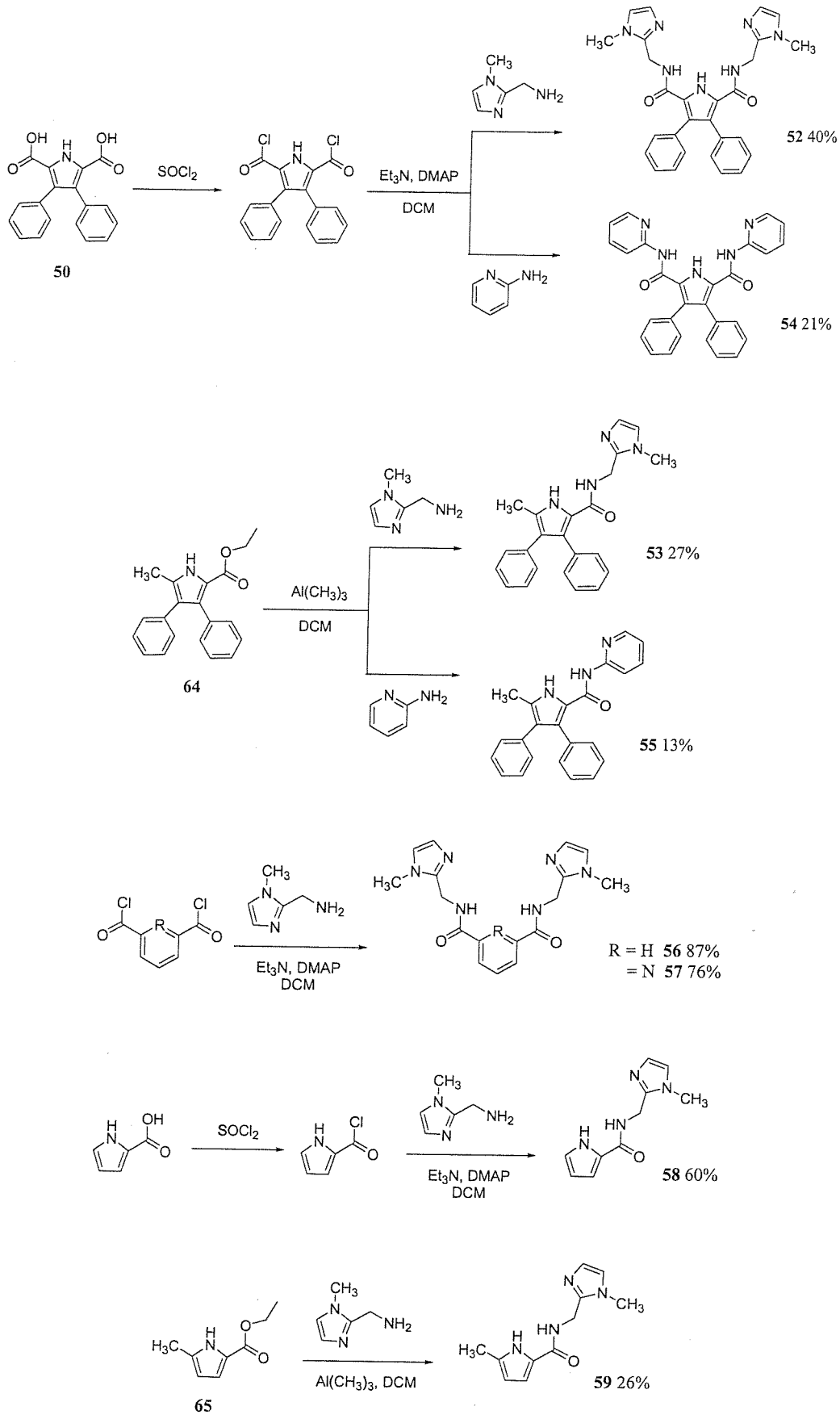

Scheme 3.2: Syntheses of compounds **52-59**.

Pyrrole-2-carboxylic acid was also converted to the acid chloride by heating at reflux in excess of thionyl chloride overnight. After removal the excess thionyl chloride, the remaining acid chloride was dissolved in dichloromethane and added to the dichloromethane solution of **60** (1.5 equiv.) in the presence of 3 equivalents of triethylamine and 5 milligrams of DMAP affording compound **58** after stirred for 72 hours in 60% yield.

5-Methyl-1H-pyrrole-2-carboxylic acid ethyl ester **65** was synthesized by literature methods.[125] This compound was added to the dichloromethane solution of **60** (2 equiv.) and trimethylaluminium (4 equiv.) and heated at reflux for 5 days to afford the last prodigiosin mimics **59** in 26% yield.

Crystals of **52** were obtained by slow evaporation of a concentrated solution of the compound in methanol. Crystallographic analysis revealed that in the solid state the receptor formed a sheet (Figure 3.5) via the two different types of hydrogen bonds, NH···N and NH···O. The N3···N2 and N5···N6 distances were found to be 2.871(3) and 2.975(3) Å respectively, whereas the N4···O1 distance was found to be 2.939(3) Å. The dihedral angles formed between the phenyl rings attached at the 3- and 4- positions and the pyrrole plane are 57.99° and 74.64°. The amide moieties deviate from the pyrrole plane by 6.40° and 16.18° with the amide NH groups pointing backwards with the respect of the pyrrole NH group (see Appendix for structure information).

X-ray quality single crystals of **53** were obtained by slow evaporation of a concentrated dichloromethane/methanol solution of the compound. The crystal structure revealed the presence of molecular tape in the solid state. In fact the molecules of the receptor were bound together via the formation of four hydrogen bonds, which were two hydrogen bonds between pyrrolic NH and the carbonyl group and the other two hydrogen bonds between amide NH and N-imidazole (Figure 3.6). In this molecular tape, the distances between N1···O1 and N2···N3 were found to be 2.8351(14) Å and 2.8837(15) Å respectively (see Appendix for structure information).

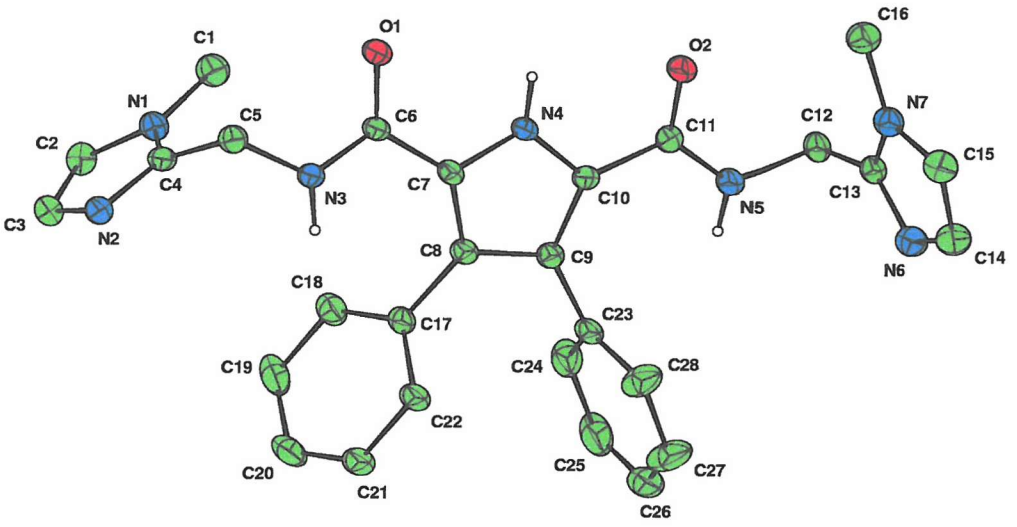

(a)

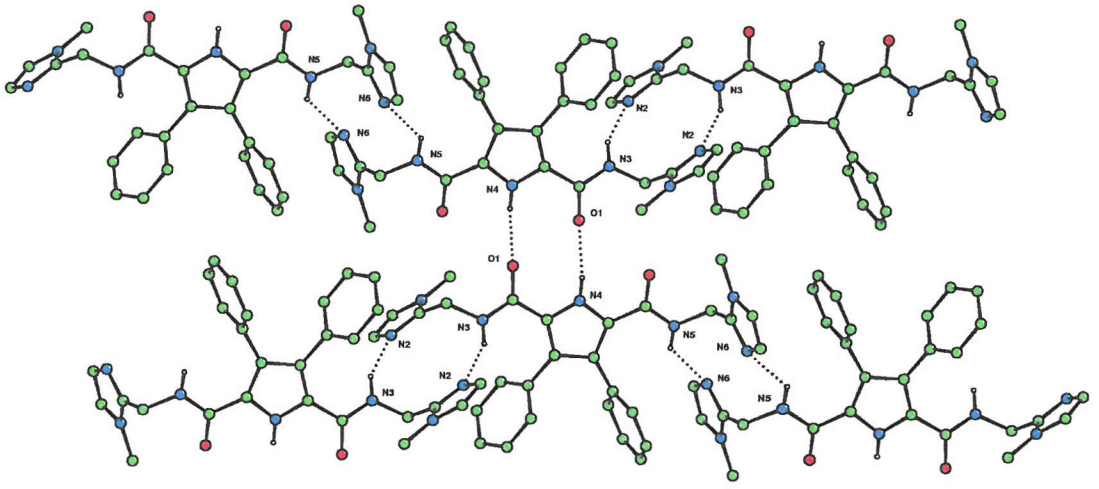

(b)

Figure 3.5: (a) The X-ray crystal structure of **52** (thermal ellipsoids drawn at the 35% probability level). (b) Sheets extending in the (1-10) plane via the formation of two hydrogen bonds ($N_{pyrrole}\cdots O$ = 2.939(3) Å, average $N_{pyrrole}\cdots N_{imidazole}$ = 2.923(3) Å). Certain hydrogen atoms are omitted for clarity.

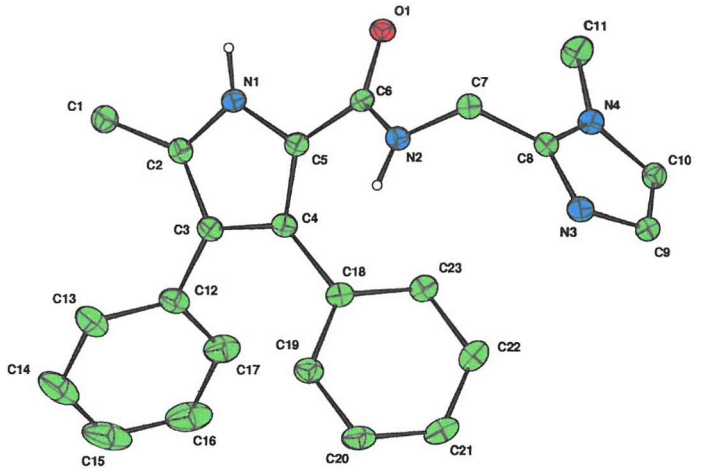

(a)

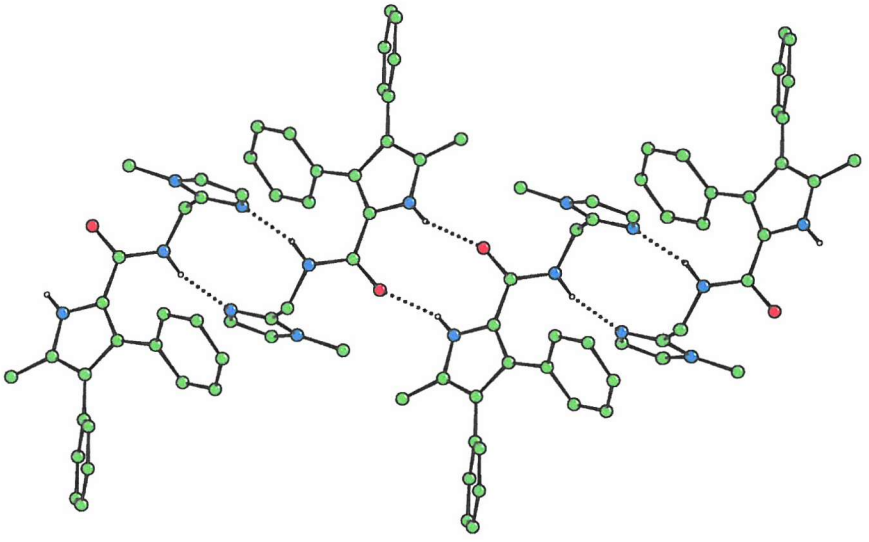

(b)

Figure 3.6: (a) The X-ray crystal structure of **53** (thermal ellipsoids drawn at the 30% probability level). (b) The structure reveals the presence of a molecular tape in the solid state. Molecules of the receptor are bound via the formation of four hydrogen bonds between the pyrrolic NH and the carbonyl group ($N_{pyrrole}\cdots O$ = 2.8351(14) Å and $N_{amide}\cdots N_{imidazole}$ = 2.8837(15) Å). Certain hydrogen atoms are omitted for clarity.

Single crystals of **54** were obtained by slow evaporation from concentrated solution of the compound in a dichloromethane/acetonitrile mixture. The X-ray crystal structure revealed the formation of dimers (Figure 3.7). The dimers were formed via two CH···N hydrogen bonds at the pyridine rings of each compound and

the distance between the N pyridine and the C pyridine is 3.493(6) Å. The phenyl rings in the 3- and 4- position deviate from the pyrrole plane by 106.22° and 114.54°. The dihedral angles formed between the amide CONH moieties and the pyrrole ring are –6.76° and –13.63°, and again the amide NH groups point backwards with respect to the pyrrole NH (see Appendix for structure information).

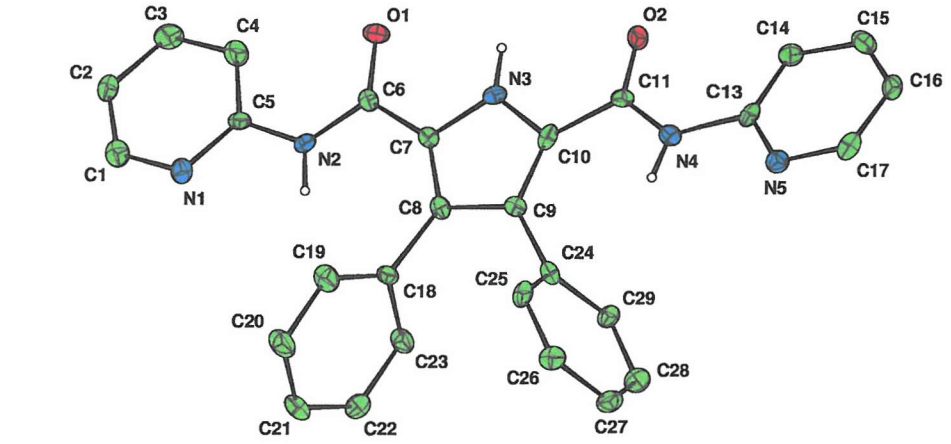

(a)

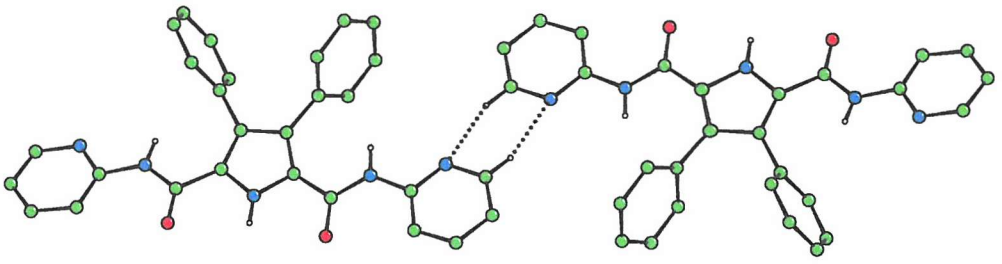

(b)

Figure 3.7: (a) The X-ray crystal structure of **54** (thermal ellipsoids drawn at the 50% probability level). (b) The dimerization of two hydrogen bonds between N-pyridine and CH-pyridine ($C_{pyridine}$···$N_{pyridine}$ = 3.493(6) Å). Certain hydrogen atoms are omitted for clarity.

X-ray quality single crystals of **58** and **59** were obtained by slow evaporation from concentrated solutions of the compounds in dichloromethane/methanol and methanol respectively. The crystal structures of **58** and **59** (Figure 3.8) revealed the presence of molecular tapes in the solid state.

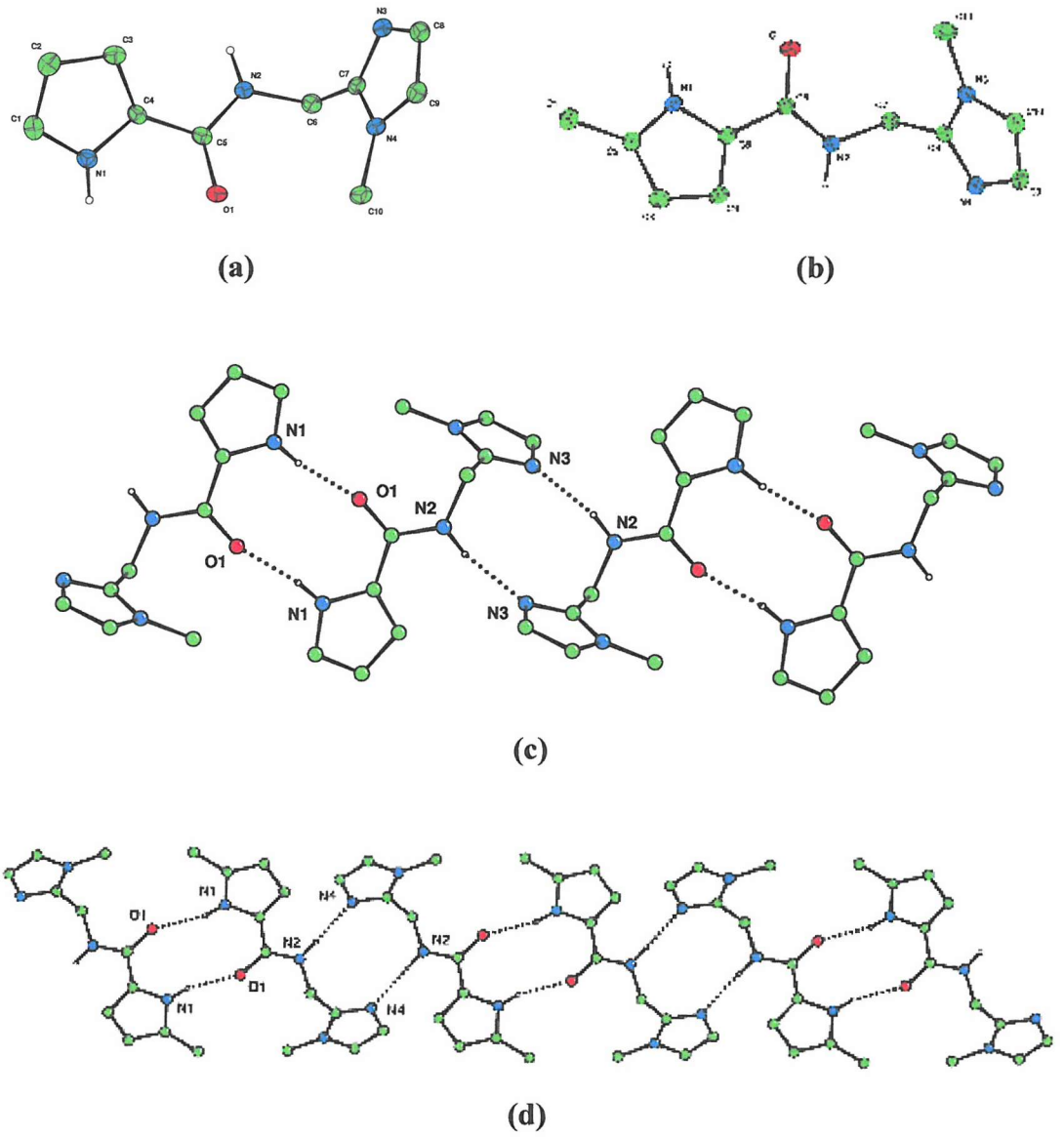

Figure 3.8: The X-ray crystal structures of (a) **58** (thermal ellipsoids drawn at the 35% probability level). (b) **59** (Thermal ellipsoids drawn at the 35% probability level). (c) Part of one of the hydrogen bonded chains running in the [101] direction of **58** (N1···O1 = 2.8175(19) Å and N2···N3 = 2.929(2) Å). (d) **59** (N1···O1 = 2.8204(19) Å and N2···N4 = 2.957(2) Å) . Non-interacting hydrogens have been omitted for clarity.

In each system, molecules of the compounds were linked together via the formation of two hydrogen bonds between pyrrolic NH and the carbonyl group and other two hydrogen bonds between amide NH and N-imidazole (Figure 3.8c and d). With compound **58**, the distances between N1···O1 and N2···N3 were found to be

2.8175(19) Å and 2.929(2) Å respectively. Very similar, in crystals of **59** the distances between N1···O1 and N2···N4 were 2.8204(19) Å and 2.957(2) Å respectively (see Appendix for structure information).

3.3 Coordination studies

3.3.1 NMR titration binding studies

The anion binding properties of the prodigiosin mimics **52-59** were investigated using ^{1}H NMR titration techniques with the EQNMR computer program used to the stability constants of the complexes. Anions were added as their tetrabutylammonium salts. The anion binding experiments were conducted in DCM-d_2 for compounds **52**, **53**, **54**, **55**, **58** and **59** and in DMSO-d_6-0.5% water for compounds **56**, **57** (due to the solubility problems). The results are shown in Table 3.1.

Compounds	Anions[a] and K_a/M^{-1} (Error)[b]					
	Fluoride	Chloride	Bromide	Benzoate	Dihydrogen phosphate	Hydrogen sulfate
52[c]	1,874 (138)	< 10	< 10	369 (11)	74,516 (822)	2,136 (266)
53[c]	558 (46)	< 10	< 10	97 (7)	209 (21)	764 (117)
54[c]	554 (83)	< 10	[e]	72 (11)	[f]	36 (2)
55[c]	290 (13)	< 10	[e]	13 (1)	458 (88)	122 (25)
56[d]	46 (6)	< 10	[e]	< 10	1,995 (241)	229 (26)
57[d]	46 (3)	< 10	[e]	< 10	308 (42)	< 10
58[c]	1,136 (165)	82 (2)	< 10	582 (7)	2,045 (215)	1,132 (146)
59[c]	354 (57)	112 (10)	< 10	611 (24)	370 (28)	891 (40)

[a]Anions added as tetrabutylammonium salts. [b]Error < 15%. [c]In DCM-d_2. [d]In DMSO-d_6-0.5%water. [e]No binding observed. [f]Could not follow the peaks.

Table 3.1: Association constants of receptors **52-59** with various anionic guest species at 25°C.

Stability constants were elucidated by the EQNMR computer program, which fitted the binding data to a 1:1 receptor:anion binding model. The results showed that the imidazole derivatives **52** and **53** bind oxo-anions as benzoate, dihydrogen phosphate and hydrogen sulfate also fluoride more strongly than their pyridine analogues **54** and **55**. However **55** bound dihydrogen phosphate, more strongly than compound **53**. This is presumably due to the higher basicity of the imidazole moieties as compared to the pyridine groups. Protic anions as dihydrogen phosphate and hydrogen sulfate ions bound to the bis-imidazole **52** particularly strongly, for example binding dihydrogen phosphate with an association constant 74,516 M^{-1} in dichloromethane-d_2 (possibly due a proton transfer occurring as was observed in the pendant amine systems described in chapter 2). Interestingly with compound **54** the NH amide resonance broadens and then disappears during the titration of this receptor and dihydrogen phosphate.

Bis-imidazole derivatives **56** and **57** (phenyl and pyridine as the central groups respectively) were found to only weakly bind the majority of the anions in the binding experiments in DMSO-d_6-0.5% water. Only compound **56** bound dihydrogen phosphate with moderate affinity with an association constant 1,995 M^{-1}.

The binding results showed **56** forms stronger complexes with anions than **57**. In this case, the central group played an important role for the anion guests binding. The pyridine derivative receptor **57** contains a lone pair on the central nitrogen in the pyridine head group, which might reduce the affinity for anions.

To study the chloride binding properties of these compounds when neutral and when protonated at the imidazole or pyridine groups, the chloride binding properties of the prodigiosin mimics, **52**, **53**, **54**, **55**, **58** and **59**, and their protonated hexafluorophosphate salts were studied using ^{1}H titration techniques in acetonitrile-d_3 which is more polar solvent than dichloromethane-d_2. However, compounds **56** and **57** were not used in these experiments because the preliminary chloride transport studies (see below) indicated that they do not function as H^+/Cl^- symport agents.

Protonated hexafluorophosphate compounds were prepared by dissolving the compound in methanol and adding 2 equivalents of hexafluorophospholic acid for **52** and **54**, and 1 equivalent for **53**, **55**, **58** and **59**. Tetrabutylammonium chloride was again used as the source of the chloride ion. The results of these studies are shown in Table 3.2. The NH amide chemical shifts in ppm were evaluated and the association constants elucidated using the EQNMR program. It was found again that the chloride complexes were all of 1:1 anion:receptor stoichiometry.

Compounds	K_a/M^{-1} (Error)[a]	Compounds	K_a/M^{-1} (Error)[a]
52	[b]	**52.2HPF$_6$**	649 (75)
53	60 (1)	**53.HPF$_6$**	397 (56)
54	[b]	**54.2HPF$_6$**	[b]
55	< 10	**55.HPF$_6$**	< 10
58	119 (6)	**58.HPF$_6$**	[c]
59	117 (9)	**59.HPF$_6$**	[c]

[a]Error <15%. [b]Precipitated. [c]Not soluble.

Table 3.2: Association constant of receptors **52**, **53**, **54**, **55**, **58** and **59** and their protonated hexafluorophosphate salts with tetrabutylammonium chloride in acetronitrile-d_3 at 25°C.

From the results, receptors **58** and **59** showed the highest association constants with chloride ion in acetonitrile-d_3, 119 and 117 M^{-1} respectively. However, when they were protonated as hexafluorophosphate salts, they were not

soluble in acetonitrile-d_3 solution. Compound **52** precipitated during the titration but **52.2HPF$_6$** was studied and gave the highest association constant (649 M^{-1}) in acetonitrile-d_3. The pyridine substituted compounds **54** and **55** were shown to be poor chloride receptors. Compounds **54** and **54.2HPF$_6$** precipitated during their titration, which means that its chloride complex was insoluble in acetonitrile-d_3. The receptor **55** and **55.HPF$_6$** has a low binding constant at less than 10 M^{-1} which suggested this compound was the poor chloride receptor even when it was protonated.

The most interesting of these results came from receptor **53**. This receptor showed a weak ability to bind the chloride ion, with an association constant of 60 M^{-1} in acetonitrile-d_3 but the association constant of its hexafluorophosphate salt is more than 5 times higher than the neutral compound, at 397 M^{-1} (Figure 3.9). This compound was therefore expected to be the most suitable HCl symport agent of this series because the protonated form enhanced its binding ability with this ion and there was not a solubility problem.

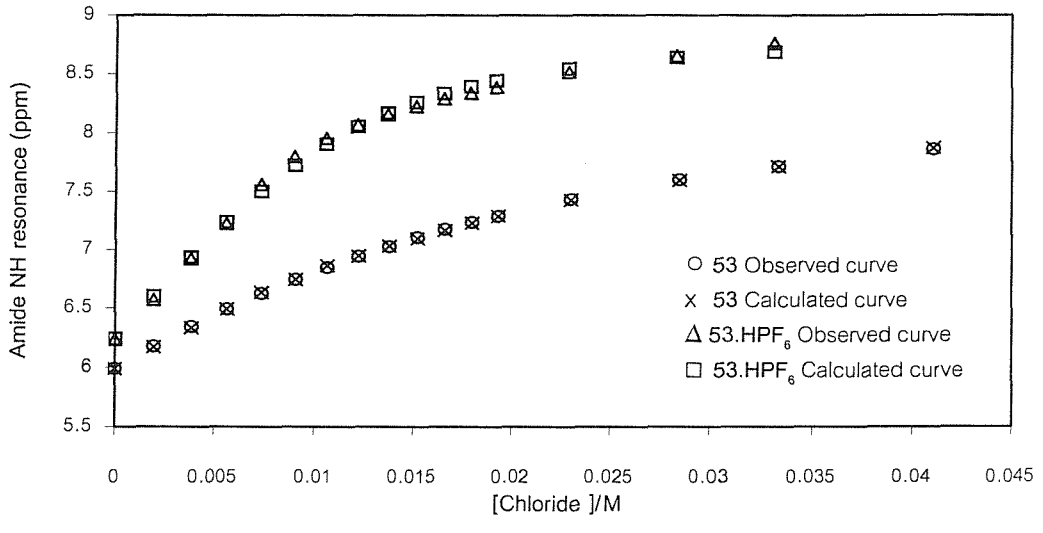

Figure 3.9: ^{1}H NMR titration curves of compounds **53** (K_a = 60 M^{-1}, error < 2%) and **53.HPF$_6$** (K_a = 397 M^{-1}, error < 15%) with tetrabutylammonium chloride in acetronitrile-d_3 at 25°C.

3.3.2 Solid-state studies

Attempts were made to crystallise all the compounds with HCl. X-ray single crystal spectroscopy techniques were used to elucidate the structures of the crystals obtained.

Crystals of **52**.HCl were obtained by slow evaporation from a concentrated solution of the receptor in dichloromethane/methanol and concentrated HCl. The receptor was protonated on one imidazole and adopts a 'semi-cleft' conformation binding a chloride ion via the formation of three hydrogen bonds between the chloride ion and pyrrolic NH ($N_{pyrrole}\cdots Cl^-$ = 3.264(7) Å), one of the amide NH group ($N_{amide}\cdots Cl^-$ = 3.108(6) Å) and one NH^+ imidazole group via a water molecule ($N_{imidazole}\cdots O_{water}$ = 2.690(9) Å, $O_{water}\cdots Cl^-$ = 3.080(4) Å), Figure 3.10. The NH amide and the imidazole groups that point toward the chloride ion deviate from the pyrrole plane by 3.97° and 65.97° respectively. On the other hand, the other NH amide and non-protonated imidazole groups point backward with respect to the pyrrole NH and showed a deviation from the pyrrole plane of 2.03° and –58.99° respectively (see Appendix for structure information).

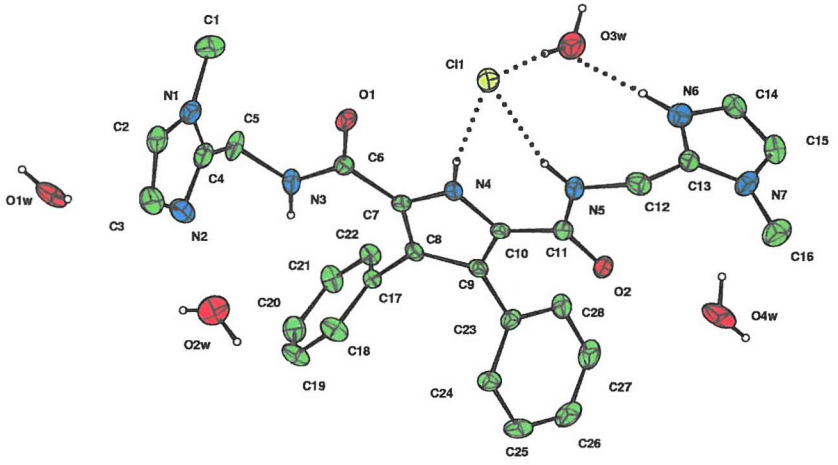

Figure 3.10: The X-ray crystal structures of the **52**+H^+/Cl^- and H_2O complex (thermal ellipsoids drawn at the 35% probability level). The receptor adopts a 'semicleft like' conformation ($N_{pyrrole}\cdots Cl^-$ = 3.264(7) Å, $N_{amide}\cdots Cl^-$ = 3.108(6) Å, $N_{imidazole}\cdots O_{water}$ = 2.690(9) Å and $O_{water}\cdots Cl^-$ = 3.080(4) Å). The certain hydrogen atoms are omitted for clarity.

This complex forms a network (Figure 3.11), which is linked together via the hydrogen bond between the one carbonyl group and water molecules.

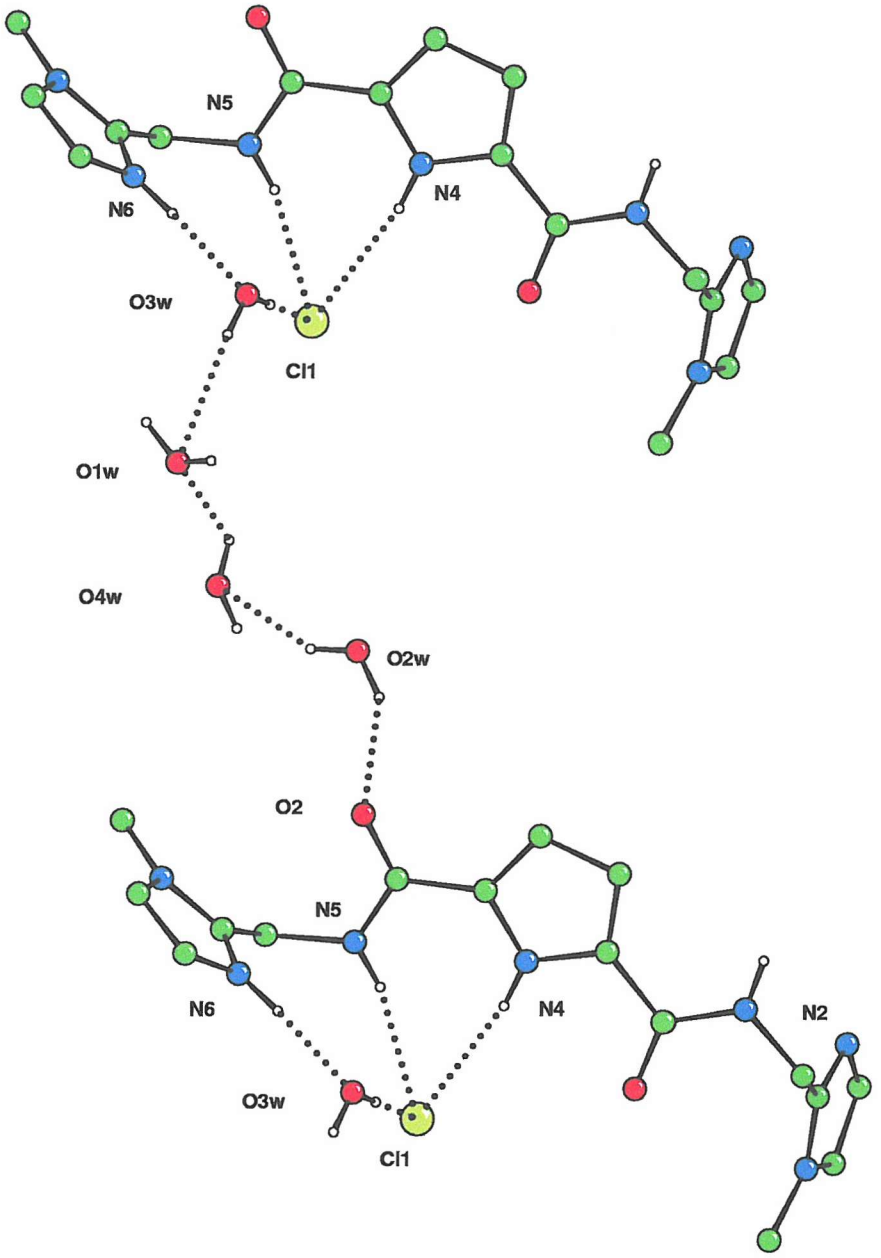

Figure 3.11: Part of the hydrogen bonded chains of the **52**+H^+/Cl^- and H_2O complex that run in the [110] direction (O2W···O2 = 2.817(7) Å, O2W···O4W = 2.831 (11) Å, O4W···O1W = 2.286 Å and O3W···O1W = 3.057(6) Å and O1W···N2 = 3.415 Å). Phenyl groups and non-interacting hydrogen atoms have been omitted for clarity

The H^+/Cl^- complex crystals of **53** were obtained by slow evaporation from concentrated mixed dichloromethane/methanol solution of the compounds and concentrated HCl. The crystal structure of the complex (Figure 3.12) showed this compound also was protonated at the N-imidazole group and this group binds directly to chloride. This chloride was bound to the pyrrole and amide NH of an adjacent molecule resulting in the formation of a 2+2 complex. Each chloride ion was bound to a pyrrolic NH ($N_{pyrrole}\cdots Cl^-$ = 3.24(2) Å), the amide NH ($N_{amide}\cdots Cl^-$ = 3.29(2) Å) and NH^+ imidazole group from other compound ($N_{imidazole}\cdots Cl^-$ = 3.10(2) Å). The NH amide and the NH^+ imidazole groups that point toward the chloride ion showed a deviation from the pyrrole plane of 8.20° and –119.07° respectively (see Appendix for structure information).

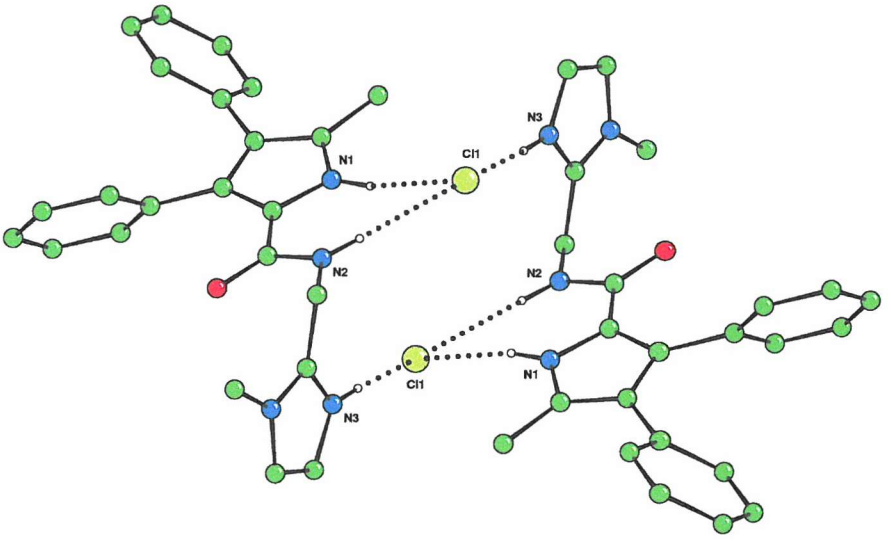

Figure 3.12: Crystal structure of H^+/Cl^- complex of **53** displaying three different hydrogen bonds between the chloride ions and pyrrolic NH ($N_{pyrrole}\cdots Cl^-$ = 3.24(2) Å), the amide NH ($N_{amide}\cdots Cl^-$ = 3.29(2) Å) and NH^+ imidazole group ($N_{imidazole}\cdots Cl^-$ = 3.10(2) Å). Non-interacting hydrogens have been omitted for clarity.

Crystals of **55** and H^+/Cl^- complex were obtained by slow evaporation from concentrated solution of the compound in dichloromethane/methanol and concentrated HCl. The crystal structure (Figure 3.13) revealed the H^+/Cl^- complex of **55** which the compound was protonated at the pyridine nitrogen. Although there are three available binding sites in this molecule, the compound used only pyrrolic

and amido protons to bind a chloride ion with distances N1···Cl1 = 3.113(5) Å and N2···Cl1 = 3.152(5) Å respectively. The pyridinium group is oriented in a reverse direction binding a chloride in an adjacent complex (N3···Cl1 = 3.164(5) Å). This may allow intramolecular hydrogen bonds between the pyridinium NH and the adjacent carbonyl group (N3···O1 = 2.645(6) Å). The pyridine ring was almost co-planar with the pyrrole ring showing a deviation of 7.90° (see Appendix for structure information).

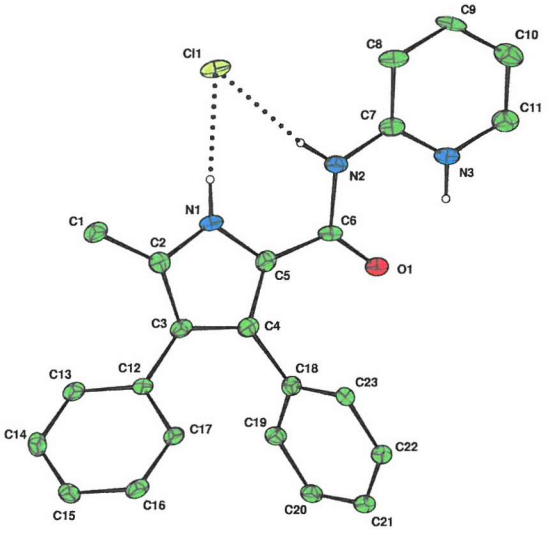

(a)

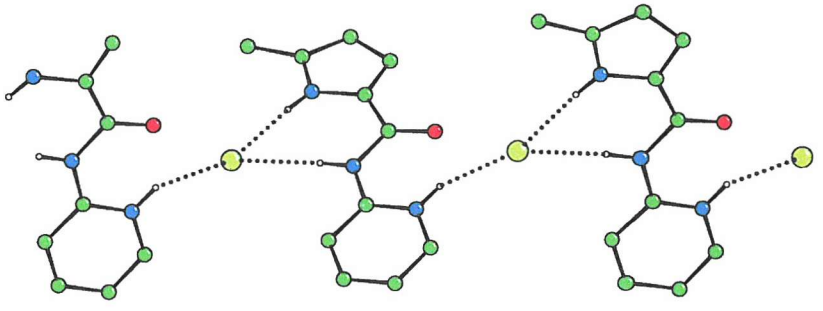

(b)

Figure 3.13: Crystal structures of (a) **55**+H^+/Cl^- complex (N1···Cl1 = 3.113(5) Å and N2···Cl1 = 3.152(5) Å) (thermal ellipsoids drawn at the 50% probability level). (b) Network showing the formation of the oligomers *via* inter hydrogen bonds with Cl^- (N3···Cl1 = 3.164(5) Å and N3···O1 = 2.645(6) Å). Phenyl groups and non-interacting hydrogen atoms have been omitted for clarity.

Crystals of **58** with H^+/Cl^- were also obtained by slow evaporation from concentrated solution of the compound in dichloromethane/methanol and concentrated HCl. Two chloride ions were located, bound in the middle between two receptors via the formation of three and four hydrogen bonds between the amide moieties (N2···Cl1 = 3.224(2) Å and N6···Cl1 = 3.210(2) Å), NH^+ imidazole (N3···Cl2 = 3.091(2) Å) and water molecules (O3···Cl1 = 3.105(2) Å, O4···Cl1 = 3.138(2) Å, O3···Cl2 = 3.099(2) Å and O4···Cl2 = 3.089(2) Å), Figure 3.14 (see Appendix for structure information).

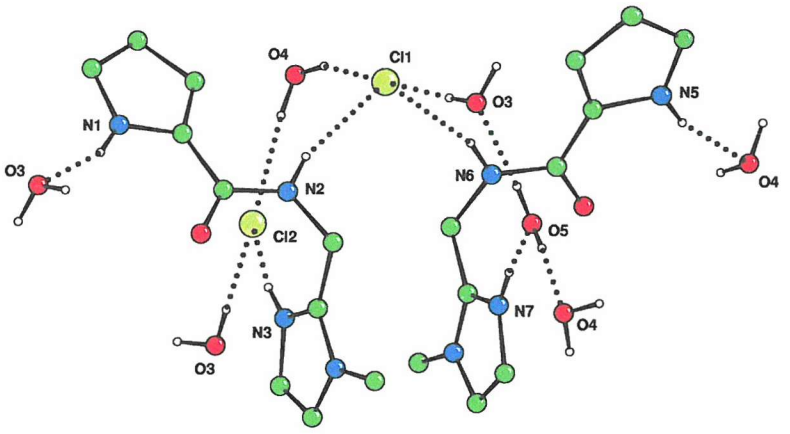

Figure 3.14: Crystal structure of the complex **58**+H^+/Cl^- shows all the unique hydrogen bonds that form a 3D network (N2···Cl1 = 3.224(2) Å, N6···Cl1 = 3.210(2) Å, N3···Cl2 = 3.091(2) Å, O3···Cl1 = 3.105(2) Å, O4···Cl1 = 3.138(2) Å, O3···Cl2 = 3.099(2) Å and O4···Cl2 = 3.089(2) Å). Non-interacting hydrogen atoms have been omitted for clarity.

X-ray quality single crystals of **52** with H_2SO_4 were isolated. These crystals were formed by slow evaporation from a concentrated solution of the compound in methanol and concentrated H_2SO_4. The crystal structure (Figure 3.15) revealed the formation of a 1:1 sulfate:receptor complex that the compound **52** was again protonated at both N-imidazoles. The sulfate ion was bound with the compounds via six hydrogen bonds. Three of them occurred between the sulfate ion and two NH^+-imidazoles (N2···O4 = 2.69(16) Å, N6···O3 = 2.7(2) Å and N6···O5 = 3.1(2) Å). Two of them formed between the sulfate ion and two NH-amide groups (N3···O3 = 2.89(16) Å and N5···O6 = 2.77(16) Å) and the last hydrogen bond formed between

the sulfate ion and the NH pyrrole ring (N4···O3 = 2.77(15) Å) (see Appendix for structure information).

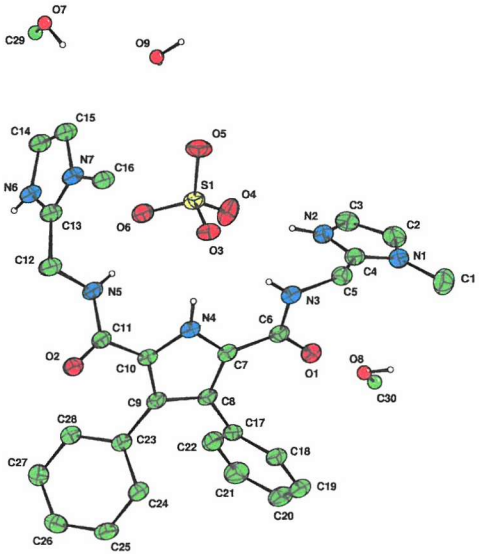

(a)

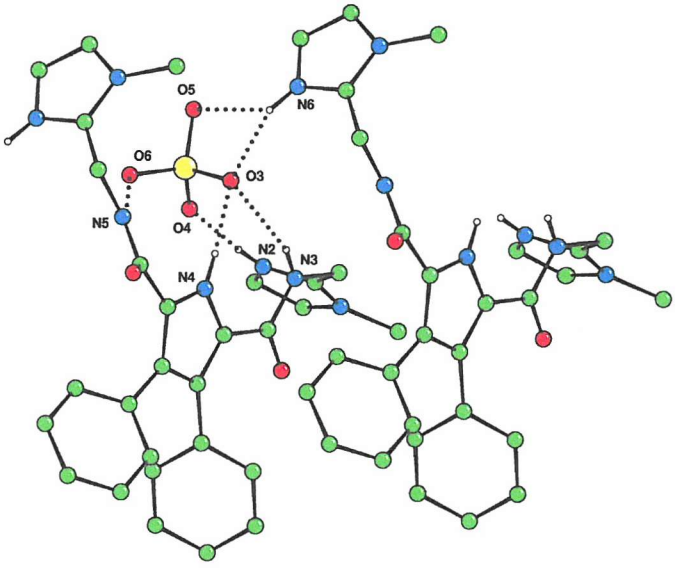

(b)

Figure 3.15: Crystal structure of **52**+2H$^+$/SO_4^{2-} complex (a) The complex (thermal ellipsoids drawn at the 50% probability level). (b) Displays all the unique hydrogen bonds that form a 3D network (N2···O4 = 2.69(16) Å, N6···O3 = 2.7(2) Å, N6···O5 = 3.1(2) Å, N6···S1 = 3.50(18) Å, N3···O3 = 2.89(16) Å, N5···O6 = 2.77(16) Å, and N5···S1 = 3.72(13) Å). Non-interacting hydrogen atoms have been omitted for clarity.

3.3.3 H^+/Cl^- symport studies

Professor Bradley D. Smith and graduate student Beth McNally conducted the membrane symport studies on these compounds at the University of Notre Dame, Indiana. Specifically, compounds **52-57** were studied for their ability to release Cl^- from artificial unilamellar vesicles in three different pH environments, pH = 4 in and out, pH = 7.2 in and out and pH = 4 in and pH = 7.2.

The vesicles were designed to mimic the biological cell membrane. These unilamellar vesicles were 200 nm mean diameter composed of 1-palmitoyl-2-oleoyl-*sn*-glycerol-3-phosphocholine (POPC) and cholesterol (70:30 POPC:cholesterol) as the vesicles membrane. The solutions inside the vesicles were 500 mM NaCl, 5 mM citric acid at pH 4 used in pH 4 and pH gradient chloride transport assay or 500 mM NaCl, 5 mM citric acid at pH 7.2 which used in pH 7.2 chloride transport assay. In the chloride transport experiments, the external solutions were 500 mM $NaNO_3$, 5 mM citric acid, pH 4 solution for pH 4 chloride transport experiments, 500 mM $NaNO_3$, 5 mM citric acid, pH 7.2 solution for pH 7.2 chloride transport experiments and 500 mM $NaNO_3$, 5 mM Na_2HPO_4, pH 7.2 solution for pH gradient chloride transport experiments. Solutions of the prodigiosin mimics were added after the vesicles were dispersed in the outside solution. The chloride levels outside the vesicles were monitored by a chloride selective electrode for 20 minutes (Figure 3.16) and the vesicles lysed with detergent at the end of the experiment (see Appendix 3 for the chloride transport assay information).

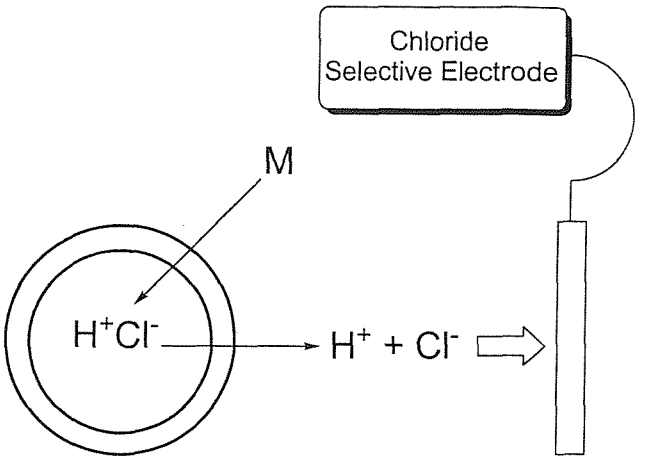

Figure 3.16: Model of the chloride transport experiments (M = prodigiosin mimics).

The results show that the best conditions to surround the unilamellar vesicles are a pH 4 inside and pH 7.2 outside; such conditions best facilitate the transport of chloride ions across the membrane. Having pH 7.2 inside and outside the unilamellar vesicles was a better environment than pH 4 inside for compounds **52** and **53**. However, there was not any significant difference between the chloride transport results with **54-57** with the two different external pH environments. The fast release of chloride (with **52** and **53**) was found when there was a pH gradient across the membrane suggesting that the proton is involved in the transport of chloride.

Compound **53** is the most effective chloride transport agent from this prodigiosin mimic series. Compounds **55**, **56** and **57** are essentially ineffective chloride transport agents. These results suggest that the basicity of the protonatable group is important for successful chloride transport; thus the imidazole-pyrrole compounds which are more basic show effective chloride transport whilst the pyridine-pyrrole systems show much less efficient transport properties.

Compounds **52**, **53**, and **54** consistently showed an increased percent chloride efflux with the pH gradient compared to the other two assays. In addition, the nature of the anion in the solution outside the vesicles was found to influence the rate of chloride transport suggesting that an anti-port process was also occurring.

A pH sensitive assay was employed to study proton transport across the vesicle membranes. Compounds **52**, **53** and **55** were studied in unilamellar vesicles composed of POPC/cholesterol (70/30 POPC:cholesterol) that were prepared as

above except that the solution inside contained varied concentrations of Oregon Green® 514 carboxylic acid[126,127] (Oregon Green) solutions (see Appendix 3 for the pH sensitive assay information). This compound's fluorescence is sensitive to pH (Figure 3.20).[128] Therefore this dye may be used to monitor the change of pH inside the vesicles during the chloride transport. The situation in which vesicle solutions were pH 4 inside and pH 7.2 outside were the optimum conditions for a chloride transport assay.

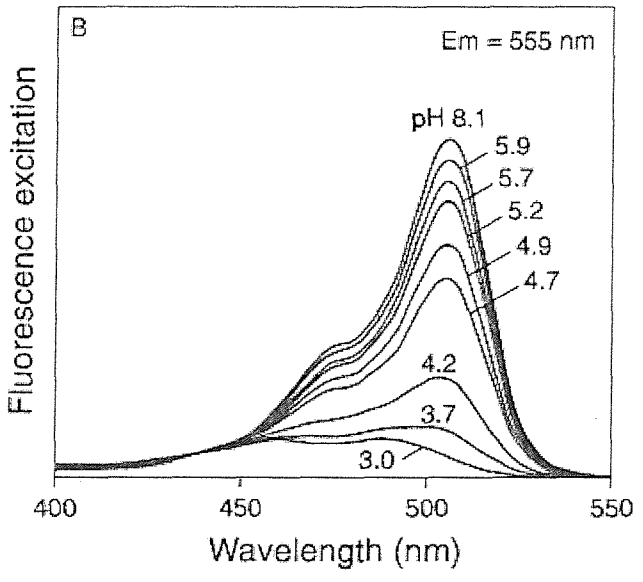

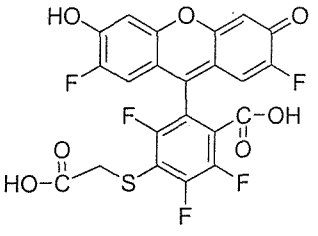

Oregon Green® 514 carboxylic acid

Figure 3.17: Fluorescence excitation at 510 nm (Em = 555 nm) of Oregon Green® 514 carboxylic acid in difference pH environments.

The Perkin Elmer luminescence spectrometer was used to measure the emission of Oregon Green at 555 nm with an excitation of 510 nm. The intensity baseline was established for 200 seconds whereupon the prodigiosin mimic was added into the experimental cell. Intensity was measured until 500 or 1000 seconds depending on the Oregon Green concentration inside solution, whereupon the vesicles were lysed with detergent (see Appendix for the pH sensitive assay information).

These studies show that the imidazole-containing receptors trigger an immediate release of protons from the vesicles, whilst the pyridine-containing compound does not significantly affect the rate of release of protons as compared to

the background release rate. Thus it is reasonable to conclude that compounds **52** and **53** are symporting both protons and chloride anions through the membranes presumably because of their basicity allowing protonation and deprotonation in the pH gradient range studied.

3.4 Conclusion

Compounds **52** and **53** show promise as synthetic HCl symport agents. Studies in vesicles have shown that these compounds are capable of symporting HCl across lipid bilayers. The behaviour of the compounds in cells is now being studied to evaluate their use as potential anti-cancer agents.

4 *Combinatorial approaches to peptide receptors containing amidopyrrole*

4.1 Introduction

The development of efficient synthetic receptors for short peptide chains or proteins is a challenging target for chemists.[129] Traditionally, individual receptors have been synthesised and their guest binding properties tested with the target guest. However, in the drug discovery and commercial research, there is a need for higher throughput techniques to generate many compounds which then may be quickly screened for a particular activity.[130] Combinatorial chemistry is one approach to solve this problem.

Much of combinatorial chemistry has focused on the creation of small molecules with pharmacological activity.[131-134] This kind of chemistry has also been developed to serve in variety of fields including host-guest (i.e. receptor-ligand) chemistry. This fusion of areas offers many advantages when compared with the typical strategy of the individual receptor synthesis, evaluation and iterative improvement. Combinatorial approaches may be used to synthesise a large library of receptors through parallel synthesis and all members are may be simultaneously evaluated for binding activity, minimizing synthetic expenditure and maximizing the possibilities of creating an effective receptor.[135]

The choice of the components from which the library is created is up to the chemist. The libraries can be designed to expand diversity of a compound collection for general screening.[136] These libraries are specifically built to be as large and diverse as possible with broad screening as their main objective. Libraries can also

be prepared to find a lead for a specific target. Typical design strategies of these libraries involve the use of privileged structure motifs or specific recognition elements that are suspected to be required for binding. Alternatively the choice of components may be made in order to improve on an existing lead.[137]

Combinatorial chemistry can be used to generate receptors in supramolecular chemistry. Much recent work in the area of peptide receptors has focused on 'tweezer' receptors, which were first used by Whitlock and coworkers[138] and Zimmerman et.al.[139] or higher order multi-armed receptors. The basic design of tweezer receptors incorporates a 'head group' or 'hinge' bearing two side arms that incorporate appropriate functionality for binding with the backbone of a suitable substrate (Figure 4.1 a). We have focused on tweezer receptors, which incorporate a 'head group' with a specific recognition site for the C-terminus of a peptide (carboxylate binding site, CBS), and peptidic side arms (Figure 4.1 b).

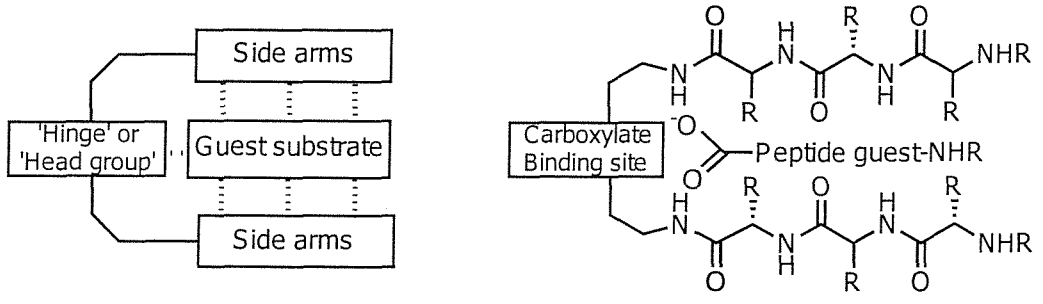

a) b)

Figure 4.1: a) Schematic of a tweezer receptor with 'hinge' or 'head group' and side arms, which provide binding interactions with a suitable guest substrate. b) Schematic of a tweezer receptor with a carboxylic acid binding site (CBS) as the 'head group'.

The combinatorial approach to these receptors proceeds by attachment of a suitably functionalised scaffold to a solid support, followed by library synthesis of the arms using a variety of monomer units and the 'split-and-mix' strategy[140,141] (Scheme 4.1). Each arm can be same sequence to give libraries of 'symmetrical' receptors, or they may be synthesized sequentially to give the more diverse libraries of 'unsymmetrical' receptors.[142]

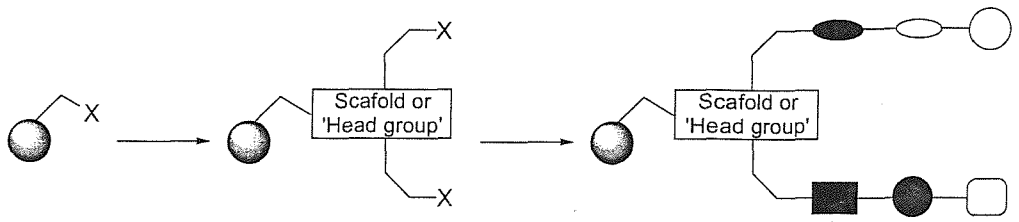

Scheme 4.1: Combinatorial approach to tweezer receptor synthesis

Tweezer receptors have been shown to have a high selectivity for certain peptide sequences in both non-polar and aqueous solvent systems. Recently, Wennemers and co-workers synthesised a series of symmetric two tripeptide side chain tweezers containing diketopiperazine head groups (Figure 4.2a).[143] These tweezer were elucidated their binding properties by screening with a library of peptide guests in chloroform. The *trans,trans* diketopiperazine scaffold was used to synthesised a tweezer receptors with a rigid 'U' shaped conformation(Figure 4.2b). They proved ideal in separating the two receptor arms and leading to highly selective receptors. However, the analogues structures which more linear scaffold *cis,cis* diketopiperazine (Figure 4.2c) were only moderately selective and structures derived from several other diamine scaffolds did not exhibit any binding at all.[144]

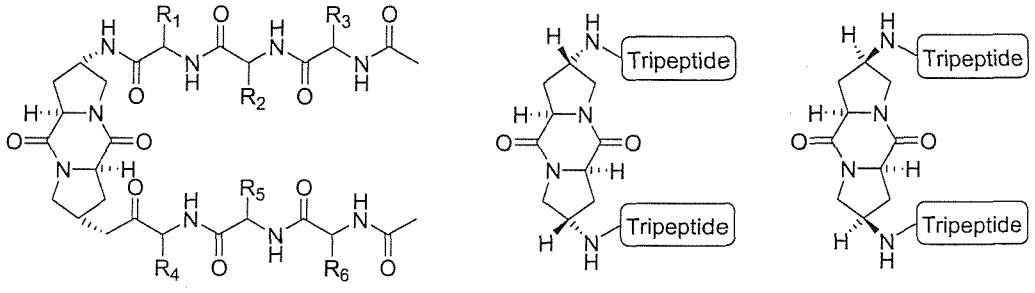

Figure 4.2: a) General structure of diketopiperazine receptors. b) *Trans,trans* structure. c) *Cis,cis* structure.

The receptor head-group can be modified to have an additional binding site for the guest target molecule. Dibenzofuran species were used as a head group to

synthesise the two peptide arms tweezer receptor **66** by LaBrenz and Kelly.[145] This receptor bound the peptidic guest **67** in water, using a combinatorial of hydrophobic and electrostatic interactions (Figure 4.3).

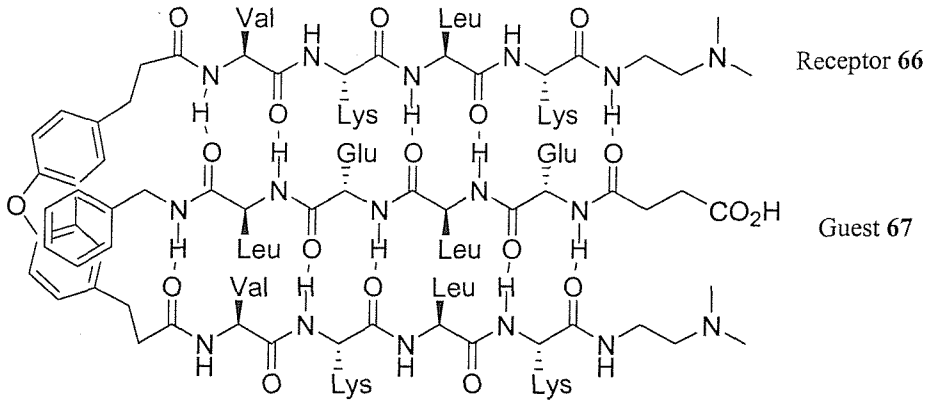

Figure 4.3: Complex of receptor **66** and guest **67**.

Incorporating a carboxylate binding site into a similar tweezer-like structure can lead to new receptors specifically for the carboxylate terminus of peptides. Kilburn and co-workers[146] used a guanidinium head group in a tweezer receptor with two peptide arms **68**.[147]

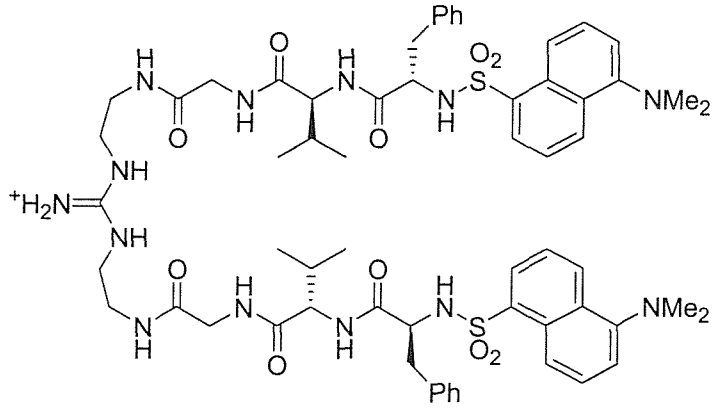

68

This receptor was used in a screening experiment in water with a 1000-member biased library of tripeptides, which attached to TentaGel resin via the amino terminus. The tweezer receptor was found to bind to ~3% of the guest library members and showed 95% selectivity for Val at the carboxy terminus of the

tripeptide and 40% selectivity for Glu(O^{t}Bu) at the amino terminus. The association constant with the selected tripeptide guest, Z-Glu(O^{t}Bu)-Ser(O^{t}Bu)-Val-OH, was determined by isothermal calorimetric technique (ITC) giving a value of K_{ass} = 4 x $10^5 \pm 5 \times 10^4$ M^{-1} in sodium borate buffer containing 16.7% DMSO at pH 9.2.

Recently, they have continued this work; however, by preparing a library of tweezer receptors. These receptors also incorporate with a guanidinium head group and two peptide derived side arms on the solid phase using an orthogonally protected guanidinium scaffold.[148] The library was screened with various tripeptide derivatives in an aqueous solvent system. A tweezer receptor **69** for the side chain protected tripeptide **70** was identified from these screening experiments having an association constant of K_{ass} = 8.2 x $10^4 \pm 2.5 \times 10^4$ M^{-1} in 15% DMSO/water system using UV-Vis titration techniques.

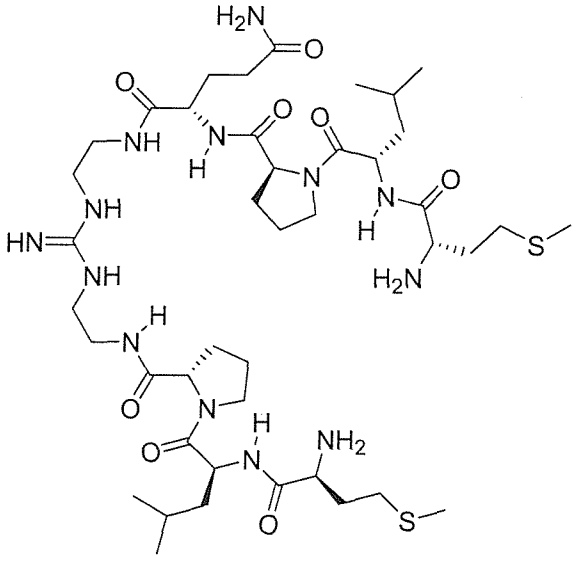

69

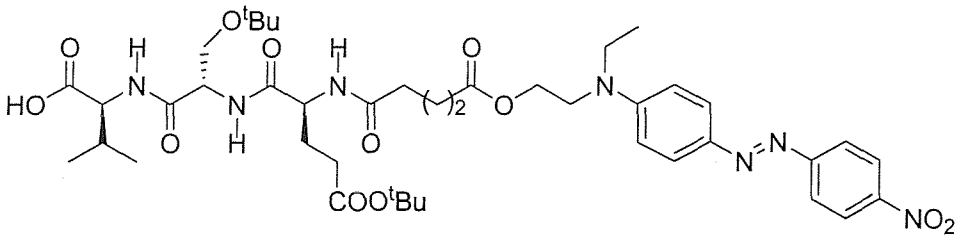

70

Schmuck and co-workers have developed receptors for carboxylate terminus peptides guests. They prepared the libraries of one-armed tripeptide based cationic

guanidiniocarbonyl pyrrole receptors using standard Fmoc couplings and the split-and-mix[149] approach in combination with radio frequency tagging technology (IRORI^{TM}).[150] Members of these libraries strongly bound the tetrapeptide L-Val-L-Ile-L-Ala which represents a model for the C-terminus of the amyloid β-peptide, in polar conditions such as in methanol ($K_{ass} \sim 10^4$)[151] and water ($K_{ass} > 4 \times 10^3$)[152] (Figure 4.4). This type of peptide is implicated in Alzheimer's disease[153-156] that is the formation of protein plaques within the brains of patients suffering from this disease.

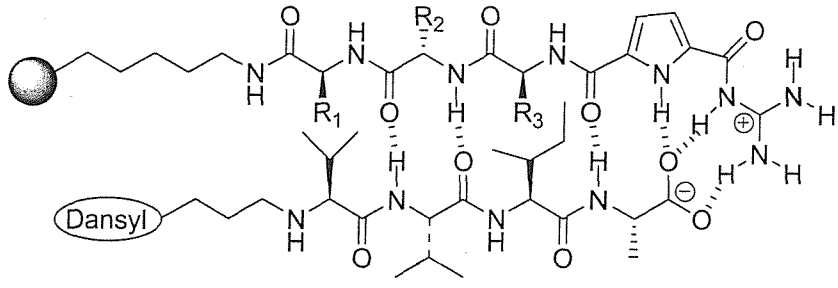

Figure 4.4: A tripeptide-based library of cationic guanidinocarbonyl pyrrole receptor bind with tetrapeptide L-Val-L-Ile-L-Ala.

HIV-1 protease (PR) is an enzyme produced from the human immunodeficiency virus (HIV). It causes acquired immune deficiency syndrome (AIDS).[157] In the active form, HIV-1 protease is a 22,000 Da homodimeric aspartic protease consisting of two 99-residue polypeptide chains that self-assemble to form an approximately 45 x 23 x 25 Å dimers. The active site is shaped at the interface of the two subunits (Figure 4.5 a), each contributing one catalytic aspartate residue.[158,159] The protease homodimer subunit is mainly stabilized by a four-stranded antiparallel β-sheet involving both the N- and C-termini of each monomer which are H-Pro-Gln-Ile-Thr and Cys-Thr-Leu-Asn-Phe-O, respectively (Figure 4.5 b). These monomers have been found to be highly conserved in HIV-1 isolates and some HIV-2 isolates.[160]

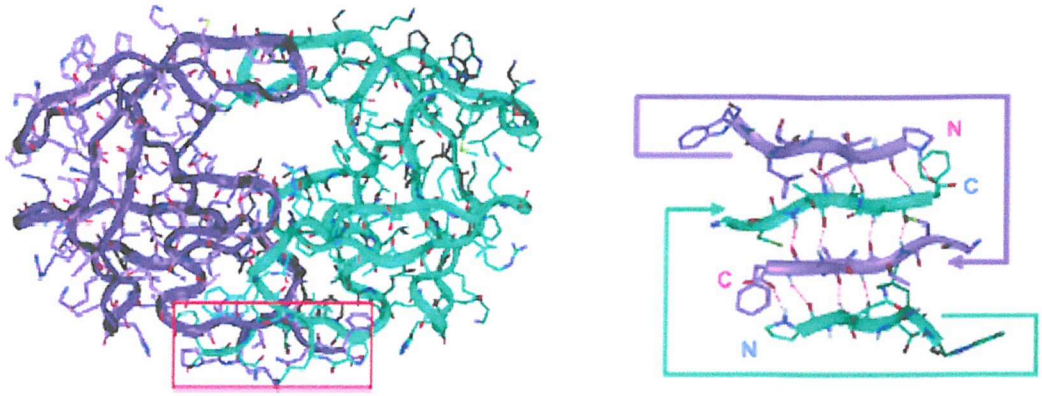

(a) **(b)**

Figure 4.5: (a) HIV-1 Protease dimers structure. The active sites are shown is the frame. (b) Antiparallel β-sheet involving both the N- and C-termini.

Since HIV-1 protease is a homodimer and most active site inhibitors used in AIDS therapy have led to resistance by rapid mutation of the virus,[161,162] preventing or disrupting the self-assembly of the monomers is one new possibility to stop or reduce its activity. Cross-linking of N- and C-terminal peptide to form a mimic of the HIV-1 protease dimerization interface has provided an alternative strategy for the development of more potent protease dimerization inhibitors.[163] The principle of this strategy is illustrated in Scheme 4.2.

Recently, Schramm, Reboud-Ravaux and co-workers[164,165] showed lipopeptides like palmitoyl-Tyr-Glu-Leu-OH and palmitoyl-Tyr-Glu-thyroxine have improved HIV-1 protease inhibitory properties. These are possibly due to the interaction of the palmitoyl residue with the hydrophobic dimerization interface of the protease. These receptors should have better bio-availability than simple peptides due to numbers of binding sites in their molecules.

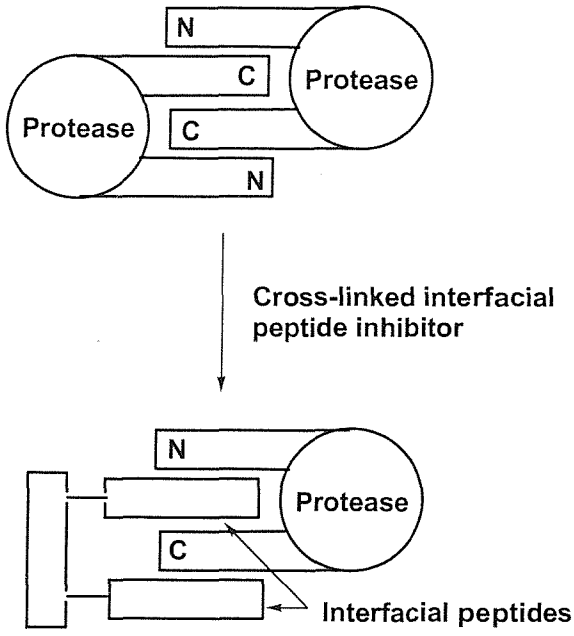

Scheme 4.2: Representation of the strategy used to inhibit protease dimerization by cross-linked interfacial peptides.

De Mendoza, also with Reboud-Ravaux and co-workers have reported that lipophilic residues linked to the side chains attached to a guanidinium scaffold such as **71**, was found to be a dimerisation inhibitor with IC_{50} = 1.6 mM and K_{id} = 150 nM.[166]

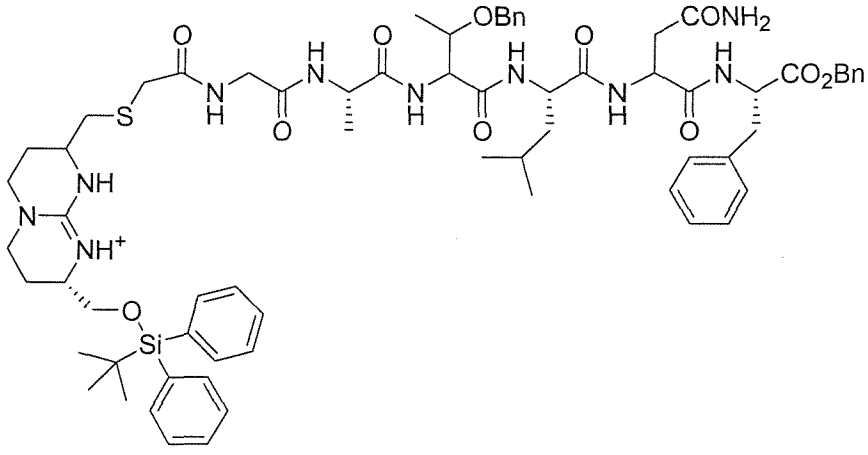

71

Tweezer receptors could be used as HIV-1 protease inhibitors. By tethering C- and N-terminal peptide sequences or arms to a scaffold, the tweezer receptors possible produce cross-linked interfacial peptides. Chemielewski and co-workers reported the 'tweezer' receptors containing cross-linked peptides from the N- and C-termini of the protease, both inhibit HIV-1 protease activity and decrease the amount of protease dimers in solution. Compound **72** was shown to inhibit activity with IC_{50} = 350 nM and K_{id} = 220 nM.[167,168]

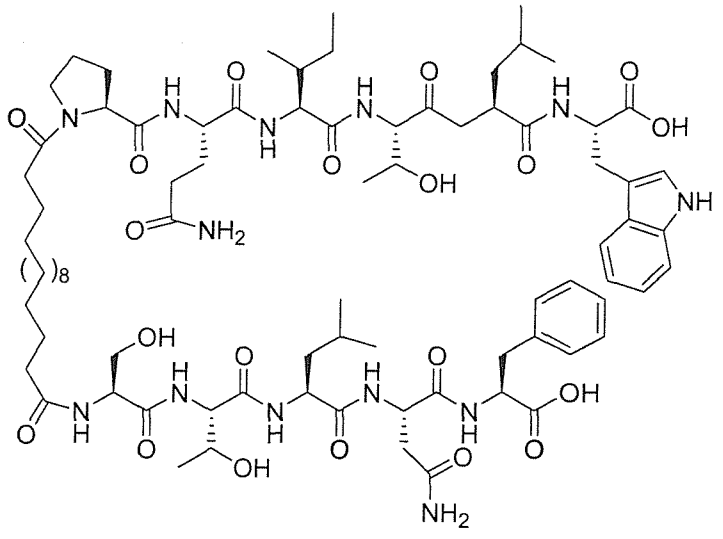

72

Using combinatorial chemistry, more recently, they synthesised a 68 member 'tweezer' receptor library and found **73** was 2.5 times more potent at half the molecular weight than a cross linked agent **72** with K_{id} = 85 nM.[169]

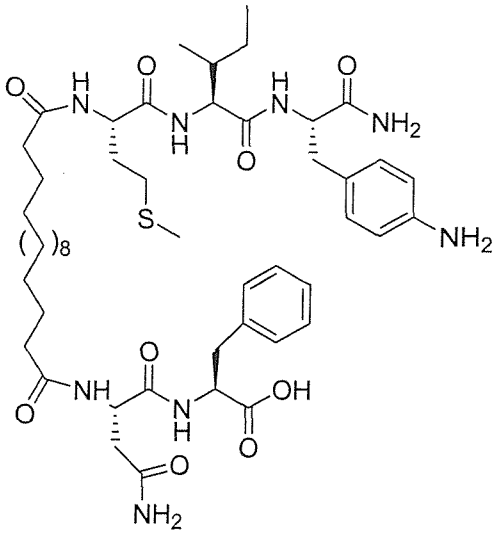

73

We took our inspiration from this work to synthesise a library of 'tweezer' receptors, which contain a 2,5-diamido pyrrole scaffold as a carboxylate binding site and two orthogonal peptide derived side arms using combinatorial chemistry with 'spilt-and-mix' methods. This tweezer receptor library would function as a cross linking agent for C-terminal of the HIV-1 protease and hence function as an HIV-1 protease inhibitor.

4.2 Synthesis and characterization

In order to prepare the library of 'tweezer' receptors, incorporating a pyrrolic 'head group' and two peptide derived side arms (Figure 4.6), an orthogonally protected pyrrole derivative **74** was prepared. Diamine pyrrole, **47**[96], prepared in the previous chapter, was used as the starting material. The pyrrolic derivative **76** was synthesised in three steps with an overall yield of 20% starting from **47** as shown in Scheme 4.3. In this way, compound **76** was suitably functionalised with a carboxylic acid moiety to allow attachment to TentaGel S NH_2 resin beads.

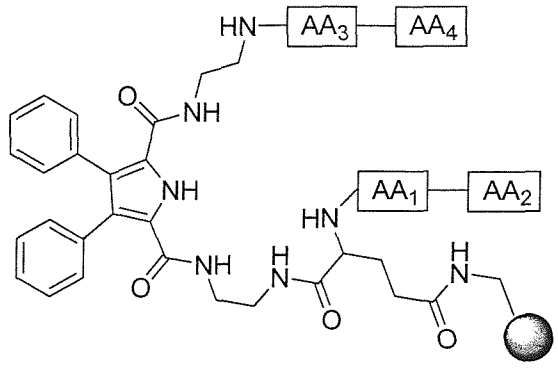

Figure 4.6: The pyrrolic-derived 'tweezer' receptor library.

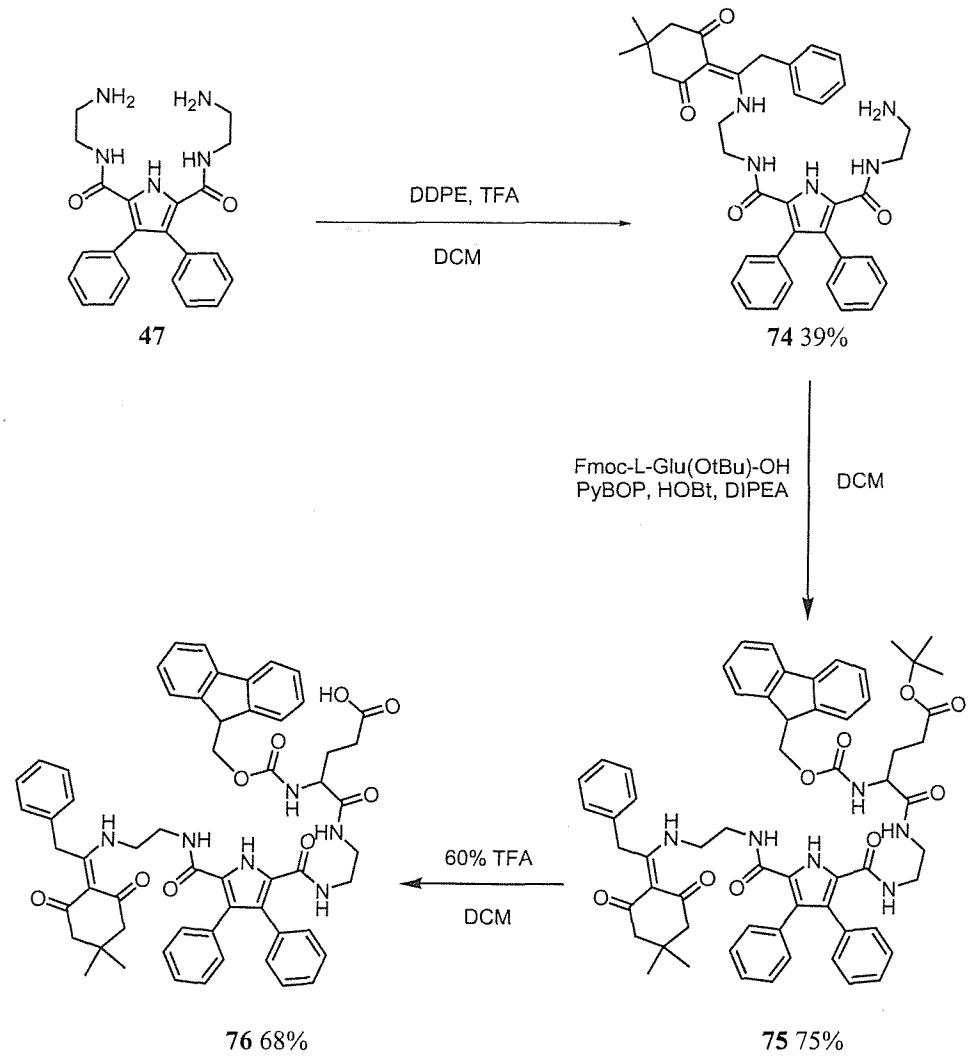

Scheme 4.3: The preparation of compound **76**.

Diamine pyrrole **47** was first converted into the mono-DDPE protected amine pyrrole **74** by stirring three equivalents of **47** with one equivalent of 2-phenylacetyldimedone (DDPE)[170] in dichloromethane and trifluoroacetic acid as catalyst. Purification by column chromatography on silica gel 60 eluting with dichloromethane/methanol (10:1 *v/v*) gave **74** in 39% yield. Coupling with N-α-Fmoc-L-glutamic acid γ-*tert*-butyl ester using PyBOP/HOBt and DIPEA in dichloromethane gave orthogonally protected 2,5-diamidopyrrole **75** in 75% yield. Boc deprotection of **75** using 60% TFA in dichloromethane led to the acid **76** in 68% yield. The orthogonal protecting groups used in the synthesis of **76** allows the

synthesis of 'unsymmetrical' tweezer receptors, that is tweezer structures where the two peptide arms can be randomised (by split-and-mix synthesis) independently.

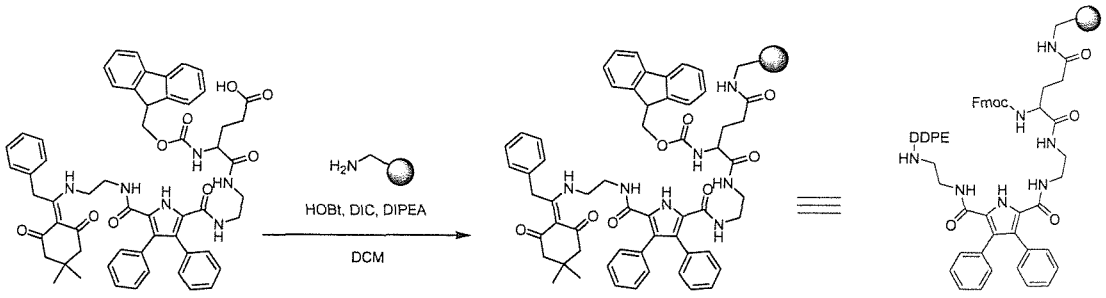

76 77

Scheme 4.4: Preparation of the pyrrolic-derived on TentaGel resin 77.

To synthesise this library, compound **76** was coupled to TentaGel resin using DIC/HOBt and DIPEA in dichloromethane (Scheme 4.4) to give **77** as a starting material. Qualitative and quantitative ninhydrin tests and quantitative Fmoc tests were used to prove that the coupling was made completely.

A 900 members library of orthogonal Fmoc- and Boc-protected tweezer receptors **82** was prepared by stepwise fourfold coupling of Fmoc- and Boc-protected amino acids to each side arm of **77** using the split-and-mix strategy (Scheme 4.5). Fmoc deprotection using 20% piperidine in dimethylformamide was carried out as the initial step to yield a free amine side arm resin **78**, which was ready for library generation. First six Fmoc-protected amino acids were used in the coupling to this free amine providing resin **79**. Then, the Fmoc-deprotection was used again followed by the coupling of another five Boc-protected amino acids to give resin **80** with two amino acids and glutamic acid on one side arm. For the other pyrrolic side arm, DDPE was deprotected using 5% $NH_2NH_2{\cdot}H_2O$ in dimethylformamide to give the free amine resin **81**. This resin was coupled with five Fmoc-protected amino acids followed by the last Fmoc-deprotection and six Fmoc-amino acids coupling gave a desired library **82** containing 900 members (6 x 5 x 5 x 6) of the pyrrole-derived tweezer compounds.

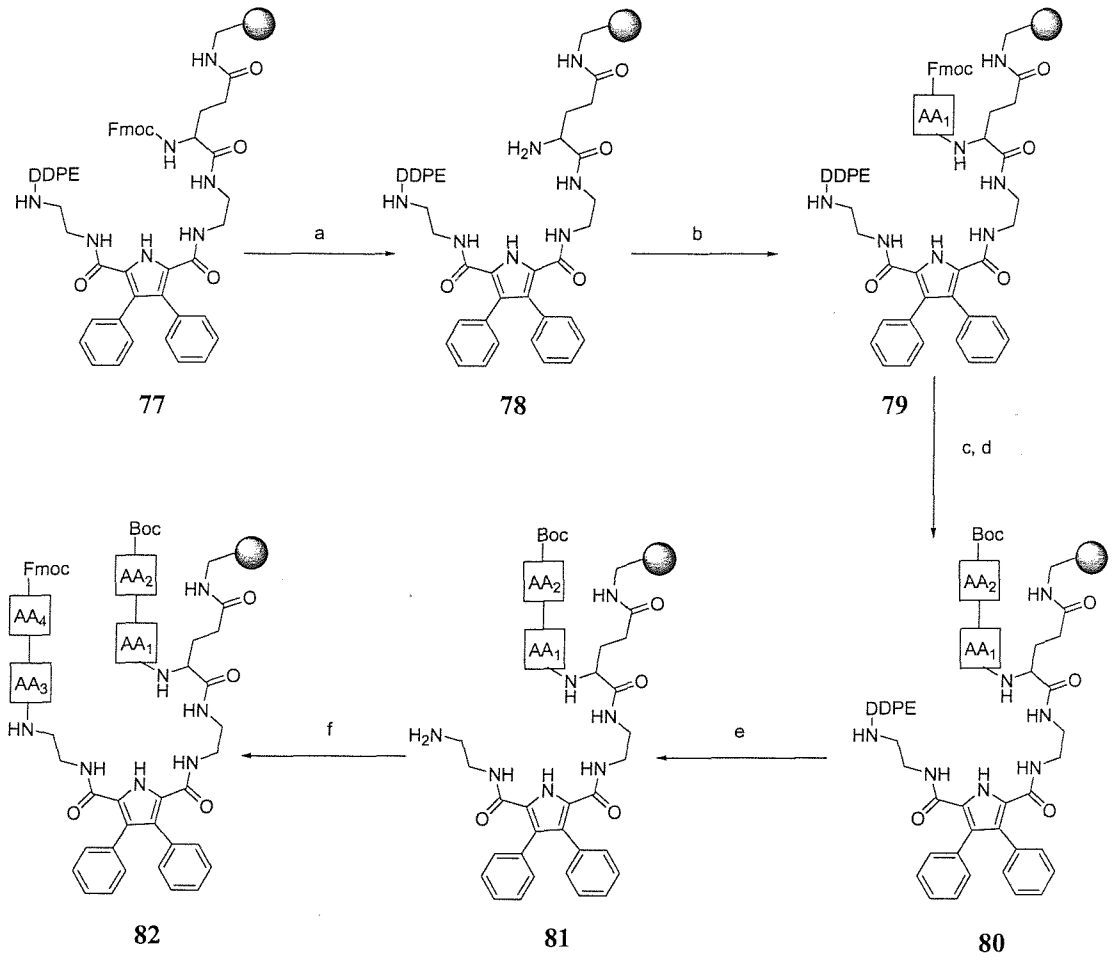

Scheme 4.5: Synthesis of pyrrole-derived tweezer receptors library **82**. a) 20% Piperidine in DMF. b) Split-and-mix Fmoc-peptide synthesis using Gly, L-Val, L-Phe, L-Lys(Boc), L-Ser(*t*Bu), Gln. c) 20% Piperidine in DMF. d) Split-and-mix Boc-peptide synthesis using Gly, L-Ala, L-Phe, L-Glu(O*t*Bu), L-Val. e) 5% $NH_2NH_2{\cdot}H_2O$ in DMF; f) Two-fold split-and-mix Fmoc-peptide synthesis using L-Glu(O*t*Bu), L-Met, L-Leu, L-Lys(Boc), L-Ala, L-Ser(*t*Bu), L-Pro, Gln.

4.3 Carboxylate binding studies: screening experiments

The carboxylate binding ability of the 900 members library **82**, which contains 2,5-diamidopyrrole as a carboxylate binding site and two orthogonal peptide derived side arms was studied using screening experiments. Dye-labelled

tripeptide guest which contains red dye 4-(4-nitro-phenylazo)-phenyl group, the tetrabutylammonium salt of the red dye-spacer-L-Leu-L-Asn-L-Phe **84** was prepared from the tripeptide **83** (Scheme 4.6). This tripeptide is a mimic for the last three amino acids at the C-terminus of HIV-1 protease.[160]

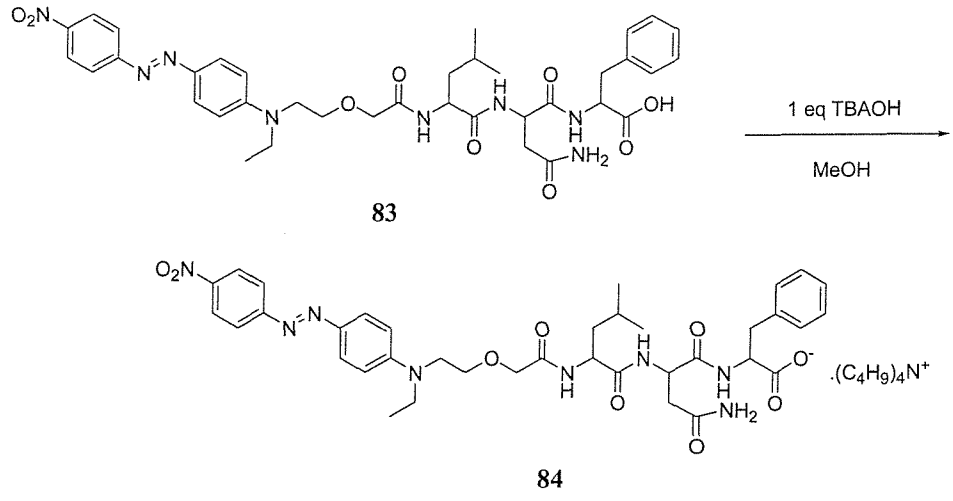

83

84

Scheme 4.6: Preparation of **84**.

In a typical screening experiment a sample of around 5 mg (~5000 beads or 5% of the beads produced) of the library was added to 1 ml of dye-labelled peptide solution (starting concentration ~ 1 μM) in a chosen solvent and incubated for at least 24 hours. It was essential that the receptor library in the peptide-guest solution was left for more than 12 hours to reach equilibrium, indicating that binding with the resin-bound receptors has relatively slow kinetics. Beads were analysed in flat-bottomed glass pots under a microscope (magnification up to 40x). The concentration of dye-labelled peptide guest was increased to provide optimal selectivity as adjudged by the number of the stained beads against a background of non- or lighter stained beads, visualised under a microscope.

Using this strategy, the tweezer receptors library **82** was screened with dye-labelled tripeptide **84**. The screening experiments were carried out in two different solutions, which were 1%DMSO:99%$CHCl_3$ and neat DMSO. When library **82** was screened in 1%DMSO:99%$CHCl_3$, there was no evidence for any selective binding

observed in the experiments. More than 20% of beads were the same colour at each concentration of dye-labelled peptide **84** solution.

The library **82** was then incubated with tripeptide guest **84** in DMSO. Highly selective binding was observed in this solution. One highly stained bead and two moderately stained beads, that is less than 0.1% of beads, were found at 10 μM of the tripeptide guest **84**. However, these stained beads could not be analysed due to the technical problems of the analysing machine. Therefore, the experiment was repeated under the same conditions. Another 5 mg of the library **82** was incubated with 10 μM of tripeptide **84** in dimethyl sulfoxide solution. Once again one highly stained bead and two moderately stained beads were found and then collected. The results showed these screening experiments were reproducible. Moreover, the experiment was carried on until the concentration of tripeptide guest **84** reached 25 μM. At this concentration, more than 20% of beads sample were highly stained, showing non-selectively binding between the library and this tripeptide guest. Portions of water were added to the solution. All the beads in the sample were stained and the solution became colourless when water was added up to 50 μl or 15% (*v/v*). This presumably indicates that a hydrophobic effect is causing the tweezer receptors library **82** to bind the carboxylate dye-labelled peptide guest **84** non-selectively upon addition of water.

The screening experiment has been repeated with larger numbers of beads, which the library **82** was studied their carboxylate binding properties with the tripeptide guest **84** in DMSO. A sample of beads 25 mg (~25,000 beads) was used and was incubated in the dimethyl sulfoxide solution of **84**. Sixteen highly stained beads were found and collected at 5.12 μM (20.46 nmol, 4 ml) of **84** solution, which was less than 0.1% of beads sample. Some of these bead samples are shown in Figure 4.7.

Two most highly stained beads, **85** and **86** from the first screening experiment and another five highest stained beads, **87**, **88**, **89**, **90** and **91** from the last screening experiment were deprotected using 20% piperidine and 60% trifluoroacetic acid respectively (Scheme 4.7).

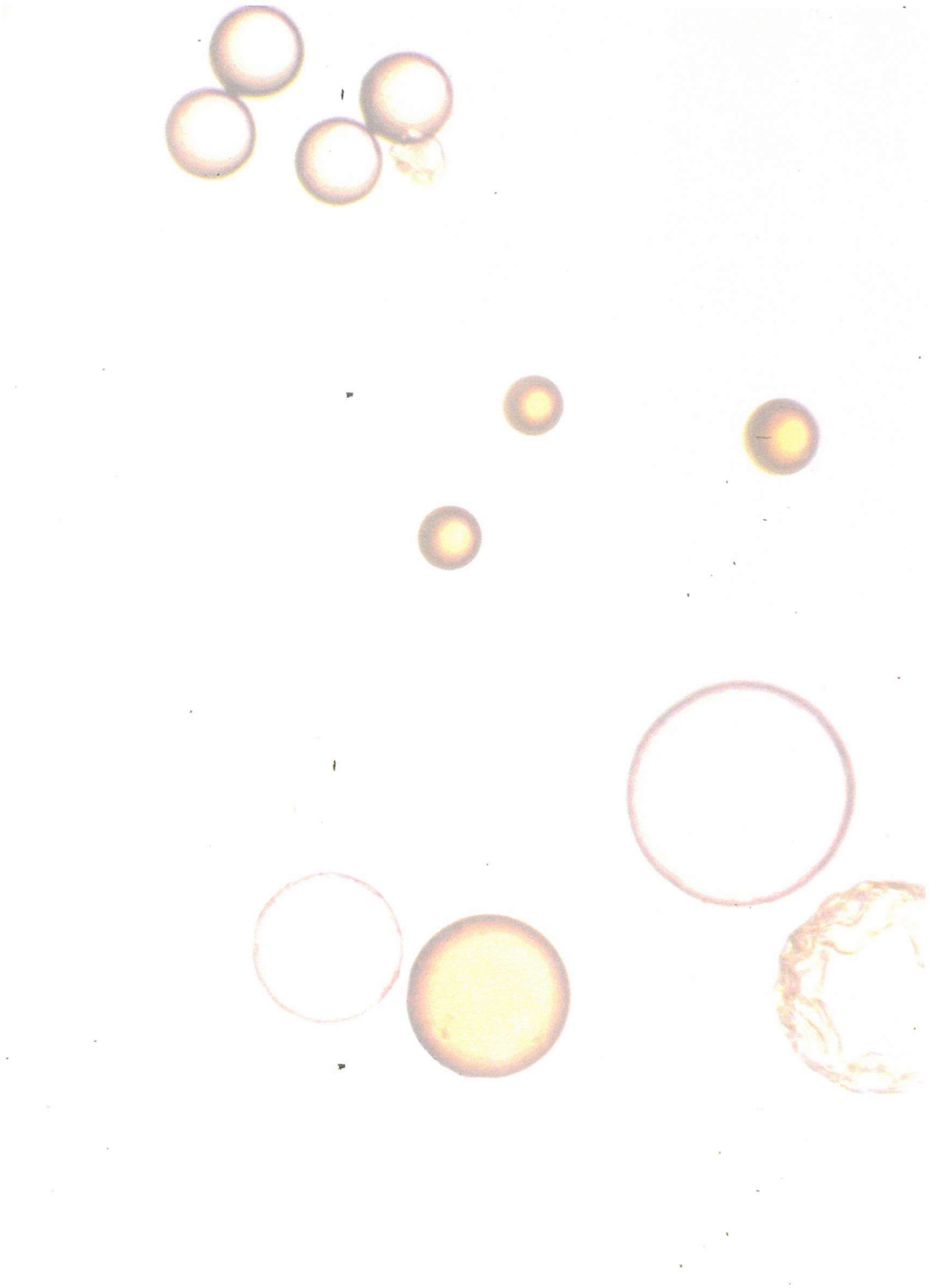

Figure 4.7: Comparison between stained beads and unstained beads.

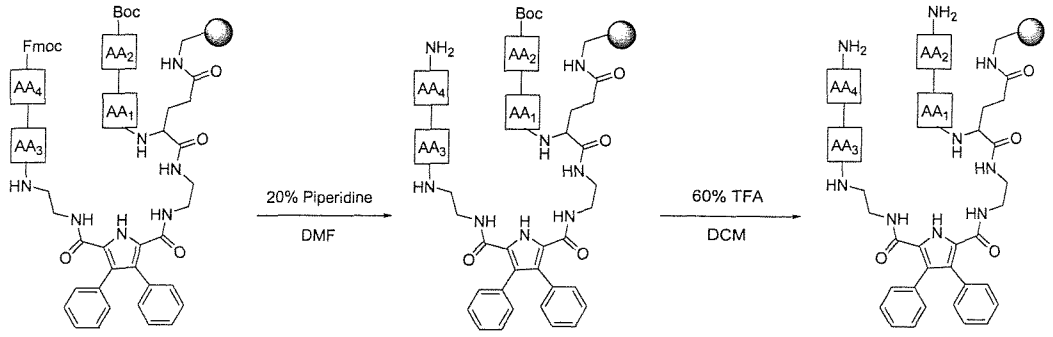

Scheme 4.7: Deprotection of beads **85-91**.

The free amine beads **85-91** were analysed using Edman degradation techniques to determine their composition.[171] Sequencing was performed by Bio-Medical school at University of Southampton using an Applied Biosystems 477A pulsed liquid-phase sequencer coupled online to an Applied Biosystem 120A Phenylthiohydantonin (PTH)-derivative analyser. The sequencing results are shown in Table 4.1. The proposed structures of **85-89** (Figure 4.8) and **90** and **91** (Figure 4.9) are shown.

Bead	AA_1	AA_2	AA_3	AA_4
85	Phenylalanine	Glutamic acid	Proline	Leucine
86*	Lysine	Valine	Proline	Leucine
87	Phenylalanine	Glycine	Proline	Proline
88	Valine	Alanine	Proline	Proline
89	Lysine	Glycine	Proline	Proline
90	Serine	Glycine	Proline	Proline
91	Valine	Valine	Proline	Proline

*Pale stained bead.

Table 4.1: Sequencing results of beads **85-91**.

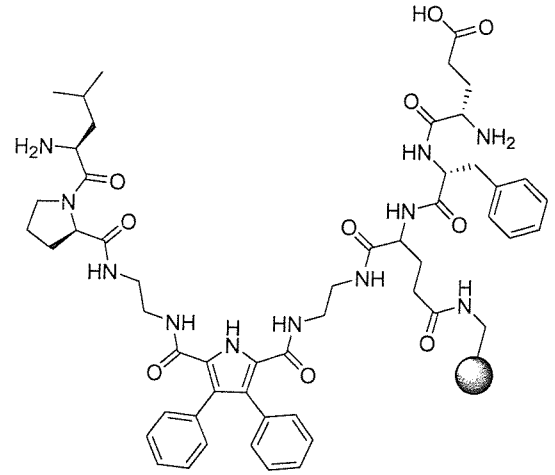

85

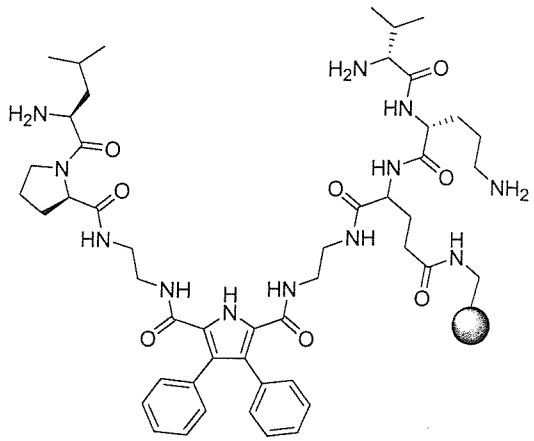

86

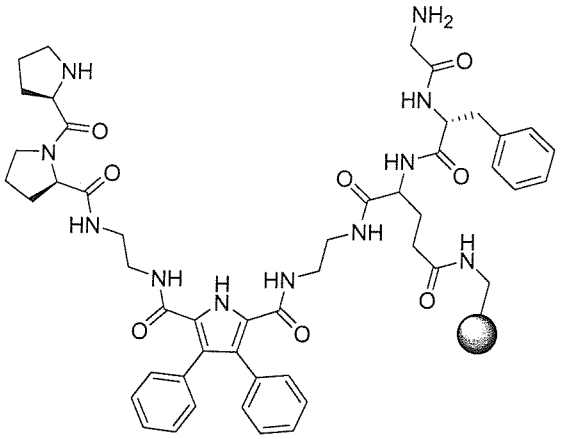

87

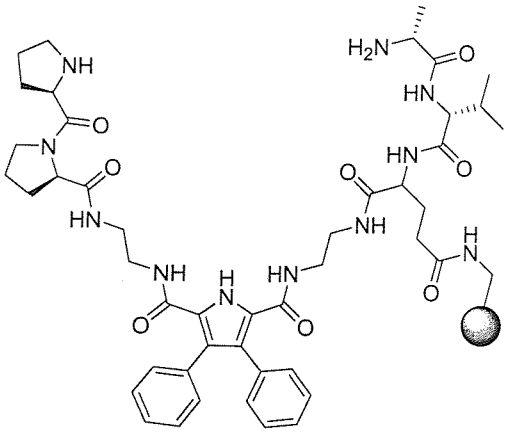

88

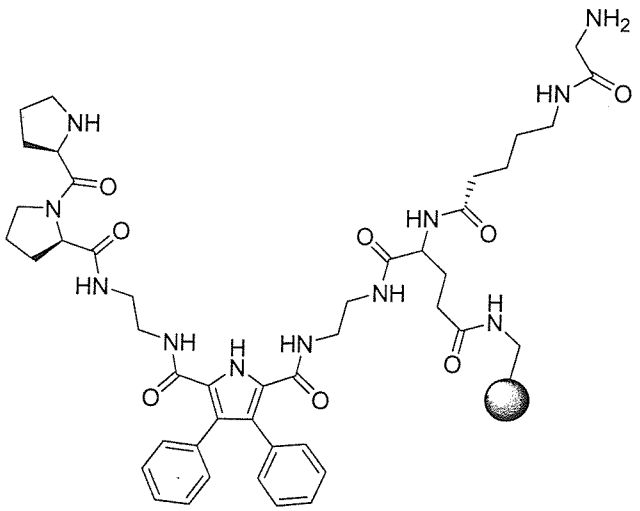

89

Figure 4.8: Proposed structures of beads **85-89**.

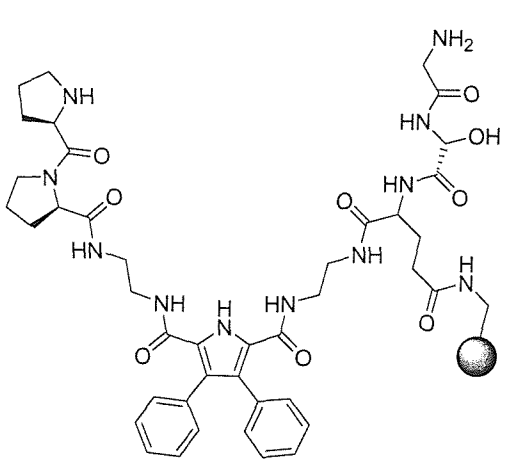

90

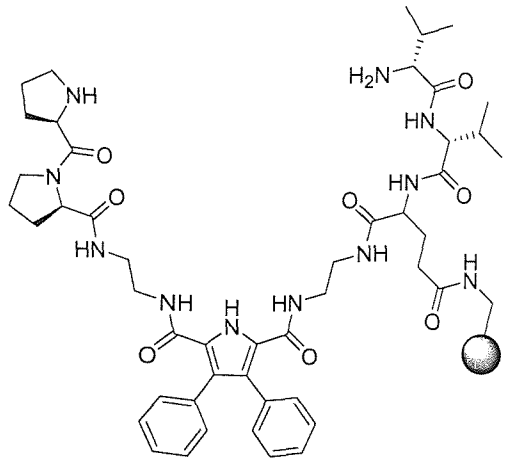

91

Figure 4.8: Proposed structures of beads **90** and **91**.

The structures of the pyrrolic-derived tweezer receptor library which bound the guest identified from the screening experiments showed the third amino acid (AA_3) was proline in all cases. The forth amino acid (AA_4) was leucine in beads **85** and **86**. However, the remaining beads contained proline in this position. The different sequencing results showed that the amino acids in the second position (AA_2) were glutamic acid, valine, glycine and alanine. Glycine was found three times in this position. The first position (AA_1) was also less well conserved, but phenylalanine was found in two cases, also valine and lysine. However, the sequencing result of **86** was less conserved because it was pale stained bead in the experiment. These results suggest that the pyrrole scaffold head group tweezer receptors which contain proline in the third and forth positions, glycine in the second position and probably phenylalanine or valine in the first position are important in binding the carboxylate tripeptide guest, L-Leu-L-Asn-L-Phe, selectively.

4.4 Conclusion

The 900 member orthogonal tweezer receptors library **82** was synthesised using split-and-mix strategy. These receptors contain a 2,5-diamido pyrrole scaffold head group as a carboxylate binding site and two orthogonal peptide derived side arms. Screening experiments have been used to study the carboxylate binding properties with dye-labelled carboxylate tripeptide **84**, L-Leu-L-Asn-L-Phe which mimics the last three peptides sequences of C-termini of HIV-1 protease, in both 1%DMSO:99%$CHCl_3$ and in neat DMSO solutions. The screening results in DMSO solution showed that some members of the receptor library have high selectively for the tripeptide guest. The peptide side arm sequences of the selected receptor beads were analysed by Edman degradation. The sequences analysis results showed the third and forth positions were proline and proline respectively. Future work will involve the synthesis of individual tweezer receptors containing these amino acids in order to study their properties both *in vitro* and *in vivo*.

5 *Anion-anion assembly: interlocking pyrrole dimers*

5.1 Introduction

In recent years, several strategies have been developed by coordination chemists to predict the outcome of self-assembly processes and this has lead on to the development of the field of crystal engineering.[172-174] Several research groups have explored metal-assisted self–assembly processes which has led to a plethora of structural motifs such as grids,[175,176] boxes,[177,178] cylinders,[179] helicates[180-183] and molecular polyhedra.[184,185] In contradistinction to these results, relatively few reports detailing anion directed self-assembly processes have been reported, despite there being considerable current interest in the development of molecular and supramolecular systems which have the ability to bind negatively charged ions.[186,187] Therefore, the use of anionic components to direct self-assembly is a relatively new area of supramolecular chemistry. For example, Lehn and co-workers have reported the chloride-templated pentametallic circular helicate **92**, which self-assembles from five tris-bipyidine ligands and five Fe(II) ions in the presence of chloride anions.[188,189]

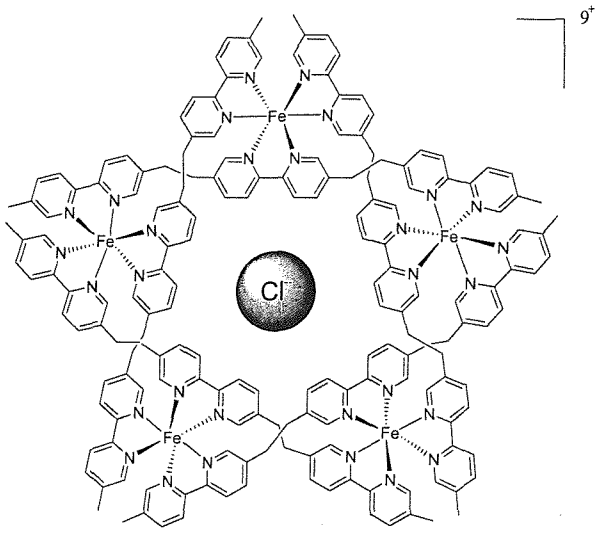

92

Kruger and co-workers have recently reported the anion directed assembly of a dinuclear double helicate of compound **93**.[190] This double helicate formed via pyridinium N-H-Cl^- hydrogen bond formation when hydrochloric acid was added to a methanolic solution of **93**.

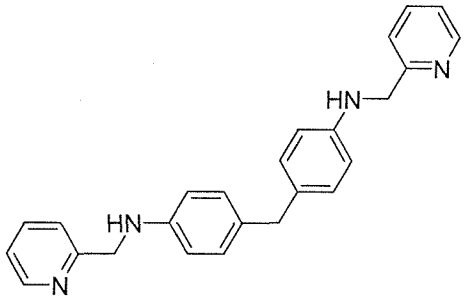

93

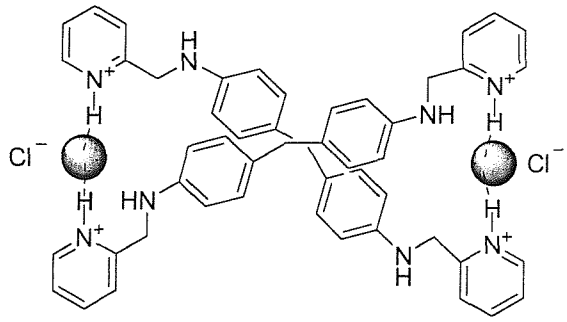

$(H_4(93)Cl)_2.6Cl.H_2O$

Gale and co-workers have synthesised anion receptors **94** and **95** which contain 3-nitrophenyl and 3,5-dinitrophenyl groups respectively.[191] The solid-state anion-directed assembly properties these isophthalamide clefts including the first example of a helix formed by anion templation of an amide ligand has been reported. Crystals of the tetrabutylammonium fluoride complex of **95** formed by slow evaporation of an acetronitrile solution of the receptor in the presence of excess tetrabutylammonium fluoride revealed a double helix formed around two fluoride anions via NH···F^- hydrogen bonds (Figure 5.1).

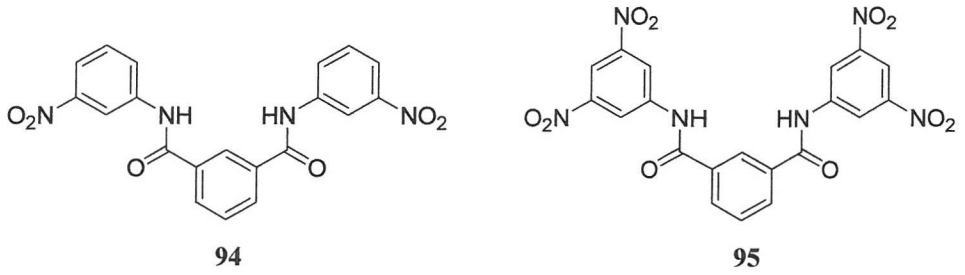

94 **95**

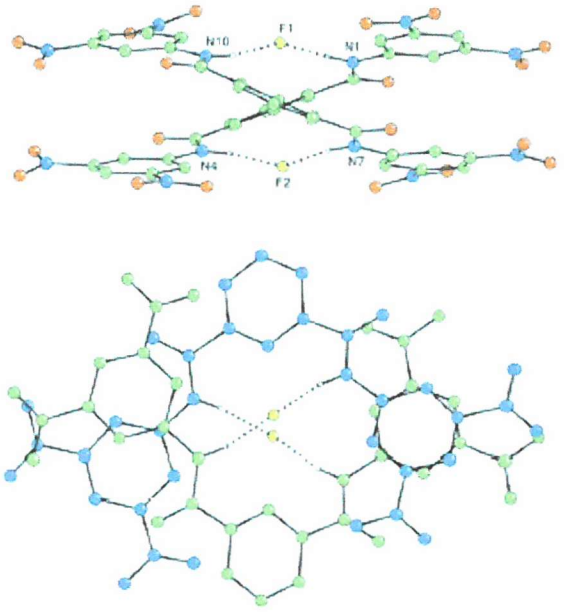

Figure 5.1: Side view of the X-ray crystal structure of the fluoride complex of receptor **95** (above) and top view of the helix showing π-stacking interactions (below). Tetrabutylammonium counter cations and certain hydrogen atoms are omitted for clarity.

Gale and co-workers have recently synthesised anion receptors containing electron withdrawing nitrophenyl groups. Two new pyrrole 2,5-diamide clefts have been synthesized containing 4-nitrophenyl **96** or 3,5-dinitrophenyl groups **97** appended to the amide positions.[192] The 3,5-dinitrophenyl derivative **97** has been shown to deprotonate in the present of tetrabutylammonium fluoride or hydroxide (Figure 5.1) resulting in the formation of a narcissistic dimer in the solid state whereby the N^- is stabilized by the formation of two amide NH-N^- hydrogen bonds from another anion. The N^- centre on the second anion was also stabilized by two NH-N^- hydrogen bonds from the first anion.

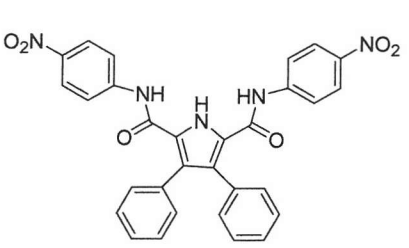

96

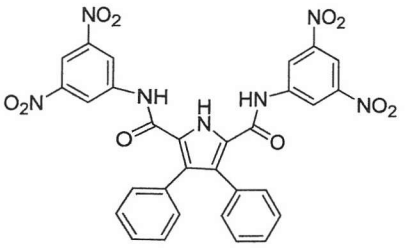

97

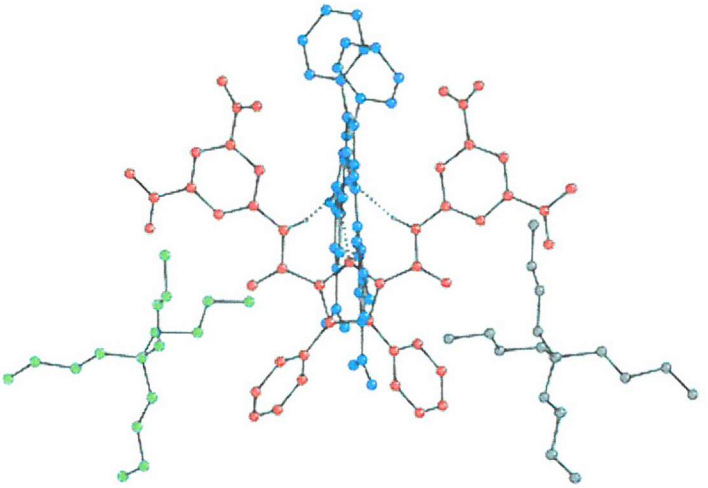

Figure 5.2: The X-ray crystal structure of the tetrabutylammonium salt of **97**-H^+. Colours represent individual components of the assembly. Certain hydrogen atoms have been omitted for clarity.

Similarly, 3,4-dichloropyrrole diamides such as compound **98** have been shown to self-assemble in the solid state when deprotonated.[193] Crystallographic evidence revealed again that the pyrrole NH proton could be removed by basic anions such as fluoride (Figure 5.3).

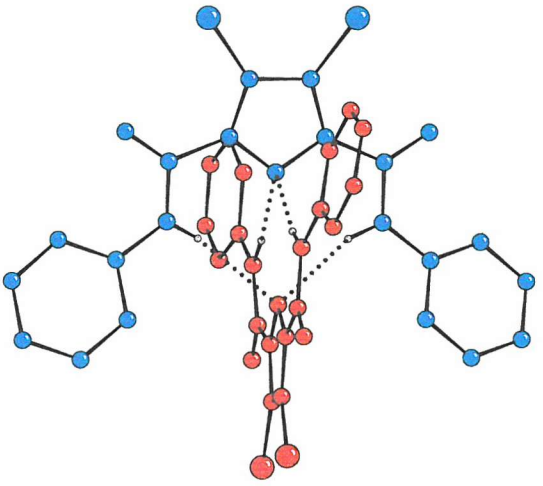

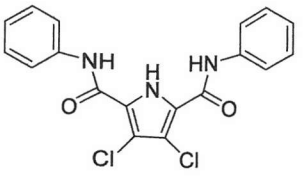

98

Figure 5.3: X-ray crystal structure of the tetrabutylammonium salt of **98**-H revealing NH···N$^-$ hydrogen bonds (tetrabutylammonium counter cations omitted for clarity).

Lehn and co-workers have recently reported a new family of oligoamide strands derived from 2,6-diaminopyridine and 2,6-pyridinedicarboxylic acid. These compounds not only self-organize into single helical conformers, but they reversibly form double-helical dimers.[194-196] Moreover, they have reported the protonation induced reversible folding/unfolding of pyridine oligoamide molecular strands **99** and **100**.[197]

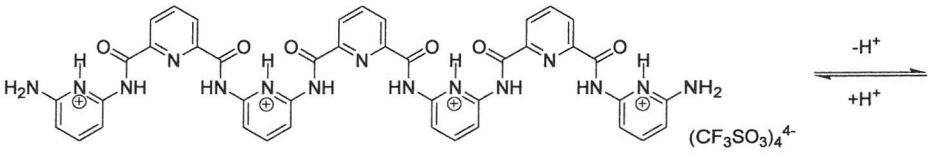

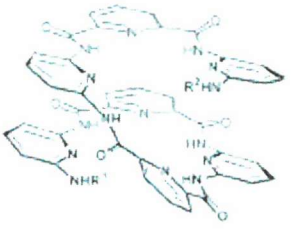

99

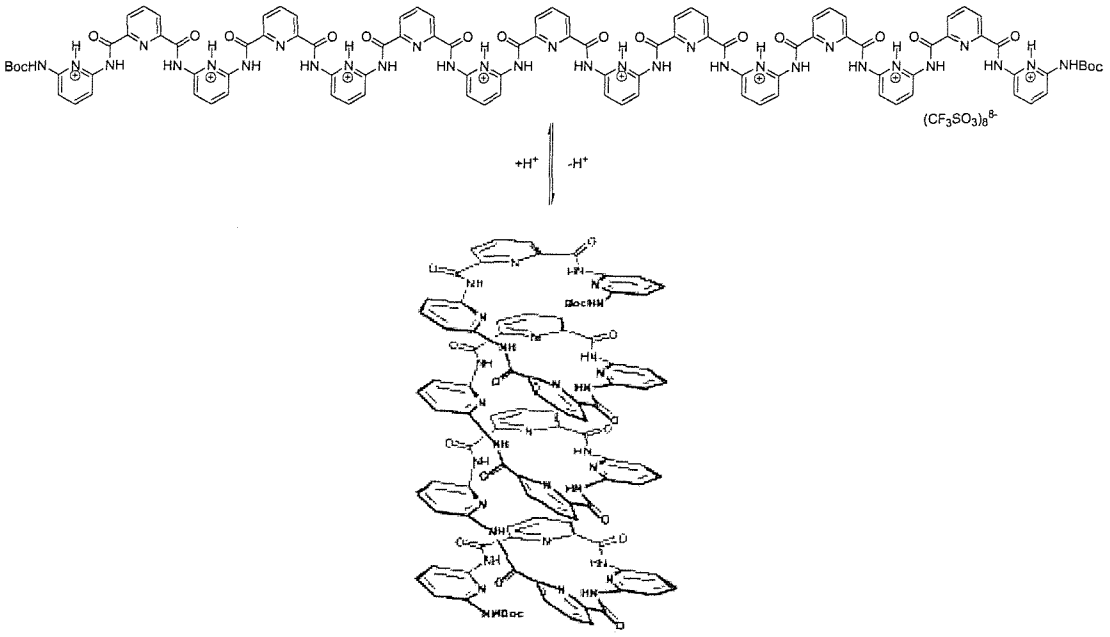

100

We wished to investigate whether we could make new types of coordination polymer based upon the deprotonated pyrrole interlocked dimer motif. We therefore synthesised a variety of ligands containing two deprotonatable pyrrole groups and studied the crystal structures of tetrabutylammonium salts of these deprotonated systems.

5.2 Synthesis and characterization

Six dimers **101**,[198] **102**,[198] **103**, **104**, **105** and **106** and two trimers **107** and **108** were synthesised. All of these compounds contain 2,5-diamidopyrroles and chlorine atoms at 3- and 4- positions of the pyrrole rings.

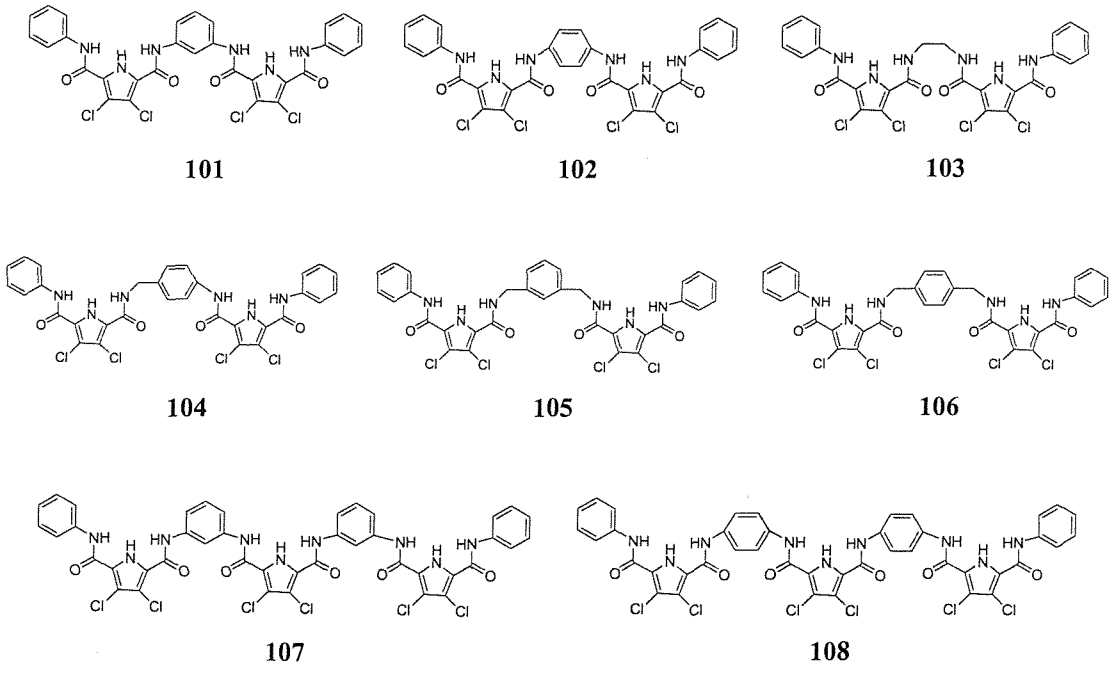

Figure 5.4: Potential interlocked compounds **101-108**.

To synthesise the dimers, 3,4-dichloro-5-phenylcarbamoyl-1H-pyrrole-2-carboxylic acid **111**[198] was prepared as the starting material (Scheme 5.1).

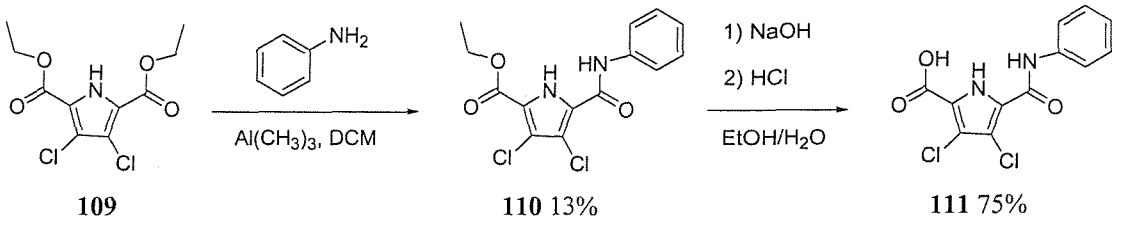

Scheme 5.1: Synthesis of compound **111**.

3,4-Dichloro-1H-pyrrole-2,5-dicarboxylic acid diethyl ester **109** was synthesised by literature methods.[125] Compound **109** was added to a dichloromethane solution of aniline (1 equiv.) and trimethylaluminium[124] (1 equiv.) to afford compound **110** after heating at reflux for three days in 13% yield. To prepare the monoacid **111**, sodium hydroxide (aqueous solution) (10 equiv.) was added to compound **110** suspended in ethanol. After heating at reflux overnight, the solution was acidified to pH =1 using hydrochloric acid. Purification by column chromatography on silica gel 60 eluting with dichloromethane/methanol (10:1 *v/v*) afforded **111** in 75% yield.

X-ray quality single crystals of **109** were obtained by slow evaporation of a concentrated methanol/acetonitrile solution of the compound. The crystal structure (Figure 5.5) revealed the presence of dimers in the solid state via two NH pyrrole and O carbonyl ($N_{pyrrole}\cdots O = 2.841(4)$ Å).

Crystals of **110** were obtained by slow evaporation of a concentrated solution of the compound in acetronitrile. Crystallographic analysis revealed (Figure 5.6) that in the solid state the receptor formed the hydrogen-bonding network via three different types of hydrogen bonds, N1H1···O1 (N1···O1 = 2.911(14) Å), N1H1···Cl1 (N1···Cl1 = 3.181(12) Å) and N2H2···O2 (N2···O2 = 2.844(12) Å) (see Appendix for structure information).

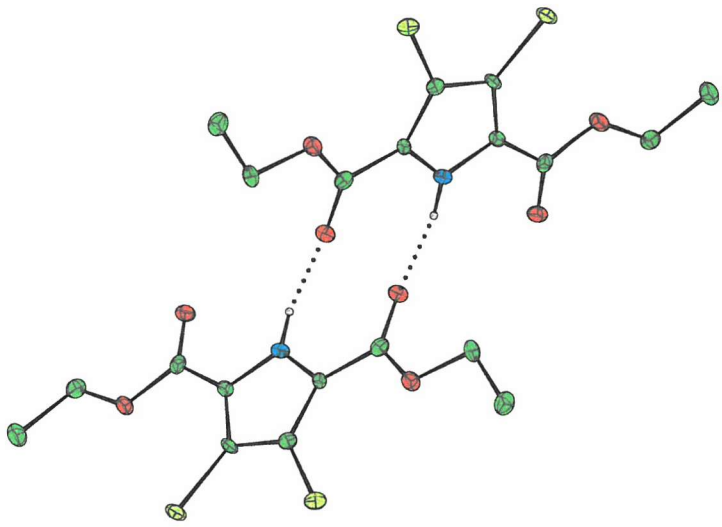

(a)

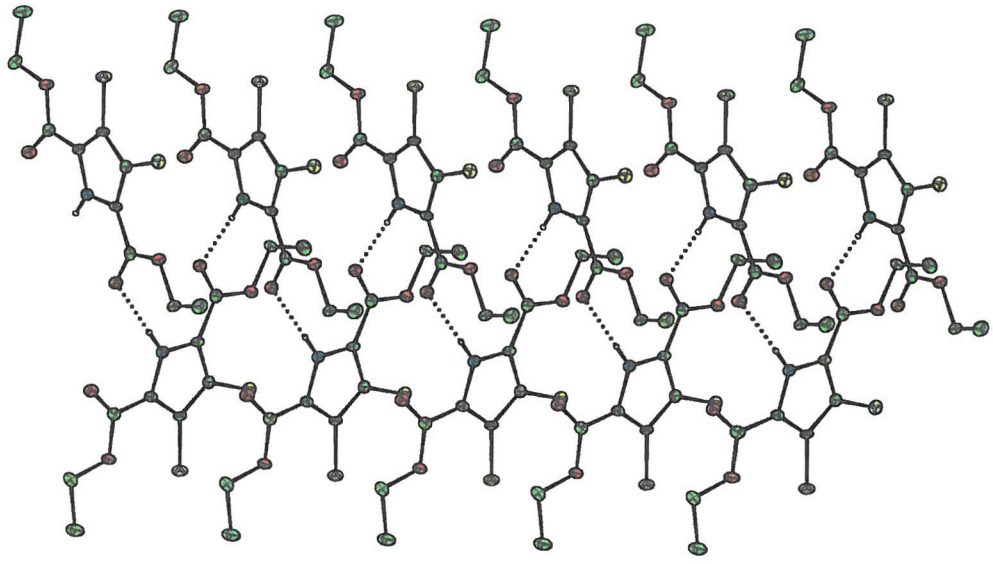

(b)

Figure 5.5: (a) The X-ray crystal structure of **109** (thermal ellipsoids drawn at the 50% probability level). The dimerization via the formation of two hydrogen bonds between NH pyrrole and the carbonyl group ($N_{pyrrole}\cdots O$ = 2.841(4) Å). (b) Displaying the hydrogen bonding network in the solid state (thermal ellipsoids drawn at the 50% probability level). Certain hydrogen atoms are omitted for clarity.

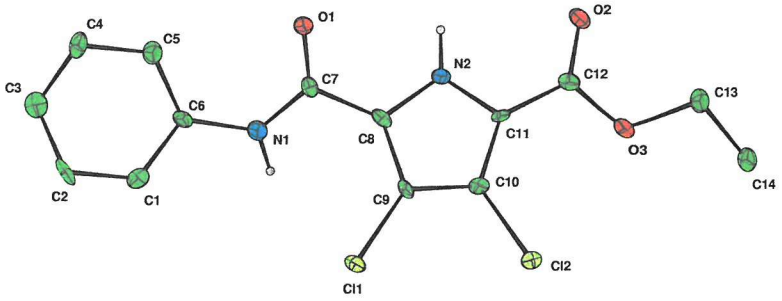

(a)

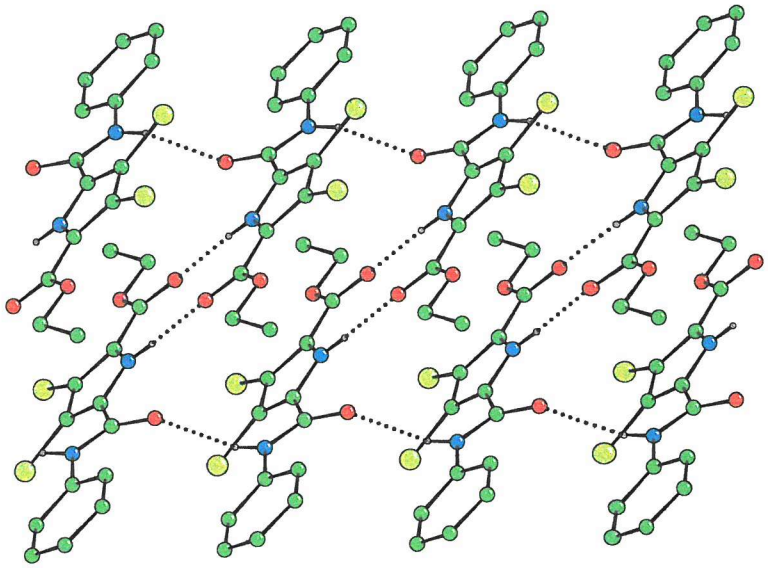

(b)

Figure 5.6: (a) The X-ray crystal structure of **110** (thermal ellipsoids drawn at the 35% probability level). (b) The hydrogen bonding network in the solid state. Molecules of the receptor are bound via the formation of three types of hydrogen bonds N1H1···O1 (N1···O1 = 2.911(14) Å), N1H1···Cl1 (N1···Cl1 = 3.181(12) Å) and N2H2···O2 (N2···O2 = 2.844(12) Å). Certain hydrogen atoms are omitted for clarity.

Six dimers containing two amidopyrrole and chlorine atoms at 3- and 4-positions in the pyrrole ring **101-106** were synthesised in a stepwise procedure (Scheme 5.2). These compounds contain different spacers between two pyrrole subunits, which are 1,3-phenyl, 1,4-phenyl, ethylene, 1,4-benzyl, *m*-xylene and *p*-xylene in compounds **101**, **102**, **103**, **104**, **105** and **106** respectively.

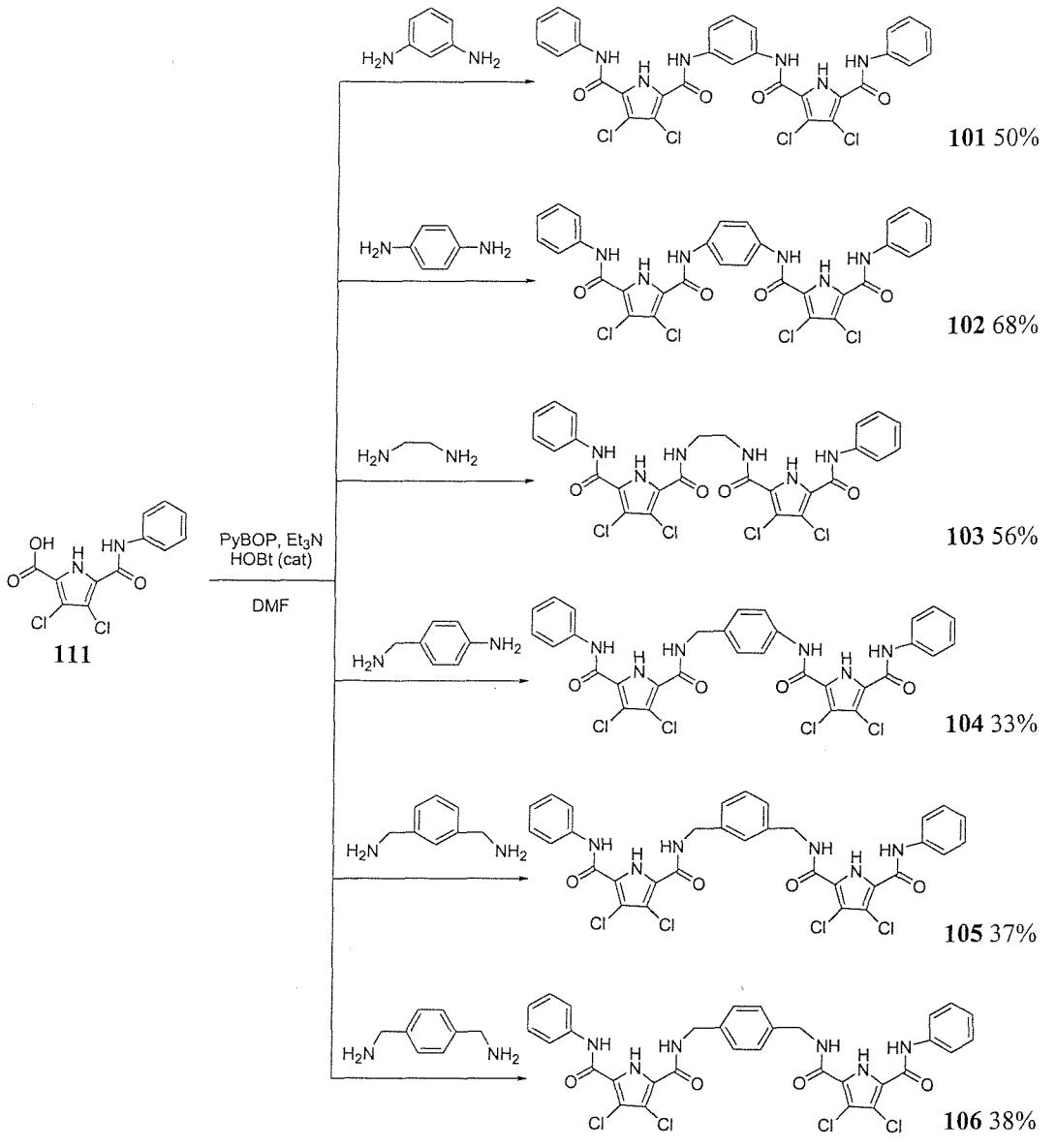

Scheme 5.2: Syntheses of compounds **101-106**.

Compound **111** was used as the starting material in all cases. This compound (2 equiv.) was coupled with 1 equivalent of diamine compounds which were 1,3-phenylenediamine, 1,4-phenylenediamine, ethylenediamine, 4-aminobenzylamine, *m*-xylenediamine and *p*-xylenediamine in DMF to give dimers **101** (50%), **102** (68%), **103** (56%), **104** (33%), **105** (37%) and **106** (38%) respectively. After stirring for three days, removal of the solvent and precipitation or extraction into suitable solvents such as acetronitrile or diethyl ether. Dimer **103** was coupled twice due to incomplete reaction of the first coupling reaction. PyBOP[199] (2 equiv.) was used as

the coupling reagent in the presence of 5 mg HOBt (catalytic quantity) and triethylamine (2 equiv.).

To synthesise the trimers, 3,4-dichloro-2,5-dicarboxylic acid-1H-pyrrole **112** was prepared following the method in Scheme 5.3. Sodium hydroxide in ethanol (28 equiv.) was added to compound **109** suspended in ethanol. After heating at reflux overnight, the solution was acidified to pH =1 using hydrochloric acid. Extraction from diethyl ether and recrystallization from acetronitrile afforded **112** in 31% yield.

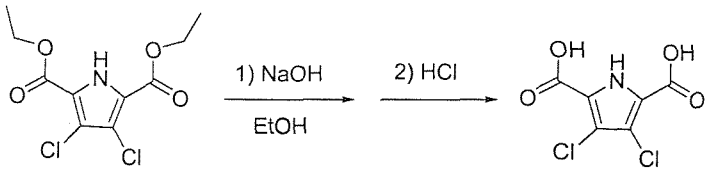

109 **112** 31%

Scheme 5.3: Preparation of **111**.

The trimers **107** and **108** containing three amidopyrrole groups were synthesised in a stepwise procedure (Scheme 5.4). These compounds contained 1,3-phenyl and 1,4-phenyl linkage moieties in **107** and **108** respectively.

Di-*tert*-butyldicarbonate was used as amine protecting group in these syntheses because the protecting formed is stable under basic conditions and it is inert to many other nucleophillic reagents.[200] Initially, the diamine linkages, 1,3-phenylenediamine and 1,4-phenylenediamine, were first converted into the mono-Boc protected species **113** and **114** by stirring of five equivalents of diamine with one equivalent of di-*tert*-butyldicarbonate (Boc) in dichloromethane. Purification by column chromatography on silica gel 60 eluting with dichloromethane/methanol (10:1 *v/v*) gave **113** and **114** in 72% and 75% yield respectively. Coupling **113** and **114** with pyrrole mono-acid **111** using PyBOP/HOBt and triethylamine in DMF gave Boc protected 3,4-dichloro-2,5-diamidopyrrole **115** and **116** in 61% and 89% yields respectively. Boc deprotection of **115** and **116** using 60% TFA in dichloromethane led to the formation of the ammonium salts **117** and **118** in 76% and 83% yield respectively. Finally, coupling **117** and **118** with bis-acid **112** using PyBOP/HOBt and triethylamine in DMF gave trimers **107** and **108** respectively.

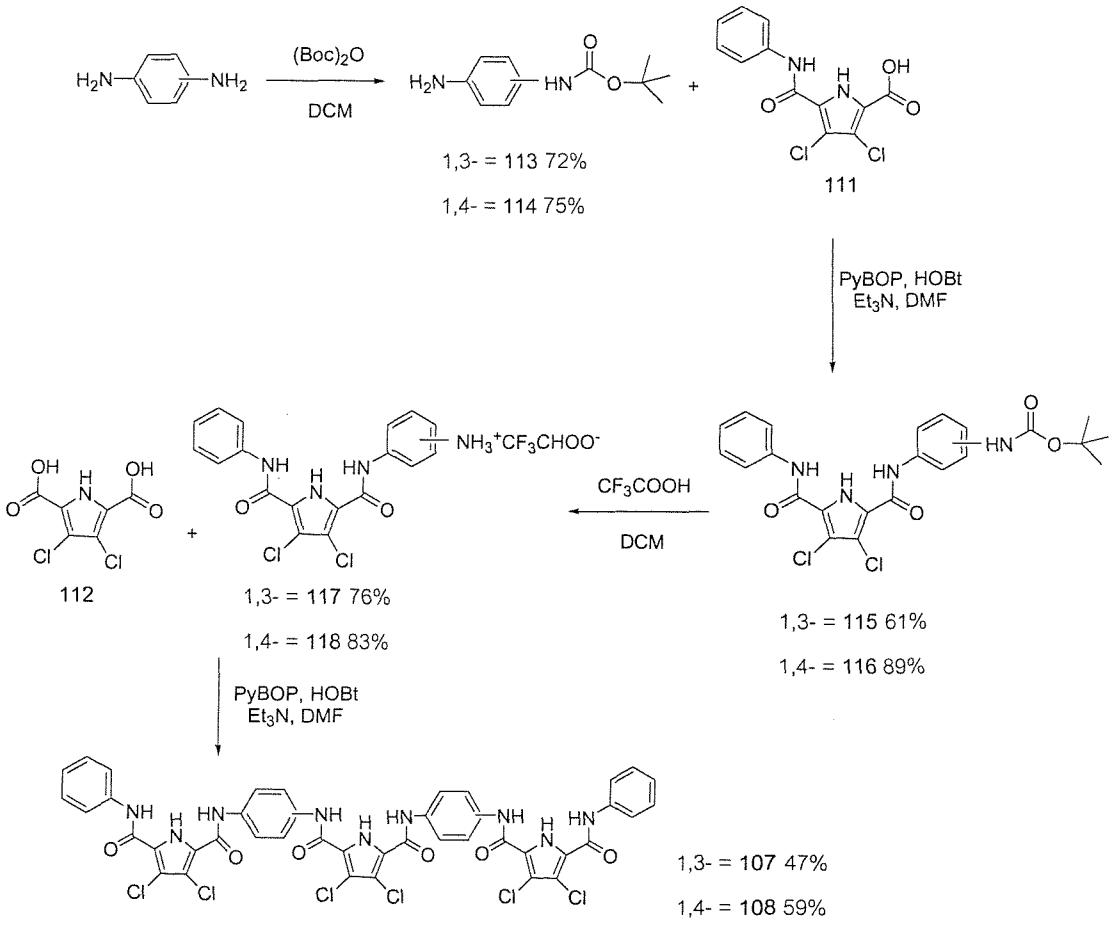

Scheme 5.4: Synthesis pathway of **107** and **108**.

The resulting dimers and trimers have limited solubility; however, it was possible to obtain ^{1}H NMR, ^{13}C NMR in DMSO-d_6 and mass spectra of some materials. Solubility was improved upon addition of tetrabutylammonium fluoride allowing complete characterization.

5.3 Deprotonation and assembly in the solid-state

The deprotonation of compound **98** was attempted with tetrabutylammonium hydroxide instead of tetrabutylammonium fluoride. Slow evaporation of an ethanolic solution of the compound **98** in the presence of tetrabutylammonium hydroxide

resulted in the formation of X-ray quality crystals. Just as was found when this compound was crystallised from dichloromethane in the presence of tetrabutylammonium fluoride, the deprotonated pyrrole again forms a narcissistic dimer via NH-N^- hydrogen bonds ($N_{amide}\cdots N^-$ = 3.152(6) - 3.287(7) Å) (Figure 5.7) but in this case crystallises as an ethanol solvate. In addition, there are π-H interactions between the *ortho* phenyl hydrogen atoms and the pyrrole ring in the range 2.580-3.310 Å; however, their distances are more variable than these hydrogen bonds in previous example[193] (see Appendix for structure information).

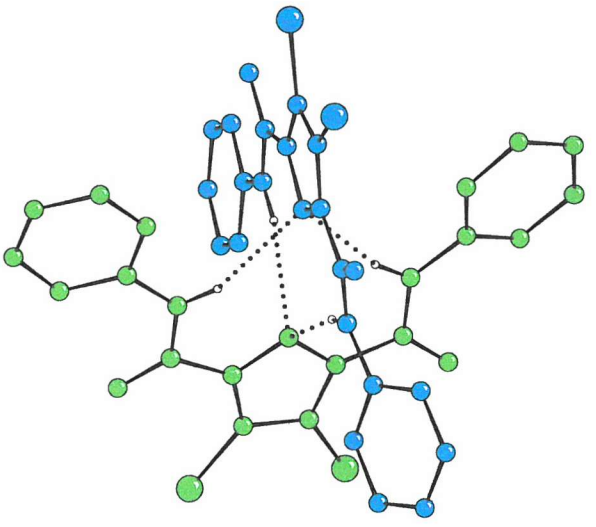

Figure 5.7: Crystal structure of the deprotonated **98** dimerized in the deprotonated form, via the formation of four hydrogen bonds between the amide NH groups and the deprotonated pyrrolic nitrogen ($N_{amide}\cdots N_{pyrrole}$ = 3.287(7), 3.152(6), 3.228(6), 3.182(7) Å). Ethanol molecule is omitted for clarity.

The dimeric and trimeric systems synthesised had poor solubility in some cases making characterisation difficult. In order to increase solubility, either the compound could be deprotonated or complexed to an anion such as chloride. The crystal structure of compound **102** was obtained as the tetrabutylammonium salt, showing two chloride ions bound to the pyrrole dimer (Figure 5.8). These crystals were formed by slow evaporation from a concentrated solution of the compound in acetronitrile and excess TBACl. The chloride ions were bound via three hydrogen bonds. Two of them occurred between the chloride ion and two NH amides (N1···Cl3

= 3.269(3) Å, N3···Cl3 = 3.273(3) Å) and other hydrogen bond formed between the chloride ion and the NH pyrrole ring (N2···Cl3 = 3.068(3) Å) (see Appendix for structure information).

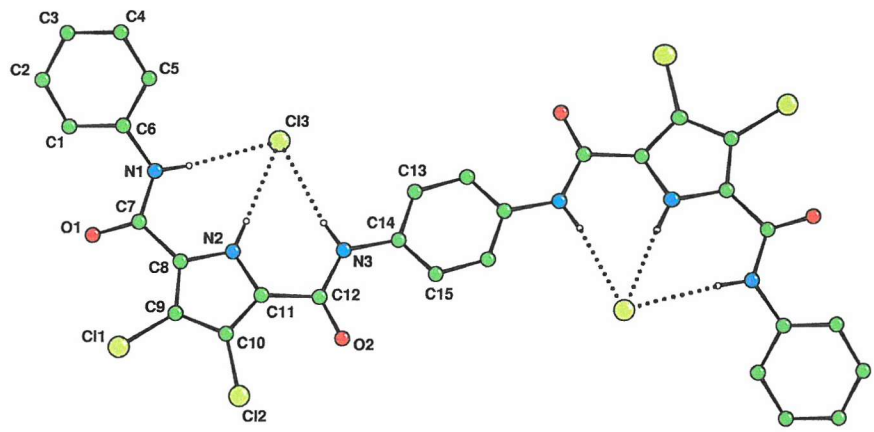

Figure 5.8: Crystal structure of **102**/2Cl$^-$ complex (N1···Cl3 = 3.269(3) Å, N3···Cl3 = 3.273(3) Å and N2···Cl3 = 3.068(3) Å). Tetrabutylammonium counter cations and non-interacting hydrogen atoms are omitted for clarity.

Attempts were made to obtain crystals of the deprotonated forms of the dimers and trimers using TBAF and TBAOH to deprotonated the pyrrole rings followed by slow evaporation of a solution of the deprotonated pyrrole. Crystals of bis-tetrabutylammonium **101**-2H$^+$ and **102**-2H$^+$ were obtained by slow evaporation from concentrated solutions of each compound in acetronitrile in the presence of excess TBAF. The X-ray crystal structure of both systems (Figure 5.9 and Figure 5.10) revealed that two pyrrole heterocycles in the molecules have indeed been deprotonated (see Appendix for structure information).

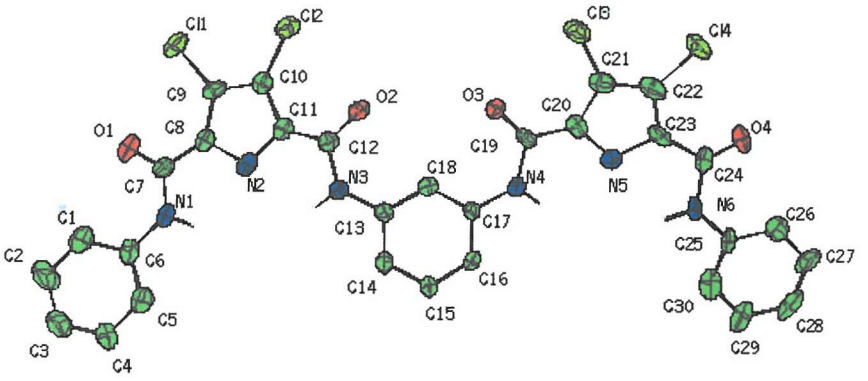

Figure 5.9: The X-ray crystal structures of tetrabutylammonium salt of **101**-$2H^+$ (thermal ellipsoids drawn at the 30% probability level). Displaying two deprotonated N^- pyrrole moieties. Tetrabutylammonium counter cations and certain hydrogen atoms are omitted for clarity.

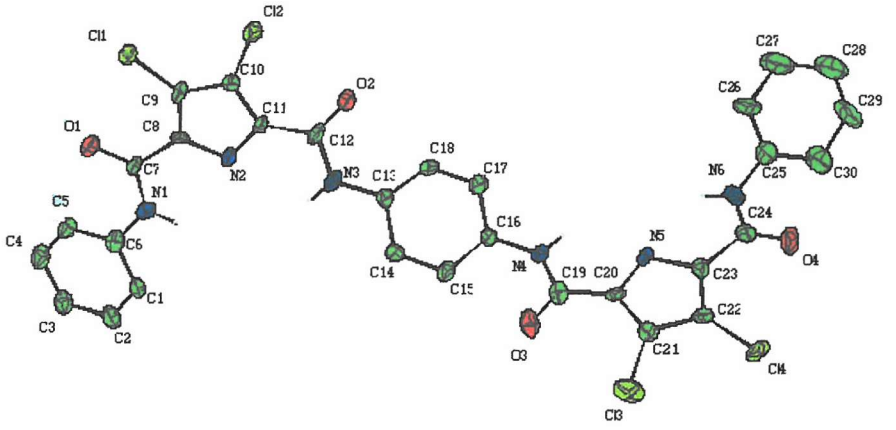

Figure 5.10: The X-ray crystal structures of tetrabutylammonium salt of **102**-$2H^+$ (thermal ellipsoids drawn at the 30% probability level). Displaying two deprotonated N^- pyrrole moieties. Tetrabutylammonium counter cations and certain hydrogen atoms are omitted for clarity.

Both systems formed interlocked chains via NH-N^- hydrogen bonds in the solid-state. In **101**-$2H^+$+$2TBA^+$ (Figure 5.11), the anionic chains consist of a single crystallographically unique molecule with NH-N^- interactions (N1···N5 = 3.103(13) Å, N3···N5 = 3.239(13) Å, N4···N2 = 3.20(3) Å, N6···N2 = 3.10(4) Å) and extend along the *a* direction (see Appendix for structure information).

In **102**-$2H^+$+$2TBA^+$ (Figure 5.12), there are one and two half unique amidopyrrole anions in the unit cell. These anions form chains that repeat in a 123123212… sequence extending in the 101 direction. The two half molecules are

essentially planar, while the complete molecule, occurring at every other position in the chain, is twisted such that the angle between the least-squares planes of the pyrrole rings is 61.79(5)° and the NH-N interactions are in the range 3.112(9)-3.491(9) Å. In both cases the tetrabutylammonium counter cations occupy the spaces between the chains (see Appendix for structure information).

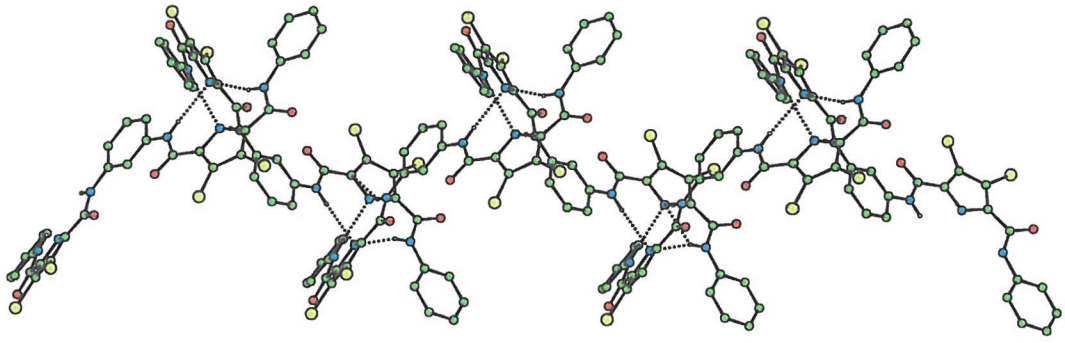

(a)

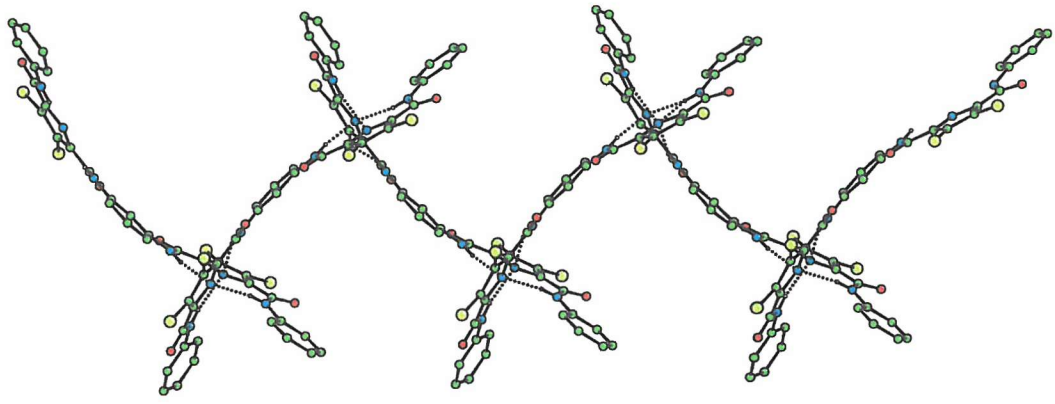

(b)

Figure 5.11: The X-ray crystal structures of tetrabutylammonium salt of **101**-$2H^+$ formed interlocked chains of anion via NH-N^- hydrogen bonds. (a) Top views. (b) Side views. Tetrabutylammonium counter cations and certain hydrogen atoms are omitted for clarity.

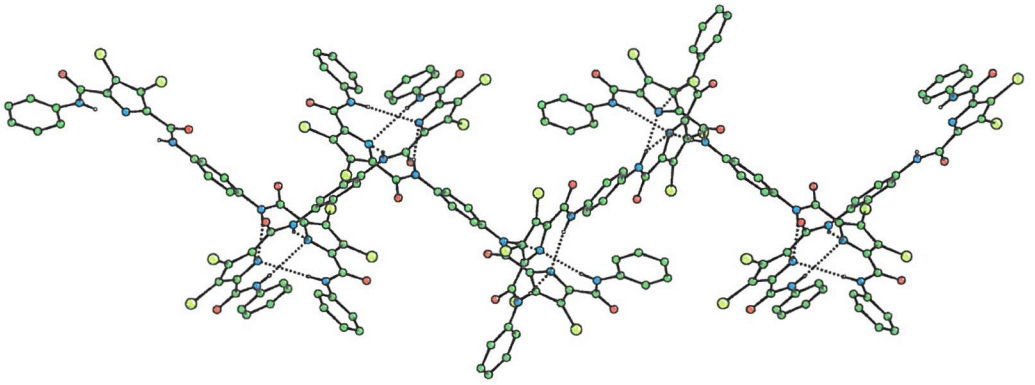

Figure 5.12: The X-ray crystal structures of tetrabutylammonium salt of **102**-$2H^+$ formed interlocked chains of anion via NH-N^- hydrogen bonds. Tetrabutylammonium counter cations and certain hydrogen atoms are omitted for clarity.

Crystals of bis-tetrabutylammonium **103**-$2H^+$ and **106**-$2H^+$ were also obtained by slow evaporation from a concentrated solution of each material in acetronitrile and excess TBAF. The X-ray crystal structures of both revealed that the two pyrrole heterocycles in the molecules have been deprotonated. However, in both cases they are not interlocked in the solid-state.

In bis-tetrabutylammonium **103**-$2H^+$ (Figure 5.13), crystallographic analysis revealed that in the solid state this material contains intramolecular hydrogen bonds ($NH_{amide}\cdots N^-_{pyrrole}$ 2.649-2.697 Å). It also formed a sheet via weak $CH_{phenyl}\cdots Cl$ hydrogen bond interactions (3.508-4.064 Å) (Figure 5.14) (see Appendix for structure information).

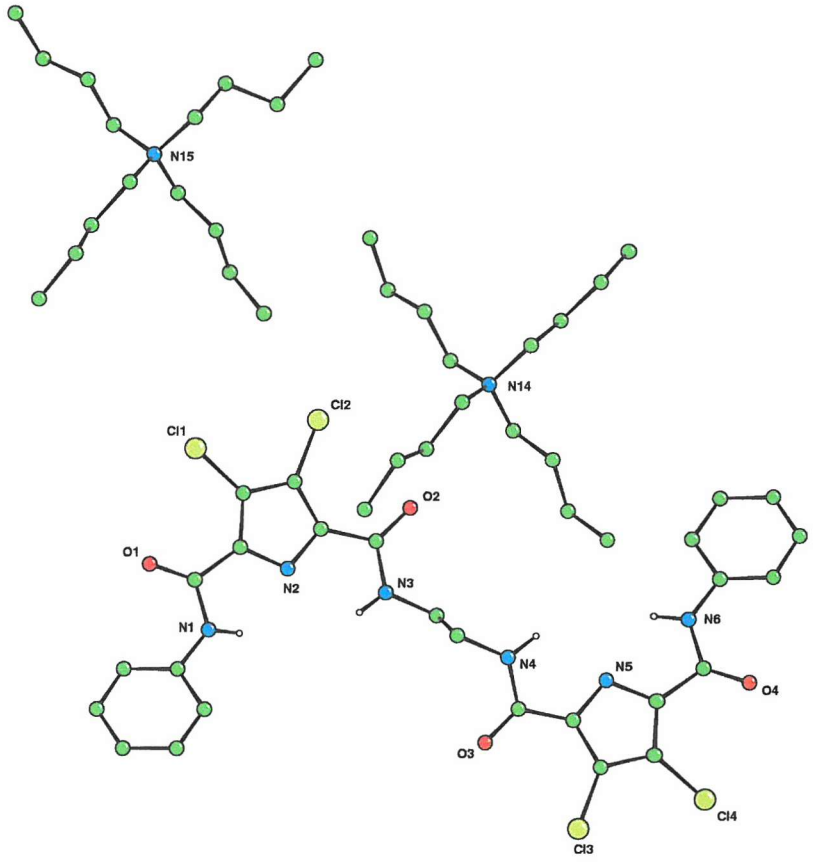

Figure 5.13: The X-ray crystal structures of tetrabutylammonium salt of **103**-$2H^+$. Certain hydrogen atoms are omitted for clarity.

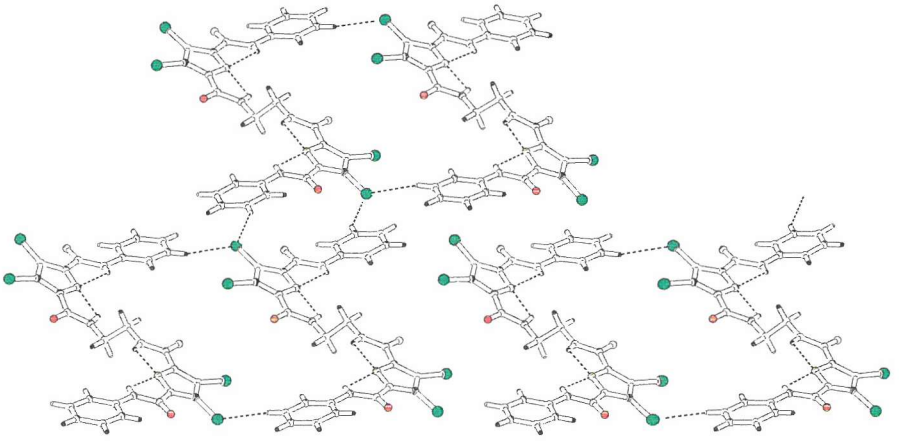

Figure 5.14: Sheets of the tetrabutylammonium salt of **103**-$2H^+$ formed via of two hydrogen bonds ($C_{phenyl}\cdots Cl$ in the range 3.508-4.064 Å and $N_{amide}\cdots N^-_{pyrrole}$ in the range 2.649-2.697 Å respectively). Tetrabutylammonium counter cations and certain hydrogen atoms are omitted for clarity.

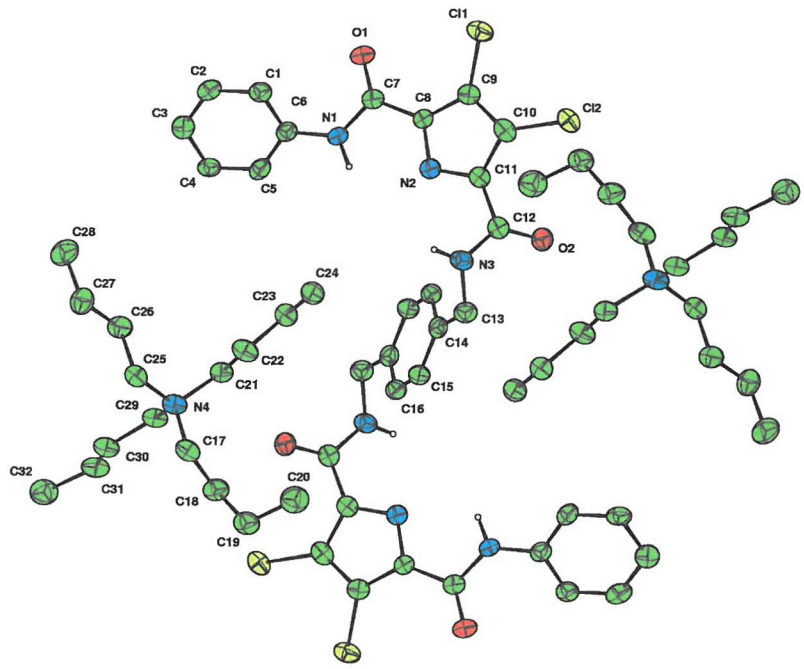

Figure 5.15: The X-ray crystal structures of tetrabutylammonium salt of **106**-$2H^+$ (thermal ellipsoids drawn at the 50% probability level). Certain hydrogen atoms are omitted for clarity.

In bis-tetrabutylammonium **106**-$2H^+$ (Figure 5.15), The $N_{amide}\cdots N^-_{pyrrole}$ distances were found in the range 2.656-2.657 Å. (see Appendix for structure information).

Attempts were also made to crystallise the other dimers and trimers that were synthesised, however, to date these attempts have been unsuccessful.

5.4 Conclusion

Six dimers **101**, **102**, **103**, **104**, **105** and **106** which consist of two 3,4-dichloro amidopyrrole subunits and varieties of the linkages and two trimers **107** and **108** consisting of three 3,4-dichloro amidopyrrole subunits were synthesised. The solid-state results showed the more rigid structures compound **101** and **102** formed the interlocked systems, whilst the less rigid molecules **103** and **106** do not form the interlocked dimer when deprotonated. The crystal structures of **101**-$2H^+$ and **102**-$2H^+$ show that there may be a CH-π interaction between the pendant phenyl groups and the π system of the pyrrole ring. In the structures of the tetrabutylammonium salts of **103**-$2H^+$ and **106**-$2H^+$, the absence of directly attached phenyl groups on both sides of the pyrrole means that this interaction could only occur on one side. Due to the limited number of structures we have obtained we are not in a position to draw general conclusion from these results. Attempts are continuing in the Gale group to crystallise there and similar oligomeric amidopyrrole systems.

6. *Experimental*

6.1 Solvent and reagent pre-treatment

Where necessary solvents were purified prior to use. Dichloromethane was distilled over calcium hydride. Diethyl ether was ditilled from sodium using benzophenone as an indicator. Anyhydrous acetronitrile (water <0.003%) was purchased from Fisher. Anhydrous methanol was bought from Aldrich (99.8%) as was anhydrous dimethylformamide (99.8%). Thionyl chloride was distilled from 10% (*w/w*) triphenyl phosphite and stored under nitrogen. TentaGel S NH_2 resin was purchased from Rapp Polymer, Tübingen (Germany). Peptide and library syntheses on solid phase were performed in polypropylene filtration tubes with polyethylene frits on a Visiprep SPE Vacuum Manifold from Supelco. The reaction containers were agitated either on a shaker (Stuart Scientific Flash Shaker SF1) or on a blood tube rotator (Stuart Scientific Blood Tube Rotator SB1). Thin layer chromatography (TLC) was performed on PET-backed plates Fluka silica gel 60 F_{254}. Fluka silica gel 60, 220-440 mesh, was used for the column chromatography. Commercial grade reagents were used without further purification. Reagents prepared in accordance with literature are so referenced. All of the syntheses were performed under an inert atmosphere of nitrogen. Tetrabutylammonium salts of the anions used during ^1H NMR titration were thoroughly dried overnight under high vacuum.

6.2 Instrumental methods

NMR data were recorded on Bruker AM300, AC300, AV300 and DPX400 spectrometers. The spectra were referenced internally using the residual protio-solvent (^{1}H), the signal of the solvent (^{13}C) and chemical shifts reported in ppm. Low resolution mass spectra were recorded on a Micromass Platform single quadrupole mass spectrometer, wheras high resolution mass spectra were recorded on a VG 70-250-SE normal geometry double focusing mass spectrometer by the mass spectrometry service at the University of Southampton. Elemental analysis were carried out at the University of Strathclyde and by Medac Ltd. Company. Melting points were recorded in open capillaries on a Gallenkamp melting point apparatus and are uncorrected.

6.3 Synthesis

6.3.1 Synthesis included in chapter 2

3,4-Diphenyl-1H-pyrrole-2,5-dicarboxylic acid bis-[(2-amino-ethyl)-amide 47:

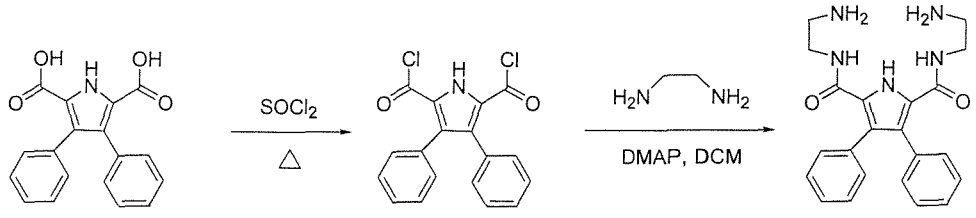

50 **47**

3,4-Diphenylpyrrole-2,5-dicarboxylic acid **50** (1.33 g, 3.4 mmol, 1 equiv.) was heated at reflux in thionyl chloride (30 ml, 411 mmol, 120 equiv.) for 12 h to obtain the acid chloride. The excess of thionyl chloride was removed by rigorous

drying under high vacuum pump. After dissolving the resulting acid chloride in dichloromethane (220 ml), this solution was added dropwise to the solution of ethylenediamine (2.66 g, 34.0 mmol, 10 equiv.) and 5 mg (0.04 mmol, 0.01 equiv.) of DMAP in dichloromethane (20 ml). The reaction was stirred for 48 hours, leading to the pale yellow suspension. The solvent was removed in vacuo and the residue was purified by column chromatography using dichloromethane/methanol (10:3 *v/v*) to yield compound **47**, pale yellow solid (0.93 g, 2.38 mmol, 70%)

M.p. 74°C. R_f = 0.74 (DCM/MeOH (10:3 *v/v*)). ^{1}H NMR 300 MHz in $CDCl_3$ δ (ppm): 2.62 (m, 4H, CH_2NH_2), 3.24 (m, 4H, CONHCH_2), 5.87 (s, 2H, CON*H*), 7.07-7.28 (m, 10H, Ar*H*, + obscured amine NH_2, 4H). ^{13}C NMR 75 MHz in DMSO-d_6 δ (ppm): 41.0, 42.3, 124.4, 126.2, 126.5, 127.6, 130.6, 134.2, 160.4. ES$^+$ mass spectrum, m/z (%): 392 (15) $[M+H]^+$, 785 (15) $[2M+H]^+$. ES$^+$ HRMS: m/z: Calc. for $C_{22}H_{25}N_5O_2$ $[M+H]^+$: 392.2080; found: 392.2081. Elemental analysis: Calc. for $C_{22}H_{25}N_5O_2 \cdot 0.2CH_2Cl_2$: C 65.28, H 6.27, N 17.15; found: C 65.24, H 6.06, N 16.52.

The hexafluorophosphate salt of 3,4-diphenyl-1H-pyrrole-2,5-dicarboxylic acid bis-[(2-amino-ethyl)-amide 48:

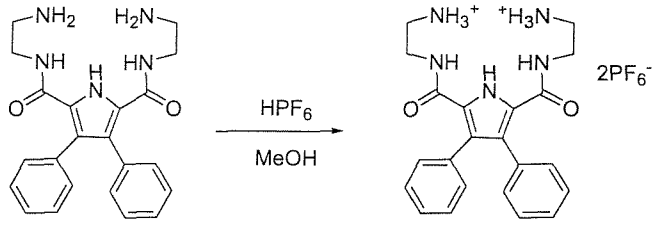

47 **48**

3,4-Diphenyl-1H-pyrrole-2,5-dicarboxylic acid bis-[(2-amino-ethyl)-amide **47** (251 mg, 0.64 mmol, 1 equiv.) was dissolved in methanol (20 ml). Hexafluorophosphatephoric acid (311 mg, 1.28 mmol, 2 equiv.) was added into the solution and stirred for 5 minutes. The solvent was removed in vacuo to yield compound **48**, plae yellow solid (440 mg, 0.64 mmol, 100%).

M.p. 114°C. ^{1}H NMR 300 MHz in DMSO-d_6 δ (ppm): 2.95 (m, 4H, $CH_2NH_3^+$), 3.45 (s, br, 4H, CONHCH_2), 7.14-7.28 (m, 10H, Ar*H*). 7.62 (s, 2H, CON*H*), 7.80 (s, br, 6H, NH_3^+), 12.01 (s, br, ^{1}H, NH-Pyrr). ^{13}C NMR 75 MHz in DMSO-d_6 δ (ppm): 37.3, 39.2, 124.7, 127.4, 128.2, 128.4, 131.3, 134.3, 161.7. ES$^-$

mass spectrum, m/z (%): 144.7 (100) $[PF_6]^-$. ES^+ mass spectrum, m/z (%): 392 (100) $[C_{22}H_{25}N_5O_2+H]^+$. Elemental analysis: Calc. for $C_{22}H_{39}F_{12}N_5O_8P_2 \cdot 0.2CH_2Cl_2$: C 33.38, H 4.97, N 8.85; found: C 33.06, H 4.65, N 7.47.

3,4-Diphenyl-1H-pyrrole-2,5-dicarboxylic acid bis-[(2-acetylamino-ethyl) -amide] 49:

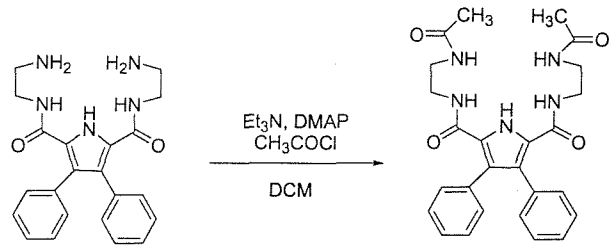

47 **49**

3,4-Diphenyl-1H-pyrrole-2,5-dicarboxylic acid bis-[(2-amino-ethyl)-amide **47** (0.50 g, 1.3 mmol, 1 equiv.) was stirred for 24 h with acetyl chloride (0.25 g, 3.2 mmol, 2.5 equiv.) added with triethylamine (0.52 g, 5.1 mmol, 4 equiv.) and 5 mg (0.04 mmol, 0.03 equiv.) of DMAP in dichloromethane (120 ml). The solvent was removed in *vacuo* and the residue was purified by column chromatography using dichloromethane/methanol (10:1 *v/v*) to yield compound **49**, pale yellow solid (0.25 g, 0.52 mmol, 41%)

M.p. 82°C. R_f = 0.54 (DCM/MeOH (10:1 *v/v*)). ^{1}H NMR 300 MHz in DMSO-d_6 δ (ppm): 1.88 (s, 6H, C*H*$_3$), 3.12 (q, 4H, J = 5.5, C*H*$_2$NHCOCH$_3$), 3.20 (q, 4H, J = 5.5, Pyrrole-CONHC*H*$_2$), 7.14-7.32 (m, 10H, Ar*H*). 7.36 (t, 2H, J = 5.5, N*H*COCH$_3$), 7.94 (t, 2H, J = 5.5, N*H*CO-Pyrr), 11.99 (s, br, 1H, N*H*-Pyrr). ^{13}C NMR 75 MHz in $CDCl_3$ δ (ppm): 23.2, 38.9, 40.1, 123.9, 126.7, 128.3, 128.9, 130.7, 133.1, 161.5, 170.7. ES^+ mass spectrum, m/z (%): 476 (15) $[M+H]^+$, 498 (50) $[M+Na]^+$, 951 (10) $[2M+H]^+$, 973 (50) $[2M+Na]^+$. ES^+ HRMS: m/z: Calc. for $C_{52}H_{58}N_{10}O_8Na$ $[2M+Na]^+$: 973.4331; found: 973.4342. Elemental analysis: Calc. for $C_{26}H_{29}N_5O_4 \cdot 0.25CH_2Cl_2 \cdot 0.25CH_3OH$: C 63.05, H 6.09, N 13.87; found: C 63.14, H 5.86, N 13.44.

6.3.2 Synthesis included in chapter 3

1-Methyl-2-imidazole carboxaldehyde 62:

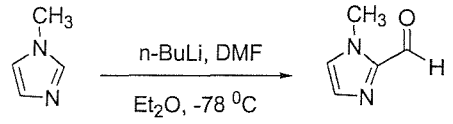

61 **62**

This compound was synthesised via the method in the literature.[122]

1-Methyl imidazole **61** (3.28 g, 40 mmol, 1 equiv.) was dissolved in dry diethyl ether (100 ml) at -78°C. The n-BuLi, 2.5 M in hexane, (16.8 ml, 0.042 mmol, 1.05 equiv.) was then added dropwise and a suspension was formed. This was stirred at -78°C for 1 h and dry DMF (5 ml, 64 mmol, 1.6 equiv.) in dry diethyl ether (8 ml) was quickly added. The reaction was stirred for 12 h and the temperature allowed to rise slowly 5°C. Then over a period of 10 min, water (4 ml) was cautiously added, followed by 4 N HCl (26 ml). The layers were separated and the diethyl ether was washed with 4 N HCl (5 x 6 ml) and the aqueous phase was collected. The combined acid extracts were saturated with K_2CO_3 and extracted with chloroform (4 x 12 ml). The combined chloroform layers were then dried over $MgSO_4$ and the solvent removed under vacuum to yield compound **62**, orange oil (3.74 g, 34 mmol, 85%).

The compound gave ^1H NMR spectrum in $CDCl_3$ accordance with literature.[122]

1-Methyl-2-imidazole carboxaldehyde oxime 63:

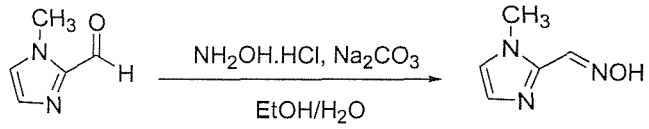

62 **63**

This compound was synthesised via the method in the literature. [122]

A solution of 1-methyl-2-imidazole carboxaldehyde **62** (4.4 g, 40 mmol, 1 equiv.) in ethanol (10 ml) was added to $NH_2OH.HCl$ (2.78 g, 40 mmol, 1 equiv.) and Na_2CO_3 (2.12 g, 20 mmol, 0.5 equiv.) aqueous solution (40 ml) and cooled to 0°C. The resulting white precipitate was filtered and washed with cold 33% ethanol in water (3 x 10 ml) and dried under high vacuum to obtain compound **63** white solid (3.20 g, 29 mmol, 72%).

The compound gave ^1H NMR spectrum in $CDCl_3$ accordance with literature.[122]

1-Methyl-2-aminomethylimidazole 60:

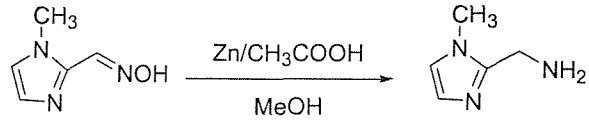

63 **60**

This compound was synthesised via the modified method in the literatures.[122,123] 1-Methyl-2-imidazole carboxaldehyde oxime **63** (1.5 g, 12 mmol, 1 equiv.) was dissolved in methanol (15 ml) and acetic acid (15 ml) solution. Zinc powder (15 g, 153 mmol, 12.75 equiv.) was added by small portion. The reaction mixture was stirred for 12 h and then undissolved zinc was removed by filtration and washed with methanol (10 ml). The solvent was removed and water (3 x 8 ml) was added and evaporated to remove the acetic acid. The mixture was neutralized and then made strong basic (pH > 12) by addition of saturated aqueous KOH solution (8 ml) until the $Zn(OH)_2$ precipitate redissolved. The aqueous solution was extracted with chloroform (3 x 15 ml). The organic layer was collected and dried over $MgSO_4$, and the solvent removed under vacuum to yield compound **60**, orange oil (1.0 g, 9 mmol, 75%).

^1H NMR 300 MHz in $CDCl_3$ δ (ppm): 3.66 (s, 3H, CH_3), 3.92 (2, 2H, CH_2), 6.84 (s, 1H, imidazole*H*), 6.95 (s, 1H, imidazole*H*). ^{13}C NMR 75 MHz in $CDCl_3$ δ (ppm): 32.4, 38.3, 121.0, 127.0, 148.4. ES^+ mass spectrum: *m/z* (%): 112 (100) $[M+H]^+$.

3,4-Diphenyl-1H-pyrrole-2,5-dicarboxylic acid bis-[(1-methyl-1H-imidazol-2-ylmethyl)-amide] 52:

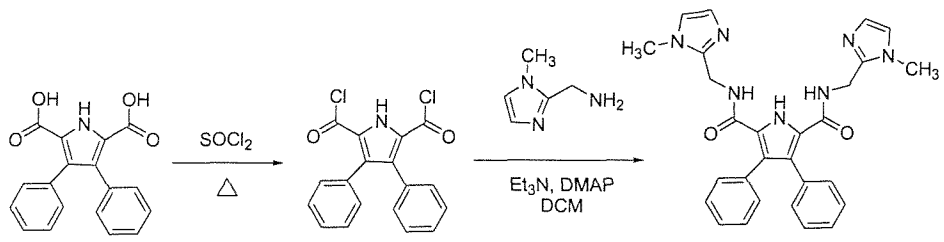

50 **52**

3,4-Diphenyl-*1H*-pyrrole-2,5-dicarboxylic acid **50** (0.50 g, 1.28 mmol, 1 equiv.) was heated at reflux in thionyl chloride (15 ml, 205 mmol, 160 equiv.) overnight to obtain the acid chloride. The excess of thionyl chloride was removed by rigorous drying under high vacuum. After dissolving the resulting acid chloride in dichloromethane (100 ml), this solution was added dropwise to the solution of 1-methyl-2-aminomethylimidazole **60** (0.28 g, 2.56 mmol, 2 equiv.), Et_3N (0.26 g, 2.56 mmol, 2.5 equiv.) and a 5 mg (0.04 mmol, 0.03 equiv.) of DMAP in dichloromethane (20 ml). The solution was stirred for 48 hours. The solvent was removed in *vacuo* and the residue was neutralised with aqueous solution of K_2CO_3 (14.0 g in 100 ml water) and then extracted with dichloromethane (3 x 50 ml). After removing the organic solvent, the residue was recrystallized with acetronitrile to yield compound **52**, pale yellow solid (0.26 g, 0.52 mmol, 40%).

M.p. 234 - 235°C (decom.). ^{1}H NMR 300 MHz in $CDCl_3$ δ (ppm): 3.62 (s, 6H, C*H*$_3$), 4.49 (d, 4H, *J* = 5.4, C*H*$_2$), 6.23 (t, 2H, *J* = 5.4, CON*H*) 6.79 (d, 2H, *J* = 1.2, imidazole*H*), 6.83 (d, 2H, *J* = 1.2, imidazole*H*), 7.10-7.28 (m, 10H, Ar*H*), 10.31 (s, br, 1H, N*H*-Pyrrole). ^{13}C NMR 75 MHz in $CDCl_3$ δ (ppm): 32.8, 35.6, 121.5, 123.6, 126.7, 127.6, 128.0, 128.2, 128.9, 130.5, 132.6, 143.9, 160.2. ES^+ mass spectrum: *m/z* (%): 494 (100) $[M+H]^+$, 987 (90) $[2M+H]^+$. Elemental analysis: Calc. for $C_{28}H_{27}N_7O_2 \cdot 0.5CH_3OH \cdot 0.3CH_2Cl_2 \cdot H_2O$: C 64.63, H 5.59, N 18.26; found: C 64.92, H 5.59, N 17.99.

5-Methyl-3,4-diphenyl-1H-pyrrole-2-carboxylic acid (1-methyl-1H-imidazol-2-ylmethyl)-amide 53:

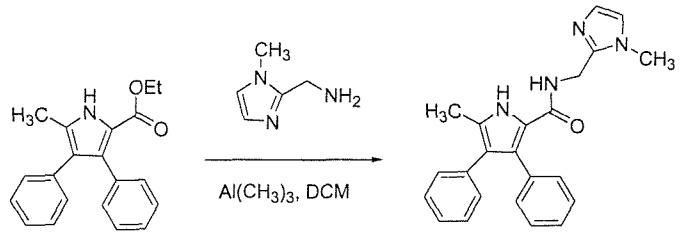

64 **53**

1-Methyl-2-aminomethylimidazole **60** (260 mg, 2.4 mmol, 2 equiv.) was stirred with 2.0 M trimethylaluminium solution in hexane (3 ml, 6 mmol, 5 equiv.) in dichloromethane (40 ml) for 30 min. 5-Methyl-3,4-diphenyl-*1H*-pyrrole-2-carboxylic acid ethyl ester **64** (365 mg, 1.2 mmol, 1 equiv.) was added into the solution and was heated at reflux for 7 days. A diluted hydrochloric acid solution was added dropwise, followed with water (100 ml) and extracted with dichloromethane (2 x 50 ml). The organic solvent was removed in *vacuo* and the residue was purified by column chromatography using dichloromethane/methanol (10:1 *v/v*). The solvent was removed to yield compound **53**, white solid (123 mg, 0.33 mmol, 27%).

M.p. 209 - 210°C (decom.). R_f = 0.40 (MeOH/DCM (1:10 *v/v*)). ^{1}H NMR 300 MHz in $CDCl_3$ δ (ppm): 2.36 (s, 3H, C*H*$_3$Pyrrole), 3.61 (s, 3H, C*H*$_3$imidazole), 4.50 (d, 2H, *J* = 5.4, C*H*$_2$), 6.04 (t, 1H, *J* = 5.4, CON*H*) 6.79 (s, 1H, imidazole*H*), 6.85 (s, 1H, imidazole*H*), 6.99-7.28 (m, 10H, Ar*H*), 9.33 (s, br, 1H, N*H*-Pyrrole). ^{13}C NMR 75 MHz in $CDCl_3$ δ (ppm): 1.1, 12.3, 35.5, 121.5, 125.9, 127.6, 127.8, 128.0, 138.5, 129.0, 130.1, 130.5, 134.4, 134.6, 161.0. ES^+ mass spectrum: *m/z* (%): 371 (100) $[M+H]^+$, 741 (10) $[2M+H]^+$. Elemental analysis: Calc. for $C_{23}H_{22}N_4O \cdot 0.8CH_3OH$: C 72.17, H 6.41, N 14.15; found: C 72.02, H 6.20, N 14.19.

3,4-Diphenyl-1H-pyrrole-2-carboxylic acid pyridin-2-ylamide 54:

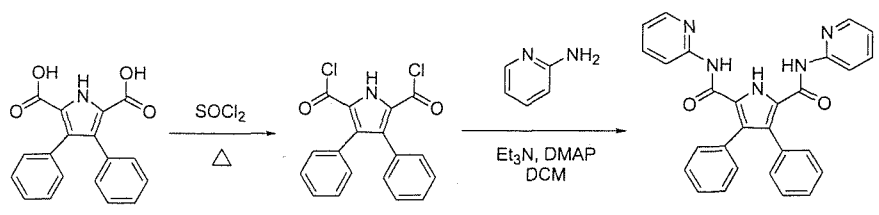

50 **54**

3,4-Diphenyl-*1H*-pyrrole-2,5-dicarboxylic acid **50** (2.0 g, 6.5 mmol, 1 equiv.) was heated at reflux in thionyl chloride (40 ml, 548 mmol, 84 equiv.) overnight to obtain the acid chloride. The excess of thionyl chloride was removed by rigorous drying under high vacuum. After dissolving the resulting acid chloride in dichloromethane (100 ml), this solution was added dropwise to the solution of 2-amino pyridine (1.22 g, 12.9 mmol, 2 equiv.), Et_3N (1.57 g, 15.1 mmol, 2.3 equiv.) and a 5 mg (0.04 mmol, 0.005 equiv.) of DMAP in dichloromethane (20 ml). The solution was stirred for 24 hours. The solvent was removed in *vacuo* and the residue was neutralised with aqueous solution of H_2CO_3 (14.0 g in 100 ml water) and then extracted with dichloromethane (2 x 100 ml). After removing the organic solvent, the residue was recrystallized with acetronitrile to yield compound **54**, yellow solid (0.62 g, 1.35 mmol, 21%).

M.p. >245°C. R_f = 0.16 (DCM/MeOH (100:2 *v/v*)). ^{1}H NMR 300 MHz in $CDCl_3$ δ (ppm): 6.95-8.26 (m, 20H, Ar*H* and Pyr*H*), 8.04 (s, 2H, CON*H*Ar), 10.46 (s, br, 1H, N*H*-Pyrrole). ^{13}C NMR 75 MHz in DMSO-d_6 δ (ppm): 114.4, 119.9, 124.6, 127.6, 128.8, 129.3, 130.8, 132.3, 138.2, 148.3, 151.0, 158.4. ES^+ mass spectrum: *m/z* (%): 460 (100) $[M+H]^+$. ES^+ HRMS: m/z: Calc. for $C_{28}H_{22}N_5O_2$ $[M+H]^+$: 460.1768; found: 460.1761. Elemental analysis: Calc. for $C_{28}H_{21}N_5O_2 \cdot 0.2H_2O$: C 72.62, H 4.66, N 15.12; found: C 72.76, H 4.48, N 15.12.

5-Methyl-3,4-diphenyl-1H-pyrrole-2-carboxylic acid pyridin-2-ylamide 55:

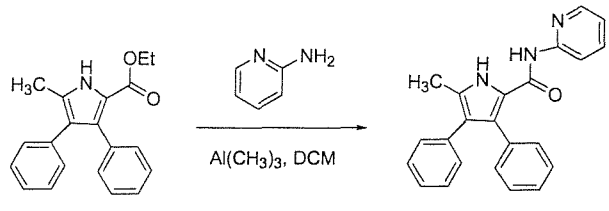

64 **55**

2-Amino pyridine (3.08 g, 32.7 mmol, 10 equiv.) was stirred with 2.0 M Trimethylaluminium solution in hexane (12 ml, 24 mmol, 7 equiv.) in dichloromethane (50 ml) for 30 min. 5-Methyl-3,4-diphenyl-*1H*-pyrrole-2-carboxylic acid ethyl ester **64** (1 g, 3.3 mmol, 1 equiv.) was added into the solution

and was heated at reflux for 5 days. A diluted hydrochloric acid solution was added dropwise, followed with water (50 ml) and extracted with dichloromethane (2 x 50 ml). The organic solvent was removed in *vacuo* and the residue was purified by column chromatography using dichloromethane/methanol (100:2 *v/v*). The solvent was removed and the residue was recrystallized with acetronitrile to yield compound **55**, white solid (157 mg, 0.44 mmol, 13%).

M.p. 225 – 227°C. R_f = 0.24 (DCM/MeOH (100:2 *v/v*)). ^{1}H NMR 300 MHz in $CDCl_3$ δ (ppm): 2.40 (s, 3H, C*H*$_3$), 6.70-8.11 (m, 16H, Ar*H* and Pyr*H*), 7.98 (s, 1H, CON*H*Ar), 9.42 (s, br, 1H, N*H*-Pyrrole). ^{13}C NMR 75 MHz in DMSO-d_6 δ (ppm): 12.5, 114.2, 119.3, 126.1, 128.1, 128.3, 129.3, 130.2, 130.9, 134.1, 134.5, 137.9, 148.3, 151.7, 154.4. ES$^+$ mass spectrum: *m/z* (%): 354 (100) [M+H]$^+$, 707 (10) [2M+H]$^+$. ES$^+$ HRMS: m/z: Calc. for $C_{23}H_{20}N_3O$ [M+H]$^+$: 354.1601; found: 354.1599. Elemental analysis: Calc. for $C_{23}H_{19}N_3O{\cdot}0.9H_2O$: C 74.74, H 5.67, N 11.37; found: C 74.99, H 5.57, N 11.11.

N,N'-bis-(1-methyl-1H-imidazol-2-ylmethyl)-isophthalamide 56:

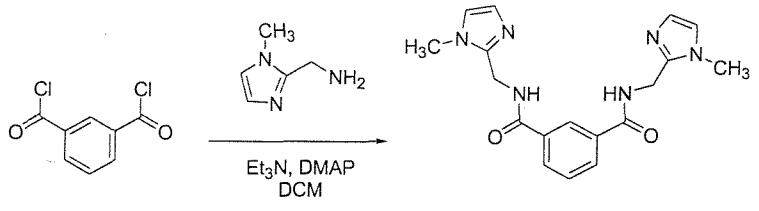

56

Isophthaloyl chloride (300 mg, 1.48 mmol, 1 equiv.) was dissolved in dry dichloromethane (30 ml), this solution was added dropwise to the solution of 1-methyl-2-aminomethylimidazole **60** (410 mg, 3.69 mmol, 2.5 equiv.), Et_3N (373 mg, 3.69 mmol, 2.5 equiv.) and a 5 mg (0.04 mmol, 0.03 equiv.) of DMAP in dichloromethane (10 ml). The solution was stirred for 24 hours. The solvent was removed in *vacuo* and the residue was neutralised with aqueous solution of K_2CO_3 (14.0 g in 100 ml water). The precipitate was collected by filtration and washed with diethyl ether (2 x 10 ml) to yield compound **56**, white solid (456 mg, 1.29 mmol, 87%).

M.p. 218 - 219°C. ^{1}H NMR 300 MHz in DMSO-d_6 δ (ppm): 3.65 (s, 6H, C*H*$_3$), 4.53 (s, 4H, C*H*$_2$), 6.79 (s, 2H, imidazole*H*), 7.08 (s, 2H, imidazole*H*), 7.54 (t,

1H, J = 8.2, Ar*H* meta to C=O), 8.00 (d, 2H, J = 8.2, Ar*H* para to C=O), 8.36 (s, 1H, Ar*H* ortho to both C=O), 9.04 (s, br, 2H, CON*H*). ^{13}C NMR 75 MHz in DMSO-d_6 δ (ppm): 32.4, 35.4, 121.8, 126.4, 126.5, 128.3, 130.0, 134.1, 144.5, 165.6. ES$^+$ mass spectrum: *m/z* (%): 177 (100) $[M+2H]^{2+}$, 353 (20) $[M+H]^+$. Elemental analysis: Calc. for $C_{18}H_{20}N_6O_2 \cdot 0.67CH_2Cl_2 \cdot 1.67H_2O$: C 51.07, H 5.66, N 19.14; found: C 50.78, H 5.49, N 19.29.

Pyridine-2,6-dicarboxylic acid bis-[(1-methyl-1H-imidazol-2-ylmethyl)-amide] 57:

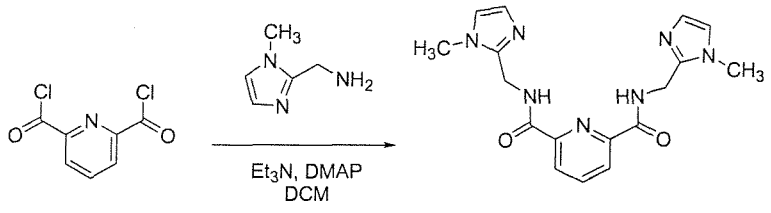

57

2,6-Pyridinedicarbonyl dichloride (177 mg, 0.87 mmol, 1 equiv.) was dissolved in dry dichloromethane (30 ml), this solution was added dropwise to the solution of 1-methyl-2-aminomethylimidazole **60** (241 mg, 2.17 mmol, 2.5 equiv.), Et_3N (219 mg, 2.17 mmol, 2.5 equiv.) and a 5 mg (0.04 mmol, 0.05 equiv.) of DMAP in dichloromethane (10 ml). The solution was stirred for 24 hours. The solvent was removed in *vacuo* and the residue was neutralised with aqueous solution of K_2CO_3 (14.0 g in 100 ml water) and then extracted with dichloromethane (3 x 50 ml) and a few amount of methanol. After removing the organic solvent, the residue was collected to yield compound **57**, white solid (234 mg, 0.66 mmol, 76%).

M.p. 239 - 240°C (decom.). ^{1}H NMR 300 MHz in DMSO-d_6 δ (ppm): 3.65 (s, 6H, C*H*$_3$), 4.61 (d, 4H, J = 5.9 C*H*$_2$), 6.79 (s, 2H, imidazole*H*), 7.06 (s, 2H, imidazole*H*), 8.13-8.24 (m, 3H, pyridine*H*), 9.91 (t, 2H, J = 5.9, CON*H*). ^{13}C NMR 75 MHz in DMSO-d_6 δ (ppm): 32.5, 34.9, 122.0, 124.7, 126.4, 139.5, 144.6, 148.6, 163.0. ES$^+$ mass spectrum: *m/z* (%): 354 (100) $[M+H]^+$, 707 (90) $[2M+H]^+$. Elemental analysis: Calc. for $C_{17}H_{19}N_7O_2 \cdot 0.5CH_3OH \cdot 0.5H_2O$: C 55.55, H 5.86, N 25.91; found: C 55.81, H 5.65, N 25.96.

1H-pyrrole-2-carboxylic acid (1-methyl-1H-imidazol-2-ylmethyl)-amide 58:

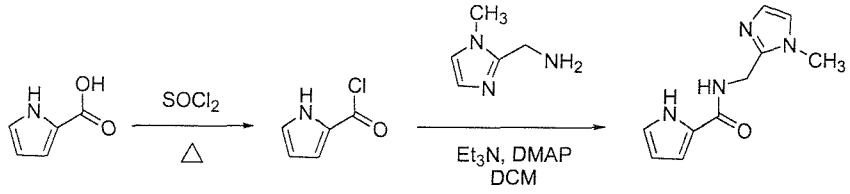

58

Pyrrole-2-carboxylic acid (300 mg, 2.70 mmol, 1 equiv.) was heated at reflux in thionyl chloride (15 ml, 205 mmol, 76 equiv.) for 12 h to obtain the acid chloride. The excess of thionyl chloride was removed by rigorous drying under high vacuum. After dissolving the resulting acid chloride in dichloromethane (50 ml), this solution was added dropwise to the solution of 1-methyl-2-aminomethylimidazole **60** (450 mg, 4.05 mmol, 1.5 equiv.), Et_3N (818 mg, 8.10 mmol, 3 equiv.) and a 5 mg (0.04 mmol, 0.01 equiv.) of DMAP in dichloromethane (10 ml). The solution was stirred for 72 hours. The solvent was removed in *vacuo* and the residue was neutralised with aqueous solution of K_2CO_3 (14.0 g in 100 ml water) and then extracted with dichloromethane (2 x 50 ml). After removing the organic solvent, the residue was purified by column chromatography using dichlomethane/methanol (10:1 *v/v*). The solvent was removed to yield compound **58**, white solid (332 mg, 1.63 mmol, 60%).

M.p. 197 - 199°C. R_f = 0.38 (MeOH/DCM (1:10 *v/v*)). ^{1}H NMR 300 MHz in DMSO-d_6 δ (ppm): 3.63 (s, 3H, C*H*$_3$), 4.47 (d, 2H, *J* = 5.1, C*H*$_2$), 6.07 (m, 1H, *H*-Pyrrole), 6.79 (d, 1H, *J* = 1.5, imidazole*H*), 6.85 (m, 2H, *H*-Pyrrole), 7.06 (d, 1H, *J* = 1.2, imidazole*H*), 8.46 (t, 1H, *J* = 5.1, CON*H*), 11.48 (s, br, 1H, N*H*-Pyrrole). ^{13}C NMR 75 MHz in DMSO-d_6 δ (ppm): 32.4, 34.6, 108.7, 110.5, 121.5, 121.8, 125.8, 126.4, 145.0, 160.4. ES$^+$ mass spectrum: *m/z* (%): 205 (100) [M+H]$^+$. Elemental analysis: Calc. for $C_{10}H_{12}N_4O_2$: C 58.81, H 5.92, N 27.42; found: C 58.52, H 6.19, N 27.14.

1H-pyrrole-2-carboxylic acid (1-methyl-1H-imidazol-2-ylmethyl)-amide 59:

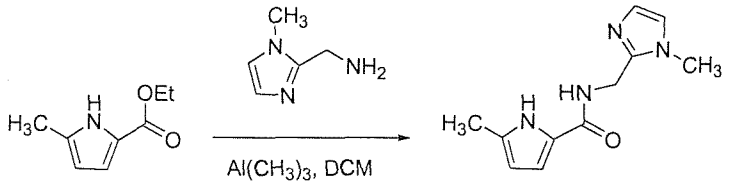

65 **59**

1-Methyl-2-aminomethylimidazole **60** (0.72 g, 6.54 mmol, 2 equiv.) was stirred with 2.0 M trimethylaluminium solution in hexane (6.6 ml, 13.08 mmol, 4 equiv.) in dichloromethane (50 ml) for 30 min. 5-Methyl-1H-pyrrole-2-carboxylic acid ethyl ester **65** (0.50 g, 3.27 mmol, 1 equiv.) was added into the solution and was heat at reflux for 5 days. A diluted hydrochloric acid solution was added dropwise, followed with water (50 ml) and extracted with dichloromethane (2 x 50 ml). The organic solvent was removed in *vacuo* and the residue was purified by column chromatography using dichlomethane/methanol (100:5 *v/v*). The solvent was removed to yield compound **59**, pale yellow solid (185 mg, 0.85 mmol, 26%).

M.p. 230 - 232°C (decom.). R_f = 0.43 (DCM/MeOH (10:1 *v/v*)). ^{1}H NMR 300 MHz in DMSO-d_6 δ (ppm): 2.16 (s, 3H, CH_3-Pyrrole), 3.63 (s, 3H, C*H*$_3$), 4.45 (d, 2H, *J* = 5.5, C*H*$_2$), 5.76 (s, br, 1H, *H*-Pyrrole), 6.71 (s, br, 1H, imidazole*H*), 6.78 (s, 1H, *H*-Pyrrole), 7.06 (s, 1H, imidazole*H*), 8.27 (t, 1H, *J* = 5.5, CON*H*), 11.22 (s, br, 1H, N*H*-Pyrrole). ^{13}C NMR 75 MHz in DMSO-d_6 δ (ppm): 12.6, 32.4, 34.6, 107.1, 111.1, 121.8, 124.3, 126.3, 131.6, 145.1, 160.4. ES$^+$ mass spectrum: *m/z* (%): 219 (100) $[M+H]^+$, 437 (47) $[2M+H]^+$, 459 (49) $[2M+Na]^+$. Elemental analysis: Calc. for $C_{11}H_{14}N_4O_2 \cdot 0.33CH_3OH$: C 59.46, H 6.75, N 24.47; found: C 59.21, H 6.46, N 24.32.

Preparation of the hexafluorophosphate salts of 52-59:

The compound (1 equiv.) was dissolved in methanol (10 ml) and hexafluorophosphoric acid (60% *wt* in water) 1 or 2 equiv. depended on numbers of amido group of the compound was added. The solution was stirred for 5 minutes and the solvent was removed and dried in high vacuum pump.

6.3.3 Synthesis included in chapter 4

3,4-Diphenyl-1H-pyrrole-2,5-dicarboxylic acid 2-[(2-amino-ethyl)-amide] 5-({2-[1-(4,4-dimethyl-2,6-dioxo-cyclohexylidene)-2-phenyl-ethylamino]-ethyl]}-amide) 74:

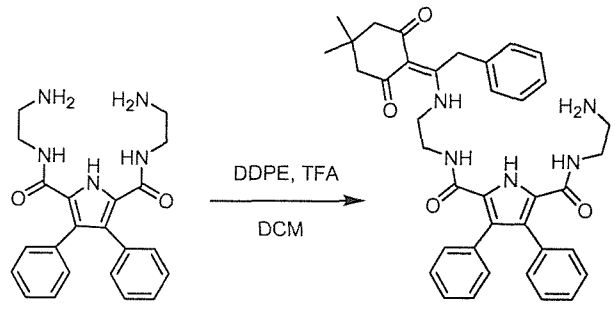

47 **74**

3,4-Diphenyl-1H-pyrrole-2,5-dicarboxylic acid bis-[(2-amino-ethyl)-amide] **47** (1.50 g, 3.83 mmol, 3 equiv.) was dissolved in dichloromethane (50 ml) and a catalyst quantity of TFA was added. 2-Phenylacetyldimedone (0.33 g, 1.28 mmol, 1 equiv.) was dissolved in dichloromethane (200 ml) and the solution was added dropwise into the former solution. After stirred for 48 h, the solution was washed with 2 M Na_2CO_3 (2 x 100 ml) and water (2 x 100 ml). The organic solvent was removed in *vacuo* and the residue was purified by column chromatography using dichlomethane/methanol (10:1 *v/v*) to yield compound **74**, pale yellow solid (0.32 g, 0.50 mmol, 39%).

M.p. 118 - 120°C. R_f = 0.35 (DCM/MeOH (10:1 *v/v*)). ^{1}H NMR 300 MHz in $CDCl_3$ δ (ppm): 1.07 (s, 6H, $(CH_3)_2C$), 2.42 (br s, 4H, CH_2CO), 2.63 (t, 2H, J = 5.7, CH_2NH), 3.27 (q, 4H, J = 5.7, Pyrrole-CONHCH_2), 3.39 (m, 2H, $OCNHCH_2CH_2NH$), 4.51 (s, 2H, CH_2-Ph), 5.71 (t, 1H, J = 5.7, $OCNHCH_2CH_2NH$), 5.87 (t, 1H, J = 5.5, $NHCH_2CH_2NH_2$), 7.05 – 7.31 (m, 15H, Ar*H*), 13.55 (m, 1H, NHC=C). ^{13}C NMR 75 MHz in $CDCl_3$ δ (ppm): 28.5, 30.2, 35.0, 39.1, 41.3, 42.3, 42.7, 53.1, 108.4, 123.4, 124.7, 126.3, 126.7, 126.8, 128.2, 128.3, 128.9, 129.0, 130.8, 130.9, 133.3, 133.4, 135.9, 160.8, 161.0, 174.2. ES^+ mass spectrum: *m/z* (%): 632 (100) $[M+H]^+$, 1264 (53) $[2M+H]^+$. ES^+ HRMS: m/z: Calc. for $C_{38}H_{42}N_5O_4$

$[M+H]^+$: 632.3231; found: 632.3255. Elemental analysis: Calc. for $C_{38}H_{41}N_5O_4 \cdot 0.33CH_2Cl_2$: C 69.75, H 6.36, N 10.61; found: C 69.81, H 6.52, N 10.61.

4-{2-[(5-{2-{1-(4,4-Dimethyl-2,6-dioxo-cyclohexylidene)-2-phenyl-ethyl-amino]-ethylcarbamoyl}-3,4-diphenyl-1H-pyrrole-2-carbonyl)-amino]-ethylcar-bamo-yl}-4-(9H-fluoren-9-ylmethoxycarbonylamino)-butyric acid tert-butyl ester 75:

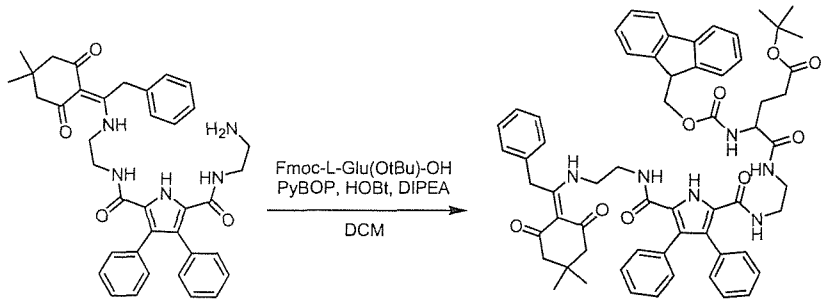

74 **75**

A solution of N-α-Fmoc-L-glutamic acid γ-*tert*-butyl ester (213 mg, 0.50 mmol, 1.05 equiv.), PyBOP (247 mg, 0.475 mmol, 1 equiv.), and HOBt (73 mg, 0.475 mmol, 1 equiv.) in dichloromethane (15 ml) was stirred at room temperature for 15 min and then added to a solution of compound **74** (300 mg, 0.475 mg, 1 equiv.) in dichloromethane (5 ml). After addition of DIPEA (0.19 ml, 1.09 mmol, 2.3 equiv.) the resulting reaction mixture was stirred for 48 h. More dichloromethane (50 ml) was added and the mixture was washed with water (50 ml) to removed unwanted salts. The organic layer was dried over $MgSO_4$ and the solvent was removed in *vacuo*. The residue was purified by column chromatography using dichlomethane/methanol (10:1 *v/v*) to yield compound **75**, pale yellow solid (371 mg, 0.36 mmol, 75%).

M.p. 126 - 128°C. R_f = 0.63 (DCM/MeOH (10:1 *v/v*)). ^{1}H NMR 300 MHz in $CDCl_3$ δ (ppm): 1.07 (s, 6H, $(CH_3)_2C$), 1.45 (s, 9H, $(CH_3)_3C$), 1.88 (m, 1H, $CH_aH_bCH_2$-Boc), 2.04 (m, 1H, $CH_aH_bCH_2$-Boc), 2.29 (m, 1H, CH_aH_b-Boc), 2.42 (br s, 4H, $(CH_3)_2CCH_2CO$ and 1H, CH_aH_b-Boc), 3.26 (br m, 4H, Pyrrole-$CONHCH_2$), 3.37 (br m, 4H, $OCNHCH_2CH_2NH$), 4.13 (m, 1H, $COCH(CH_2)_2$-Boc), 4.21 (m, 1H, CH_2CH-fluorenyl), 4.40 (d, 2H, J = 6.4, CH_2-fluorenyl), 4.51 (br s, 2H, CH_2Ph), 5.71 (m, 1H, $OCNH(CH_2)_2NHC{=}C$), 5.81 (m, 1H, $OCNH(CH_2)_2NHCO$), 6.76 (m,

1H, N*H*C=C), 7.06 (d, 2H, *J* = 7.3, fluorenyl*H*), 7.17 – 7.31 (m, 15H, Ar*H*), 7.39 (t, 2H, *J* = 7.3, fluorenyl*H*), 7.59 (m, 2H, fluorenyl*H*), 7.75 (d, 2H, *J* = 7.3, fluorenyl*H*), 10.38 (m, 1H, N*H*-Fmoc), 13.55 (m, 1H, NHC=C). ^{13}C NMR 100 MHz in $CDCl_3$ δ (ppm): 28.2, 28.4, 30.2, 31.9, 35.0, 36.5, 39.1, 42.7, 47.3, 53.2, 81.2, 108.4, 120.1, 125.3, 126.6, 126.7, 127.2, 127.9, 128.1, 128.4, 128.9, 129.0, 129.1, 130.7, 130.8, 135.8, 141.4, 160.8, 171.8, 174.2. ES$^+$ mass spectrum: *m/z* (%): 1039 (25) $[M+H]^+$, 1061 (55) $[M+Na]^+$. Elemental analysis: Calc. for $C_{62}H_{66}N_6O_9{\cdot}2CH_2Cl_2.3CH_3OH$: C 61.65, H 6.33, N 6.44; found: C 61.52, H 6.47, N 6.30.

4-{2-[(5-{2-{1-(4,4-Dimethyl-2,6-dioxo-cyclohexylidene)-2-phenyl-ethyl-amino]-ethylcarbamoyl}-3,4-diphenyl-1H-pyrrole-2-carbonyl)-amino]-ethylcar-bamo-yl}-4-(9H-fluoren-9-ylmethoxycarbonylamino)-butyric acid 76:

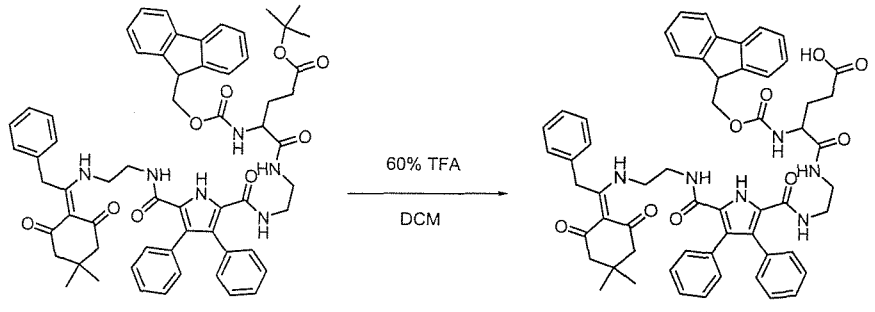

75 **76**

Compound **75** (450 mg, 0.43 mmol) was stirred vigorously in 60% TFA in dichloromethane (10 ml) for 24 h at room temperature. Toluene (150 ml) was added and the solvents were removed under *vacuo*. The residue was purified by column chromatography using dichlomethane/methanol (10:1 *v/v*) to yield the cream solid. After washed with Et_2O, compound **76** obtained as a white solid (290 mg, 0.29 mmol, 68%).

M.p. 138 – 140°C. R_f = 0.50 (DCM/MeOH (10:1 *v/v*)). ^{1}H NMR 300 MHz in $CDCl_3$ δ (ppm): 1.04 (s, 6H, $(CH_3)_2C$), 1.95 (m, 1H, $CH_aH_bCH_2$-Boc), 2.11 (m, 1H, $CH_aH_bCH_2$-Boc), 2.41 (m, 4H, $(CH_3)_2CCH_2CO$ and 2H, CH_2-Boc), 3.32 (br m, 8H, Pyrrole-CONH$(CH_2)_2$), 4.12 (m, 1H, COC*H*$(CH_2)_2$-Boc), 4.27 (m, 1H, CH_2CH-fluorenyl and 2H, CH_2-fluorenyl), 4.46 (br s, 2H, CH_2Ph), 5.98 (m, 2H, Pyrrole-CON*H*), 6.16 (m, 1H, N*H*C=C), 7.02 (d, 2H, *J* = 7.3, fluorenyl*H*), 7.12 – 7.27 (m, 15H, Ar*H*), 7.35 (t, 2H, *J* = 7.3, fluorenyl*H*), 7.72 (d, 2H, *J* = 7.3, fluorenyl*H*), 11.32

(br s, 1H, N*H*-Fmoc), 13.42 (m, 1H, NHC=C). ^{13}C NMR 75 MHz in $CDCl_3$ δ (ppm): 28.3, 30.2, 35.1, 38.8, 39.6, 42.5, 47.1, 52.8, 54.3, 67.1, 108.3, 120.0, 123.6, 125.2, 126.8, 127.2, 127.6, 127.8, 128.0, 128.7, 128.9, 130.7, 132.8, 133.1, 135.6, 141.3, 143.9, 156.3, 161.5, 161.6, 174.3, 176.3. ES^- mass spectrum: *m/z* (%): 981 (100) $[M-H]^-$. ES^+ HRMS: m/z: Calc. for $C_{58}H_{58}N_6O_9Na$ $[M+Na]^+$: 1005.4157; found: 1005.4128. Elemental analysis: Calc. for $C_{58}H_{58}N_6O_9 \cdot 1.2CH_3OH$: C 69.60, H 6.20, N 8.23; found: C 69.35, H 5.95, N 8.32.

Preparation of 77:

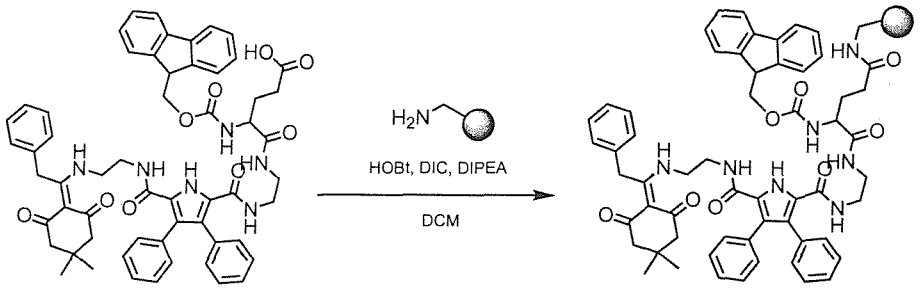

76 **77**

A solution of **76** (38 mg, 0.04 mmol, 1.5 equiv.), DIC (5 mg, 0.04 mmol, 1.5 equiv.), and HOBt (5 mg, 0.04 mmol, 1.5 equiv.) in dichloromethane (2 ml) was stirred for 15 min and then added to pre-swollen resin (100 mg, 0.026 mmol free NH_2, 1 equiv.) in dichloromethane (1 ml) followed by addition of neat DIPEA (18 µl, 0.10 mmol, 4 equiv.). After agitation on a tube rotator for 24 h at room temperature the resin was drained, washed with DMF (3 x 5 ml), dichloromethane (3 x 5 ml), methanol (3 x 5 ml) and diethyl ether (3 x 5 ml) and dried in high vacuum. A quantitative ninhydrin test indicated almost complete coupling of free amino groups on the resin (0.009 mmol/g, 3%).

Quantitative ninhydrin test:

Reagent A: Solution 1; Reagent grade phenol (40 ml) was dissolved in hot absolute ethanol (10 ml). After cooling down, the solution was stirred with Amberlite mixed-bed resin MB-3 (4 g) for 60 min, which was removed by filtration. Solution 2; Potassium cyanide (65 mg) was dissolved in distilled water (100 ml). An

aliquot (2 ml) of this solution was diluted with distilled pyridine (100 ml) and stirred with Amberlite mixed-bed MB-3 (4 g) for 60 min, which was removed by filtration. Solution 1 and 2 were mixed together.

Reagent B: Ninhydrin (25 g) was dissolved in absolute ethanol (50 ml) and stored in the dark. To a known quantity of resin (3 – 5 mg) was added reagent A (7 drops) and reagent B (3 drops). A control was prepared using the stains without the resin present. Both test tubes were heated at 100 °C for 5 min. A 60% solution of ethanol in water was added to each test tube and the solution transferred to 25 ml volumetric flasks through a wool plug in a pipette. A concentrated solution of $Et_4N^+Cl^-$ in CH_2Cl_2 (2 x 0.5 ml) was used to wash each sample tube. A 60% solution of ethanol in water was added to a volume of 10 ml. The UV absorbance was measured at 570 nm. The control sample was used as blank to run the background. The loading of the resin was calculated using the following formula:

$$\text{Substitution (mmol/g)} = (A_{570} \times V \times 10^3) / (\varepsilon_{570} \times W)$$

Where ε_{570} (1.5×10^4 $M^{-1}cm^{-1}$) is the extinction coefficient of the piperidyl-fulvene adduct at $\lambda = 570$ nm, V is the final volume (ml), W is the weight of the resin sample (mg) and A_{570} is the measured absorbance.

Quantitative Fmoc-test:

A known quantity of resin (3 – 5 mg) was treated with a solution of 20% piperidine in DMF (1 ml) for 15 min. The solution was filtered through glass wool and the volume of filtrate made up to 25 ml with 20% piperidine in DMF. The absorbance was deduced from the following equation:

$$\text{mmol/g} = (A_{302} \times V \times 10^3) / (\varepsilon_{302} \times W)$$

Where ε_{302} (7800 $M^{-1}cm^{-1}$) is the extinction coefficient of the piperidyl-fulvene adduct at $\lambda = 302$ nm, V is the final volume (ml), W is the weight of the resin sample (mg) and A_{302} is the measured absorbance of the pipiperidyl-fulvene adduct.

General procedure for Fmoc deprotection on the solid-phase:

The Fmoc-resin was suspended in a solution of 20% piperidine in DMF (20 ml per g resin) and agitated for 30 to 45 min. The resin was drained and washed with

dichloromethane (3 x), DMF (3 x) and dichloromethane (3 x) (10 ml solvent per g resin). The procedure was repeated once and the progress of the deprotection monitored by the ninhydrin test.

General procedure for DDPE deprotection on the solid-phase:

The DDPE-resin was suspended in a solution of 5% $NH_2NH_2{\cdot}H_2O$ in DMF (20 ml per g resin) and agitated for 120 to 150 min. The resin was drained and washed with dichloromethane (3 x), DMF (3 x) and dichloromethane (3 x) (10 ml solvent per g resin). The progress of the deprotection monitored by the ninhydrin test.

Synthesis of the tweezer receptor receptor library 82:

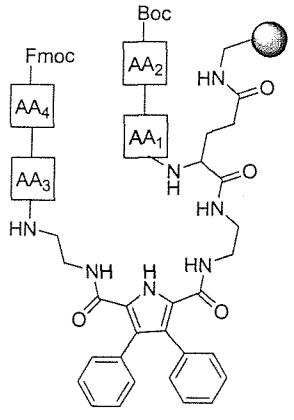

82

After performing **77** (100 mg, 26 μmol) with the Fmoc deprotection step (as described in the general procedure) a qualitative ninhydrin test showed free amino functions, as expected. Following a subsequent Fmoc deprotection (see general procedure) to achieve **78**, the resin was then divided into 6 equal portions. Each portion was pre-swollen in DMF (1 ml). A solution of a Fmoc-protected amino acid (8.7 μmol, 2 equiv.), DIC (1.1 mg, 8.7 μmol) and HOBt (1.2 mg, 8.7 μmol) in DMF (1 ml) was pre-activated for 15 minutes and then added to each portion followed by DIPEA (2.23 mg, 17.3 μmol, 3 μl). Each portion was agitated on a tube rotator for at least 18-24 h at room temperature. The portions were washed with dichloromethane (3 x 2 ml), DMF (3 x 2 ml) and dichloromethane (3 x 2 ml) and dried. The success of

the coupling step was monitored by a qualitative ninhydrin test. Each coupling cycle was repeated until a ninhydrin test showed no free amino functions to achieve **79**. The quantities of Fmoc-amino acid used per coupling cycle were as follows: Gly (2.6 mg), L-Val (2.9 mg), L-Phe (3.4 mg), L-Lys(Boc) (4.1 mg), L-Ser(*t*Bu) (3.3 mg), Gln (3.2 mg).

After each successful coupling step, the resin was re-combined and Fmoc-deprotected as described in the general procedure and monitored by a qualitative ninhydrin test. The resin was divided into 5 equal portions. Each portion was pre-swollen in DMF (1 ml). A solution of a Boc-protected amino acid (10.4 μmol, 2 equiv.), DIC (1.3 mg, 10.4 μmol) and HOBt (1.4 mg, 10.4 μmol) in DMF (1 ml) was pre-activated for 15 minutes and then added to each portion followed by DIPEA (2.68 mg, 20.8 μmol, 3.6 μl). Each portion was agitated on a tube rotator for at least 18-24 h at room temperature. The portions were washed with dichloromethane (3 x 2 ml), DMF (3 x 2 ml) and dichloromethane (3 x 2 ml) and dried. The success of the coupling step was monitored by a qualitative ninhydrin test. Each coupling cycle was repeated until a ninhydrin test showed no free amino functions to achieve **80**. The quantities of Boc-amino acid used per coupling cycle were as follows: Gly (1.8 mg), L-Ala (1.9 mg), L-Phe (2.8 mg), L-Glu(O*t*Bu) (3.2 mg), L-Val (2.3 mg).

After each successful coupling step, the resin was re-combined and DDPE-deprotected as described in the general procedure and monitored by a qualitative ninhydrin test to achieve **81**. The resin was divided into 5 equal portions. Each portion was pre-swollen in DMF (1 ml). A solution of a Fmoc-protected amino acid (10.4 μmol, 2 equiv.), DIC (1.3 mg, 10.4 μmol) and HOBt (1.4 mg, 10.4 μmol) in DMF (1 ml) was pre-activated for 15 minutes and then added to each portion followed by DIPEA (2.68 mg, 20.8 μmol, 3.6 μl). Each portion was agitated on a tube rotator for at least 18-24 h at room temperature. The portions were washed with dichloromethane (3 x 2 ml), DMF (3 x 2 ml) and dichloromethane (3 x 2 ml) and dried. The success of the coupling step was monitored by a qualitative ninhydrin test. Each coupling cycle was repeated until a ninhydrin test showed no free amino functions. The quantities of Fmoc-amino acid used per coupling cycle were as follows: L-Glu(O*t*Bu) (4.4 mg), L-Met (3.9 mg), L-Leu (3.7 mg), L-Ala (3.2 mg), L-Pro (3.5 mg).

After each successful coupling step, the resin was re-combined and Fmoc-deprotected as described in the general procedure and monitored by a qualitative ninhydrin test. The resin was divided into 6 equal portions. Each portion was pre-swollen in DMF (1 ml). A solution of a Fmoc-protected amino acid (8.7 μmol, 2 equiv.), DIC (1.1 mg, 8.7 μmol) and HOBt (1.2 mg, 8.7 μmol) in DMF (1 ml) was pre-activated for 15 minutes and then added to each portion followed by DIPEA (2.23 mg, 17.3 μmol, 3 μl). Each portion was agitated on a tube rotator for at least 18-24 h at room temperature. The portions were washed with dichloromethane (3 x 2 ml), DMF (3 x 2 ml) and dichloromethane (3 x 2 ml) and dried. The success of the coupling step was monitored by a qualitative ninhydrin test. Each coupling cycle was repeated until a ninhydrin test showed no free amino functions to yield library **82**. The quantities of Fmoc-amino acid used per coupling cycle were as follows: L-Met (3.2 mg), L-Leu (3.1 mg), L-Pro (2.9 mg), L-Lys(Boc) (4.1 mg), L-Ser(*t*Bu) (3.3 mg), Gln (3.2 mg).

Tetrabutylammonium salt of the red dye-spacer-L-Leu-L-Asn-L-Phe 84:

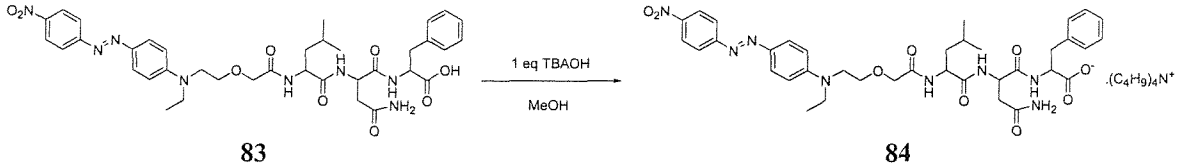

83 **84**

Tetrabutylammonium hydroxide, 0.1 M in methanol, (0.40 ml, 40 μM, 1 equiv.) was added to the solution of the red dye-spacer-L-Leu-L-Asn-L-Phe **83** (30 mg, 40 μM, 1 equiv.) in methanol (10ml). After stirred for 1 h, the solvent was removed and dried in high vacuum pump.

6.3.4 Synthesis included in chapter 5

3,4-Dichloro-5-phenylcarbamoyl-1H-pyrrole-2-carboxylic acid ethyl ester 110:

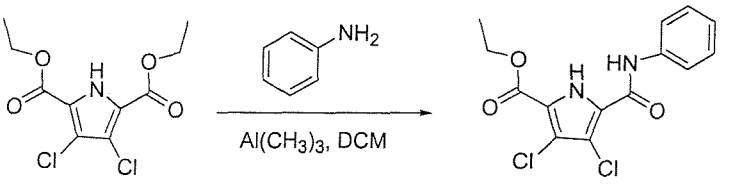

109 **110**

Aniline (1.65, 17.85 mmol, 1 equiv.) was stirred with 0.2 M trimethylaluminium solution in hexane (8.9 ml, 17.85 mmol, 1 equiv.) in dichloromethane (100 ml) for 30 minutes. 3,4-Dichloro-1H-pyrrole-2,5-dicarboxylic acid diethyl ester **109** (5.0 g, 17.85 mmol) was added into the solution and was heated at reflux for 72 h. A diluted hydrochloric acid solution was added dropwise, followed with water (100 ml) and extracted with dichloromethane (2 x 100 ml). The organic solvent was removed in vacuo and the residue was recrystallized with acetonitrile to yield compound **110**, white solid (0.80 g, 2.86 mmol, 13%).

M.p. 148°C. ^{1}H NMR 300 MHz in $CDCl_3$ δ (ppm): 1.42 (t, 3H, J = 7.0, CH_3), 4.42 (q, 2H, J = 7.0, CH_2), 7.21 (t, 1H, J = 7.5, *p*-Ar*H*), 7.41 (t, 2H, J = 7.5, *m*-Ar*H*), 7.64 (d, 2H, J = 7.5, *o*-Ar*H*), 8.57 (s, 1H, CON*H*), 10.08 (s, br, 1H, N*H*-Pyrrole). ^{13}C NMR 75 MHz in DMSO-d_6 δ (ppm): 14.8, 61.7, 114.9, 116.9, 119.4, 120.5, 124.7, 126.2, 129.5, 138.9, 156.9, 159.3. ES^+ mass spectrum: *m/z* (%): 327 (10) $[M+H]^+$, 677 (20) $[2M+Na]^+$, 1004 (30) $[3M+Na]^+$. Elemental analysis: Calc. for $C_{14}H_{12}Cl_2N_2O_3 \cdot 0.2CH_2Cl_2$: C 49.56, H 3.63, N 8.14; found: C 49.63, H 3.80, N 7.98.

3,4-Dichloro-5-phenylcarbamoyl-1H-pyrrole-2-carboxylic acid 111:

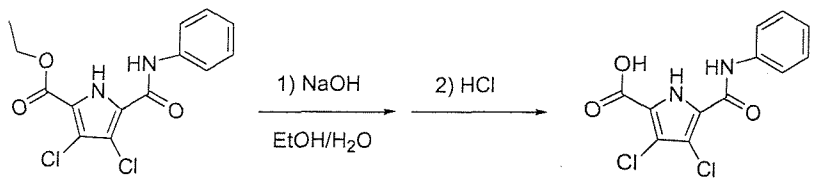

110 **111**

3,4-Dichloro-5-phenylcarbamoyl-1H-pyrrole-2-carboxylic acid ethyl ester **110** (0.5 g, 1.5 mmol, 1 equiv.) was heat at reflux in absolute ethanol (40 ml). The sodium hydroxide aqueous solution (0.6 g, 15 mmol, 10 equiv., 10 ml) was added and the solution was refluxed at 80°C for 12 h. The solution was acidified to pH = 1 using hydrochloric acid and the solvent was removed in *vacuo*. Water (50 ml) was added and the white solid was collected by filtration. The residue was purified by column chromatography using dichloromethane/methanol (10:1 *v/v*) to yield compound **111**, white solid (0.33 g, 1.10 mmol, 75%).

M.p. 239°C (decom.). R_f = 0.49 (DCM/MeOH (10:1 *v/v*)). ^{1}H NMR 300 MHz in DMSO-d_6 δ (ppm): 7.21 (t, 1H, J = 7.3, *p*-Ar*H*), 7.46 (t, 2H, J = 7.3, *m*-Ar*H*), 7.81 (d, 2H, J = 7.3, *o*-Ar*H*), 10.38 (s, 1H, CON*H*), 13.27 (s, br, 1H, COO*H*). ^{13}C NMR 75 MHz in DMSO-d_6 δ (ppm): 114.5, 119.7, 121.5, 122.5, 123.6, 125.5, 128.6, 138.4, 156.3, 160.3. ES$^-$ mass spectrum: *m/z* (%): 297 (30) [M-H]$^-$, 411 (45) [M+CF_3COO]$^-$. Elemental analysis: Calc. for $C_{12}H_8Cl_2N_2O_3 \cdot 0.3CH_3OH \cdot 0.3CH_2Cl_2$: C 45.28, H 2.96, N 8.38; found: C 45.41, H 3.05, N 8.11.

1,3-Phenylene-bis-(3,4-dichloro-5-phenylcarbamoyl-1H-pyrrole-2-carboxylic acid amide) 111:

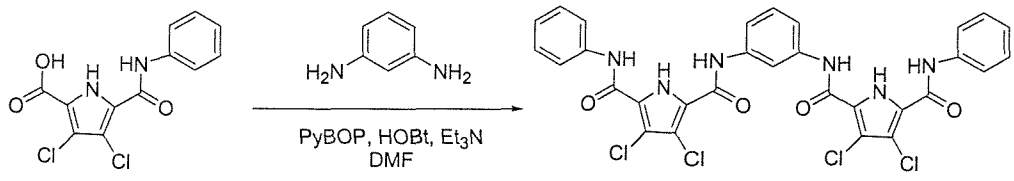

111 **101**

3,4-Dichloro-5-phenylcarbamoyl-1H-pyrrole-2-carboxylic acid **111** (300 mg, 1 mmol, 2 equiv.) was dissolved in DMF (30 ml). 1,3-Phenylenediamine (54 mg, 0.5

mmol, 1 equiv.), triethylamine (0.10 g, 1 mmol, 2 equiv.) PyBOP (0.57 g, 1.1 mmol, 2.2 equiv.) and 5 mg (0.04 mmol, 0.07 equiv.) of HOBt was added and the solution was stirred for 72 h. After removing the solvent, the white solid was recrystallized with acetonitrile to yield compound **101**, white solid (167 mg, 0.25 mmol, 50%).

M.p. 272 °C (decom.). ^{1}H NMR 300 MHz in DMSO-d_6 δ (ppm): 7.23 (t, 2H, J = 7.3, *p*-Ar*H*), 7.44-7.58 (m, 7H, CONH(*m*-Ar*H*)NHCO, *m*-Ar*H*, CONH(*o*- and *p*-Ar*H*)NHCO), 7.81 (d, 4H, J = 7.3, *o*-Ar*H*), 8.31 (s, 1H, J = 7.3, CONH(*o*-Ar*H*)NHCO, 10.10 (s, 2H, terminal-CON*H*), 10.20 (s, 2H, bridging-CON*H*), 13.12 (s, br, 2H, N*H*-Pyrrole). ^{13}C NMR 75 MHz in DMSO-d_6 δ (ppm) with 2 equiv. of TBAF: 13.4, 19.1, 23.0, 57.5, 110.5, 111.4, 111.5, 113.8, 119.1, 122.3, 126.2, 128.5, 128.6, 139.6, 139.7, 160.1, 160.3. ES$^-$ mass spectrum (with 2 equiv. of TBAF): *m/z* (%): 334 (100) $[M-2H]^{2-}$, 669 (35) $[M-H]^-$. ES$^-$ HRMS (with 2 equiv. of TBAF): m/z: Calc. for $C_{46}H_{54}N_6O_5Cl_4$ $[M-2H+TBA]^-$: 910.2904; found: 910.2924. Elemental analysis: Calc. for $C_{30}H_{20}Cl_4N_6O_4$: C 53.75, H 3.01, N 12.54; found: C 53.48, H 2.98, N 12.30.

1,4-Phenylene-bis-(3,4-dichloro-5-phenylcarbamoyl-1H-pyrrole-2-carboxylic acid amide) 102:

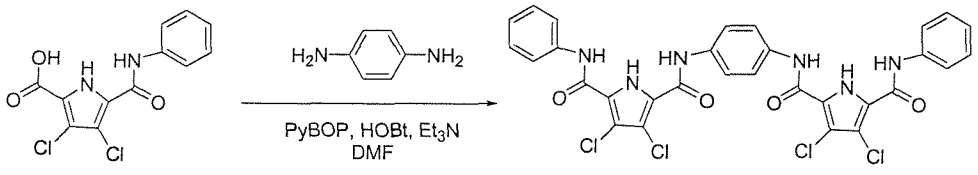

111 **102**

3,4-Dichloro-5-phenylcarbamoyl-1H-pyrrole-2-carboxylic acid **111** (300 mg, 1 mmol, 2 equiv.) was dissolved in DMF (30 ml). 1,4-Phenylenediamine (54 mg, 0.5 mmol, 1 equiv.), triethylamine (0.10 g, 1 mmol, 2 equiv.) PyBOP (0.57 g, 1.1 mmol, 2.2 equiv.) and 5 mg (0.04 mmol, 0.07 equiv.) of HOBt was added and the solution was stirred for 72 h. After removing the solvent, the white solid was recrystallized with acetonitrile to yield compound **102**, white solid (230 mg, 0.34 mmol, 68%).

M.p. >300°C. ^{1}H NMR 300 MHz in DMSO-d_6 δ (ppm): 7.23 (t, 2H, J = 7.3, *p*-Ar*H*), 7.48 (t, 2H, J = 7.3, *m*-Ar*H*), 7.81 (s, 8H, CONH(Ar*H*)NHCO, *o*-Ar*H*), 10.11 (s, 2H, terminal-CON*H*), 10.13 (s, 2H, bridging-CON*H*), 13.09 (s, br, 2H,

N*H*-Pyrrole). ^{13}C NMR 75 MHz in DMSO-d_6 δ (ppm) with 2 equiv. of TBAF: 13.4, 19.1, 23.0, 57.5, 111.2, 118.8, 119.1, 122.0, 126.6, 126.9, 128.5, 134.5, 139.8, 160.6, 160.9. ES$^-$ mass spectrum (with 2 equiv. of TBAF): *m/z* (%): 334 (100) $[M-2H]^{2-}$, 669 (15) $[M-H]^-$. ES$^-$ HRMS (with 2 equiv. of TBAF): m/z: Calc. for $C_{46}H_{54}N_6O_5Cl_4$ $[M-2H+TBA]^-$: 910.2904; found: 910.2898. Elemental analysis: Calc. for $C_{30}H_{20}Cl_4N_6O_4$: C 53.75, H 3.01, N 12.54; found: C 53.97, H 3.26, N 12.39.

Ethyl-bis-(3,4-dichloro-5-phenylcarbamoyl-1H-pyrrole-2-carboxylic acid amide) 103:

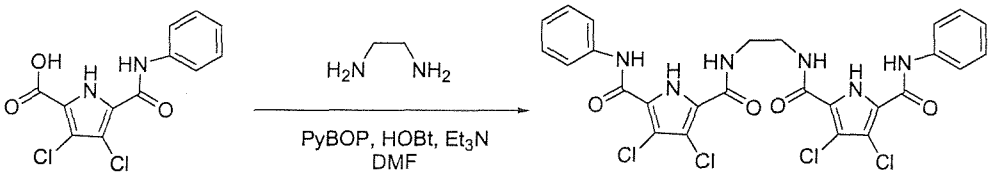

111 **103**

3,4-Dichloro-5-phenylcarbamoyl-1H-pyrrole-2-carboxylic acid **111** (300 mg, 1 mmol, 2 equiv.) was dissolved in DMF (30 ml). Ethylenediamine (30 mg, 0.5 mmol, 1 equiv.), triethylamine (0.10 g 1 mmol, 2 equiv.), PyBOP (0.57 g, 1.1 mmol, 2.2 equiv.) and 5 mg (0.04 mmol, 0.04 equiv.) of HOBt was added and the solution was stirred for 72 h. After removing the solvent, the solid was recrystallized with acetonitrile and collected by filtration to provide white solid (370 mg). This residue (150 mg) was dissolved in DMF (15 ml) and 3,4-dichloro-5-phenylcarbamoyl-1H-pyrrole-2-carboxylic acid **111** (130 mg, 0.44 mmol) was added. Triethylamine (50 mg 0.48 mmol), PyBOP (0.24 g, 0.46 mmol) and 5 mg (0.04 mmol) of HOBt was added and the solution was stirred for 72 h. After removing the solvent, the solid was recrystallized with dichloromethane and acetonitrile. The white solid, compound **103**, obtained after filtration (167 mg, 0.25 mmol, 56%).

M.p. >240°C. ^{1}H NMR 300 MHz in DMSO-d_6 δ (ppm): 3.53 (s, 4H, N(CH_2)$_2$N), 7.11 (t, 2H, *J* = 7.7, *p*-Ar*H*), 7.35 (t, 4H, *J* = 7.7, *m*-Ar*H*), 7.67 (d, 4H, *J* = 7.7, *o*-Ar*H*), 8.07 (s, br, 2H, *H*NCH$_2$), 10.03 (s, 2H, CON*H*Ar), 12.78 (s, br, 2H, N*H*-Pyrrole). ^{13}C NMR 75 MHz in DMSO-d_6 δ (ppm): 38.7, 119.8, 123.0, 123.8, 128.7, 138.2, 156.4, 158.4. ES$^+$ mass spectrum: *m/z* (%): 643 (80) $[M_{35}Cl+Na]^+$, 645 (100) $[M_{37}Cl+Na]^+$. ES$^-$ mass spectrum: *m/z* (%): 619 (76) $[M_{35}Cl-H]^-$, 621 (100)

$[M_{37}Cl\text{-}H]^-$. Elemental analysis: Calc. for $C_{26}H_{20}Cl_4N_6O_4 \cdot 0.33CH_2Cl_2 \cdot H_2O$: C 47.30, H 3.42, N 12.57; found: C 47.54, H 3.75, N 12.17.

4-Aminomethyl-phenylamino-bis-(3,4-dichloro-5-phenylcarbamoyl-1H-pyrrole-2-carboxylic acid amide) 104:

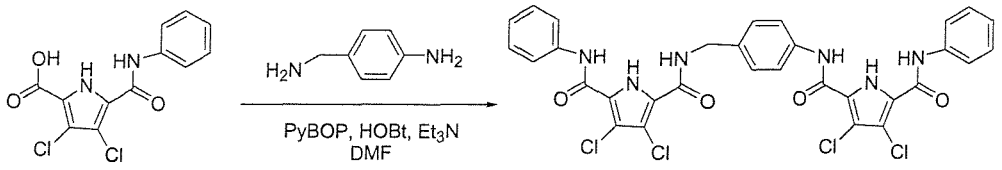

111 **104**

4-Aminobenzylamine (61 mg, 0.5 mmol, 1 equiv.) was added to a solution of 3,4-dichloro-5-phenylcarbamoyl-1H-pyrrole-2-carboxylic acid **111** (300 mg, 1 mmol, 2 equiv.) in DMF (30 ml) under a nitrogen atmosphere. Triethyamine (104 mg, 1 mmol, 2 equiv.), PyBOP (572 mg, 1.1 mmol, 2.2 equiv.) and 5 mg (0.04 mmol, 0.04 equiv.) of HOBt were added and the reaction was stirred for 72 h. Then the solvent was removed and water (50 ml) was added. The product was extracted with dichloromethane (3 x 50 ml). The organic phase was collected and the solvent was removed. The product was washed with diethyl ether (75 ml) and a small quantity of 10% MeOH in DCM (*v/v*). The white solid, compound **104**, occurred (114 mg, 0.17 mmol, 33%).

M.p. 254 - 256°C (decom.). ^{1}H NMR 300 MHz in DMSO-d_6 δ (ppm): 4.43 (d, J = 5.8, 2H, CH_2), 7.02-7.64 (m, 14H, Ar*H*), 8.39 (t, 1H, J = 5.8, CH_2-CON*H*), 9.91 (s, 2H, outer-CON*H*), 9.95 (s, 1H, central-CON*H*), 12.71 (s, 1H, N*H*-Pyrrole), 12.89 (s, 1H, N*H*-Pyrrole). ^{13}C NMR 75 MHz in DMSO-d_6 δ (ppm): 45.4, 111.8, 113.4, 119.5, 119.6, 119.7, 122.6, 122.7, 127.6, 128.4, 128.5, 137.9, 138.0, 156.1, 157.7, 166.2. Elemental analysis: Calc. for $C_{31}H_{22}Cl_4N_6O_4 \cdot 0.6H_2O$: C 53.56, H 3.36, N 12.09; found: C 53.32, H 3.38, N 12.19.

3-Aminomethyl-phenylamino-bis-(3,4-dichloro-5-phenylcarbamoyl-1H-pyrrole-2-carboxylic acid amide) 105:

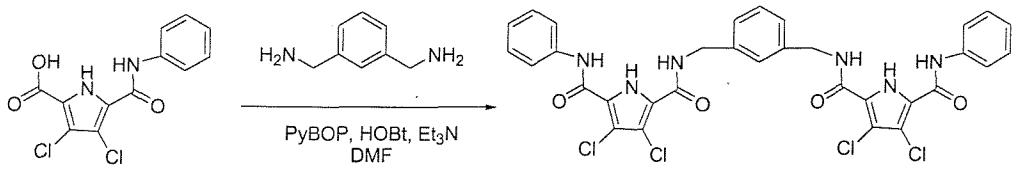

111 **105**

m-Xylenediamine (68 mg, 0.5 mmol, 1 equiv.) was added to a solution of 3,4-dichloro-5-phenylcarbamoyl-1H-pyrrole-2-carboxylic acid **111** (300 mg, 1 mmol, 2 equiv.) in DMF (30 ml) under a nitrogen atmosphere. Triethyamine (104 mg, 1 mmol, 2 equiv.), PyBOP (572 mg, 1.1 mmol, 2.2 equiv.) and 5 mg (0.04 mmol, 0.04 equiv.) of HOBt were added and the reaction was stirred for 72 h. Then the solvent was removed and water (50 ml) was added. The product was extracted with dichloromethane (3 x 50 ml). The organic phase was collected and the solvent was removed. The product was washed with diethyl ether (75 ml) and a small quantity of 10% MeOH in DCM (*v/v*). The white solid, compound **105**, occurred (130 mg, 0.19 mmol, 37%).

M.p. 283°C (decom.). ^{1}H NMR 300 MHz in DMSO-d_6 δ (ppm): 4.51 (d, J = 5.4, 4H, CH_2), 7.00-7.70 (m, 14H, Ar*H*), 8.50 (t, 2H, J = 5.4, central-CON*H*), 10.10 (s, 2H, outer-CON*H*), 12.75 (s, 2H, N*H*-Pyrrole). ^{13}C NMR 75 MHz in DMSO-d_6 δ (ppm): 42.5, 119.8, 122.9, 123.2, 123.9, 126.0, 128.4, 128.8, 138.4, 139.1, 158.2, 160.1. ES$^+$ mass spectrum: *m/z* (%): 699.1 (100) [M+H]$^+$. Elemental analysis: Calc. for $C_{32}H_{24}Cl_4N_6O_4 \cdot H_2O$: C 53.65, H 3.66, N 11.73; found: C 53.82, H 3.46, N 11.78.

4-Aminomethyl-phenylamino-bis-(3,4-dichloro-5-phenylcarbamoyl-1H-pyrrole-2-carboxylic acid amide) 106:

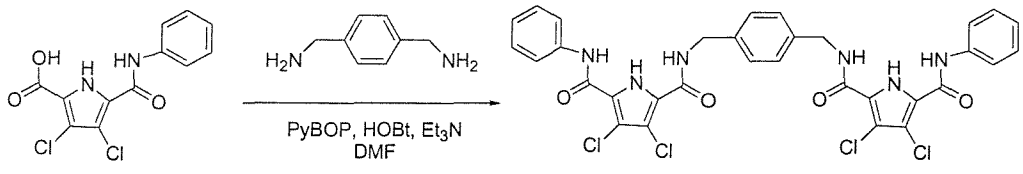

111 **106**

p-Xylenediamine (68 mg, 0.5 mmol, 1 equiv.) was added to a solution of 3,4-dichloro-5-phenylcarbamoyl-1H-pyrrole-2-carboxylic acid **111** (300 mg, 1 mmol, 2 equiv.) in DMF (30 ml) under a nitrogen atmosphere. Triethyamine (104 mg, 1 mmol, 2 equiv.), PyBOP (572 mg, 1.1 mmol, 2.2 equiv.) and 5 mg (0.04 mmol, 0.04 equiv.) of HOBt were added and the reaction was stirred for 72 h. Then the solvent was removed and water (50 ml) was added. The product was extracted with dichloromethane (3 x 50 ml). The organic phase was collected and the solvent was removed. The product was washed with diethyl ether (75 ml) and a small quantity of 10% MeOH in DCM (*v/v*). The white solid, compound **106**, occurred (132 mg, 0.19 mmol, 38%).

M.p. 317°C (decom.). ^{1}H NMR 300 MHz in DMSO-d_6 δ (ppm): 4.50 (d, J = 5.4, 4H, CH_2), 7.00-7.70 (m, 14H, Ar*H*), 8.50 (t, 2H, J = 5.4, central-CON*H*), 10.04 (s, 2H, outer-CON*H*), 12.79 (s, 2H, N*H*-Pyrrole). ^{13}C NMR 75 MHz in DMSO-d_6 δ (ppm): 42.3, 112.0, 113.6, 119.8, 122.9, 123.1, 123.9, 127.4, 128.7, 137.6, 138.3, 156.5, 158.1. TOF LD$^+$ mass spectrum: *m/z* (%): 472 (100) $[C_{23}H_{22}Cl_2N_4O_3]^+$. Elemental analysis: Calc. for $C_{32}H_{24}Cl_4N_6O_4 \cdot H_2O$: C 53.65, H 3.66, N 11.73; found: C 53.28, H 3.73, N 12.03.

3,4-Dichloro-2,5-dicarboxylic acid-1H-pyrrole 112:

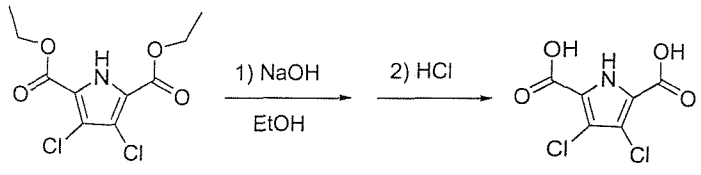

109 **112**

3,4-Dichloro-1H-pyrrole-2,5-dicarboxylic acid diethyl ester **109** (2.0 g, 7.14 mmol, 1 equiv.) was suspended in ethanolic NaOH solution (8.0 g, 200 mmol, 28 equiv. 100 ml) and was heat at reflux for 12 h. The solution was acidified to pH =1 with concentrated HCl. The product was extracted with diethyl ether (3 x 100 ml) and collected the diethyl ether phase. The solvent was removed and the solid was recrystallized from acetronitrile. The pale orange, compound **112**, was collected (0.50 g, 2.2 mmol, 31%).

M.p. 230°C (decom.). ^{1}H NMR 300 MHz in DMSO-d_6 δ (ppm): 12.93 (s, br, 1H, N*H*-Pyrrole), 13.52 (s, br, 2H, COO*H*). ^{13}C NMR 75 MHz in DMSO-d_6 δ (ppm): 116.2, 121.8, 159.8. ES$^-$ mass spectrum, m/z (%): 336 (100) [M + TFA]$^-$, 222 (15) [M-H]$^-$. ES$^-$ HRMS, m/z: Calc. for $C_6H_3Cl_2NO_4$ [M-H]$^-$: 221.9366, found: 221.9371. Elemental analysis: Calc. for $C_6H_3Cl_2NO_4 \cdot 1.33H_2O \cdot 0.5C_2H_5OH \cdot 0.17(C_2H_5)_2O$: C 32.49, H 3.68, N 4.94; found: C 32.76, H 3.53, N 4.67.

(3-Amino-phenyl)-carbamic acid tert-butyl ester 113:

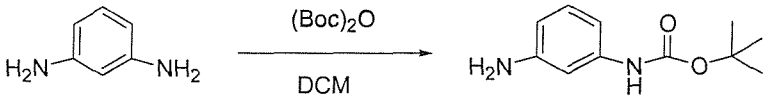

113

1,3-Phenylenediamine (3 g, 27.7 mmol, 5 equiv.) was dissolved in dichloromethane (20 ml). A solution of di-*tert*-butyldicarbonate (1.21 g, 5.54 mmol, 1 equiv.) in dichloromethane (200 ml) was added dropwise slowly over 6 h and the reaction was stirred for 12 h. The solvent was removed and the residue treated with K_2CO_3 aqueous solution (14 g in water 100 ml). This solution was extracted with dichloromethane (2 x 100 ml) and dried over $MgSO_4$. The solvent was removed and the product was purified using column chromatography using dichloromethane/methanol (10:1 *v/v*). The pale brown solid, compound **113**, occurred (0.83 g, 3.98 mmol, 72%).

M.p. 106 - 108°C (decom.). R_f = 0.43 (DCM/MeOH (100:5 *v/v*)). ^{1}H NMR 300 MHz in $CDCl_3$ δ (ppm): 1.52 (s, 9H, C*H*$_3$), 2.75 (s, br, 2H, N*H*$_2$), 6.40-7.09 (m, 5H, Ar*H* and CON*H*). ^{13}C NMR 75 MHz in $CDCl_3$ δ (ppm): 80.4, 105.1, 108.6, 109.9, 129.7, 139.4, 147.3, 152.8. ES$^+$ mass spectrum: *m/z* (%): 250 (100) [M+CH_3CN]$^+$, 209 (35) [M+H]$^+$.

(4-Amino-phenyl)-carbamic acid tert-butyl ester 114:

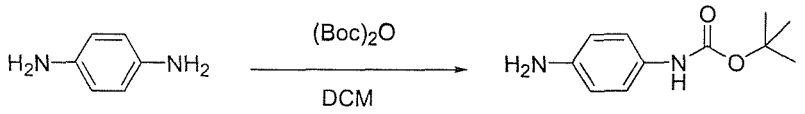

114

1,4-Phenylenediamine (3 g, 27.7 mmol, 5 equiv.) was dissolved in dichloromethane (20 ml). A solution of di-*tert*-butyldicarbonate (1.21 g, 5.54 mmol, 1 equiv.) in dichloromethane (200 ml) was added dropwise slowly over 6 h and the reaction was stirred for 12 h. The solvent was removed and the residue treated with K_2CO_3 aqueous solution (14 g in water 100 ml). This solution was extracted with dichloromethane (2 x 100 ml) and dried over $MgSO_4$. The solvent was removed and the product was purified using column chromatography using dichloromethane/methanol (10:1 *v/v*). The pale brown solid, compound **114**, occurred (0.87 g, 4.1 mmol, 75%).

M.p. 109 - 111°C (decom.). R_f = 0.31 (DCM/MeOH (10:1 *v/v*)). ^{1}H NMR 300 MHz in DMSO-d_6 δ (ppm): 1.48 (s, 9H, CH_3), 4.73 (s, br, 2H, NH_2), 6.51 (d, J = 8.1, 2H, ArHCONH), 7.11 (d, J = 8.1, 2H, ArHNH_2), 8.78 (s, br, 1H CONH). ^{13}C NMR 75 MHz in $CDCl_3$ δ (ppm): 28.2, 78.1, 113.9, 120.2, 128.5, 143.8, 153.0. ES$^+$ mass spectrum: *m/z* (%): 250 (100) $[M+CH_3CN]^+$, 209 (50) $[M+H]^+$.

{3-[(3,4-Dichloro-5-phenylcarbamoyl-1H-pyrrole-2-carbonyl)-amino]-phenyl}-carbamic acid tert-butyl ester 115:

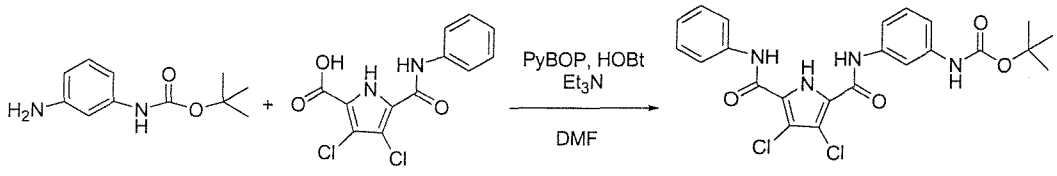

113 **111** **115**

3,4-Dichloro-5-phenylcarbamoyl-1H-pyrrole-2-carboxylic acid **111** (300 mg, 1 mmol, 1 equiv.), (3-amino-phenyl)-carbamic acid tert-butyl ester **113** (314 mg, 1.51, 1.5 equiv.), triethylamine (303 mg, 3 mmol, 3 equiv.) PyBOP (780 mg, 1.5 mmol, 1.5 equiv.) and 5 mg (0.04 mmol, 0.04 equiv.) of HOBt were dissolved in DMF (30 ml). The reaction was stirred for 72 h. Then the solvent was removed and the product was purified by column chromatography using dichloromethane/methanol (100:5 *v/v*). The pale brown solid, compound **115**, occurred (300 mg, 0.61 mmol, 61%).

M.p. 118 - 120°C (decom.). R_f = 0.90 (DCM/MeOH (100:5 *v/v*)). ^{1}H NMR 300 MHz in $CDCl_3$ δ (ppm): 1.55 (s, 9H, CH_3), 6.97-7.60 (m, 9H, ArH), 7.89 (s, br,

1H, OCONH), 8.46 (s, br, 2H, Pyrrole-CONH), 10.88 (s, br, 1H, NH-Pyrrole). ^{13}C NMR 75 MHz in $CDCl_3$ δ (ppm): 28.4, 80.7, 110.3, 112.1, 114.5, 115.0, 120.4, 123.2, 123.3, 125.1, 129.2, 129.6, 137.0, 137.5, 139.6, 152.9, 156.0. ES$^+$ mass spectrum, m/z (%): 511 (100) [M + Na]$^+$. Elemental analysis: Calc. for $C_{23}H_{22}Cl_2N_4O_4$: C 56.45, H 4.53, N 11.44; found: C 56.20, H 4.70, N 11.17.

{4-[(3,4-Dichloro-5-phenylcarbamoyl-1H-pyrrole-2-carbonyl)-amino]-phenyl}-carbamic acid tert-butyl ester 116:

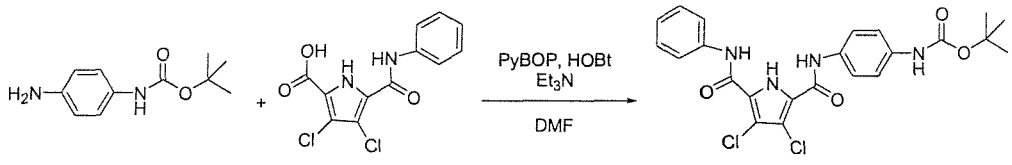

114 **111** **116**

3,4-Dichloro-5-phenylcarbamoyl-1H-pyrrole-2-carboxylic acid **111** (370 mg, 1.24 mmol, 1 equiv.), (4-amino-phenyl)-carbamic acid tert-butyl ester **114** (387 mg, 1.86, 1.5 equiv.), triethylamine (188 mg, 1.86 mmol, 1.5 equiv.) PyBOP (967 mg, 1.86 mmol, 1.5 equiv.) and 5 mg (0.04 mmol, 0.03 equiv.) of HOBt were dissolved in DMF (30 ml). The reaction was stirred for 72 h. Then the solvent was removed and the product was purified by column chromatography using dichloromethane/methanol (100:5 *v/v*). The pale brown solid, compound **116**, occurred (540 mg, 1.10 mmol, 89%).

M.p. 200 - 202°C. R_f = 0.55 (DCM/MeOH (100:5 *v/v*)). ^{1}H NMR 300 MHz in $CDCl_3$ δ (ppm): 1.54 (s, 9H, CH_3), 6.51 (s, br, 1H, OCONH), 7.17-7.66 (m, 9H, ArH), 8.45 (s, br, 1H, Pyrrole-CONHAr), 8.50 (s, br, 1H, ArCONH-Pyrrole), 10.40 (s, br, 1H, NH-Pyrrole). ^{13}C NMR 75 MHz in $CDCl_3$ δ (ppm): 28.3, 80.7, 111.6, 119.1, 120.3, 121.1, 122.9, 125.1, 129.2, 131.9, 135.6, 136.8, 155.5, 156.6, 162.5. ES$^+$ mass spectrum, m/z (%): 511 (15) [M + Na]$^+$. Elemental analysis: Calc. for $C_{23}H_{22}Cl_2N_4O_4$·0.8CH3OH: C 55.51, H 4.93, N 10.88; found: C 55.62, H 5.20, N 11.04.

Boc deprotection of {3-[(3,4-Dichloro-5-phenylcarbamoyl-1H-pyrrole-2-carbonyl)-amino]-phenyl}-carbamic acid tert-butyl ester 117:

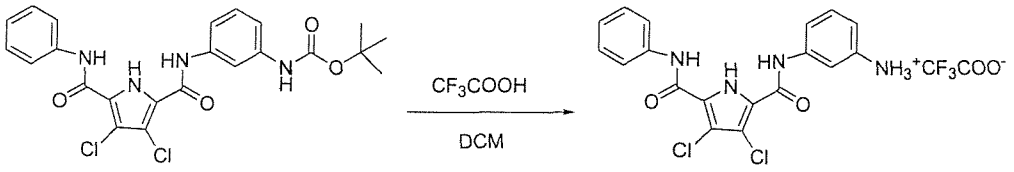

115 **117**

{3-[(3,4-Dichloro-5-phenylcarbamoyl-1H-pyrrole-2-carbonyl)-amino]-phenyl}-carbamic acid tert-butyl ester **115** (548 mg, 1.12 mmol, 1 equiv.) was dissolved in dichloromethane (30 ml). Solution of 60% trifluoro acetic acid in dichloromethane (22 ml) was added and stirred for 12 h. Then the solvent was removed. Toluene (100 ml) was added and removed and the product was washed with diethyl ether (2 x 10 ml). The compound **117**, grey solid, was collected (428 mg, 0.85 mmol, 76%).

M.p. 180°C (decom.). ^{1}H NMR 300 MHz in DMSO-d_6 δ (ppm): 4.01 (s, br, 2H, NH_3^+), 6.71-7.71 (m, 9H, Ar*H*), 9.98 (s, br, 2H, CON*H*), 12.95 (s, br, 1H, N*H*-Pyrrole). ^{13}C NMR 75 MHz in DMSO-d_6 δ (ppm): 112.3, 112.5, 119.0, 122.5, 123.1, 127.8, 128.7, 131.8, 137.2, 138.1, 155.6, 155.7. ES$^+$ mass spectrum, m/z (%): 389 (100) $[C_{18}H_{14}Cl_2N_4O_2 + H]^+$. Elemental analysis: Calc. for $C_{20}H_{15}Cl_2N_4O_4F_3$: C 47.73, H 3.00, N 11.13; found: C 47.58, H 3.10, N 11.16.

Boc deprotection of {4-[(3,4-Dichloro-5-phenylcarbamoyl-1H-pyrrole-2-carbonyl)-amino]-phenyl}-carbamic acid tert-butyl ester 118:

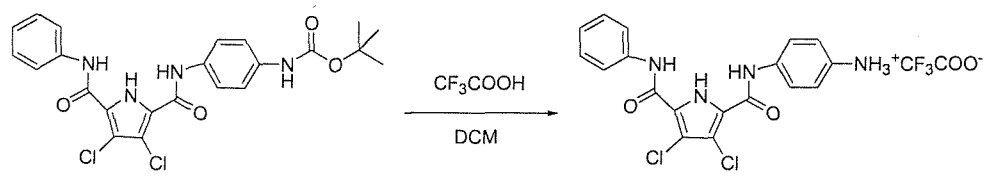

116 **118**

{4-[(3,4-Dichloro-5-phenylcarbamoyl-1H-pyrrole-2-carbonyl)-amino]-phenyl}-carbamic acid tert-butyl ester **116** (500 mg, 1.02 mmol, 1 equiv.) was dissolved in dichloromethane (50 ml). Solution of 60% trifluoro acetic acid in dichloromethane (20 ml) was added and stirred for 12 h. Then the solvent was

removed. Toluene (100 ml) was added and removed and the product was washed with diethyl ether (2 x 10 ml). The compound **118**, pale brown solid, was collected (430 mg, 0.85 mmol, 83%).

M.p. 198 - 200°C (decom.). ^{1}H NMR 300 MHz in DMSO-d_6 δ (ppm): 3.99 (s, br, 3H, NH_3^+), 7.10-7.70 (m, 9H, Ar*H*), 9.98 (s, br, 1H, Pyrrole-CON*H*-Ar), 9.99 (s, br, 1H, Ar-CON*H*-Pyrrole). ^{13}C NMR 75 MHz in DMSO-d_6 δ (ppm): 113.3, 119.9, 120.5, 121.2, 123.3, 124.0, 128.8, 134.5, 138.2, 156.4, 156.5. ES$^+$ mass spectrum, m/z (%): 389 (50) $[C_{18}H_{14}Cl_2N_4O_2 + H]^+$. Elemental analysis: Calc. for $C_{20}H_{15}Cl_2N_4O_4F_3 \cdot 0.67CH_2Cl_2 \cdot 0.33C_7H_8$: C 46.77, H 3.24, N 9.49; found: C 46.97, H 2.97, N 9.52.

Synthesis of Trimer 107:

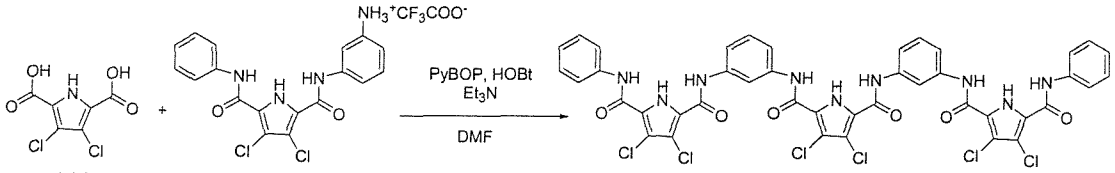

112 **117** **107**

3,4-Dichloro-2,5-dicarboxylic acid-1H-pyrrole **112** (79 mg, 0.35 mmol, 1 equiv), compound **117** (300 mg, 0.77 mmol, 2 equiv.), triethyamine (78 mg, 0.77 mmol, 2 equiv.), PyBOP (402 mg, 0.77 mmol, 2 equiv.) and 5 mg (0.04 mmol, 0.01 equiv.) of HOBt were dissolved in DMF (30 ml) and the reaction was stirred for 72 h. Then the solvent was removed and water (50 ml) was added. The product was extracted with dichloromethane (3 x 50 ml). The organic phase was collected and the solvent was removed. The product was recrystallized from acetronitrile (25 ml) and washed with dichloromethane (2 x 5 ml) to yield brown solid, compound **107** (158 mg, 0.16 mmol, 47%).

M.p. 195°C (decom.). ^{1}H NMR 300 MHz in DMSO-d_6 δ (ppm): 7.14 (t, J = 7.3, 2H, terminal-*p*-ArH_2), 7.39 (t, J =7.3, 6H, terminal-*m*-Ar*H*, bridging-*m*-Ar*H*), 7.48 (d, J =7.3, 4H, bridging-*o* and *p*-Ar*H*), 7.71 (d, J =7.3, 4H, terminal-*o*-Ar*H*), 8.21 (s, 2H, bridging-*o*-Ar*H*), 10.02 (s, br, 2H, terminal-CON*H*), 10.15 (s, br, 4H, bridging-CON*H*), 13.03 (s, br, 3H, N*H*-Pyrrole). ^{13}C NMR 75 MHz in DMSO-d_6 δ (ppm): 109.0, 109.1, 113.2, 117.5, 121.0, 121.5, 121.9, 126.3, 126.6, 135.8, 136.2,

136.3, 153.8, 157.4. Elemental analysis: Calc. for $C_{42}H_{27}Cl_6N_9O_6 \cdot CH_2Cl_2 \cdot 0.6HCON(CH_3)_2$: C 49.13, H 3.06, N 12.28; found: C 48.98, H 2.69, N 12.64.

Synthesis of Trimer 108:

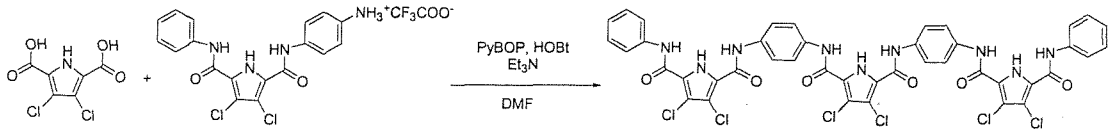

112 **118** **108**

3,4-Dichloro-2,5-dicarboxylic acid-1H-pyrrole **112** (80 mg, 0.36 mmol, 1 equiv), compound **118** (395 mg, 0.78 mmol, 2 equiv.), triethyamine (80 mg, 0.78 mmol, 2 equiv.), PyBOP (412 mg, 0.78 mmol, 2 equiv.) and 5 mg (0.03 mmol, 0.08 equiv.) of HOBt were dissolved in DMF (30 ml) and the reaction was stirred for 72 h. Then the solvent was removed and water (50 ml) was added. The product was extracted with dichloromethane (3 x 50 ml). The organic phase was collected and the solvent was removed. The product was recrystallized from diethyl ether (50 ml) and washed with dichloromethane (2 x 5 ml) to yield brown solid, compound **108** (208 mg, 0.21 mmol, 59%).

M.p. >300°C (decom.). ^{1}H NMR 300 MHz in DMSO-d_6 δ (ppm) with TBAF: 6.97 (t, J = 7.1, 2H, terminal-p-ArH_2), 7.28 (t, J =7.1, 4H, terminal-m-ArH), 7.64-7.84 (m, 12H, terminal-o-ArH and bridging-ArH), 9.88 (s, br, 4H, bridging-CONH), 9.95 (s, br, 4H, terminal-CONH). ^{13}C NMR 75 MHz in DMSO-d_6 δ (ppm) with TBAF: 110.4, 110.5, 110.6, 118.6, 118.8, 119.0, 121.7, 127.0, 127.2, 127.3, 128.3, 134.5, 134.6, 140.0, 161.2, 161.2, 161.4. Elemental analysis: Calc. for $C_{42}H_{27}Cl_6N_9O_6 \cdot 0.6CH_2Cl_2$: C 50.29, H 2.79, N 12.39; found: C 50.10, H 2.75, N 12.61.

6.4 General method used for an NMR titration

All the ^{1}H NMR titration experiments were performed on a Bruker AM300 and AV300 NMR spectrometer. The anions were added as their tetrabutylammonium salts and would be dried under high vacuum pump overnight without heating. The receptor would be made up as a 0.01 M solution in a cooled yet previously oven dried NMR tube (5mm), the top would be sealed using a suba-seal rubber septum which was secured using laboratory film. The anion would made up as 0.1 M solution in a separate vial, the lid was made airtight so that the concentration would not change through the evaporation of the solvent. These solutions can be made quite simply; (1) for the receptor, molecule mass of the receptor divided by two hundreds gives the required mass in milligram to be dissolved in 500 μl of the chosen solvent and accuracy percentage volume of water sometimes when it needed. (2) for the anion, molecular mass of the salt divided by ten gives the required mass in milligram to be dissolved in 1 ml of the same solvent. Small aliquots of the anionic guest would be introduced via syringe addition to the NMR tube after which a proton NMR spectrum of the receptor:anion solution would be recorded. The chemical shift of proton resonances believed to be involved in hydrogen bonding were recorded and the resulting data subsequently processed using the EQNMR program[98] to calculate both the association constant and corresponding errors. The titration would be repeated if the error was estimated to be more than 15%.

References

1. Lehn, J.-M. *Struct. Bonding* **1973**, *16*, 1.
2. Lehn, J.-M. *Pure Appl. Chem.* **1978**, *50*, 871.
3. Lehn, J.-M. *Acc. Chem. Res.* **1978**, *11*, 49.
4. Lehn, J.-M. *Angew. Chem. Int. Ed.* **1988**, *27*, 89.
5. Lehn, J.-M. *Supramolecular Chemistry, Concepts and Perspectives*, VCH, Weinheim, **1995**.
6. Beer, P. D.; Gale, P. A.; Smith, D. K. *Supramolecular Chemistry*, Oxford University Press, **1999**.
7. Steed, J. W.; Atwood, J. L. *Supramolecular Chemistry*, Wiley & sons, Ltd., **2000**.
8. Smithrud, D. B.; Sanford, E. M.; Chao, I.; Ferguson, S. B.; Carcanague, D. R.; Evanseck, J. D.; Houk, K. N.; Diederich, F. *Pure Appl. Chem.* **1990**, *62*, 2227.
9. Beer P. D.; Gale, P. A. *Angew. Chem. Int. Ed.* **2001**, *40*, 486.
10. Shannon, R. D. *Acta Crystallogr. Sect. A* **1976**, *32*, 751.
11. Hofmeister, F. *Arch. Exp. Pathol. Pharmakol.* **1888**, *24*, 247.
12. Pedersen, C. J. *Angew. Chem. Int. Ed.* **1988**, *27*, 1021.
13. Dietrich, B.; Lehn, J.-M.; Sauvage, J. P. *Tetrahedron Lett.* **1969**, 2885.
14. Park, C. H.; Simmons, H. E. *J. Am. Chem. Soc.* **1968**, *90*, 2431.
15. Bianchi, A.; Bowman-James, K.; García-España, E. Eds. *Supramolecular Chemistry of Anions*, Wiley-VCH, New York, **1997**.
16. Gale, P. A. *Coord. Chem. Rev.* **2003**, *240*, 191.
17. Gale, P. A. *Coord. Chem. Rev.* **2001**, *213*, 79.
18. Gale, P. A. *Coord. Chem. Rev.* **2000**, *199*, 181.
19. Chakrabarti, P. *J. Mol. Biol.* **1993**, *234*, 463.

20. Mangani, S.; Ferraroni, M. In *Supramolecular Chemistry of Anions*; Bianchi, A.; Bowman-James, K.; García-España, E. Eds., Wiley-VCH, New York, **1997**.
21. Glidewell, C. *Chem. Br.* **1990**, *26*, 137.
22. Moss, B. *Chem. Ind.* **1996**, 407.
23. Holloway, J. M.; Dahlgren, R. A.; Hansen B.; Casey, W. H. *Nature* **1998**, *395*, 785.
24. Scheele, J.; Timmerman P.; Reinhoudt, D. N. *Chem. Commun.* **1998**, 2613.
25. Sessler, J. L.; Sansom, P. I.; Andriersky, A.; Král, V. In *Supramolecular Chemistry of Anions*; Bianchi, A.; Bowman-James, K.; García-España, E. Eds., Wiley-VCH, New York, **1997**.
26. Watson, J. D.; Crick, F. H. C. *Nature*, **1953**, *171*, 573.
27. Christianson, D. W.; Lipscomb, W. N. *Acc. Chem. Res.* **1989**, *22*, 62.
28. Rees, D. C.; Lipscomb, W. N. *Proc. Natl. Acad. Sci. USA* **1981**, *78*, 5455.
29. Berg, J. M. *Acc. Chem. Res.* **1995**, *28*, 14.
30. Puglisi, J. D.; Chen, L.; Frankel, A. D.; Williamson, J. R. *Proc. Nat. Acad. Sci. USA* **1993**, *90*, 3680.
31. Martinez-Cruz, L. A.; Dreyer, M. K.; Boisvert, D. C.; Yokota, H.; Martinez-Chantar, M. L.; Kim, R.; Kim, S.-H. *Structure* **2002**, *10*, 195.
32. Sierra-Callay, I. L. L.; Collinet, B.; Graille, M.; Quevillon-Cheruel, S.; Liger, D.; Minard, P.; Blondeau, K.; Henckes, G.; Aufrère, R.; Leulliot, N.; Zhou, C.-Z.; Sorel, I.; Ferrer, J.-L.; Poupon, A.; Janin, J.; van Tilbeurgh, H. *PROTEINS* **2004**, *54*, 776.
33. Quiocho, F. A. *Annu. Rev. Biochem.* **1986**, *55*, 287.
34. Quiocho, F. A. *Phil. Trans. R. Soc.* **1990**, *B341*, 341.
35. Choi, K.; Hamilton, A. D. *Coord. Chem. Rev.* **2003**, *240*, 101.
36. Dutzler, R.; Campbell, E. B.; Cadene, M.; Chait, B. T.; MacKinnon, R. *Nature* **2002**, *415*, 287.
37. Boat, T. F.; Welsh, M. J.; Beaudet, A. L. In *The Metabolic Basis of Inherited Disease,* 6th ed., Scriver. C. R.; Beaudet, A. L.; Sly, W. S.; Valle, D. Eds., McGraw-Hill, New York, **1989**, 2649.
38. Quinton, P. M. *FASEB* **1990**, *4*, 2709.
39. Davis, P. B. *N. Engl. J. Med.* **1991**, *325*, 575.

40. Calnan, B. J.; Tidor, B.; Biancalana, S.; Hudson, D.; Frankel, A. D. *Science* **1991**, *252*, 1167.
41. van Axel Castelli, V.; Cort, A. D.; Mandolini, L. *J. Am. Chem. Soc.* **1998**, *120*, 12688.
42. Kavallieratos, K.; Crabtree, R. H. *Chem. Commun.* **1999**, 2109.
43. Hosseini, M. W. In *Supramolecular Chemistry of Anions*; Bianchi, A.; Bowman-James, K.; García-España, E. Eds., Wiley-VCH, New York, **1997**.
44. Hosseini, M. W.; Lehn, J.-M. *Helv. Chim. Acta* **1987**, *70*, 1312.
45. Hosseini, M. W.; Lehn, J.-M. Maggiora, L.; Mertes, K. B.; Mertes, M. P. *J. Am. Chem. Soc.* **1987**, *109*, 537.
46. Schmidtchen, F. P. In *Supramolecular Chemistry of Anions*; Bianchi, A.; Bowman-James, K.; García-España, E. Eds., Wiley-VCH, New York, **1997**.
47. Bondy, C. R.; Loeb, S. J. *Coord. Chem. Rev.* **2003**, *240*, 77.
48. Kavallieratos, K.; de Gala, S. R.; Austin, D. J.; Crabtree, R. H. *J. Am. Chem. Soc.*, **1997**, *119*, 2325.
49. Szumna, A.; Jurczak, J. *Eur. J. Org. Chem.* **2001**, 4031.
50. Choi, K. H.; Hamilton, A. D. *J. Am. Chem. Soc.*, **2001**, *123*, 2456.
51. Choi, K. H.; Hamilton, A. D. *Angew. Chem. Int. Ed. Engl.* **2001**, *40*, 3912.
52. Kubik, S.; Goddard, R.; Kirchner, R.; Nolting, D.; Seidal, J. *Angew. Chem. Int. Ed. Engl.*, **2001**, *40*, 2648.
53. Kubik, S.; Bitta, J.; Goddard, R.; Kubik, D.; Pohl, S. *Mater. Sci. Eng. C* **2001**, *18*, 125.
54. Demuth, C.; Zerbe, O.; Rognan, D.; Söll, R.; Beck-Sickinger, A.; Folkers, G.; Spichiger, U. E. *Biosensors & Bioelectronics* **2001**, *16*, 783.
55. Maison, W.; Kennedy, R. J.; Kemp, D. S. *Angew. Chem. Int. Ed. Engl.* **2001**, *40*, 3819.
56. Hinzen, B.; Seiler, P.; Diederich, F. *Helv. Chim. Acta* **1996**, *79*, 942.
57. Davis, A. P.; Gilmer, J. F.; Perry, J. J. *Angew. Chem. Int. Ed. Engl.* **1996**, *35*, 1312.
58. Lazzarotto, M.; Sansone, F.; Baldini, L.; Casnati, A.; Cozzini, P.; Ungaro, R. *Eur. J. Org.* **2001**, 595.
59. Kelley, T. R.; Kim, M. H. *J. Am. Chem. Soc.* **1994**, *116*, 7072.

60. Buhlmann, P.; Nishizawa, S.; Xiao, K. P.; Umezawa, Y. *Tetrahedron*, **1997**, *53*, 1647.
61. Kyne, G. M.; Light, M. E.; Hursthouse, M. B.; de Mendoza, J.; Kilburn. J. D. *J. Chem. Soc., Perkin Trans. 1* **2001**, 1258.
62. Best, M. D.; Tobey, S. L.; Anslyn, E. V. *Coord. Chem. Rev.* **2003**, *240*, 3.
63. Müller, G.; Riede, J.; Schmidtchen, F. P. *Angew. Chem.* **1988**, *100*, 1574; *Angew. Chem. Int. Ed. Engl.* **1988**, *27*, 1516.
64. Echavarren, A.; Galan, A.; de Mendoza, J.; Salmeron, A.; Lehn, J.-M. *J. Am. Chem. Soc.* **1989**, *111*, 4994.
65. Galán, A.; Pueyo, E.; Salmerón, A.; de Mendoza, J. *Tetrahedron Lett.* **1991**, *31*, 1827.
66. Lawlwss, L. J.; Blackburn, A. G.; Ayling, A. J.; Perez-Payan, M. N.; Davis, A. P. *J. Chem. Soc., Perkin Trans. 1* **2001**, 1329.
67. Coles, S. J.; Gale, P. A.; Hursthouse, M. B. *Cryst. Eng. Comn.* **2001**, *53*.
68. Sessler, J. L.; Gale, P. A. In *The Porphyrin Handbook*; Kadish, K. M.; Smith, K. M.; Guilard, R. Eds. Academic Press:San Diego, **2000**, *6*, 257.
69. Sessler, J. L.; Cyr, M. J.; Lynch, V.; McGhee, E.; Ibers, J. A. *J. Am. Chem. Soc.* **1990**, *112*, 2810.
70. Sessler, J. L.; Cyr, M.; Furuta, H.; Král, V.; Mody, T.; Morishima, T.; Shionoya, M.; Weghorn, S. J. *Pure Appl. Chem.* **1993**, *65*, 393.
71. Shionoya, M.; Furuta, H.; Lynch, V.; Harriman, A.; Sessler, J. L. *J. Am. Chem. Soc.* **1992**, *114*, 5714.
72. Black, C. B.; Andrioletti, B.; Try, A. C.; Ruiperez, C. Sessler, J. L. *J. Am. Chem. Soc.* **1999**, *121*, 10438.
73. Anzenbacher Jr., P.; Try, A. C.; Miyaji, H.; Jursíková, K.; Lynch, V. M.; Marquez, M.; Sessler, J. L. *J. Am. Chem. Soc.* **2000**, *122*, 10268.
74. Furuta, H.; Maeda, H.; Osuka, A. *J. Am. Chem. Soc.* **2001**, *123*, 6435.
75. Gale, P. A.; Camiolo, S.; Chapman, C. P.; Light, M. E.; Hursthouse, M. B. *Tetrahedron Lett.*, **2001**, *42*, 5095.
76. Denuault, G.; Gale, P. A.; Hursthouse, M. B.; Light, M. E.; Warriner, C. N. *New J. Chem.* **2002**, 811.
77. Sessler, J. L.; Camiolo, S.; Gale, P. A. *Coord. Chem. Rev.* **2003**, *240*, 17.
78. Scherer, M.; Sessler, J. L.; Gebauer, A.; Lynch, V. *Chem. Commun.* **1998**, 85.

79. Schmuck, C.; Lex, J. *Org. Lett.* **1999**, *1*, 1779.
80. Schmuck, C.; Heil, M. *Org. Lett.* **2001**, *3*, 1253.
81. Schmuck, C. *Chem. Eur. J.* **2000**, *6*, 709.
82. Klug, A. *Angew. Chem. Int. Ed. Engl.* **1983**, *22*, 565.
83. Greig, L. M.; Philp, D. *Chem. Soc. Rev.* **2001**, *30*, 287.
84. Lehn, J.-M.; Sauvage, J. P.; Simon, J. *Nouv. J. Chem.* **1983**, *7*, 413.
85. Youinou, M. T.; Rahmouni, N.; Fischer, J.; Osborn, A. *Angew. Chem. Int. Ed. Engl.* **1992**, *31*, 733.
86. Baxter, P. N. W.; Lehn, J.-M.; Fischer, J.; Youinou, M. T. *Angew. Chem. Int. Ed. Engl.* **1994**, *33*, 2284.
87. Sánchez-Quesada, J.; Seel, C.; Prados, P.; de Mendoza, J. *J. Am. Chem Soc.* **1996**, *118*, 277.
88. Peczuh, M. W.; Hamilton, A. D.; Sánchez-Quesada, J.; de Mendoza, J.; Haack, T.; Giralt, E. *J. Am. Chem Soc.* **1997**, *119*, 9327.
89. Hübner, G. M.; Glaser, J.; Seel, C.; Vögtle, F. *Angew. Chem. Int. Ed.* **1999**, *38*, 383.
90. Reuter, C.; Wienand, W.; Hübner, G. M.; Seel, C.; Vögtle, F. *Chem. Eur. J.* **1999**, *5*, 2692.
91. Wisner, J. A.; Beer, P. D.; Drew, M. G. B. *Angew. Chem. Int. Ed.* **2001**, *40*, 3606.
92. Coles, S. J.; Gale, P. A.; Horton, P. N.; Hursthouse, M. B.; Light, M. E.; Warriner, C. N. *Polyhedron* **2003**, *22*, 699.
93. Gale, P.A.; Camiolo, S.; Tizzard, G. J.; Chapman, C. P.; Light, M. E.; Coles, S. J.; Hursthouse, M. B. *J. Org. Chem.* **2001**, *66*, 7849.
94. Camiolo, S.; Gale, P.A.; Hursthouse, M. B.; Light, M. E. *Tetrahedron Lett.* **2002**, *43*, 6995.
95. Hossain, M. A.; Llinares, J. M.; Powell, D.; Bowman-James, K. *Inorg. Chem.* **2001**, *40*, 2936.
96. Navakhun, K.; Gale, P.A.; Camiolo, S.; Light, M. E.; Hursthouse, M. B. *Chem. Commun.* **2002**, 2084.
97. Friedman, M. *J. Org. Chem.* **1965**, *30*, 859.
98. Hynes, M. J. *J. Chem. Soc., Dalton Trans.* **1993**, 311.

99. Jentsch, T. J.; Stein, V.; Weinreich, F.; Zdebik, A. A. *Physiol. Rev.* **2002**, *82*, 503.
100. Smith, B. D.; Lambert, T. N. *Chem. Commun.* **2003**, 2261.
101. Koulov, A. V.; Lambert, T. N.; Mahim Jain, R. S.; Boon, J. N.; Smith, B. D.; Li, H.; Sheppard, D. N.; Joos, J-B.; Clare, J. P.; Davis, A. P. *Angew. Chem. Int. Ed.* **2003**, *42*, 4931.
102. Broughman, J. R.; Shank, L. P.; Takeguchi, W.; Schultz, B. D.; Iwamoto, T.; Mitchell, K. E.; Tomich, J. M. *Biochemistry* **2002**, *41*, 7350.
103. Boon, J. M.; Smith, B. D. *Curr. Opin. Chem. Biol.* **2002**, *6*, 749.
104. Fürstner, A. *Angew. Chem. Int. Ed.* **2003**, *42*, 3582.
105. Harashima, K.; Tanaka, T.; Nagatsu, J. *Agric. Biol. Chem.* **1967**, *31*, 481.
106. Gerber, N. N. *Crit. Rev. Microbiol.* **1974**, *3*, 469.
107. Bennett, J. W.; Bentley, R. *Adv. Appl. Microbiol.* **2000**, *47*, 1.
108. Castro, A. J. *Nature* **1967**, *213*, 903.
109. Lazaro, J. E. H.; Nitcheu, J.; Predicala, R. Z.; Mangalindan, G. C.; Nesslany, F.; Marzin, D.; Concepcion, G. P.; Diquet, B. *J. Nat. Toxins* **2002**, *11*, 367.
110. Kim, H. S.; Hayashi, M.; Shibata, Y.; Wataya, Y.; Mitamura, T.; Horii, T.; Kawauchi, K.; Hirata, H.; Tsuboi, S.; Moriyama, Y. *Biol. Pharm. Bull.* **1999**, *22*, 532.
111. Yamamoto, C.; Takemoto, H.; Kuno, H.; Yamamoto, D.; Tsubura, A.; Kamata, K.; Hirata, H.; Yamamoto, A.; Kano, H.; Seki, T.; Inoue, K. *Hepatology* **1999**, *30*, 894.
112. Kataoka, T.; Muroi, M.; Ohkuma, S.; Waritani, T.; Magae, J.; Takatsuki, A.; Kondo, S.; Yamasaki, M.; Nagai, K. *FEBS Lett.* **1995**, *359*, 53.
113. Sato, T.; Konno, H.; Tanaka, Y.; Kataoka, T.; Nagai, K.; Wasserman, H. H.; Ohkuma, S. *J. Biol. Chem.* **1998**, *273*, 21455.
114. Gottlieb, R. A.; Nordberg, J.; Showronski, E.; Babior, B. M. *Proc. Natl. Acad. Sci. U.S.A.* **1996**, *93*, 654.
115. Manderville, R. A. *Curr. Med. Chem.-Anti-Cancer Agents* **2001**, *1*, 195.
116. Melvin, M. S.; Tomlinson, J. T.; Park, G.; Day, C. S.; Saluta, G. R.; Kucera, G. L.; Manderville, R. A. *Chem. Res. Toxicol.* **2002**, *15*, 734.
117. Boger, D. L.; Patel, M. *J. Org. Chem.* **1988**, *53*, 1405.
118. Boger, D. L.; Patel, M. *Tetrahedron Lett.* **1987**, *28*, 2499.

119. Ohkuma, S.; Sato, T.; Okamoto, M.; Matsuya, H.; Arai, K.; Kataoka, T.; Nagai, K.; Wasserman, H. H. *Biochem. J.* **1998**, *334*, 731.
120. Povirk, L. F. *In Molecular Aspects of Anti-cancer Drug Design:* Neidle, S. and Waring, M. Ed., MacMillan: London, **1983**, 157.
121. Melvin, M. S.; Tomlinson, J. T.; Saluta, G. R.; Kucera, G. L.; Lindquist, N.; Manderville, R. A. *J. Am. Chem. Soc.* **2000**, *122*, 6333.
122. Oberhansen, K. J.; Richardson, J. F.; Buchanan, R. M.; Pierce, W. *Polyhedron*, **1989**, *8*, 659.
123. Canary, J. W.; Wang, Y.; Richard, R. Jr. *Inorganic Syntheses*, **1998**, *32*, 70.
124. Basha, A.; Lipton, M.; Weinreb, S. M. *Tetrahedron Lett.* **1977**, *18*, 4171.
125. Motekaitis, R. J.; Heinert, D. H.; Martell, A. E. *J. Org. Chem.* **1970**, *35*, 2504.
126. Delmotte, C.; Delmas, A. *Bioorg. Med. Chem. Lett.* **1999**, *9*, 2989.
127. Rusinova, E.; Tretyachenko-Ladokhina, V.; Vele, O.E.; Senear, D. F.; Alexander Ross, J. B. *Anal. Biochem.* **2002,** *308*, 18.
128. *Handbook of Fluorescent Probes and Research Products*, Molecular Probes, Inc., (www.probes.com/handbook/) **2004**.
129. Hunter, C. A.; Tomas, S. *Chem. Biol.* **2003**, *10*, 1023.
130. Otto, S.; Kubik, S. *J. Am. Chem. Soc.* **2003**, *125*, 7804.
131. Otto, S.; Furlan, R. L. E.; Sanders, J. K. M. *Curr. Opin. Chem. Biol.* **2002**, *6*, 321.
132. Otto, S.; Furlan, R. L. E.; Sanders, J. K. M. *Drug Discovery Today* **2002**, *7*, 117.
133. Lehn, J.-M.; Eliseev, A. V. *Science* **2001**, *291*, 2331.
134. Karan, C.; Miller, B. L. *Drug Discovery Today* **2000**, *5*, 67.
135. Linton, B.; Hamilton, A. D. *Curr. Opin. Chem. Biol.* **1999**, *3*, 307.
136. Spaller, M. R.; Burger, M. T.; Fardis, M.; Bartlett, P. A. *Curr. Opin. Chem. Biol.* **1997**, *1*, 47.
137. Antel, J. *Curr. Opin. Drug Discovery Dev.* **1999**, *2*, 224.
138. Chen, C. W.; Whitlock, H. W. Jr. *J. Am. Chem. Soc.* **1978**, *100*, 4921.
139. Zimmerman, S. C.; Wu, W.; Zeng, Z. *J. Am. Chem. Soc.* **1991**, *113*, 196.
140. Furka, A.; Sebestyen, F.; Asgedom, M.; Dibo, G. *J. Pept. Protein Res.* **1991**, *36*, 487.

141. Lam, K. S.; Salmon, S. E.; Hersh, E. M.; Hruby, V. J.; Kazmierski, W. M.; Knapp, R. J. *Nature* **1991**, *354*, 82.
142. Srinivasan, N.; Kilburn, J. D. *Curr. Opin. Chem. Biol.* **2004**, *8*, 305.
143. Conza, M. M.; Wennemers, H. *J. Org. Chem.* **2002**, *67*, 2696.
144. Wennemes, H.; Nold, M. C.; Conza, M. M.; Kulicke, K. J.; Neuburger, M. *Chem. Eur. J.* **2003**, *9*, 442.
145. LaBrenz, S. R.; Kelly, J. W. *J. Am. Chem. Soc.* **1995**, *117*, 1655.
146. Bonnat, M.; Bradley, M.; Kilburn, J. D. *Tetrahedron Lett.* **1996**, *37*, 5409.
147. Davies, M.; Bonnat, M.; Guillier, F.; Kilburn, J. D.; Bradley, M. *J. Org. Chem.* **1998**, *63*, 8696.
148. Jensen, K. B.; Braxmeier, T. B.; Demarcus, M.; Frey, J. G.; Kilburn, J. D. *Chem. Eur. J.* **2002**, *8*, 1300.
149. Lam, K. S.; Lebl, M.; Krchnak, V. *Chem. Rev.* **1997**, *97*, 411.
150. Czarnik, A. W. *Curr. Opin. Chem. Biol.* **1997**, *1*, 60.
151. Schmuck, C.; Heil, M. *Org. Biomol. Chem.* **2003**, *1*, 633.
152. Schmuck, C.; Heil, M. *ChemBioChem* **2003**, *4*, 1232.
153. Zerovnik, E. *Eur. J. Biochem.* **2002**, *269*, 3362.
154. Hardy, J.; Selkoe, D. J. *Science* **2002**, *297*, 353.
155. Lansbury, Jr. P. T. *Acc. Chem. Res.* **1996**, *29*, 317.
156. Yanker, B. A. *Neuron* **1996**, *16*, 921.
157. Debouck, C. *AIDS Res. Hum. Retroviruses* **1992**, *8*, 153.
158. Wlodawer, A.; Miller, A.; Jaskolski, M.; Sathyanarayana, B.; Baldwin, E.; Webber, I.; Selk, L.; Clawson, L.; Schneider, J.; Kent, S. *Science* **1989**, *245*, 616.
159. Pearl, L. H.; Taylor, W. R. *Nature* **1987**, *329*, 351.
160. Gustchina, A.; Weber, I. T. *Proteins* **1991**, *10*, 325.
161. Hoetelmans, R. M.; Meenhorst, P. L.; Mulder, J. W.; Burger, D. M.; Koks, C. H.; Beijnen, J. H. *Pharm. World Sci.* **1997**, *19*, 159.
162. Larder, B. *AIDS* **2001**, *15* (Suppl. 5), S27-S34.
163. Sluis-Cremer, N.; Tachedjian, G. *Eur. J. Biochem.* **2002**, *269*, 5103.
164. Schramm, H. J.; de Rosny, E.; Rebound-Ravaux, M.; Büttner, J.; Dick, A.; Schramm, W. *Biol. Chem.* **1999**, *380*, 593.

165. Dumond, J.; Boggetto, N.; Schramm, H. J.; Schramm, W.; Takahashi, M.; Reboud-Ravaux, M. *Biochem. Pharmacol.* **2003**, *65*, 1097.

166. Breccia, P.; Boggetto, N.; Pérez-Fernándaz, R.; Van Gool, M.; Takahashi, M.; René, L.; Prados, P.; Badet, B.; Reboud-Ravaux, M.; de Mendoza J. *J. Med. Chem.* **2003**, *46*, 5196.

167. Zutshi, R.; Franciskovich, J.; Shultz, M.; Schweitzer, B.; Bishop, P.; Wilson, M.; Chmielewski, J. *J. Am. Chem. Soc.* **1997**, *119*, 4841.

168. Shultz, M. D.; Bowman, M. J.; Ham, Y.-W.; Zhao, X.; Tora, G.; Chmielewski, J. *Angew. Chem. Int. Ed.* **2000**, *39*, 2710.

169. Shultz, M. D.; Ham, Y.-W.; Lee, S.-G.; Davis, D. A.; Brown, C.; Chmielewski, J. *J. Am. Chem. Soc.* **2004**, *126*, 9886.

170. Kellam, B.; Chan, W. C.; Chhabra, S. R.; Bycroft, B. W. *Tetrahedron Lett.* **1997**, *38*, 5391.

171. Edman, P.; Begg, G. *Eur. J. Biochem.* **1967**, *1*, 80.

172. Desiraju, G. R. *Crystal Engineering: The Design of Organic Solids*, Elsevier, Amsterdam, **1989**.

173. Atwood, J. L.; Davies, J. E. D.; MacNicol, D. D.; Vögtle, F.; Lehn, J.-M. *Comprehensive Supramolecular Chemistry*, Pergamon, Oxford, **1996**, *9*, 165.

174. Swiegers, G. F.; Malefetse, T. J. *Chem. Rev.* **2000**, *100*, 3483.

175. Breuning, E.; Ruben, M.; Lehn, J.-M.; Renz, F.; Garcia, Y.; Ksenofontov, V.; Gütlich, P.; Wegelius, E.; Rissanen, K. *Angew. Chem. Int. Ed.* **2000**, *39*, 2504.

176. Zhao, L. A.; Xu, Z. Q.; Thompson, L. K.; Heath, S. L.; Miller, D. O.; Ohba, M. *Angew. Chem. Int. Ed.* **2000**, *39*, 3114.

177. Bu, X. H.; Morishita, H.; Tanaka, K.; Biradha, K.; Furusho, S.; Shionoya, M. *Chem. Commun.* **2000**, 971.

178. Fujita, M.; Ume-moto, K.; Yoshizawa, M.; Fujita, N.; Kusukawa, T.; Bitadha, K. *Chem. Commun.* **2001**, 509.

179. John, D. W.; Xu, J. D.; Saalfrank, R. W.; Raymond, K. N. *Angew. Chem. Int. Ed.* **1999**, *38*, 2882.

180. Mamula, O.; von Zelewsky, A. *J. Chem. Soc., Dalton Trans.* **2000**, 219.

181. Mamula, O.; von Zelewsky, A.; Bark, T.; Bernardinelli, G. *Angew. Chem. Int. Ed.* **1999**, *38*, 2945.

182. Piguet, C.; Bernardinelli, G.; Hopfgartner, G. *Chem. Rev.*, **1997**, *97*, 2005.
183. Albrecht, M. *Chem. Eur. J.* **2000**, *6*, 3485.
184. Holliday, B. J.; Mirkin, C. A. *Angew. Chem. Int. Ed.* **2001**, *40*, 2022.
185. Stang, P. J.; Olenyuk, B. *Acc. Chem. Res.* **1997**, *30*, 502.
186. Schmidtchen, F. P.; Berger, M. *Chem. Rev.* **1997**, *97*, 1609.
187. Dietrich, B. *Pure Appl. Chem.* **1993**, *65*, 1457.
188. Hasenknof, B.; Lehn, J.-M.; Kniesel, B. O.; Baum, G.; Fenske, D. *Angew. Chem. Int. Ed. Engl.* **1996**, *35*, 1838.
189. Hasenknof, B.; Lehn, J.-M.; Kniesel, B. O.; Baumediene, N.; Dupont-Gervais, A.; van Dorsselar, A.; Fenske, D. *J. Am. Chem. Soc.* **1997**, *119*, 10956.
190. Keegan, J.; Kruger, P. E.; Nieuwenhuyzen, M.; O'Brien, J.; Martin, N. *Chem. Commun.* **2001**, 2192.
191. Coles, S. J.; Frey, J. G.; Gale, P. A.; Hursthouse, M. B.; Light, M. E.; Navakhun, K.; Thomas, G. L. *Chem. Commun.* **2003**, 568.
192. Camiolo, S.; Gale, P.A.; Hursthouse, M. B.; Light, M. E. *Org. Biomol. Chem.* **2003**, *1*, 741.
193. Camiolo, S.; Gale, P.A.; Hursthouse, M. B.; Light, M. E.; Shi, A. J. *Chem. Commun.* **2002**, 758.
194. Berl, V.; Huc, I.; Khoury, R.; Krische, M. J.; Lehn, J.-M. *Nature* **2000**, *407*, 720.
195. Berl, V.; Huc, I.; Khoury, R.; Krische, M. J.; Lehn, J.-M. *Chem. Eur. J.* **2001**, *7*, 2798.
196. Berl, V.; Huc, I.; Khoury, R.; Krische, M. J.; Lehn, J.-M. *Chem. Eur. J.* **2001**, *7*, 2810.
197. Kolomiets, E.; Berl, V.; Odriozola, I.; Stadler, A.-M.; Kyritsakas, N.; Lehn, J.-M. *Chem. Commun.* **2003**, 2868.
198. Gale, P. A.; Navakhun, K.; Camiolo, S.; Light, M. E.; Hursthouse, M. B. *J. Am. Chem. Soc.* **2002**, *124*, 11228.
199. Coste, J.; Le-Nguyen, D.; Castro, B. *Tetrahedron Lett.* **1990**, *31*, 205.
200. Greene, T. W.; Wuts, P. G. M. *Protective Groups In Organic Synthesis*, Wiley-Interscience, **1999**, 507 and 518.

Appendix 1: Crystal data

A1.1 Introduction

The crystal structures presented in the chapter 2, 3 and 5 were solved by the EPSRC National Crystallography Service (Dr. M. E. Light, Dr. S. Coles and Prof. M. B. Hursthouse). The refinement of the structures and the fractional coordinates are reported for the sake of completeness and so that the structure may be regenerated from the text of this thesis if necessary.

A1.2 Crystal data

The hexafluorophosphate salt of 3,4-diphenyl-1H-pyrrole-2,5-dicarboxylic acid bis-[(2-amino-ethyl)-amide (48)

Table A1.1: Crystal data and structure refinement.

Identification code	**48**
Empirical formula	$C_{22}H_{30}F_6N_5O_4P$
Formula weight	573.48
Temperature	120(2) K
Wavelength	0.71073 Å
Crystal system	Orthorhombic
Space group	Pbca
Unit cell dimensions	a = 16.1973(5) Å b = 9.3378(2) Å c = 34.0104(12) Å
Volume	5144.0(3) Å^3
Z	8
Density (calculated)	1.481 Mg / m^3
Absorption coefficient	0.190 mm^{-1}
F(000)	2384
Crystal	Colourless Plate
Crystal size	0.10 × 0.10 × 0.02 mm^3
θ range for data collection	3.09 – 25.03°
Index ranges	$-19 \le h \le 13, -11 \le k \le 9, -40 \le l \le 39$
Reflections collected	18704
Independent reflections	4519 [R_{int} = 0.1556]
Completeness to θ = 25.03°	99.6 %
Absorption correction	Semi–empirical from equivalents
Max. and min. transmission	0.9962 and 0.9813
Refinement method	Full-matrix least-squares on F^2
Data / restraints / parameters	4519 / 6 / 382
Goodness-of-fit on F^2	0.929
Final R indices [$F^2 > 2\sigma(F^2)$]	$R1$ = 0.0653, $wR2$ = 0.1377
R indices (all data)	$R1$ = 0.1738, $wR2$ = 0.1769
Extinction coefficient	none
Largest diff. peak and hole	0.681 and –0.501 e Å^{-3}

Table A1.2: Atomic coordinates [$\times 10^4$], equivalent isotropic displacement parameters [$Å^2 \times 10^3$] and site occupancy factors. U_{eq} is defined as one third of the trace of the orthogonalized U^{ij} tensor.

Atom	*x*	*y*	*z*	U_{eq}	*S.o.f.*
N1	3930(3)	1084(6)	11512(1)	25(1)	1
N2	3210(2)	−731(4)	10596(1)	23(1)	1
N3	3836(2)	−431(4)	9569(1)	18(1)	1
N4	3321(2)	−305(4)	8529(1)	29(1)	1
N5	3316(3)	1231(7)	7517(1)	35(1)	1
O1	4462(2)	−482(4)	10321(1)	31(1)	1
O2	4562(2)	−346(3)	8835(1)	28(1)	1
C1	3479(3)	896(5)	11135(1)	28(1)	1
C2	3525(3)	−651(5)	10993(1)	26(1)	1
C3	3714(3)	−570(5)	10285(1)	22(1)	1
C4	3330(3)	−506(5)	9890(1)	19(1)	1
C5	2511(3)	−520(4)	9758(1)	19(1)	1
C6	2547(3)	−442(4)	9341(1)	20(1)	1
C7	3373(2)	−386(5)	9236(1)	16(1)	1
C8	3801(3)	−342(5)	8850(1)	22(1)	1
C9	3639(3)	−74(6)	8131(1)	35(1)	1
C10	3074(4)	956(6)	7927(1)	46(2)	1
C11	1754(3)	−550(5)	10005(1)	21(1)	1
C12	1530(3)	656(5)	10225(1)	28(1)	1
C13	840(3)	641(6)	10463(1)	33(1)	1
C14	359(3)	−574(6)	10482(2)	31(1)	1
C15	561(3)	−1750(6)	10259(1)	31(1)	1
C16	1256(3)	−1755(5)	10025(1)	27(1)	1
C17	1822(3)	−374(5)	9069(1)	19(1)	1
C18	1340(3)	−1566(5)	8992(1)	25(1)	1
C19	707(3)	−1507(6)	8722(1)	29(1)	1
C20	543(3)	−267(6)	8520(2)	33(1)	1
C21	1008(3)	949(5)	8596(1)	27(1)	1
C22	1628(3)	883(5)	8873(1)	26(1)	1
P1	1309(1)	2461(2)	7092(1)	33(1)	1
F1	752(2)	3904(3)	7233(1)	37(1)	1
F2	1177(2)	1698(3)	7530(1)	58(1)	1
F3	2157(2)	3265(3)	7264(1)	59(1)	1
F4	1897(2)	1022(3)	6956(1)	41(1)	1
F5	1461(2)	3214(3)	6652(1)	63(1)	1
F6	481(2)	1652(3)	6923(1)	53(1)	1
O1W	−765(3)	3714(5)	7581(1)	66(1)	1
O2W	1613(2)	6121(4)	6574(1)	44(1)	1

3,4-Diphenyl-1H-pyrrole-2,5-dicarboxylic acid bis-[(1-methyl-1H-imida- zol-2-ylmethyl)-amide] (52)

Table A1.3: Crystal data and structure refinement.

Identification code	**52**	
Empirical formula	$C_{28}H_{27}N_7O_2$	
Formula weight	493.57	
Temperature	120(2) K	
Wavelength	0.71073 Å	
Crystal system	Triclinic	
Space group	*P*-1	
Unit cell dimensions	a = 9.3875(10) Å	α = 89.878(7)°
	b = 11.7030(10) Å	β = 70.435(4)°
	c = 12.1367(13) Å	γ = 80.149(7)°
Volume	1235.7(2) Å^3	
Z	2	
Density (calculated)	1.327 Mg / m^3	
Absorption coefficient	0.088 mm^{-1}	
F(000)	520	
Crystal	Colourless Slab	
Crystal size	0.40 × 0.20 × 0.06 mm^3	
θ range for data collection	3.18 – 25.03°	
Index ranges	$-11 \le h \le 11$, $-13 \le k \le 13$, $-14 \le l \le 14$	
Reflections collected	16236	
Independent reflections	4334 [R_{int} = 0.0704]	
Completeness to θ = 25.03°	99.4 %	
Absorption correction	Semi–empirical from equivalents	
Max. and min. transmission	0.9948 and 0.9658	
Refinement method	Full-matrix least-squares on F^2	
Data / restraints / parameters	4334 / 0 / 337	
Goodness-of-fit on F^2	0.980	
Final R indices [$F^2 > 2\sigma(F^2)$]	*R1* = 0.0552, *wR2* = 0.1290	
R indices (all data)	*R1* = 0.1106, *wR2* = 0.1511	
Extinction coefficient	0.010(3)	
Largest diff. peak and hole	0.218 and –0.254 e Å^{-3}	

Table A1.4: Atomic coordinates [$\times 10^4$], equivalent isotropic displacement parameters [$Å^2 \times 10^3$] and site occupancy factors. U_{eq} is defined as one third of the trace of the orthogonalized U^{ij} tensor.

Atom	*x*	*y*	*z*	U_{eq}	*S.o.f.*
C1	−3591(3)	5908(2)	3457(2)	44(1)	1
C2	−4296(3)	5900(2)	1627(2)	41(1)	1
C3	−3551(3)	5446(2)	519(2)	42(1)	1
C4	−2011(3)	4923(2)	1466(2)	31(1)	1
C5	−652(3)	4399(2)	1780(2)	34(1)	1
C6	274(3)	5481(2)	3041(2)	29(1)	1
C7	1051(3)	6447(2)	3170(2)	29(1)	1
C8	1425(3)	7400(2)	2529(2)	30(1)	1
C9	2139(3)	8038(2)	3129(2)	31(1)	1
C10	2164(3)	7446(2)	4121(2)	29(1)	1
C11	2715(3)	7615(2)	5108(2)	34(1)	1
C12	3858(3)	8763(2)	6139(2)	37(1)	1
C13	5543(3)	8331(2)	5815(2)	33(1)	1
C14	7978(3)	8211(2)	5047(2)	43(1)	1
C15	7767(3)	7202(2)	5572(2)	41(1)	1
C16	5471(3)	6403(2)	6773(2)	48(1)	1
C17	1097(3)	7759(2)	1451(2)	33(1)	1
C18	−390(3)	7982(2)	1437(2)	43(1)	1
C19	−677(4)	8337(2)	424(3)	55(1)	1
C20	524(5)	8480(2)	−562(3)	61(1)	1
C21	1994(4)	8259(3)	−550(3)	58(1)	1
C22	2287(4)	7906(2)	446(2)	43(1)	1
C23	2722(3)	9115(2)	2701(2)	38(1)	1
C24	1720(4)	10112(2)	2705(3)	55(1)	1
C25	2259(5)	11099(3)	2193(3)	73(1)	1
C26	3806(6)	11043(3)	1658(3)	72(1)	1
C27	4821(5)	10067(3)	1661(3)	71(1)	1
C28	4292(4)	9106(3)	2181(3)	56(1)	1
N1	−3307(3)	5564(2)	2231(2)	36(1)	1
N2	−2121(2)	4832(2)	414(2)	36(1)	1
N3	165(2)	5285(2)	1992(2)	31(1)	1
N4	1502(2)	6493(2)	4123(2)	29(1)	1
N5	3255(2)	8588(2)	5197(2)	35(1)	1
N6	6601(3)	8918(2)	5197(2)	40(1)	1
N7	6199(3)	7278(2)	6062(2)	37(1)	1
O1	−251(2)	4909(1)	3889(2)	40(1)	1
O2	2679(2)	6850(2)	5813(2)	46(1)	1

5-Methyl-3,4-diphenyl-1H-pyrrole-2-carboxylic acid (1-methyl-1H-imidazol-2-ylmethyl)-amide (53)

Table A1.5: Crystal data and structure refinement.

Identification code	**53**	
Empirical formula	$C_{23}H_{22}N_4O$	
Formula weight	370.45	
Temperature	120(2) K	
Wavelength	0.71073 Å	
Crystal system	Triclinic	
Space group	*P*-1	
Unit cell dimensions	a = 7.3267(2) Å	α = 82.523(2)°
	b = 10.4025(3) Å	β = 76.069(2)°
	c = 13.6141(4) Å	γ = 82.898(2)°
Volume	993.93(5) Å^3	
Z	2	
Density (calculated)	1.238 Mg / m^3	
Absorption coefficient	0.078 mm^{-1}	
F(000)	392	
Crystal	Colourless block	
Crystal size	0.30 × 0.20 × 0.10 mm^3	
θ range for data collection	2.94 – 25.02°	
Index ranges	$-8 \le h \le 8, -12 \le k \le 12, -16 \le l \le 16$	
Reflections collected	17926	
Independent reflections	3507 [R_{int} = 0.0702]	
Completeness to θ = 25.02°	99.8 %	
Absorption correction	Semi–empirical from equivalents	
Max. and min. transmission	0.9922 and 0.9769	
Refinement method	Full-matrix least-squares on F^2	
Data / restraints / parameters	3507 / 0 / 256	
Goodness-of-fit on F^2	1.053	
Final R indices [$F^2 > 2\sigma(F^2)$]	*R1* = 0.0404, *wR2* = 0.1053	
R indices (all data)	*R1* = 0.0470, *wR2* = 0.1099	
Extinction coefficient	0.030(5)	
Largest diff. peak and hole	0.201 and –0.201 e Å^{-3}	

Table A1.6: Atomic coordinates [$\times 10^4$], equivalent isotropic displacement parameters [$Å^2 \times 10^3$] and site occupancy factors. U_{eq} is defined as one third of the trace of the orthogonalized U^{ij} tensor.

Atom	*x*	*y*	*z*	U_{eq}	*S.o.f.*
C1	7717(2)	300(2)	2053(1)	42(1)	1
C2	5922(2)	1071(1)	2502(1)	34(1)	1
C3	4667(2)	1882(1)	2040(1)	34(1)	1
C4	3196(2)	2402(1)	2828(1)	32(1)	1
C5	3637(2)	1875(1)	3743(1)	30(1)	1
C6	2679(2)	1963(1)	4813(1)	29(1)	1
C7	586(2)	3315(1)	6057(1)	32(1)	1
C8	−1466(2)	3288(1)	6096(1)	30(1)	1
C9	−4308(2)	3879(1)	5947(1)	37(1)	1
C10	−4174(2)	2567(1)	6133(1)	35(1)	1
C11	−1641(2)	849(1)	6478(2)	51(1)	1
C12	4758(2)	2073(1)	932(1)	41(1)	1
C13	6393(3)	2440(2)	238(1)	55(1)	1
C14	6469(4)	2592(2)	−793(2)	78(1)	1
C15	4921(5)	2413(2)	−1148(2)	88(1)	1
C16	3291(4)	2069(2)	−470(2)	78(1)	1
C17	3215(3)	1879(2)	564(1)	55(1)	1
C18	1466(2)	3214(1)	2659(1)	34(1)	1
C19	1580(2)	4253(1)	1894(1)	42(1)	1
C20	−40(2)	4917(2)	1654(1)	50(1)	1
C21	−1805(2)	4585(2)	2185(1)	49(1)	1
C22	−1944(2)	3590(2)	2966(1)	44(1)	1
C23	−328(2)	2903(1)	3200(1)	38(1)	1
O1	2753(1)	998(1)	5455(1)	34(1)	1
N1	5274(2)	1062(1)	3525(1)	32(1)	1
N2	1758(2)	3112(1)	5052(1)	31(1)	1
N3	−2608(2)	4332(1)	5923(1)	36(1)	1
N4	−2364(2)	2189(1)	6233(1)	33(1)	1

3,4-Diphenyl-1H-pyrrole-2-carboxylic acid pyridin-2-ylamide (54)

Table A1.7: Crystal data and structure refinement.

Identification code	**54**	
Empirical formula	$C_{28}H_{21}N_5O_2$	
Formula weight	459.50	
Temperature	120(2) K	
Wavelength	0.71073 Å	
Crystal system	Triclinic	
Space group	*P*-1	
Unit cell dimensions	a = 8.5279(3) Å	α = 86.8860(10)°
	b = 9.7128(3) Å	β = 87.5470(10)°
	c = 14.0884(7) Å	γ = 78.889(3)°
Volume	1142.75(8) $Å^3$	
Z	2	
Density (calculated)	1.335 Mg / m^3	
Absorption coefficient	0.087 mm^{-1}	
F(000)	480	
Crystal	Colourless shard	
Crystal size	0.25 x 0.03 x 0.02 mm^3	
θ range for data collection	5.04 – 25.02°	
Index ranges	10 *h* -10, 11 *k* -11, 16 *l* -16	
Reflections collected	4259	
Independent reflections	1710 [R_{int} = 0.0716]	
Completeness to θ = 25.02°	42.4 %	
Absorption correction	Semiempirical from equivalents	
Max. and min. transmission	0.9983 and 0.9785	
Refinement method	Ful-matrix least-quares on F^2	
Data / restraints / parameters	1710 / 0 / 317	
Goodnessoffit on F^2	0.793	
Final *R* indices [$F^2 > 2\sigma(F^2)$]	*R1* = 0.1011, *wR2* = 0.2618	
R indices (all data)	*R1* = 0.1371, *wR2* = 0.2816	
Extinction coefficient	0.018(3)	
Largest diff. peak and hole	0.277 and 0.305 e $Å^{-3}$	

Table A1.8: Atomic coordinates [$\times 10^4$], equivalent isotropic displacement parameters [$Å^2 \times 10^3$] and site occupancy factors. U_{eq} is defined as one third of the trace of the orthogonalized U^{ij} tensor.

Atom	*x*	*y*	*z*	U_{eq}	*S.o.f.*
C1	5642(15)	6726(13)	9481(9)	32(3)	1
C2	6538(15)	8038(14)	9416(9)	34(3)	1
C3	5828(16)	9100(14)	8964(11)	42(4)	1
C4	4278(16)	8719(13)	8580(10)	41(4)	1
C5	3463(13)	7367(12)	8709(9)	24(3)	1
C6	827(14)	7679(12)	8016(8)	24(3)	1
C7	746(13)	6912(12)	7729(8)	23(3)	1
C8	1604(14)	5538(12)	7739(9)	24(3)	1
C9	3098(14)	5548(12)	7271(8)	25(3)	1
C10	3158(12)	6905(11)	6996(9)	21(3)	1
C11	4358(12)	7688(13)	6521(8)	23(3)	1
C13	7180(12)	7271(12)	5900(8)	21(3)	1
C14	7150(15)	8533(13)	5404(9)	32(3)	1
C15	8546(14)	8785(14)	4978(10)	35(3)	1
C16	9905(14)	7778(13)	5011(9)	32(3)	1
C17	9811(14)	6560(13)	5518(8)	30(3)	1
C18	1014(12)	4221(12)	8091(9)	21(3)	1
C19	1033(14)	3830(13)	9048(10)	29(3)	1
C20	609(17)	2571(14)	9370(9)	39(4)	1
C21	271(14)	1658(14)	8719(10)	31(3)	1
C22	262(15)	2037(13)	7770(10)	32(3)	1
C23	674(16)	3296(14)	7446(10)	35(3)	1
C24	4320(13)	4252(11)	7096(8)	22(3)	1
C25	5089(14)	3495(12)	7878(9)	28(3)	1
C26	6176(14)	2268(12)	7758(9)	28(3)	1
C27	6480(14)	1744(12)	6835(9)	30(3)	1
C28	5744(13)	2487(12)	6063(9)	27(3)	1
C29	4681(14)	3722(12)	6199(8)	27(3)	1
N1	4150(10)	6347(10)	9152(7)	23(2)	1
N2	1888(11)	6873(11)	8364(8)	26(2)	1
N3	1778(10)	7742(10)	7295(7)	22(2)	1
N4	5846(11)	6874(10)	6372(7)	27(2)	1
N5	8492(10)	6254(10)	5963(7)	25(2)	1
O1	1140(10)	8972(9)	7959(6)	30(2)	1
O2	3979(9)	8907(8)	6272(6)	30(2)	1

1H-pyrrole-2-carboxylic acid (1-methyl-1H-imidazol-2-ylmethyl)-amide (58)

Table A1.9: Crystal data and structure refinement.

Identification code	**(58)**	
Empirical formula	$C_{10}H_{12}N_4O$	
Formula weight	204.24	
Temperature	120(2) K	
Wavelength	0.71073 Å	
Crystal system	Triclinic	
Space group	*P*-1	
Unit cell dimensions	a = 7.9042(4) Å	α = 71.895(3)°
	b = 8.1598(5) Å	β = 73.760(3)°
	c = 8.6434(4) Å	γ = 80.527(3)°
Volume	506.88(5) Å^3	
Z	2	
Density (calculated)	1.338 Mg / m^3	
Absorption coefficient	0.092 mm^{-1}	
F(000)	216	
Crystal	Colourless Block	
Crystal size	0.30 × 0.10 × 0.10 mm^3	
θ range for data collection	3.12 – 25.02°	
Index ranges	$-9 \le h \le 9$, $-9 \le k \le 9$, $-10 \le l \le 10$	
Reflections collected	8638	
Independent reflections	1783 [R_{int} = 0.0827]	
Completeness to θ = 25.02°	99.5 %	
Absorption correction	Semi–empirical from equivalents	
Max. and min. transmission	0.9909 and 0.9729	
Refinement method	Full-matrix least-squares on F^2	
Data / restraints / parameters	1783 / 0 / 138	
Goodness-of-fit on F^2	1.016	
Final R indices [$F^2 > 2\sigma(F^2)$]	*R1* = 0.0408, *wR2* = 0.0993	
R indices (all data)	*R1* = 0.0608, *wR2* = 0.1097	
Extinction coefficient	0.049(9)	
Largest diff. peak and hole	0.219 and –0.195 e Å^{-3}	

Table A1.10: Atomic coordinates [$\times 10^4$], equivalent isotropic displacement parameters [$Å^2 \times 10^3$] and site occupancy factors. U_{eq} is defined as one third of the trace of the orthogonalized U^{ij} tensor.

Atom	*x*	*y*	*z*	U_{eq}	*S.o.f.*
C1	−1538(2)	1005(2)	1356(2)	30(1)	1
C2	−879(2)	2251(2)	−73(2)	31(1)	1
C3	551(2)	2857(2)	188(2)	27(1)	1
C4	711(2)	1965(2)	1784(2)	23(1)	1
C5	1859(2)	2142(2)	2776(2)	24(1)	1
C6	4474(2)	3404(2)	2758(2)	26(1)	1
C7	4164(2)	5234(2)	2828(2)	22(1)	1
C8	4265(2)	7984(2)	2177(2)	30(1)	1
C9	3135(2)	7537(2)	3714(2)	28(1)	1
C10	2077(2)	4722(2)	5710(2)	30(1)	1
N1	−589(2)	845(2)	2486(2)	26(1)	1
N2	3298(2)	2990(2)	1926(2)	26(1)	1
N3	4910(2)	6546(2)	1622(2)	26(1)	1
N4	3066(2)	5781(2)	4124(2)	23(1)	1
O1	1484(2)	1562(2)	4331(1)	32(1)	1

1H-pyrrole-2-carboxylic acid (1-methyl-1H-imidazol-2-ylmethyl)-amide (59)

Table A1.11: Crystal data and structure refinement.

Identification code	**59**	
Empirical formula	$C_{11}H_{14}N_4O$	
Formula weight	218.26	
Temperature	120(2) K	
Wavelength	0.71073 Å	
Crystal system	Triclinic	
Space group	*P*-1	
Unit cell dimensions	$a = 7.7936(15)$ Å	$\alpha = 71.287(17)°$
	$b = 8.653(2)$ Å	$\beta = 78.524(16)°$
	$c = 9.1498(18)$ Å	$\gamma = 69.712(17)°$
Volume	545.5(2) $Å^3$	
Z	2	
Density (calculated)	1.329 Mg / m^3	
Absorption coefficient	0.090 mm^{-1}	
F(000)	232	
Crystal	Colourless Cut Block	
Crystal size	0.20 × 0.15 × 0.10 mm^3	
θ range for data collection	3.33 – 25.03°	
Index ranges	$-9 \le h \le 9, -10 \le k \le 10, -10 \le l \le 10$	
Reflections collected	8563	
Independent reflections	1918 [$R_{int} = 0.0325$]	
Completeness to $\theta = 25.03°$	99.6 %	
Absorption correction	Semi–empirical from equivalents	
Max. and min. transmission	0.9910 and 0.9822	
Refinement method	Full-matrix least-squares on F^2	
Data / restraints / parameters	1918 / 0 / 156	
Goodness-of-fit on F^2	1.050	
Final *R* indices [$F^2 > 2\sigma(F^2)$]	*R1* = 0.0387, *wR2* = 0.1087	
R indices (all data)	*R1* = 0.0470, *wR2* = 0.1155	
Extinction coefficient	0.042(11)	
Largest diff. peak and hole	0.251 and –0.275 e $Å^{-3}$	

Table A1.12: Atomic coordinates [$\times 10^4$], equivalent isotropic displacement parameters [$Å^2 \times 10^3$] and site occupancy factors. U_{eq} is defined as one third of the trace of the orthogonalized U^{ij} tensor.

Atom	*x*	*y*	*z*	U_{eq}	*S.o.f.*
N1	−402(2)	2553(2)	937(2)	23(1)	1
N2	3301(2)	2025(2)	3089(2)	25(1)	1
N3	2889(2)	4308(2)	5512(2)	25(1)	1
N4	4834(2)	1706(2)	6247(2)	27(1)	1
O1	1666(2)	4426(1)	1440(1)	33(1)	1
C1	−2808(2)	1826(2)	116(2)	31(1)	1
C2	−1379(2)	1463(2)	1147(2)	24(1)	1
C3	−801(2)	110(2)	2413(2)	27(1)	1
C4	579(2)	389(2)	2973(2)	25(1)	1
C5	817(2)	1913(2)	2041(2)	22(1)	1
C6	1961(2)	2884(2)	2144(2)	23(1)	1
C7	4473(2)	2826(2)	3428(2)	26(1)	1
C8	4092(2)	2942(2)	5057(2)	23(1)	1
C9	4075(2)	2320(2)	7515(2)	30(1)	1
C10	2887(2)	3911(2)	7088(2)	30(1)	1
C11	1861(2)	5927(2)	4517(2)	33(1)	1

3,4-Diphenyl-1H-pyrrole-2,5-dicarboxylic acid bis-[(1-methyl-1H-imida- zol-2-ylmethyl)-amide] (52 hydrogenchloride complex)

Table A1.13: Crystal data and structure refinement.

Identification code	**52·H⁺·Cl⁻·H₂O**	
Empirical formula	$C_{28}H_{36}ClN_7O_6$	
Formula weight	602.09	
Temperature	120(2) K	
Wavelength	0.71073 Å	
Crystal system	Triclinic	
Space group	*P*-1	
Unit cell dimensions	a = 10.070(8) Å	α = 101.54(6)°
	b = 11.263(5) Å	β = 106.48(4)°
	c = 14.195(12) Å	γ = 100.72(4)°
Volume	1461.3(18) Å^3	
Z	2	
Density (calculated)	1.368 Mg / m^3	
Absorption coefficient	0.185 mm^{-1}	
F(000)	636	
Crystal	Colourless cut slab	
Crystal size	0.16 × 0.13 × 0.04 mm^3	
θ range for data collection	3.02 – 23.26°	
Index ranges	$-11 \le h \le 11$, $-12 \le k \le 12$, $-15 \le l \le 15$	
Reflections collected	15227	
Independent reflections	4185 [R_{int} = 0.1532]	
Completeness to θ = 23.26°	99.5 %	
Absorption correction	Semi–empirical from equivalents	
Max. and min. transmission	0.9926 and 0.9709	
Refinement method	Full-matrix least-squares on F^2	
Data / restraints / parameters	4185 / 12 / 407	
Goodness-of-fit on F^2	1.047	
Final R indices [$F^2 > 2\sigma(F^2)$]	*R1* = 0.0919, *wR2* = 0.2299	
R indices (all data)	*R1* = 0.1869, *wR2* = 0.2856	
Extinction coefficient	0.005(4)	
Largest diff. peak and hole	1.057 and –0.442 e Å^{-3}	

Table A1.14: Atomic coordinates [$\times 10^4$], equivalent isotropic displacement parameters [$Å^2 \times 10^3$] and site occupancy factors. U_{eq} is defined as one third of the trace of the orthogonalized U^{ij} tensor.

Atom	*x*	*y*	*z*	U_{eq}	*S.o.f.*
O1W	685(4)	3619(4)	−4721(4)	58(2)	1
O2W	−534(5)	1394(5)	−2842(6)	100(3)	1
O3W	6726(3)	4125(4)	3604(5)	60(2)	1
O4W	498(4)	1662(3)	5533(5)	70(2)	1
Cl1	4200(2)	5296(2)	2941(2)	47(1)	1
N1	1932(8)	5627(6)	−1663(5)	45(2)	1
N2	290(8)	3889(7)	−2382(6)	61(2)	1
N3	2663(7)	2764(6)	−1264(5)	41(2)	1
N4	3057(6)	2538(5)	1300(4)	31(2)	1
N5	3327(7)	2722(5)	3382(4)	38(2)	1
N6	6083(7)	2680(6)	4792(5)	45(2)	1
N7	4952(8)	1689(6)	5581(5)	47(2)	1
O1	3455(6)	4251(5)	205(4)	45(1)	1
O2	2791(6)	635(4)	3031(4)	39(1)	1
C1	3313(10)	6515(8)	−1100(7)	65(3)	1
C2	638(9)	5914(8)	−1974(6)	46(2)	1
C3	−370(10)	4840(9)	−2424(7)	62(3)	1
C4	1717(9)	4387(7)	−1953(6)	44(2)	1
C5	2832(10)	3665(7)	−1845(6)	47(2)	1
C6	3007(8)	3139(7)	−263(6)	32(2)	1
C7	2853(7)	2158(6)	288(5)	30(2)	1
C8	2525(7)	861(6)	−12(5)	31(2)	1
C9	2547(7)	465(6)	886(5)	29(2)	1
C10	2855(7)	1514(6)	1670(5)	28(2)	1
C11	2986(7)	1586(7)	2741(6)	33(2)	1
C12	3557(8)	2829(7)	4461(6)	42(2)	1
C13	4850(9)	2409(7)	4941(6)	38(2)	1
C14	7038(9)	2167(7)	5382(6)	47(2)	1
C15	6321(10)	1541(8)	5862(7)	53(2)	1
C16	3858(11)	1214(8)	5988(7)	65(3)	1
C17	2272(8)	47(6)	−1034(5)	31(2)	1
C18	925(9)	−422(8)	−1738(6)	47(2)	1
C19	706(9)	−1187(8)	−2683(6)	50(2)	1
C20	1836(9)	−1487(8)	−2939(6)	47(2)	1
C21	3178(9)	−1030(8)	−2248(6)	46(2)	1
C22	3386(8)	−274(7)	−1310(6)	38(2)	1
C23	2229(8)	−884(6)	889(6)	34(2)	1
C24	890(8)	−1689(6)	315(6)	39(2)	1
C25	596(9)	−2942(7)	298(7)	49(2)	1
C26	1653(11)	−3403(8)	836(7)	55(3)	1
C27	2984(11)	−2645(8)	1383(7)	55(2)	1
C28	3281(9)	−1363(7)	1433(6)	40(2)	1

5-Methyl-3,4-diphenyl-1H-pyrrole-2-carboxylic acid (1-methyl-1H-imidazol-2-ylmethyl)-amide (53 hydrogenchloride complex)

Table A1.15: Crystal data and structure refinement.

Identification code	**53·H$^+$·Cl$^-$**
Empirical formula	$C_{23}H_{25}ClN_4O_2$
	$C_{23}H_{23}N_4O^+ \cdot Cl^- \cdot H_2O$
Formula weight	424.92
Temperature	120(2) K
Wavelength	0.71069 Å
Crystal system	Monoclinic
Space group	*C*2/*c*
Unit cell dimensions	a = 35.854(5) Å
	b = 6.249(5) Å β = 120.620(9)°
	c = 22.020(5) Å
Volume	4246(4) Å^3
Z	8
Density (calculated)	1.330 Mg / m^3
Absorption coefficient	0.208 mm^{-1}
F(000)	1792
Crystal	Colourless Plate
Crystal size	0.10 × 0.06 × 0.02 mm^3
θ range for data collection	3.39 – 23.26°
Index ranges	$-39 \le h \le 39$, $-6 \le k \le 6$, $-24 \le l \le 24$
Reflections collected	12382
Independent reflections	3025 [R_{int} = 0.0689]
Completeness to θ = 23.26°	99.3 %
Absorption correction	None
Max. and min. transmission	0.9959 and 0.9795
Refinement method	Full-matrix least-squares on F^2
Data / restraints / parameters	3025 / 18 / 287
Goodness-of-fit on F^2	1.061
Final R indices [$F^2 > 2\sigma(F^2)$]	*R1* = 0.0685, *wR2* = 0.1693
R indices (all data)	*R1* = 0.0955, *wR2* = 0.1872
Extinction coefficient	0.008(7)
Largest diff. peak and hole	0.606 and –0.482 e Å^{-3}

Table A1.16: Atomic coordinates [$\times 10^4$], equivalent isotropic displacement parameters [$Å^2 \times 10^3$] and site occupancy factors. U_{eq} is defined as one third of the trace of the orthogonalized U^{ij} tensor.

Atom	*x*	*y*	*z*	U_{eq}	*S.o.f.*
N1	−712(6)	3600(30)	227(10)	43(5)	1
N2	−768(6)	7320(30)	−535(10)	44(5)	1
N3	−690(6)	7440(30)	−1793(10)	44(5)	1
N4	−1088(6)	10260(30)	−2168(10)	41(5)	1
O1	−1447(5)	6460(30)	−1369(8)	49(5)	1
C1	−415(7)	1070(40)	1237(12)	50(6)	1
C2	−780(7)	1920(40)	556(12)	43(6)	1
C3	−1214(7)	1370(40)	160(12)	42(6)	1
C4	−1415(7)	2800(40)	−427(12)	43(6)	1
C5	−1093(7)	4170(40)	−372(12)	42(6)	1
C6	−1122(8)	6030(40)	−805(12)	43(6)	1
C7	−798(8)	9350(40)	−890(12)	46(6)	1
C8	−860(7)	9010(40)	−1606(11)	40(6)	1
C9	−806(8)	7670(40)	−2486(12)	48(6)	1
C10	−1058(8)	9430(40)	−2726(13)	48(6)	1
C11	−1326(8)	12210(40)	−2187(13)	48(6)	1
C12	−1427(7)	−270(40)	368(11)	43(6)	1
C13	−1234(8)	−2260(40)	633(11)	45(6)	1
C14	−1429(8)	−3770(40)	849(12)	50(7)	1
C15	−1821(8)	−3310(40)	801(13)	52(7)	1
C16	−2017(8)	−1340(50)	536(13)	53(7)	1
C17	−1825(7)	150(40)	326(12)	44(6)	1
C18	−1883(7)	2780(40)	−985(12)	43(6)	1
C19	−2073(7)	940(40)	−1385(12)	47(6)	1
C20	−2511(8)	880(50)	−1895(13)	52(7)	1
C21	−2766(8)	2670(50)	−2008(13)	54(7)	1
C22	−2579(8)	4510(50)	−1612(12)	51(7)	1
C23	−2146(8)	4560(40)	−1108(12)	47(6)	1
Cl1	−155(2)	6514(10)	4060(3)	51(2)	1
O2	−108(18)	5440(70)	2130(30)	129(14)	0.67
O3	0	6970(110)	2500	129(14)	0.67

5-Methyl-3,4-diphenyl-1H-pyrrole-2-carboxylic acid pyridin-2-ylamide (55 hydrogenchloride complex)

Table A1.17: Crystal data and structure refinement.

Identification code	**55·H⁺·Cl⁻**
Empirical formula	$C_{23}H_{20}ClN_3O$
Formula weight	389.87
Temperature	120(2) K
Wavelength	0.71073 Å
Crystal system	Monoclinic
Space group	*Pn*
Unit cell dimensions	a = 5.6831(4) Å
	b = 11.8280(9) Å β = 100.422(3)°
	c = 14.4722(13) Å
Volume	956.77(13) Å^3
Z	2
Density (calculated)	1.353 Mg / m^3
Absorption coefficient	0.219 mm^{-1}
F(000)	408
Crystal	Colourless Lath
Crystal size	0.30 × 0.07 × 0.04 mm^3
θ range for data collection	3.44 – 25.02°
Index ranges	$-6 \le h \le 6, -12 \le k \le 14, -17 \le l \le 17$
Reflections collected	3036
Independent reflections	3027 [R_{int} = 0.0356]
Completeness to θ = 25.02°	99.4 %
Absorption correction	Semi–empirical from equivalents
Max. and min. transmission	0.9913 and 0.9373
Refinement method	Full-matrix least-squares on F^2
Data / restraints / parameters	3027 / 2 / 256
Goodness-of-fit on F^2	0.977
Final R indices [$F^2 > 2\sigma(F^2)$]	$R1$ = 0.0677, $wR2$ = 0.1665
R indices (all data)	$R1$ = 0.0940, $wR2$ = 0.1850
Extinction coefficient	0.024(8)
Largest diff. peak and hole	0.420 and –0.365 e Å^{-3}

Table A1.18: Atomic coordinates [$\times 10^4$], equivalent isotropic displacement parameters [$Å^2 \times 10^3$] and site occupancy factors. U_{eq} is defined as one third of the trace of the orthogonalized U^{ij} tensor.

Atom	*x*	*y*	*z*	U_{eq}	*S.o.f.*
C1	2698(11)	8429(6)	9318(4)	33(1)	1
C2	4156(9)	8075(5)	10229(4)	26(1)	1
C3	4132(10)	8395(5)	11162(4)	26(1)	1
C4	5943(9)	7758(5)	11746(4)	26(1)	1
C5	7042(10)	7088(5)	11158(4)	28(1)	1
C6	9096(10)	6335(5)	11404(4)	24(1)	1
C7	12018(10)	5230(5)	10703(4)	28(1)	1
C8	12921(11)	4926(5)	9903(5)	35(1)	1
C9	14937(11)	4256(5)	9998(5)	36(2)	1
C10	16070(12)	3891(6)	10868(5)	38(2)	1
C11	15139(11)	4166(6)	11636(5)	38(2)	1
C12	2654(9)	9322(5)	11445(3)	22(1)	1
C13	270(9)	9465(5)	10994(4)	29(1)	1
C14	−1097(10)	10359(6)	11232(4)	33(1)	1
C15	−94(10)	11129(5)	11926(4)	31(1)	1
C16	2240(10)	10983(5)	12379(4)	31(1)	1
C17	3603(10)	10088(5)	12143(4)	29(1)	1
C18	6604(9)	7869(5)	12776(4)	24(1)	1
C19	4995(9)	7570(5)	13366(4)	25(1)	1
C20	5517(10)	7791(5)	14313(4)	29(1)	1
C21	7656(10)	8308(5)	14715(4)	32(1)	1
C22	9280(11)	8583(5)	14146(4)	29(1)	1
C23	8762(10)	8375(5)	13188(4)	27(1)	1
N1	5931(8)	7300(4)	10243(3)	26(1)	1
N2	10045(8)	5911(4)	10649(3)	30(1)	1
N3	13143(8)	4825(4)	11548(3)	31(1)	1
O1	9987(7)	6087(3)	12213(3)	33(1)	1
Cl1	7587(2)	6172(1)	8526(1)	38(1)	1

1H-pyrrole-2-carboxylic acid (1-methyl-1H-imidazol-2-ylmethyl)-amide (58 hydrogenchloride complex)

Table A1.19: Crystal data and structure refinement.

Identification code	**58·H⁺·Cl⁻**
Empirical formula	$C_{10}H_{16}ClN_4O_{2.50}$
	$C_{10}H_{13}N_4O \cdot Cl \cdot 1.5H_2O$
Formula weight	267.72
Temperature	293(2) K
Wavelength	0.71069 Å
Crystal system	Monoclinic
Space group	$P2_1/n$
Unit cell dimensions	a = 9.582(5) Å
	b = 16.519(5) Å β = 90.627(5)°
	c = 16.239(5) Å
Volume	2570.2(17) Å^3
Z	8 (2 Molecules)
Density (calculated)	1.384 Mg / m^3
Absorption coefficient	0.300 mm^{-1}
F(000)	1128
Crystal	Colourless Cut Block
Crystal size	0.22 x 0.1 x 0.08 mm^3
θ range for data collection	3.26 – 25.02°
Index ranges	$-11 \le h \le 11$, $-18 \le k \le 19$, $-19 \le l \le 19$
Reflections collected	25801
Independent reflections	4541 [R_{int} = 0.0657]
Completeness to θ = 25.02°	99.8 %
Absorption correction	Semi–empirical from equivalents
Refinement method	Full-matrix least-squares on F^2
Data / restraints / parameters	4541 / 15 / 367
Goodness-of-fit on F^2	1.027
Final R indices [$F^2 > 2\sigma(F^2)$]	$R1$ = 0.0441, $wR2$ = 0.1034
R indices (all data)	$R1$ = 0.0753, $wR2$ = 0.1170
Extinction coefficient	0.0021(6)
Largest diff. peak and hole	0.295 and –0.309 e Å^{-3}

Table A1.20: Atomic coordinates [$\times 10^4$], equivalent isotropic displacement parameters [$Å^2 \times 10^3$] and site occupancy factors. U_{eq} is defined as one third of the trace of the orthogonalized U^{ij} tensor.

Atom	*x*	*y*	*z*	U_{eq}	*S.o.f.*
N1	−497(2)	5423(1)	3200(1)	23(1)	1
N2	1087(2)	3951(1)	4585(1)	25(1)	1
N3	3765(2)	3440(1)	4046(1)	28(1)	1
N4	4798(2)	3843(1)	5146(1)	28(1)	1
O1	1821(2)	5203(1)	4245(1)	30(1)	1
C1	−1677(3)	5353(2)	2743(2)	26(1)	1
C2	−2176(3)	4582(2)	2836(2)	28(1)	1
C3	−1267(3)	4179(2)	3379(2)	26(1)	1
C4	−233(2)	4714(2)	3604(2)	21(1)	1
C5	965(2)	4652(2)	4163(2)	22(1)	1
C6	2177(2)	3863(2)	5192(2)	28(1)	1
C7	3552(3)	3716(2)	4797(2)	24(1)	1
C8	5168(3)	3391(2)	3904(2)	37(1)	1
C9	5819(3)	3640(2)	4593(2)	38(1)	1
N5	−401(2)	−394(1)	6836(1)	23(1)	1
N6	1058(2)	1017(1)	5360(1)	23(1)	1
N7	3738(2)	1586(1)	5869(1)	26(1)	1
N8	4738(2)	1148(1)	4780(1)	29(1)	1
O2	1860(2)	−201(1)	5778(1)	29(1)	1
C10	5059(3)	4124(2)	5985(2)	40(1)	1
C11	−1575(3)	−314(2)	7283(2)	26(1)	1
C12	−2126(3)	434(2)	7139(2)	26(1)	1
C13	−1260(3)	821(2)	6571(2)	23(1)	1
C14	−194(2)	298(2)	6386(2)	21(1)	1
C15	979(2)	343(2)	5826(2)	22(1)	1
C16	2125(2)	1085(2)	4748(2)	27(1)	1
C17	3503(3)	1269(2)	5127(2)	23(1)	1
C18	5151(3)	1665(2)	5997(2)	34(1)	1
C19	5777(3)	1394(2)	5320(2)	37(1)	1
C20	4958(3)	822(2)	3951(2)	40(1)	1
O3	596(2)	7019(1)	3219(1)	32(1)	1
O4	1178(2)	−1941(1)	6899(1)	31(1)	1
O5	2004(2)	2284(1)	7013(1)	39(1)	1
Cl1	−1034(1)	2484(1)	4952(1)	27(1)	1
Cl2	1855(1)	2506(1)	2829(1)	30(1)	1

3,4-Diphenyl-1H-pyrrole-2,5-dicarboxylic acid bis-[(1-methyl-1H-imida- zol-2-ylmethyl)-amide] (52 dihydrogensulfate complex)

Table A1.21: Crystal data and structure refinement.

Identification code	**52·2H$^+$·SO$_4^{2-}$**
Empirical formula	$C_{29}H_{34}N_7O_{7.50}S$ $C_{28}H_{29}N_7O_2^{2+}$ · SO_4^{2-} · $0.5H_2O$ · CH_3OH
Formula weight	632.69
Temperature	293(2) K
Wavelength	0.69330 Å
Crystal system	Triclinic
Space group	*P*-1
Unit cell dimensions	a = 6.2644(14) Å α = 95.957(2)° b = 15.034(3) Å β = 95.068(2)° c = 16.478(4) Å γ = 94.872(2)°
Volume	1530.6(6) Å^3
Z	2
Density (calculated)	1.373 Mg / m^3
Absorption coefficient	0.166 mm^{-1}
F(000)	666
Crystal	Colourless Needle
Crystal size	0.20 × 0.01 × 0.01 mm^3
θ range for data collection	2.91 – 24.37°
Index ranges	$-7 \le h \le 7$, $-17 \le k \le 17$, $-19 \le l \le 19$
Reflections collected	11050
Independent reflections	5328 [R_{int} = 0.0296]
Completeness to θ = 24.37°	98.2 %
Absorption correction	None
Max. and min. transmission	0.9983 and 0.9676
Refinement method	Full-matrix least-squares on F^2
Data / restraints / parameters	5328 / 83 / 429
Goodness-of-fit on F^2	0.897
Final *R* indices [$F^2 > 2\sigma(F^2)$]	*R1* = 0.0662, *wR2* = 0.1910
R indices (all data)	*R1* = 0.0831, *wR2* = 0.2065
Extinction coefficient	0.1(4)
Largest diff. peak and hole	1.264 and –0.325 e Å^{-3}

Table A1.22: Atomic coordinates [$\times 10^4$], equivalent isotropic displacement parameters [$Å^2 \times 10^3$] and site occupancy factors. U_{eq} is defined as one third of the trace of the orthogonalized U^{ij} tensor.

Atom	*x*	*y*	*z*	U_{eq}	*S.o.f.*
C5	−1400(200)	−1040(100)	3140(80)	30(30)	1
C4	−700(200)	−1120(90)	4010(80)	30(30)	1
N2	1230(190)	−770(80)	4390(70)	30(30)	1
C3	1400(300)	−970(100)	5190(90)	40(40)	1
C2	−500(300)	−1450(110)	5290(90)	40(40)	1
N1	−1730(190)	−1530(80)	4550(70)	30(30)	1
C1	−3900(300)	−2030(130)	4380(110)	50(40)	1
C6	1400(200)	−1800(90)	2580(90)	30(30)	1
C7	3200(200)	−1820(90)	2060(90)	30(30)	1
C8	4300(200)	−2530(90)	1770(90)	30(30)	1
C9	5800(200)	−2210(90)	1220(80)	30(30)	1
C10	5500(200)	−1300(90)	1210(80)	30(30)	1
C11	6700(200)	−600(90)	790(90)	30(30)	1
C12A	8200(800)	1000(300)	900(300)	40(20)	0.65
C13A	8600(400)	1740(140)	1540(140)	40(20)	0.65
N6A	10300(300)	1910(120)	2090(120)	30(30)	0.65
C14A	10100(400)	2670(160)	2620(160)	40(20)	0.65
C15A	8200(400)	2960(140)	2370(140)	40(20)	0.65
N7A	7300(300)	2380(120)	1710(130)	30(30)	0.65
C16A	5100(400)	2430(170)	1310(160)	40(20)	0.65
C12B	8300(1500)	900(500)	900(600)	40(20)	0.35
C13B	7300(600)	1700(200)	1300(200)	40(20)	0.35
N6B	5400(500)	2000(200)	1000(200)	30(30)	0.35
C14B	5000(600)	2800(300)	1400(300)	40(20)	0.35
C15B	6600(600)	3000(200)	1900(200)	40(20)	0.35
N7B	8100(500)	2400(200)	1800(200)	30(30)	0.35
C16B	10100(600)	2400(300)	2400(300)	40(20)	0.35
C17	4100(200)	−3460(90)	2020(90)	30(30)	1
C18	2200(200)	−4000(100)	1910(90)	30(30)	1
C19	2100(300)	−4840(100)	2180(100)	40(40)	1
C20	3900(300)	−5160(110)	2560(110)	40(40)	1
C21	5800(300)	−4630(110)	2670(110)	40(40)	1
C22	5900(300)	−3780(100)	2400(100)	30(40)	1
C23	7200(200)	−2750(90)	730(90)	30(30)	1
C24	6400(300)	−3620(100)	370(90)	30(30)	1
C25	7700(300)	−4120(100)	−110(100)	40(40)	1
C26	9700(300)	−3770(100)	−250(100)	40(40)	1
C27	10500(200)	−2910(100)	110(90)	30(30)	1
C28	9200(200)	−2400(100)	580(90)	30(30)	1
N3	380(190)	−1050(80)	2630(70)	30(30)	1
N4	4010(190)	−1070(80)	1720(70)	30(30)	1
N5	7200(200)	190(80)	1250(80)	30(30)	1

O1	870(170)	–2460(70)	2930(70)	30(30)	1
O2	7080(170)	–730(70)	70(60)	30(20)	1
S1	4430(60)	880(20)	3090(20)	31(13)	1
O3	2840(170)	580(70)	2360(60)	30(30)	1
O4	4160(180)	250(80)	3710(70)	40(30)	1
O5	4030(190)	1780(80)	3410(70)	40(30)	1
O6	6610(170)	870(70)	2830(60)	30(30)	1
O8	1100(600)	–3650(180)	4240(170)	70(80)	0.50
C30	1900(900)	–4200(300)	4900(300)	70(130)	0.50
O7	10500(900)	4500(300)	3900(300)	130(160)	0.50
C29	12000(1100)	4000(400)	4400(400)	100(190)	0.50
O9	5900(900)	3400(200)	4100(300)	110(140)	0.50

3,4-Dichloro-1H-pyrrole-2,5-dicarboxylic acid bis-phenylamide (98 deprotanated complex)

Table A1.23: Crystal data and structure refinement.

Identification code	**2[98-H$^+$]·EtOH**
Empirical formula	$C_{70}H_{101}Cl_4N_8O_5$
Formula weight	1276.39
Temperature	150(2) K
Wavelength	0.71073 Å
Crystal system	Orthorhombic
Space group	*Pbca*
Unit cell dimensions	a = 20.800(5) Å
	b = 21.367(5) Å
	c = 31.437(5) Å
Volume	13972(5) Å^3
Z	8
Density (calculated)	1.214 Mg / m^3
Absorption coefficient	0.223 mm^{-1}
F(000)	5480
Crystal	Colourless Block
Crystal size	0.40 × 0.30 × 0.20 mm^3
θ range for data collection	2.92 – 25.03°
Index ranges	$-24 \le h \le 19$, $-23 \le k \le 25$, $-37 \le l \le 37$
Reflections collected	78085
Independent reflections	12300 [R_{int} = 0.1152]
Completeness to θ = 25.03°	99.7 %
Absorption correction	Semi–empirical from equivalents
Max. and min. transmission	0.9567 and 0.9160
Refinement method	Full-matrix least-squares on F^2
Data / restraints / parameters	12300 / 242 / 776
Goodness-of-fit on F^2	1.089
Final R indices [$F^2 > 2\sigma(F^2)$]	*R1* = 0.1000, *wR2* = 0.2798
R indices (all data)	*R1* = 0.1830, *wR2* = 0.3377
Extinction coefficient	0.0008(3)
Largest diff. peak and hole	1.462 and –0.733 e Å^{-3}

Table A1.24: Atomic coordinates [$\times 10^4$], equivalent isotropic displacement parameters [$Å^2 \times 10^3$] and site occupancy factors. U_{eq} is defined as one third of the trace of the orthogonalized U^{ij} tensor.

Atom	*x*	*y*	*z*	U_{eq}	*S.o.f.*
Cl1A	2336(1)	280(1)	5916(1)	55(1)	1
Cl2A	2610(1)	180(1)	6960(1)	51(1)	1
N1A	3911(2)	1785(2)	5535(1)	44(1)	1
N2A	3704(2)	1382(2)	6348(1)	35(1)	1
N3A	4196(2)	1761(2)	7110(1)	38(1)	1
O1A	3158(3)	1096(2)	5287(1)	66(1)	1
O2A	3633(2)	990(2)	7452(1)	46(1)	1
C1A	3810(3)	1978(3)	4764(2)	47(2)	1
C2A	4051(4)	2292(3)	4411(2)	60(2)	1
C3A	4560(4)	2688(3)	4437(2)	65(2)	1
C4A	4848(4)	2779(3)	4826(2)	65(2)	1
C5A	4632(4)	2477(3)	5185(2)	55(2)	1
C6A	4110(3)	2076(3)	5158(2)	43(2)	1
C7A	3454(3)	1326(3)	5587(2)	45(2)	1
C8A	3361(3)	1130(3)	6020(2)	40(1)	1
C9A	2919(3)	694(3)	6185(2)	42(1)	1
C10A	3020(3)	662(2)	6618(2)	37(1)	1
C11A	3503(3)	1094(2)	6709(2)	34(1)	1
C12A	3771(3)	1266(2)	7125(2)	35(1)	1
C13A	4461(3)	2059(2)	7467(2)	37(1)	1
C14A	5035(3)	2373(3)	7422(2)	44(2)	1
C15A	5320(4)	2677(3)	7766(2)	57(2)	1
C16A	5006(4)	2676(3)	8156(2)	65(2)	1
C17A	4428(4)	2381(3)	8198(2)	55(2)	1
C18A	4150(3)	2072(3)	7861(2)	47(2)	1
N1B	3672(2)	2891(2)	6389(1)	41(1)	1
N2B	4842(2)	2337(2)	6292(1)	37(1)	1
N3B	5197(2)	1110(2)	6230(1)	37(1)	1
O1B	4144(2)	3855(2)	6443(1)	52(1)	1
O2B	6231(2)	1397(2)	6072(1)	46(1)	1
Cl1B	5632(1)	4004(1)	6217(1)	77(1)	1
Cl2B	6653(1)	2806(1)	6130(1)	65(1)	1
C1B	2762(3)	3635(3)	6378(2)	42(2)	1
C2B	2118(3)	3729(3)	6409(2)	48(2)	1
C3B	1702(3)	3242(3)	6482(2)	62(2)	1
C4B	1937(4)	2652(3)	6541(3)	73(2)	1
C5B	2597(3)	2548(3)	6515(2)	61(2)	1
C6B	3015(3)	3037(3)	6432(2)	40(1)	1
C7B	4188(3)	3287(3)	6388(2)	41(1)	1
C8B	4805(3)	2970(3)	6313(2)	37(1)	1
C9B	5413(3)	3233(3)	6250(2)	46(2)	1
C10B	5834(3)	2728(3)	6198(2)	42(2)	1
C11B	5469(3)	2189(2)	6225(2)	36(1)	1
C12B	5676(3)	1540(3)	6169(2)	36(1)	1

C13B	5231(3)	451(3)	6184(2)	36(1)	1
C14B	4697(3)	102(3)	6299(2)	44(2)	1
C15B	4696(3)	−537(3)	6257(2)	47(2)	1
C16B	5217(4)	−841(3)	6093(2)	53(2)	1
C17B	5747(4)	−514(3)	5978(2)	55(2)	1
C18B	5766(3)	138(3)	6022(2)	50(2)	1
N3	2402(2)	3659(2)	4928(1)	69(2)	1
C19	2636(3)	3465(3)	4513(1)	80(2)	1
C20	2797(4)	4002(3)	4204(2)	88(3)	1
C21	3005(5)	3756(4)	3765(2)	106(3)	1
C22	3126(5)	4309(4)	3462(2)	119(4)	1
C23	1795(2)	3989(3)	4887(1)	71(2)	1
C24	1433(2)	4201(3)	5288(1)	62(2)	1
C25	794(2)	4517(2)	5167(2)	56(2)	1
C26	292(3)	4050(3)	4997(2)	58(2)	1
C27	2852(2)	4071(3)	5144(2)	72(2)	1
C28	3561(2)	3869(3)	5166(3)	85(3)	1
C29	3983(3)	4385(4)	5364(3)	88(3)	1
C30	4706(3)	4238(7)	5331(5)	157(5)	1
C31	2326(3)	3088(2)	5174(2)	90(3)	1
C32	1813(4)	2601(4)	5051(3)	116(3)	1
C33	1797(6)	2053(4)	5370(4)	164(5)	1
C34	1411(12)	1495(6)	5195(6)	302(14)	1
N4	5573(2)	127(2)	7614(1)	47(1)	1
C35	5756(2)	653(2)	7348(2)	54(2)	1
C36	6384(3)	988(3)	7469(2)	62(2)	1
C37	6567(3)	1490(3)	7138(2)	59(2)	1
C38	7171(3)	1845(3)	7285(2)	79(2)	1
C39	6031(2)	−383(2)	7573(1)	49(2)	1
C40	6134(4)	−690(3)	7135(1)	68(2)	1
C41	6638(4)	−1215(3)	7167(2)	81(2)	1
C42	6881(6)	−1435(5)	6729(3)	137(4)	1
C43	5539(3)	292(2)	8062(1)	59(2)	1
C44	5057(4)	804(3)	8195(2)	79(2)	1
C45	4963(5)	817(5)	8681(2)	150(5)	1
C46	5579(6)	1010(7)	8918(4)	161(5)	1
C47	4939(2)	−63(3)	7467(2)	62(2)	1
C48	4566(3)	−579(3)	7704(2)	68(2)	1
C49	3949(3)	−762(3)	7465(2)	79(2)	1
C50	3527(3)	−1206(3)	7730(3)	107(3)	1
O3	2271(3)	5405(3)	4623(2)	104(2)	1
C51	2688(6)	5783(6)	4402(4)	119(4)	1
C52	2463(14)	5754(15)	3937(9)	290(13)	1

3,4-Dichloro-1H-pyrrole-2,5-dicarboxylic acid diethyl ester (109)

Table A1.25: Crystal data and structure refinement.

Identification code	**109**
Empirical formula	$C_{10}H_{11}Cl_2NO_4$
Formula weight	280.10
Temperature	120(2) K
Wavelength	0.71073 Å
Crystal system	Monoclinic
Space group	$P2_1/c$
Unit cell dimensions	a = 13.0510(19) Å
	b = 4.5968(7) Å β = 101.462(5)°
	c = 20.618(4) Å
Volume	1212.3(3) Å^3
Z	4
Density (calculated)	1.535 Mg / m^3
Absorption coefficient	0.537 mm^{-1}
F(000)	576
Crystal	Colourless Rod
Crystal size	0.15 × 0.05 × 0.03 mm^3
θ range for data collection	4.03 – 25.01°
Index ranges	$-15 \le h \le 15$, $-5 \le k \le 5$, $-24 \le l \le 24$
Reflections collected	5032
Independent reflections	1965 [R_{int} = 0.0836]
Completeness to θ = 25.01°	91.5 %
Max. and min. transmission	0.9841 and 0.9238
Refinement method	Full-matrix least-squares on F^2
Data / restraints / parameters	1965 / 0 / 157
Goodness-of-fit on F^2	0.942
Final R indices [$F^2 > 2\sigma(F^2)$]	$R1$ = 0.0497, $wR2$ = 0.0910
R indices (all data)	$R1$ = 0.1157, $wR2$ = 0.1121
Extinction coefficient	0.0015(11)
Largest diff. peak and hole	0.372 and –0.454 e Å^{-3}

Table A1.26: Atomic coordinates [$\times 10^4$], equivalent isotropic displacement parameters [$Å^2 \times 10^3$] and site occupancy factors. U_{eq} is defined as one third of the trace of the orthogonalized U^{ij} tensor.

Atom	*x*	*y*	*z*	U_{eq}	*S.o.f.*
N1	1691(3)	13676(7)	3189(2)	22(1)	1
O1	−342(2)	11564(6)	2866(1)	25(1)	1
O2	0(2)	8535(6)	3747(1)	27(1)	1
O3	2832(2)	17835(6)	2637(1)	28(1)	1
O4	4259(2)	16708(6)	3418(1)	26(1)	1
Cl1	2095(1)	8615(2)	4726(1)	29(1)	1
Cl2	4164(1)	12589(2)	4563(1)	29(1)	1
C1	−1221(4)	5529(9)	4150(2)	35(1)	1
C2	−1068(3)	7416(9)	3574(2)	27(1)	1
C3	243(4)	10593(9)	3352(2)	24(1)	1
C4	1310(3)	11639(8)	3560(2)	19(1)	1
C5	2129(3)	10961(8)	4087(2)	22(1)	1
C6	2992(3)	12617(8)	4021(2)	21(1)	1
C7	2705(3)	14323(8)	3452(2)	20(1)	1
C8	3245(4)	16469(9)	3122(2)	23(1)	1
C9	4859(3)	18935(9)	3155(2)	28(1)	1
C10	5987(3)	18543(10)	3493(2)	39(1)	1

3,4-Dichloro-5-phenylcarbamoyl-1H-pyrrole-2-carboxylic acid ethyl ester (110)

Table A1.27: Crystal data and structure refinement.

Identification code	**110**
Empirical formula	$C_{14}H_{12}Cl_2N_2O_3$
Formula weight	327.16
Temperature	120(2) K
Wavelength	0.71073 Å
Crystal system	Monoclinic
Space group	$P2_1/n$
Unit cell dimensions	$a = 9.7259(8)$ Å
	$b = 4.9086(5)$ Å $\quad \beta = 8.838(3)°$
	$c = 29.937(3)$ Å
Volume	1412.2(2) Å^3
Z	4
Density (calculated)	1.539 Mg / m^3
Absorption coefficient	0.471 mm^{-1}
F(000)	672
Crystal	Colourless Needle
Crystal size	0.10 × 0.02 × 0.02 mm^3
θ range for data collection	3.18 – 23.25°
Index ranges	$-10 \le h \le 10$, $-4 \le k \le 5$, $-33 \le l \le 32$
Reflections collected	3326
Independent reflections	1968 [$R_{int} = 0.1093$]
Completeness to $\theta = 23.25°$	96.8 %
Max. and min. transmission	0.9907 and 0.9545
Refinement method	Full-matrix least-squares on F^2
Data / restraints / parameters	1968 / 0 / 192
Goodness-of-fit on F^2	1.156
Final R indices [$F^2 > 2\sigma(F^2)$]	$R1 = 0.1045$, $wR2 = 0.2932$
R indices (all data)	$R1 = 0.1810$, $wR2 = 0.3247$
Largest diff. peak and hole	0.919 and –0.513 e Å^{-3}

Table A1.28: Atomic coordinates [× 10^4], equivalent isotropic displacement parameters [$Å^2 \times 10^3$] and site occupancy factors. U_{eq} is defined as one third of the trace of the orthogonalized U^{ij} tensor.

Atom	*x*	*y*	*z*	U_{eq}	*S.o.f.*
C1	5906(14)	7050(30)	2377(5)	30(4)	1
C2	5516(17)	6890(30)	2799(5)	38(4)	1
C3	4526(15)	8700(30)	2910(5)	37(4)	1
C4	3967(15)	10680(30)	2613(4)	37(4)	1
C5	4367(15)	10790(30)	2180(5)	35(4)	1
C6	5333(14)	8970(30)	2061(4)	25(3)	1
C7	5721(14)	10940(30)	1332(4)	23(3)	1
C8	6382(14)	10270(30)	930(4)	27(4)	1
C9	7448(13)	8410(30)	861(4)	22(3)	1
C10	7697(14)	8810(20)	424(4)	25(3)	1
C11	6862(13)	10900(20)	226(4)	21(3)	1
C12	6713(14)	12210(30)	−207(4)	27(3)	1
C13	7629(16)	12510(30)	−909(4)	37(4)	1
C14	8287(15)	10500(30)	−1189(4)	35(4)	1
N1	5743(12)	8900(20)	1625(4)	34(3)	1
N2	6067(11)	11710(20)	538(3)	26(3)	1
O1	5227(10)	13229(19)	1368(3)	31(2)	1
O2	5948(10)	14099(19)	−327(3)	36(3)	1
O3	7541(10)	11111(18)	−476(3)	32(2)	1
Cl1	8298(4)	6187(7)	1244(1)	30(1)	1
Cl2	8955(4)	7035(7)	195(1)	31(1)	1

1,4-Phenylene-bis-(3,4-dichloro-5-phenylcarbamoyl-1H-pyrrole-2-car boxylic acid amide) (102 chloride complex)

Table A1.29: Crystal data and structure refinement.

Identification code	**$[102{\cdot}2Cl^-]^{2-}{\cdot}2TBA$**
Empirical formula	$C_{33}H_{49}Cl_3N_5O_2$
Formula weight	654.12
Temperature	120(2) K
Wavelength	0.71073 Å
Crystal system	Monoclinic
Space group	$P2_1/c$
Unit cell dimensions	a = 8.5720(2) Å
	b = 21.1088(5) Å β = 93.5560(10)°
	c = 19.3520(6) Å
Volume	3494.90(16) Å^3
Z	4
Density (calculated)	1.243 Mg / m^3
Absorption coefficient	0.298 mm^{-1}
F(000)	1396
Crystal	Colourless Needle
Crystal size	0.15 × 0.07 × 0.05 mm^3
θ range for data collection	3.07 – 25.03°
Index ranges	$-10 \le h \le 10$, $-25 \le k \le 24$, $-23 \le l \le 23$
Reflections collected	11999
Independent reflections	6161 [R_{int} = 0.0392]
Completeness to θ = 25.03°	99.8 %
Absorption correction	Semi–empirical from equivalents
Max. and min. transmission	0.9852 and 0.9566
Refinement method	Full-matrix least-squares on F^2
Data / restraints / parameters	6161 / 18 / 394
Goodness-of-fit on F^2	0.996
Final R indices [$F^2 > 2\sigma(F^2)$]	$R1$ = 0.0647, $wR2$ = 0.1661
R indices (all data)	$R1$ = 0.0911, $wR2$ = 0.1809
Extinction coefficient	0.0027(7)
Largest diff. peak and hole	1.733 and –0.894 e Å^{-3}

Table A1.30: Atomic coordinates [$\times 10^4$], equivalent isotropic displacement parameters [$Å^2 \times 10^3$] and site occupancy factors. U_{eq} is defined as one third of the trace of the orthogonalized U^{ij} tensor.

Atom	*x*	*y*	*z*	U_{eq}	*S.o.f.*
Cl1	1684(1)	7067(1)	6076(1)	32(1)	1
Cl2	3847(1)	5789(1)	6482(1)	34(1)	1
Cl3	1879(1)	6940(1)	9566(1)	28(1)	1
N1	571(4)	7816(2)	8263(2)	28(1)	1
N2	2001(3)	6613(2)	8025(2)	25(1)	1
N3	3595(4)	5717(2)	8903(2)	30(1)	1
O1	−101(4)	7867(2)	7111(2)	49(1)	1
O2	4267(3)	5178(1)	7941(1)	36(1)	1
C1	−1005(5)	8795(2)	8074(2)	33(1)	1
C2	−1508(5)	9362(2)	8346(2)	38(1)	1
C3	−1072(5)	9545(2)	9015(2)	39(1)	1
C4	−140(5)	9145(2)	9428(2)	40(1)	1
C5	365(5)	8571(2)	9171(2)	33(1)	1
C6	−47(4)	8401(2)	8491(2)	28(1)	1
C7	564(4)	7592(2)	7606(2)	29(1)	1
C8	1448(4)	7005(2)	7501(2)	26(1)	1
C9	1974(4)	6761(2)	6896(2)	26(1)	1
C10	2861(4)	6221(2)	7069(2)	25(1)	1
C11	2858(4)	6130(2)	7771(2)	25(1)	1
C12	3629(4)	5628(2)	8208(2)	27(1)	1
C13	3843(5)	5431(2)	10104(2)	29(1)	1
C14	4314(4)	5333(2)	9436(2)	26(1)	1
C15	5485(5)	4896(2)	9335(2)	29(1)	1
N4	6734(4)	7885(2)	5362(2)	36(1)	1
C16	6875(5)	7170(2)	5351(2)	43(1)	1
C17	5426(5)	6823(2)	5064(2)	44(1)	1
C18	5799(6)	6146(3)	4877(3)	58(1)	1
C19	4394(6)	5786(3)	4574(3)	61(2)	1
C20	6313(5)	8144(3)	4633(2)	44(1)	1
C21	7297(6)	7880(4)	4067(2)	74(2)	1
C22	6931(8)	8250(4)	3400(3)	93(3)	1
C23	7744(11)	8765(5)	3352(6)	164(5)	1
C24	8292(5)	8156(2)	5632(2)	41(1)	1
C25	8304(5)	8854(3)	5791(2)	48(1)	1
C26	9969(5)	9093(3)	5960(3)	52(1)	1
C27	10038(6)	9789(3)	6125(3)	67(2)	1
C28	5433(5)	8094(2)	5807(2)	36(1)	1
C29	5623(5)	7912(2)	6568(2)	35(1)	1
C30	4474(5)	8303(2)	6972(2)	40(1)	1
C31	4579(6)	8152(3)	7741(2)	49(1)	1
N5	1508(7)	4076(4)	3601(4)	108(2)	1
C32	1866(7)	4521(3)	3329(3)	60(1)	1
C33	2355(6)	5085(3)	2979(3)	59(1)	1

1,3-Phenylene-bis-(3,4-dichloro-5-phenylcarbamoyl-1H-pyrrole-2-car- boxylic acid amide) (101 deprotonated complex)

Table A1.31: Crystal data and structure refinement.

Identification code	**$[101\text{-}2H^+]^{2-}\cdot 2TBA$**
Empirical formula	$C_{62}H_{90}Cl_4N_8O_4$
Formula weight	1153.22
Temperature	293(2) K
Wavelength	0.71073 Å
Crystal system	Orthorhombic
Space group	*P*212121
Unit cell dimensions	a = 13.3899(3) Å b = 16.3267(3) Å c = 28.0813(7) Å
Volume	6138.9(2) $Å^3$
Z	4
Density (calculated)	1.248 Mg / m^3
Absorption coefficient	0.246 mm^{-1}
F(000)	2472
Crystal	Colourless block
Crystal size	0.10 × 0.05 × 0.04 mm^3
θ range for data collection	2.92 – 21.96°
Index ranges	$-14 \le h \le 13$, $-17 \le k \le 17$, $-29 \le l \le 29$
Reflections collected	29984
Independent reflections	7462 [R_{int} = 0.1000]
Completeness to θ = 21.96°	99.5 %
Max. and min. transmission	0.9902 and 0.9759
Refinement method	Full-matrix least-squares on F^2
Data / restraints / parameters	7462 / 428 / 637
Goodness-of-fit on F^2	1.064
Final R indices [$F^2 > 2\sigma(F^2)$]	*R1* = 0.1119, *wR2* = 0.2814
R indices (all data)	*R1* = 0.1866, *wR2* = 0.3306
Absolute structure parameter	–0.11(18)
Largest diff. peak and hole	0.764 and –0.330 e $Å^{-3}$

Table A1.32: Atomic coordinates [$\times 10^4$], equivalent isotropic displacement parameters [$Å^2 \times 10^3$] and site occupancy factors. U_{eq} is defined as one third of the trace of the orthogonalized U^{ij} tensor.

Atom	*x*	*y*	*z*	U_{eq}	*S.o.f.*
C1	3279(5)	9773(5)	−1520(2)	137(7)	1
C2	2753(6)	9819(6)	−1946(3)	165(9)	1
C3	3063(6)	10355(6)	−2300(2)	124(6)	1
C4	3898(6)	10846(5)	−2229(2)	92(4)	1
C5	4423(5)	10800(4)	−1803(2)	93(4)	1
C6	4113(4)	10264(4)	−1448(2)	84(4)	1
C7	4428(10)	9835(7)	−602(5)	63(3)	1
N2	6073(4)	10324(3)	−325(2)	64(3)	1
C8	5199(3)	9848(3)	−250(2)	61(3)	1
C9	5299(5)	9442(4)	195(2)	69(3)	1
C10	6233(5)	9668(4)	395(2)	63(3)	1
C11	6711(4)	10213(4)	73(2)	64(3)	1
C12	7629(8)	10604(7)	100(5)	60(3)	1
C13	8580(4)	11768(3)	−259(2)	55(3)	1
C14	8624(4)	12263(4)	−661(2)	69(3)	1
C15	9285(5)	12919(4)	−676(2)	63(3)	1
C16	9902(4)	13080(3)	−290(1)	63(3)	1
C17	9858(3)	12585(2)	113(1)	55(3)	1
C18	9197(4)	11929(3)	128(2)	55(3)	1
C19	10602(9)	12390(8)	923(4)	58(3)	1
N5	11484(4)	13662(3)	1195(2)	62(2)	1
C20	11247(3)	12819(3)	1250(1)	68(3)	1
C21	11700(5)	12538(4)	1677(2)	83(4)	1
C22	12216(4)	13207(4)	1886(2)	78(4)	1
C23	12082(4)	13902(4)	1589(2)	67(3)	1
C24	12442(9)	14715(7)	1641(5)	65(3)	1
C25	12417(6)	16034(4)	1189(3)	64(3)	1
C26	13007(8)	16465(7)	1510(3)	143(8)	1
C27	13148(9)	17302(7)	1453(4)	147(8)	1
C28	12699(8)	17709(4)	1074(5)	110(6)	1
C29	12109(7)	17278(6)	753(4)	105(5)	1
C30	11968(6)	16440(6)	811(3)	104(5)	1
N1	4630(7)	10244(6)	−1007(4)	67(3)	1
N3	7858(7)	11154(5)	−252(3)	59(2)	1
N4	10445(6)	12807(5)	502(3)	56(2)	1
N6	12216(7)	15199(6)	1234(3)	66(3)	1
O1	3647(7)	9487(5)	−527(3)	88(3)	1
O2	8227(6)	10472(4)	436(3)	72(2)	1
O3	10270(7)	11713(5)	1000(3)	76(2)	1
O4	12861(6)	14951(5)	1987(3)	81(2)	1
Cl1	4485(3)	8765(2)	440(1)	98(1)	1
Cl2	6664(3)	9293(2)	922(1)	93(1)	1
Cl3	11670(4)	11568(2)	1903(1)	125(2)	1

Cl4	12856(3)	13167(2)	2399(1)	106(1)	1
N7	5596(11)	5500(7)	234(4)	350(30)	1
C31	5080(20)	6017(19)	−130(5)	231(15)	1
C32	4403(17)	6652(11)	71(6)	205(12)	1
C33	3702(12)	6992(13)	−300(7)	208(12)	1
C34	4236(17)	7432(11)	−692(5)	154(8)	1
C35	6085(12)	4810(10)	−47(6)	170(10)	1
C36	6869(14)	5143(12)	−383(7)	229(13)	1
C37	7297(14)	4503(9)	−700(6)	140(7)	1
C38	7950(20)	4813(14)	−1087(8)	210(12)	1
C39	4900(14)	5164(13)	594(6)	216(13)	1
C40	5363(11)	4551(12)	920(5)	171(9)	1
C41	4756(13)	4325(12)	1338(5)	156(8)	1
C42	5228(12)	3739(11)	1671(5)	129(6)	1
C43	6329(13)	6031(15)	475(7)	206(11)	1
C44	5996(11)	6380(8)	944(4)	100(5)	1
C45	6637(17)	7096(12)	1094(7)	230(14)	1
C46	6280(20)	7467(10)	1555(5)	168(9)	1
N8	7897(11)	1267(8)	1890(4)	104(4)	1
C47	7900(20)	1899(19)	1549(11)	244(15)	1
C48	7380(30)	2100(17)	1172(9)	220(13)	1
C49	7800(12)	3041(9)	934(6)	105(5)	1
C50	7152(18)	2941(18)	547(11)	240(14)	1
C51	8418(16)	559(14)	1712(8)	172(10)	1
C52	8900(20)	−30(15)	1828(12)	211(12)	1
C53	9387(15)	−713(10)	1644(6)	120(6)	1
C54	10372(16)	−627(17)	1481(7)	178(10)	1
C55	8390(20)	1489(15)	2351(9)	176(10)	1
C56	9310(20)	1647(16)	2446(8)	177(10)	1
C57	9586(17)	1772(19)	2964(10)	204(13)	1
C58	10510(30)	1990(30)	3021(10)	276(18)	1
C59	6880(20)	1044(16)	1999(10)	173(9)	1
C60	6060(30)	1350(30)	2072(12)	245(16)	1
C61	4890(30)	1080(30)	2191(13)	276(18)	1
C62	4870(70)	340(50)	2050(30)	620(70)	1

1,4-Phenylene-bis-(3,4-dichloro-5-phenylcarbamoyl-1H-pyrrole-2-carboxylic acid amide) (102 deprotonated complex)

Table A1.33. Crystal data and structure refinement.

Identification code	**$[102\text{-}2H^+]^{2-}\cdot 2TBA$**	
Empirical formula	$C_{124}H_{180}Cl_8N_{16}O_8$	
Formula weight	2306.44	
Temperature	120(2) K	
Wavelength	0.71069 Å	
Crystal system	Triclinic	
Space group	P-1	
Unit cell dimensions	a = 16.472(5) Å	α = 69.036(5)°
	b = 18.028(5) Å	β = 76.520(5)°
	c = 24.398(5) Å	γ = 73.183(5)°
Volume	6408(3) Å^3	
Z	2	
Density (calculated)	1.195 Mg / m^3	
Absorption coefficient	0.235 mm^{-1}	
F(000)	2472	
Crystal	Colourless Block	
Crystal size	0.10 × 0.10 × 0.10 mm^3	
θ range for data collection	2.95 – 23.25°	
Index ranges	$-18 \le h \le 18$, $-20 \le k \le 20$, $-26 \le l \le 26$	
Reflections collected	31321	
Independent reflections	17550 [R_{int} = 0.0616]	
Completeness to θ = 23.25°	95.4 %	
Max. and min. transmission	0.9769 and 0.9769	
Refinement method	Full-matrix least-squares on F^2	
Data / restraints / parameters	17550 / 948 / 1421	
Goodness-of-fit on F^2	0.992	
Final R indices [$F^2 > 2\sigma(F^2)$]	*R1* = 0.1107, *wR2* = 0.2954	
R indices (all data)	*R1* = 0.2051, *wR2* = 0.3389	
Largest diff. peak and hole	1.008 and –0.747 e Å^{-3}	

Table A1.34: Atomic coordinates [$\times 10^4$], equivalent isotropic displacement parameters [$Å^2 \times 10^3$] and site occupancy factors. U_{eq} is defined as one third of the trace of the orthogonalized U^{ij} tensor.

Atom	*x*	*y*	*z*	U_{eq}	*S.o.f.*
Cl1	−7281(1)	3371(1)	2915(1)	63(1)	1
Cl2	−5848(1)	2505(2)	1969(1)	75(1)	1
Cl3	2653(2)	1270(2)	1385(1)	107(1)	1
Cl4	3869(1)	−281(2)	910(1)	93(1)	1
N1	−5539(4)	2950(4)	4340(2)	51(2)	1
N2	−4965(3)	2401(4)	3368(3)	49(2)	1
N3	−3364(4)	1741(5)	2872(3)	72(2)	1
N4	64(4)	368(4)	2141(2)	46(2)	1
N5	1478(3)	−438(4)	1567(2)	42(2)	1
N6	1937(5)	−1959(4)	1388(3)	62(2)	1
O1	−6899(3)	3344(3)	4138(2)	59(2)	1
O2	−3962(3)	1607(4)	2162(2)	80(2)	1
O3	667(4)	1460(4)	1886(2)	74(2)	1
O4	3148(4)	−1632(4)	805(2)	78(2)	1
C1	−4914(5)	2813(5)	5165(4)	62(2)	1
C2	−4989(6)	2786(5)	5762(4)	73(3)	1
C3	−5780(6)	2940(5)	6096(4)	64(2)	1
C4	−6492(5)	3119(5)	5833(4)	66(2)	1
C5	−6436(5)	3144(5)	5253(3)	52(2)	1
C6	−5656(5)	2979(4)	4927(3)	49(2)	1
C7	−6137(5)	3032(5)	4020(3)	50(2)	1
C8	−5792(5)	2789(4)	3469(3)	45(2)	1
C9	−6241(4)	2872(5)	3019(3)	48(2)	1
C10	−5634(5)	2522(5)	2631(3)	57(2)	1
C11	−4867(4)	2238(5)	2853(3)	52(2)	1
C12	−4038(5)	1835(6)	2600(4)	68(3)	1
C13	−2513(5)	1392(6)	2698(3)	68(3)	1
C14	−1841(5)	1646(6)	2781(3)	74(3)	1
C15	−992(5)	1332(6)	2599(3)	69(3)	1
C16	−783(5)	734(5)	2337(3)	50(2)	1
C17	−1436(5)	416(5)	2285(3)	59(2)	1
C18	−2278(5)	733(6)	2473(3)	68(3)	1
C19	708(5)	760(6)	1897(3)	56(2)	1
C20	1487(5)	285(5)	1630(3)	45(2)	1
C21	2298(5)	467(5)	1396(3)	58(2)	1
C22	2796(4)	−170(5)	1191(3)	53(2)	1
C23	2278(4)	−726(5)	1294(3)	42(2)	1
C24	2496(6)	−1463(6)	1148(3)	53(2)	1
C25	1931(8)	−2647(6)	1248(4)	86(3)	1
C26	1179(9)	−2861(7)	1300(6)	131(5)	1
C27	1122(13)	−3503(9)	1159(8)	180(7)	1
C28	1863(15)	−4013(10)	980(8)	184(8)	1

C29	2670(12)	−3801(8)	915(6)	142(6)	1
C30	2695(8)	−3141(6)	1069(4)	93(3)	1
Cl5	−1430(2)	3450(2)	3726(1)	97(1)	1
Cl6	−1446(1)	1632(2)	4736(1)	72(1)	1
N7	−3903(5)	3891(5)	2874(3)	73(2)	1
N8	−3367(4)	2540(4)	3811(3)	53(2)	1
N9	−4006(4)	1183(4)	4457(2)	45(2)	1
O5	−2698(4)	4324(4)	2791(2)	79(2)	1
O6	−2939(3)	715(3)	5037(2)	54(1)	1
C31	−3972(7)	5139(7)	2017(5)	100(3)	1
C32	−4359(8)	5637(7)	1528(5)	112(4)	1
C33	−5066(7)	5493(7)	1412(4)	86(3)	1
C34	−5388(6)	4847(6)	1793(4)	79(3)	1
C35	−4998(6)	4345(6)	2272(4)	65(2)	1
C36	−4286(6)	4455(6)	2390(4)	72(3)	1
C37	−3143(6)	3824(7)	3061(4)	68(3)	1
C38	−2910(5)	3127(5)	3567(3)	51(2)	1
C39	−2194(5)	2909(6)	3854(4)	56(2)	1
C40	−2219(5)	2174(5)	4273(3)	52(2)	1
C41	−2951(4)	1954(5)	4246(3)	42(2)	1
C42	−3289(4)	1239(5)	4607(4)	47(2)	1
C43	−4496(4)	588(5)	4740(3)	44(2)	1
C44	−4431(5)	60(5)	5318(3)	50(2)	1
C45	−4938(5)	−506(5)	5568(3)	51(2)	1
Cl7	−926(2)	−3050(1)	3827(1)	72(1)	1
Cl8	−1999(2)	−2353(2)	2666(1)	100(1)	1
N10	1332(4)	−1661(4)	3000(2)	46(2)	1
N11	90(4)	−1556(3)	2380(2)	41(2)	1
N12	−163(4)	−795(4)	1226(2)	47(2)	1
O7	701(3)	−2493(3)	3846(2)	53(1)	1
O8	−1422(3)	−1192(4)	1414(2)	66(2)	1
C46	2535(4)	−1076(5)	2788(3)	47(2)	1
C47	3190(5)	−903(5)	2963(4)	58(2)	1
C48	3318(5)	−1171(5)	3521(3)	52(2)	1
C49	2770(5)	−1648(5)	3955(4)	56(2)	1
C50	2127(4)	−1818(5)	3799(3)	48(2)	1
C51	1991(4)	−1523(4)	3202(3)	39(2)	1
C52	721(5)	−2090(5)	3311(3)	46(2)	1
C53	73(5)	−2021(5)	2969(3)	48(2)	1
C54	−649(5)	−2367(5)	3148(3)	54(2)	1
C55	−1077(5)	−2104(5)	2668(3)	58(2)	1
C56	−592(5)	−1604(5)	2207(3)	45(2)	1
C57	−775(5)	−1190(5)	1584(3)	50(2)	1
C58	−98(4)	−403(4)	611(3)	42(2)	1
C59	461(5)	98(5)	356(3)	47(2)	1
C60	585(5)	488(4)	−264(3)	48(2)	1
N13	−1486(3)	−1346(3)	4951(2)	59(2)	1

C61	−2171(3)	−1253(4)	5460(3)	89(3)	1
C62	−1957(4)	−1335(7)	6019(3)	89(3)	1
C63	−2746(5)	−1091(6)	6441(3)	92(3)	1
C64	−2587(6)	−1273(7)	7059(3)	111(4)	1
C65	−844(3)	−2160(4)	5145(3)	89(3)	1
C66	−1155(4)	−2914(4)	5387(4)	85(3)	1
C67	−485(5)	−3670(4)	5541(5)	115(4)	1
C68	−701(6)	−4452(4)	5687(6)	139(5)	1
C69	−1026(4)	−641(4)	4757(2)	81(3)	1
C70	−358(5)	−607(5)	4235(3)	86(3)	1
C71	−79(5)	203(5)	4016(3)	84(3)	1
C72	625(5)	255(5)	3536(3)	82(3)	1
C73	−1885(5)	−1351(4)	4457(3)	90(3)	1
C74	−2368(5)	−574(4)	4113(3)	102(4)	1
C75	−2956(5)	−706(6)	3744(3)	100(4)	1
C76	−3609(7)	−1166(8)	4119(5)	156(6)	1
N14	3222(3)	−4143(3)	3447(2)	70(2)	1
C77	2707(4)	−3983(3)	4001(3)	67(2)	1
C78	2517(5)	−4647(4)	4515(3)	80(3)	1
C79	1868(5)	−4350(5)	4991(3)	91(3)	1
C80	1679(5)	−5009(5)	5551(4)	111(4)	1
C81	4056(3)	−4770(3)	3595(3)	64(2)	1
C82	4666(4)	−4572(4)	3842(3)	63(2)	1
C83	5362(5)	−5267(4)	4077(5)	96(3)	1
C84	6029(4)	−5137(5)	4308(4)	69(2)	1
C85	3429(4)	−3335(3)	3011(2)	71(3)	1
C86	3893(6)	−3365(5)	2424(3)	104(4)	1
C87	4136(5)	−2551(5)	2060(3)	88(3)	1
C88	4811(9)	−2401(8)	2262(5)	164(6)	1
C89	2725(4)	−4493(4)	3195(3)	84(3)	1
C90	1868(4)	−4028(4)	3069(4)	85(3)	1
C91	1467(5)	−4449(5)	2762(5)	116(4)	1
C92	545(5)	−4089(6)	2722(6)	127(5)	1
N15	−951(3)	3992(4)	1357(2)	126(4)	1
C93	−1367(5)	4871(5)	1276(4)	194(9)	1
C94	−933(8)	5397(6)	1362(10)	302(14)	1
C95	−1521(9)	6223(7)	1356(8)	303(16)	1
C96	−1080(13)	6838(9)	1358(14)	350(18)	1
C97	−440(4)	3895(4)	767(2)	88(3)	1
C98	8(7)	3075(4)	743(4)	144(6)	1
C99	448(8)	3033(6)	152(4)	150(6)	1
C100	920(9)	2249(7)	80(6)	215(9)	1
C101	−1660(4)	3509(5)	1557(3)	173(7)	1
C102	−2256(6)	3721(9)	1132(3)	180(7)	1
C103	−2989(6)	3279(9)	1410(4)	187(8)	1
C104	−3624(6)	3484(10)	1028(5)	193(8)	1
C105	−334(5)	3703(6)	1797(3)	281(13)	1

C106	−618(7)	3269(10)	2410(4)	261(11)	1
C107	113(9)	3020(8)	2805(4)	215(9)	1
C108	558(7)	3681(9)	2682(6)	163(6)	1
N16	−3617(3)	485(3)	979(2)	72(2)	1
C109	−3213(4)	−206(4)	731(3)	116(4)	1
C110	−3722(5)	−714(6)	702(5)	129(5)	1
C111	−3194(6)	−1357(6)	413(6)	133(5)	1
C112	−3655(9)	−1975(8)	443(7)	214(9)	1
C113	−4185(4)	1158(4)	550(2)	108(4)	1
C114	−4540(8)	1950(5)	653(4)	139(5)	1
C115	−5083(9)	2556(6)	217(6)	181(8)	1
C116	−5401(8)	3386(5)	241(5)	167(6)	1
C117	−2899(4)	815(4)	1054(2)	95(4)	1
C118	−2399(6)	1233(7)	505(3)	110(4)	1
C119	−1683(5)	1488(7)	649(4)	117(4)	1
C120	−1269(9)	2036(9)	146(5)	198(8)	1
C121	−4174(4)	188(5)	1558(3)	142(5)	1
C122	−3759(5)	−456(6)	2037(3)	113(4)	1
C123	−4437(5)	−730(5)	2600(3)	109(4)	1
C124	−4829(6)	−100(7)	2901(4)	113(4)	1

Ethyl-bis-(3,4-dichloro-5-phenylcarbamoyl-1H-pyrrole-2-carboxylic acid amide) (103 deprotonated complex)

Table A1.35: Crystal data and structure refinement.

Identification code	**$[103\text{-}2H^+]^{2-}\cdot 2TBA$**
Empirical formula	$C_{116}H_{180}Cl_8N_{16}O_8$
Formula weight	2210.36
Temperature	120(2) K
Wavelength	0.71073 Å
Crystal system	Triclinic
Space group	*P*–1
Unit cell dimensions	a = 11.9582(2) Å α = 79.2250(10)°
	b = 23.1506(3) Å β = 82.9650(10)°
	c = 23.5489(4) Å γ = 75.4470(10)°
Volume	6179.28(17) Å^3
Z	2
Density (calculated)	1.188 Mg / m^3
Absorption coefficient	0.241 mm^{-1}
F(000)	2376
Crystal	Colourless Block
Crystal size	0.60 × 0.40 × 0.18 mm^3
θ range for data collection	2.91 – 27.45°
Index ranges	$-15 \le h \le 15$, $-29 \le k \le 30$, $0 \le l \le 30$
Reflections collected	25507
Independent reflections	25507 [R_{int} = 0.0000]
Completeness to θ = 27.45°	90.2 %
Max. and min. transmission	0.9579 and 0.8689
Refinement method	Full-matrix least-squares on F^2
Data / restraints / parameters	25507 / 12 / 1394
Goodness-of-fit on F^2	1.013
Final *R* indices [$F^2 > 2\sigma(F^2)$]	*R1* = 0.0700, *wR2* = 0.1711
R indices (all data)	*R1* = 0.1288, *wR2* = 0.2075
Extinction coefficient	0.00000(19)
Largest diff. peak and hole	0.792 and –0.548 e Å^{-3}

Table A1.36: Atomic coordinates [$\times 10^4$], equivalent isotropic displacement parameters [$Å^2 \times 10^3$] and site occupancy factors. U_{eq} is defined as one third of the trace of the orthogonalized U^{ij} tensor.

Atom	*x*	*y*	*z*	U_{eq}	*S.o.f.*
C1	9076(2)	−1063(1)	5804(1)	22(1)	1
C2	8974(3)	−1654(1)	5809(1)	29(1)	1
C3	9868(3)	−2061(1)	5566(1)	37(1)	1
C4	10873(3)	−1889(1)	5319(1)	40(1)	1
C5	10977(3)	−1309(1)	5324(1)	36(1)	1
C6	10081(2)	−891(1)	5564(1)	26(1)	1
C7	7822(2)	−50(1)	5941(1)	17(1)	1
C8	6640(2)	201(1)	6178(1)	18(1)	1
C9	5975(2)	795(1)	6078(1)	18(1)	1
C10	4930(2)	797(1)	6410(1)	18(1)	1
C11	4991(2)	204(1)	6692(1)	18(1)	1
C12	4154(2)	−68(1)	7097(1)	22(1)	1
C13	3913(3)	−1055(1)	7652(1)	35(1)	1
C14	3606(3)	−1482(1)	7308(1)	35(1)	1
C15	3335(2)	−2458(1)	7871(1)	21(1)	1
C16	2484(2)	−2721(1)	8269(1)	18(1)	1
C17	2519(2)	−3319(1)	8541(1)	19(1)	1
C18	1472(2)	−3312(1)	8869(1)	18(1)	1
C19	821(2)	−2713(1)	8781(1)	17(1)	1
C20	−359(2)	−2459(1)	9012(1)	17(1)	1
C21	−1595(2)	−1439(1)	9151(1)	24(1)	1
C22	−2620(2)	−1596(1)	9373(1)	29(1)	1
C23	−3527(3)	−1169(1)	9590(1)	39(1)	1
C24	−3410(3)	−592(2)	9589(2)	46(1)	1
C25	−2396(3)	−430(1)	9366(2)	46(1)	1
C26	−1475(3)	−850(1)	9145(1)	37(1)	1
N1	8111(2)	−669(1)	6042(1)	22(1)	1
N2	6037(2)	−160(1)	6545(1)	18(1)	1
N3	4570(2)	−660(1)	7297(1)	37(1)	1
N4	2932(2)	−1866(1)	7663(1)	32(1)	1
N5	1441(2)	−2354(1)	8423(1)	18(1)	1
N6	−615(2)	−1840(1)	8932(1)	24(1)	1
O1	8476(2)	263(1)	5685(1)	21(1)	1
O2	3166(2)	213(1)	7246(1)	25(1)	1
O3	4323(2)	−2745(1)	7730(1)	26(1)	1
O4	−1043(2)	−2766(1)	9247(1)	22(1)	1
Cl1	6301(1)	1395(1)	5590(1)	23(1)	1
Cl2	3814(1)	1432(1)	6451(1)	26(1)	1
Cl3	3605(1)	−3962(1)	8480(1)	25(1)	1
Cl4	1117(1)	−3919(1)	9335(1)	24(1)	1
C27	3408(2)	3532(1)	9170(1)	21(1)	1
C28	3391(3)	4149(1)	9066(1)	31(1)	1

C29	2405(3)	4560(1)	9241(1)	38(1)	1
C30	1450(3)	4362(1)	9514(1)	38(1)	1
C31	1472(3)	3754(1)	9618(1)	31(1)	1
C32	2451(2)	3333(1)	9449(1)	25(1)	1
C33	4802(2)	2529(1)	9129(1)	17(1)	1
C34	6000(2)	2298(1)	8907(1)	17(1)	1
C35	6692(2)	1710(1)	9019(1)	19(1)	1
C36	7730(2)	1717(1)	8683(1)	20(1)	1
C37	7640(2)	2311(1)	8388(1)	20(1)	1
C38	8465(2)	2588(1)	7984(1)	25(1)	1
C39	8675(3)	3583(2)	7427(2)	44(1)	1
C40	8918(3)	4053(2)	7736(2)	42(1)	1
C41	9116(2)	5015(1)	7109(1)	25(1)	1
C42	9931(2)	5263(1)	6671(1)	20(1)	1
C43	9848(2)	5840(1)	6342(1)	20(1)	1
C44	10889(2)	5822(1)	5995(1)	19(1)	1
C45	11565(2)	5237(1)	6140(1)	19(1)	1
C46	12760(2)	4985(1)	5924(1)	18(1)	1
C47	14076(2)	3964(1)	5867(1)	23(1)	1
C48	15076(3)	4139(1)	5621(1)	31(1)	1
C49	16020(3)	3709(1)	5435(1)	35(1)	1
C50	15963(3)	3110(1)	5491(1)	40(1)	1
C51	14972(3)	2937(1)	5739(1)	39(1)	1
C52	14023(3)	3358(1)	5929(1)	33(1)	1
N7	4444(2)	3145(1)	8984(1)	20(1)	1
N8	6575(2)	2662(1)	8533(1)	20(1)	1
N9	8053(3)	3184(1)	7804(1)	45(1)	1
N10	9562(3)	4440(1)	7356(1)	40(1)	1
N11	10978(2)	4896(1)	6540(1)	20(1)	1
N12	13063(2)	4368(1)	6057(1)	26(1)	1
O5	4178(2)	2205(1)	9402(1)	21(1)	1
O6	9442(2)	2307(1)	7815(1)	28(1)	1
O7	8124(2)	5300(1)	7254(1)	32(1)	1
O8	13415(2)	5293(1)	5658(1)	24(1)	1
Cl5	6397(1)	1112(1)	9518(1)	24(1)	1
Cl6	8860(1)	1089(1)	8644(1)	32(1)	1
Cl7	8734(1)	6479(1)	6353(1)	33(1)	1
Cl8	11179(1)	6389(1)	5457(1)	26(1)	1
C69	611(2)	864(1)	5982(1)	24(1)	1
C70	1841(3)	485(1)	6022(1)	31(1)	1
C71	2356(3)	310(2)	5439(1)	31(1)	1
C72	3545(3)	−111(2)	5470(2)	53(1)	1
C73	610(2)	1596(1)	6643(1)	29(1)	1
C74	459(4)	2160(2)	6191(2)	48(1)	1
C75	1014(3)	2622(2)	6349(2)	47(1)	1
C76	880(60)	3233(16)	5800(40)	85(12)	0.37(10)
C76'	706(15)	3215(9)	6006(10)	47(3)	0.63(10)
C77	224(2)	608(1)	7059(1)	28(1)	1
C78	−268(3)	77(1)	7019(1)	30(1)	1
C79	117(3)	−458(2)	7498(1)	38(1)	1

C80	−378(3)	−989(2)	7450(2)	44(1)	1
C81	−1235(2)	1363(1)	6457(1)	27(1)	1
C82	−1941(3)	1663(2)	6951(1)	35(1)	1
C83	−3197(3)	1898(2)	6817(2)	39(1)	1
C84	−3950(3)	2257(2)	7254(2)	52(1)	1
N14	51(2)	1111(1)	6536(1)	24(1)	1
C53	2018(3)	939(2)	8405(1)	37(1)	1
C54	2160(3)	372(2)	8848(2)	48(1)	1
C55	1587(3)	−80(2)	8679(2)	46(1)	1
C56	1839(4)	−683(2)	9067(2)	68(1)	1
C57	3858(2)	1157(2)	8615(1)	32(1)	1
C58	4582(2)	850(2)	8123(1)	36(1)	1
C59	5834(3)	626(2)	8272(1)	38(1)	1
C60	6592(3)	260(2)	7835(2)	45(1)	1
C61	2424(3)	1922(2)	7999(1)	36(1)	1
C62	2912(3)	2454(2)	8035(1)	43(1)	1
C63	2500(4)	2988(2)	7549(2)	62(1)	1
C64	2893(5)	3535(2)	7594(2)	79(2)	1
C65	2009(2)	1666(1)	9074(1)	29(1)	1
C66	788(3)	2067(2)	9012(1)	35(1)	1
C67	243(3)	2215(2)	9605(1)	34(1)	1
C68	−909(3)	2683(2)	9559(2)	51(1)	1
N13	2582(2)	1418(1)	8521(1)	30(1)	1
C101	4485(3)	3216(2)	3573(1)	36(1)	1
C102	4595(4)	2707(2)	4090(2)	53(1)	1
C103	3999(3)	2226(2)	4011(2)	49(1)	1
C104	4078(5)	1707(2)	4511(2)	85(2)	1
C105	6311(2)	3504(1)	3709(1)	26(1)	1
C106	7046(2)	3156(1)	3250(1)	30(1)	1
C107	8319(3)	3017(1)	3364(1)	33(1)	1
C108	9106(3)	2637(2)	2948(2)	48(1)	1
C109	4446(3)	4056(1)	4115(1)	30(1)	1
C110	3222(3)	4432(2)	4030(2)	51(1)	1
C111	2655(3)	4669(2)	4575(2)	43(1)	1
C112	1481(3)	5093(2)	4509(2)	70(2)	1
C113	4861(3)	4161(2)	3034(1)	42(1)	1
C114	5388(5)	4693(2)	2975(2)	62(1)	1
C115	4927(8)	5169(2)	2464(2)	132(3)	1
C116	4802(9)	5698(3)	2439(3)	199(6)	1
N16	5030(2)	3730(1)	3608(1)	28(1)	1
C85	1416(2)	4035(1)	1175(1)	28(1)	1
C86	567(3)	4412(1)	1578(1)	33(1)	1
C87	−94(3)	4071(2)	2047(1)	41(1)	1
C88	−1280(3)	4479(2)	2233(2)	52(1)	1
C89	3188(2)	4357(1)	1351(1)	26(1)	1
C90	3055(3)	4857(1)	822(1)	35(1)	1
C91	3735(3)	5315(1)	867(2)	40(1)	1
C92	3643(4)	5827(2)	352(2)	66(1)	1
C93	3311(2)	3470(1)	851(1)	26(1)	1

C94	4571(3)	3156(2)	935(1)	34(1)	1
C95	5047(3)	2760(1)	474(1)	34(1)	1
C96	6279(3)	2407(2)	542(2)	49(1)	1
C97	2794(3)	3431(1)	1920(1)	27(1)	1
C98	2450(3)	2836(1)	1973(1)	36(1)	1
C99	2796(3)	2443(1)	2544(1)	37(1)	1
C100	2573(4)	1819(2)	2594(2)	53(1)	1
N15	2672(2)	3823(1)	1327(1)	25(1)	1

4-Aminomethyl-phenylamino-bis-(3,4-dichloro-5-phenylcarbamoyl-1H-pyrrole-2-carboxylic acid amide) (106 deprotonated complex)

Table A1.37: Crystal data and structure refinement.

Identification code	**$[106\text{-}2H^+]^{2-}\cdot 2TBA$**
Empirical formula	$C_{64}H_{94}Cl_4N_8O_4$
	$C_{32}H_{22}Cl_4N_6O_4 \cdot 2C_{16}H_{36}N$
Formula weight	1181.27
Temperature	120(2) K
Wavelength	0.71069 Å
Crystal system	Triclinic
Space group	*P*-1
Unit cell dimensions	$a = 9.524(5)$ Å $\quad \alpha = 78.293(5)°$
	$b = 10.363(5)$ Å $\quad \beta = 88.733(5)°$
	$c = 17.056(5)$ Å $\quad \gamma = 80.136(5)°$
Volume	1623.9(13) $Å^3$
Z	1
Density (calculated)	1.208 Mg / m^3
Absorption coefficient	0.234 mm^{-1}
F(000)	634
Crystal	Colourless Block
Crystal size	0.20 × 0.10 × 0.07 mm^3
θ range for data collection	3.13 – 25.02°
Index ranges	$-10 \le h \le 11$, $-12 \le k \le 12$, $-20 \le l \le 20$
Reflections collected	15744
Independent reflections	5287 [$R_{int} = 0.1073$]
Completeness to $\theta = 25.02°$	92.0 %
Absorption correction	Semi–empirical from equivalents
Max. and min. transmission	0.9838 and 0.9548
Refinement method	Full-matrix least-squares on F^2
Data / restraints / parameters	5287 / 0 / 365
Goodness-of-fit on F^2	1.048
Final *R* indices [$F^2 > 2\sigma(F^2)$]	$R1 = 0.0987$, $wR2 = 0.1724$
R indices (all data)	$R1 = 0.1980$, $wR2 = 0.2062$
Largest diff. peak and hole	0.237 and –0.236 e $Å^{-3}$

Table A1.38: Atomic coordinates [× 10^4], equivalent isotropic displacement parameters [$Å^2 \times 10^3$] and site occupancy factors. U_{eq} is defined as one third of the trace of the orthogonalized U^{ij} tensor.

Atom	*x*	*y*	*z*	U_{eq}	*S.o.f.*
Cl1	353(2)	−2073(2)	4449(1)	62(1)	1
Cl2	−2406(2)	544(2)	4153(1)	59(1)	1
N1	802(5)	−2732(5)	1767(3)	49(1)	1
N2	−1072(5)	−824(5)	2225(3)	43(1)	1
N3	−2724(5)	1256(5)	1331(3)	51(1)	1
O1	1697(4)	−3547(4)	3030(2)	56(1)	1
O2	−4028(4)	1744(4)	2402(2)	54(1)	1
C1	3028(7)	−4189(6)	1558(4)	49(2)	1
C2	3809(6)	−4995(6)	1103(4)	50(2)	1
C3	3231(7)	−5225(6)	415(4)	52(2)	1
C4	1852(7)	−4605(6)	184(4)	50(2)	1
C5	1075(6)	−3806(6)	642(4)	51(2)	1
C6	1644(7)	−3573(6)	1336(4)	46(2)	1
C7	865(6)	−2732(6)	2571(4)	45(2)	1
C8	−192(6)	−1672(6)	2795(3)	39(1)	1
C9	−506(6)	−1353(6)	3541(3)	46(2)	1
C10	−1617(7)	−278(6)	3426(3)	47(2)	1
C11	−1956(6)	44(6)	2587(3)	43(2)	1
C12	−3009(7)	1093(6)	2118(4)	44(2)	1
C13	−3800(6)	1883(6)	722(3)	53(2)	1
C14	−4401(6)	907(6)	344(4)	45(2)	1
C15	−4925(6)	1253(6)	−433(3)	48(2)	1
C16	−5530(6)	392(6)	−774(3)	46(2)	1
N4	1867(5)	2167(5)	3108(3)	47(1)	1
C17	2263(6)	765(6)	3622(3)	51(2)	1
C18	3848(6)	303(6)	3804(4)	60(2)	1
C19	4237(7)	−1235(6)	3995(4)	64(2)	1
C20	4372(8)	−1837(7)	3262(4)	83(2)	1
C21	2296(6)	2153(6)	2237(3)	48(2)	1
C22	1520(7)	1334(6)	1811(3)	56(2)	1
C23	1877(6)	1538(6)	943(3)	53(2)	1
C24	1181(6)	710(6)	483(3)	58(2)	1
C25	262(6)	2585(6)	3169(3)	48(2)	1
C26	−351(6)	3941(6)	2662(4)	58(2)	1
C27	−1950(7)	4262(7)	2749(4)	67(2)	1
C28	−2615(7)	5598(8)	2262(5)	82(2)	1
C29	2667(6)	3149(6)	3386(3)	48(2)	1
C30	2327(6)	3381(6)	4224(3)	52(2)	1
C31	3379(7)	4151(6)	4504(4)	61(2)	1
C32	2939(7)	4509(7)	5311(4)	78(2)	1

Appendix 2: ^{1}H NMR Titration curves

A2.1 Introduction

Standard ^{1}H NMR titration techniques were used to study the anion binding properties of the receptors presented in chapter 2 and 3 and also the deprotonation processes of the materials occurring in chapter 5. The titration experiments were carried out in various solvents. The anion was added as the tetrabutylammonium salt. The amide NH resonances in ppm unit were observed in each titration. The EQNMR program[98] was used to elucidate both the constants and corresponding errors.

A2.2 ^{1}H NMR Titration curves in chapter 2

Figure A2.1: ^{1}H NMR titration curves of **47** with anions in DMSO-d_6-0.5% water at 25°C. (a) Chloride. (b). Benzoate. (c). Hydrogensulfate. And in DMSO-d_6-5% water (d) Dihydrogenphosphate.

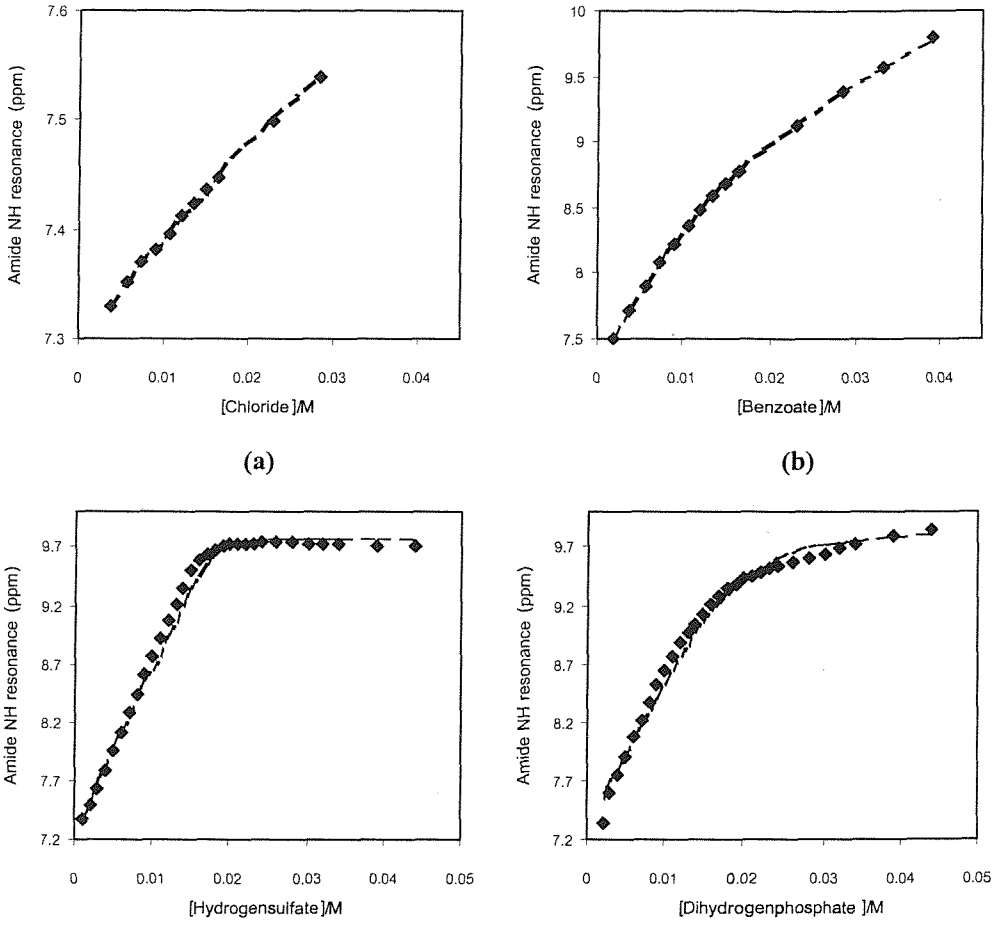

Figure A2.2: ^1H NMR titration curves of **48** with anions in DMSO-d_6-0.5% water at 25°C. (a) Chloride (1). (b). Chloride (2). (c). Chloride (3). (d) Bromide. (e) Dihydrogenphosphate. (f) Benzoate. (g) Hydrogensulfate (1). (h) Hydrogensulfate (2).

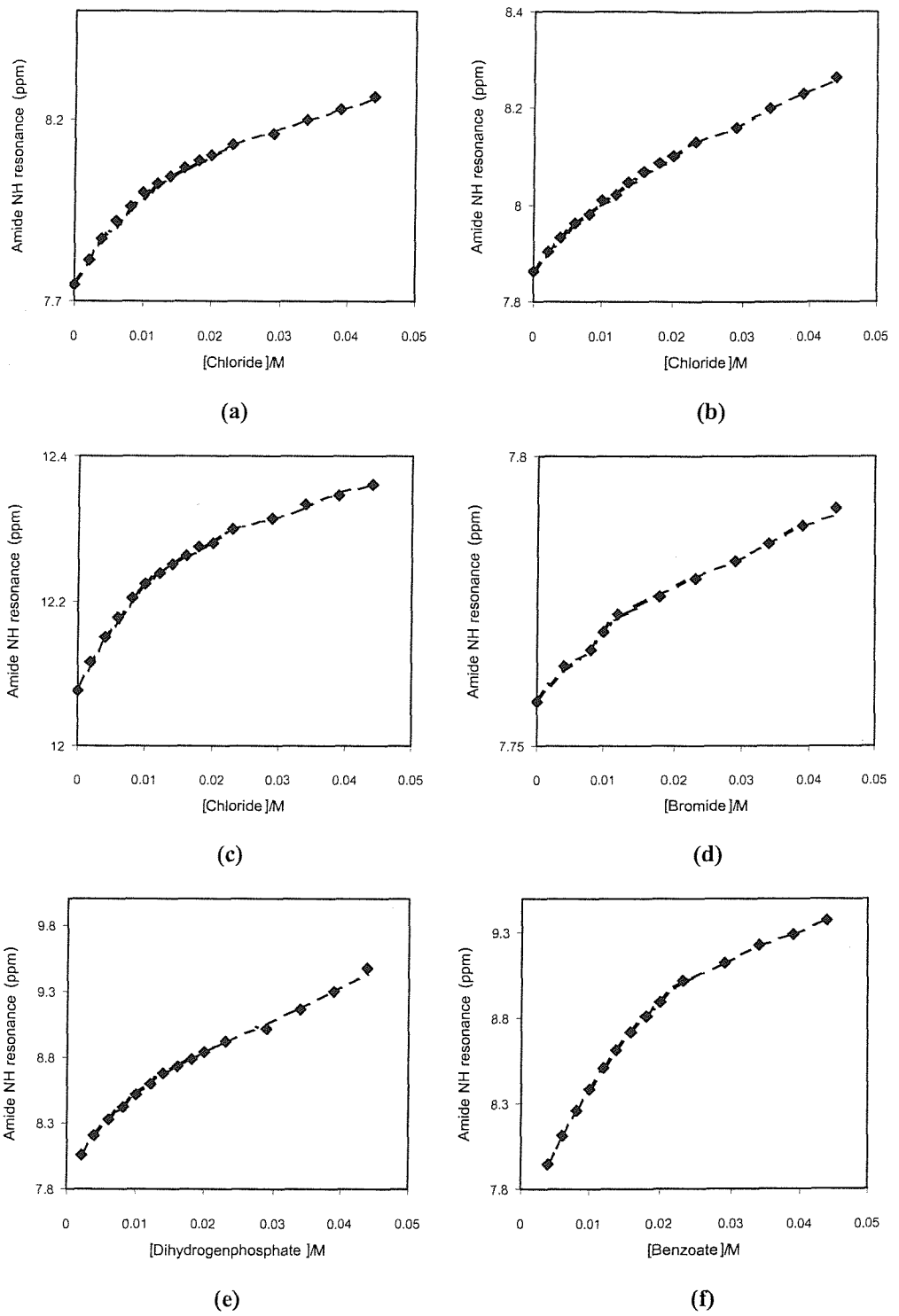

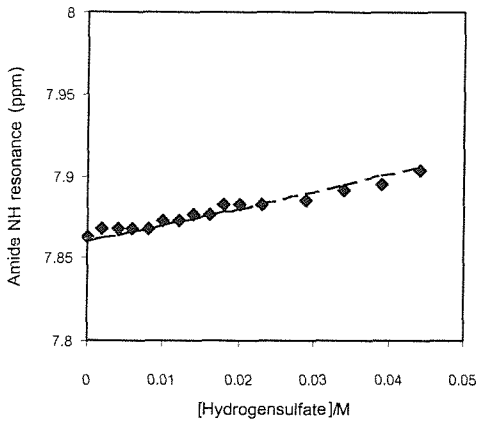
8
7.95
7.9
7.85
7.8
Amide NH resonance (ppm)
0
0.01
0.02
0.03
0.04
0.05
[Hydrogensulfate]/M

(g)

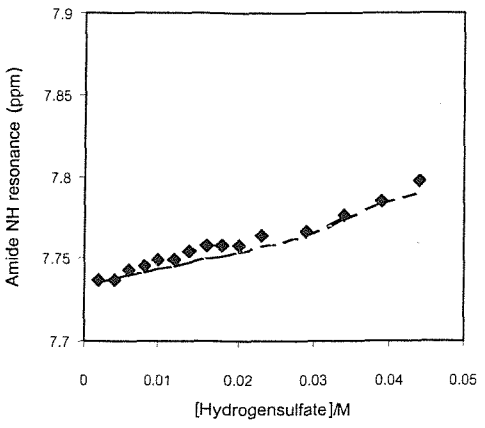
7.9
7.85
7.8
7.75
7.7
Amide NH resonance (ppm)
0
0.01
0.02
0.03
0.04
0.05
[Hydrogensulfate]/M

(h)

Figure A2.3: ^1H NMR titration curves of **49** with anions in DMSO-d_6-0.5% water at 25°C. (a) Chloride. (b). Dihydrogenphosphate (1). (c) Dihydrogenphosphate (2). (d) Benzoate (1). (e) Benzoate (2).

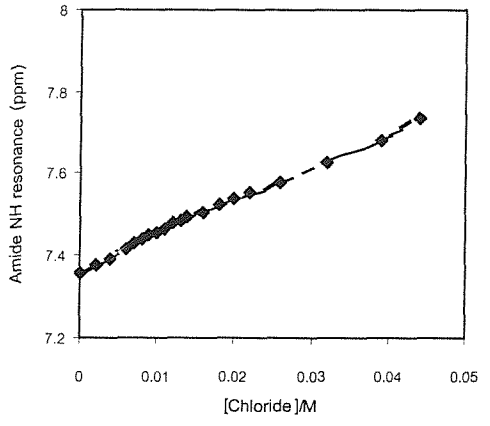

(a)

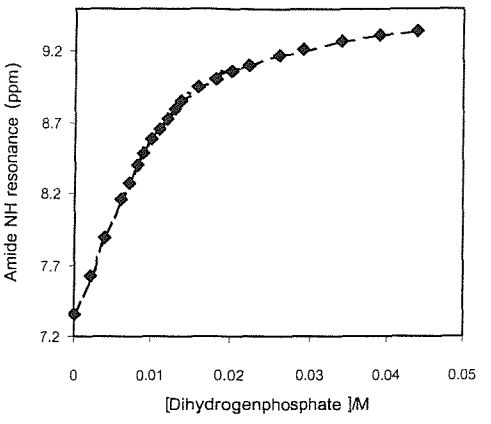

(b)

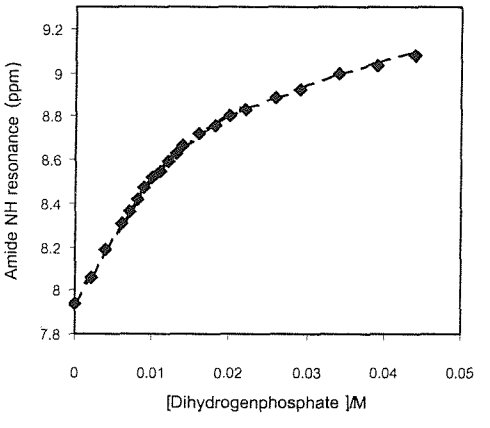

(c)

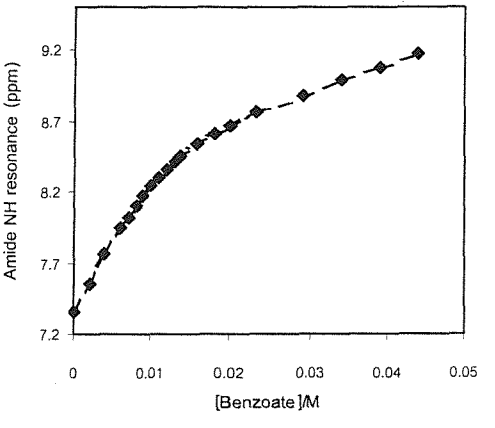

(d)

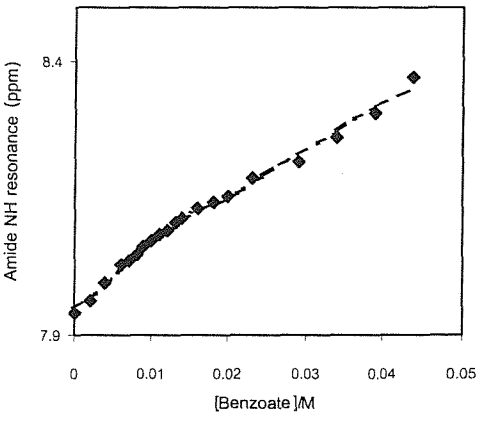

(e)

A2.3 ^{1}H NMR Titration curves in chapter 3

Figure A2.4: ^{1}H NMR titration curves of **52** with anions in DCM-d_2 at 25°C. (a) Fluoride. (b) Chloride. (c) Bromide. (d) Benzoate. (e) Dihydrogenphosphate. (f) Hydrogensulfate.

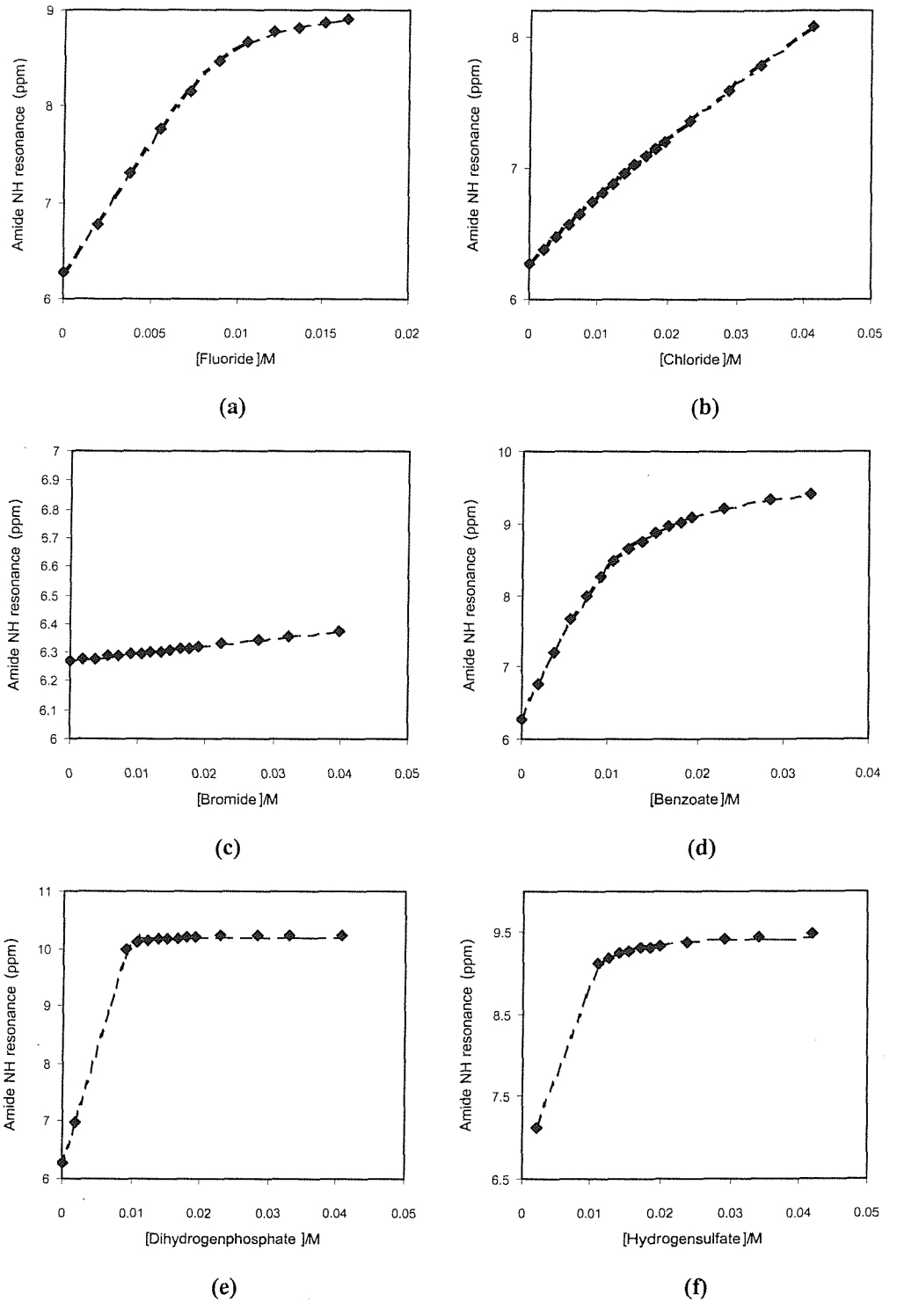

Figure A2.5: ^{1}H NMR titration curves of **53** with anions in DCM-d_2 at 25°C. (a) Fluoride. (b) Chloride. (c) Bromide. (d) Benzoate. (e) Dihydrogenphosphate. (f) Hydrogensulfate.

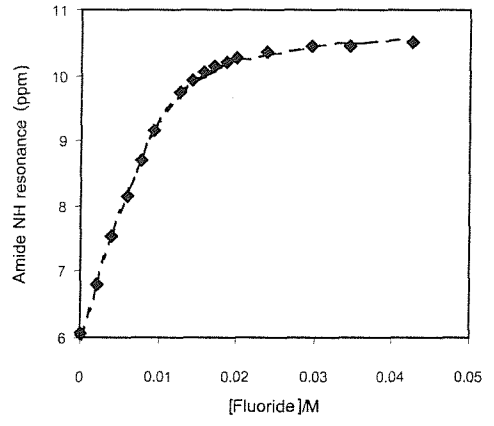

(a)

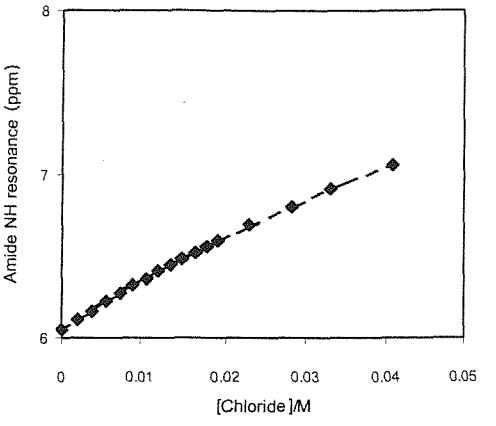

(b)

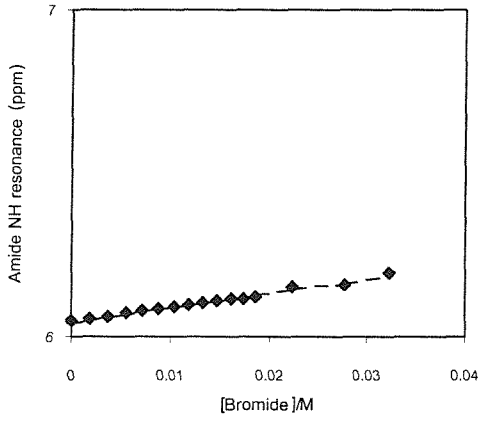

(c)

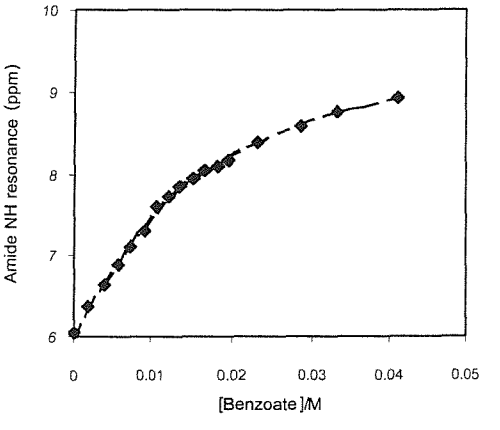

(d)

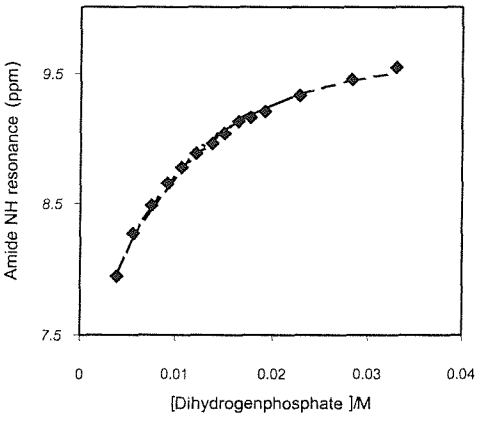

(e)

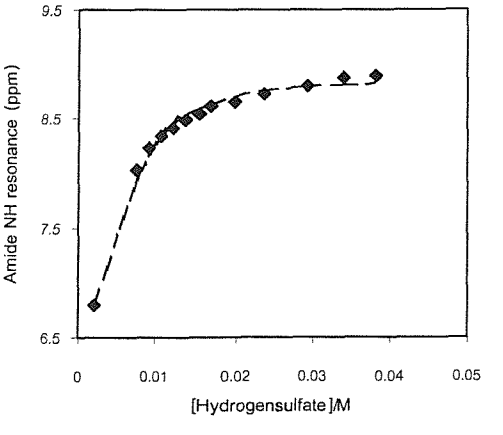

(f)

Figure A2.6: ^{1}H NMR titration curves of **54** with anions in DCM-d_2 at 25°C. (a) Fluoride. (b) Chloride. (c) Benzoate. (d) Hydrogensulfate.

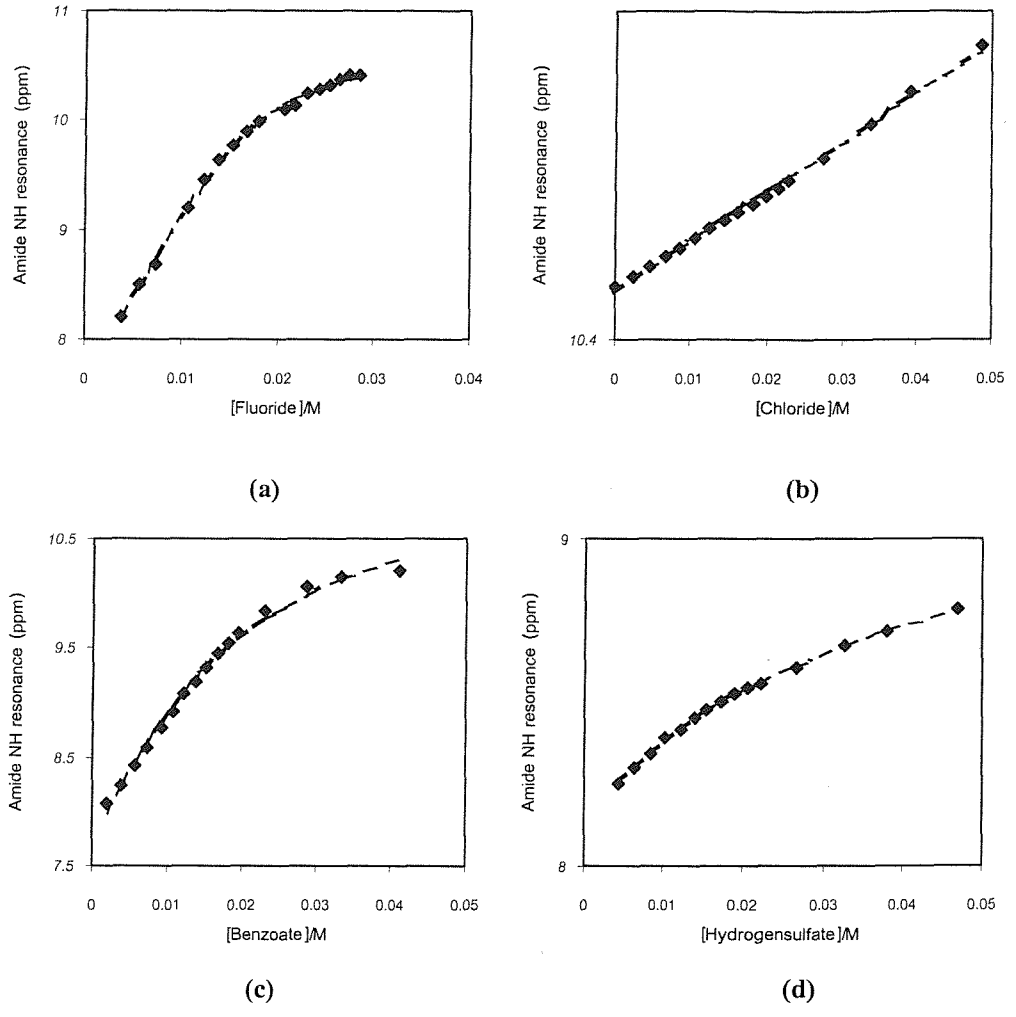

Figure A2.7: ^{1}H NMR titration curves of **55** with anions in DCM-d_2 at 25°C. (a) Fluoride. (b) Chloride. (c) Benzoate. (d) Dihydrogenphosphate. (e) Hydrogensulfate.

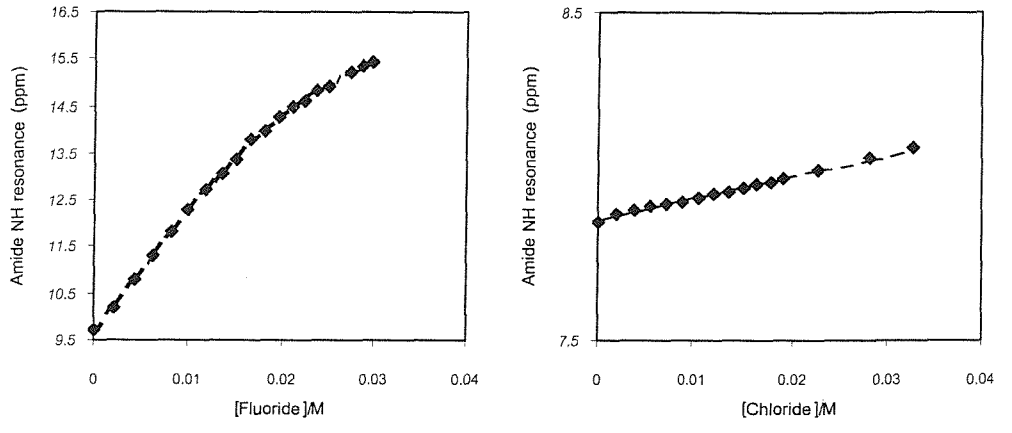

(a)

(b)

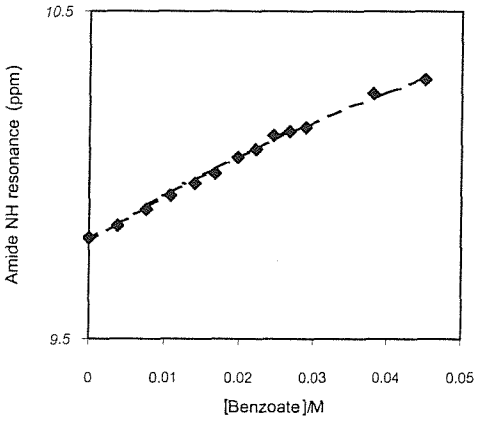

(c)

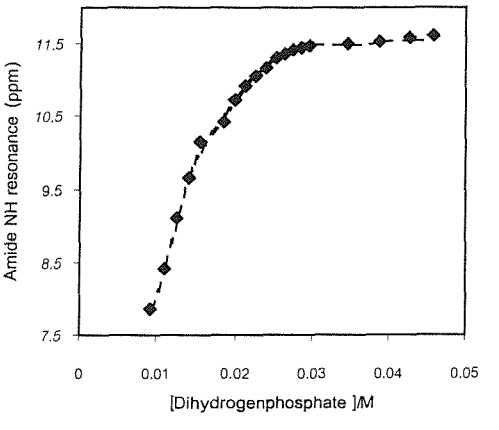

(d)

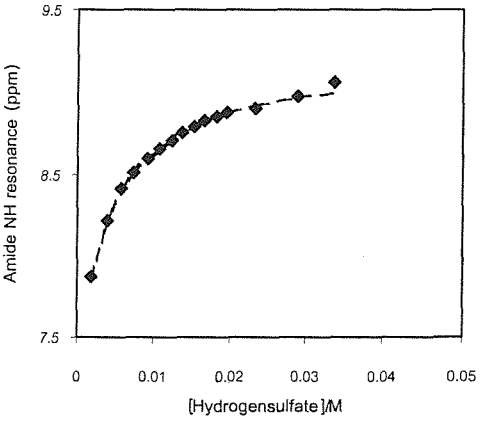

(e)

Figure A2.8: ^{1}H NMR titration curves of **56** with anions in DMSO-d_6-0.5% water at 25°C. (a) Fluoride. (b) Chloride. (c) Benzoate. (d) Dihydrogenphosphate. (e) Hydrogensulfate.

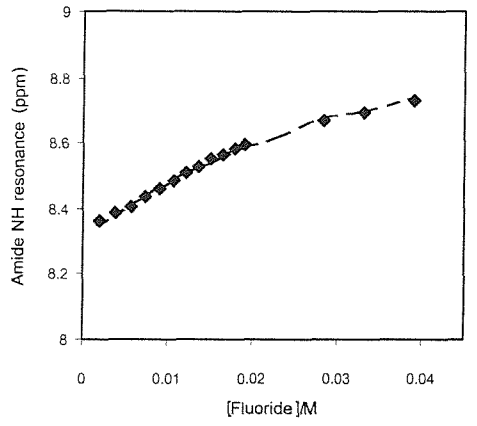

(a)

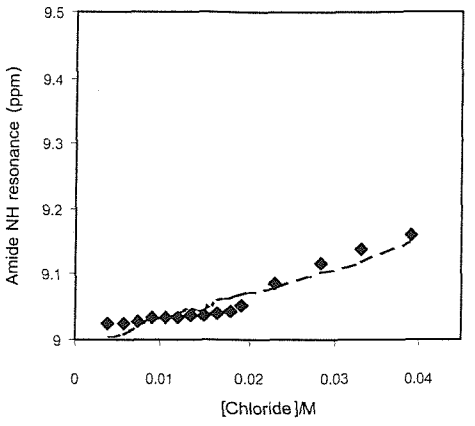

(b)

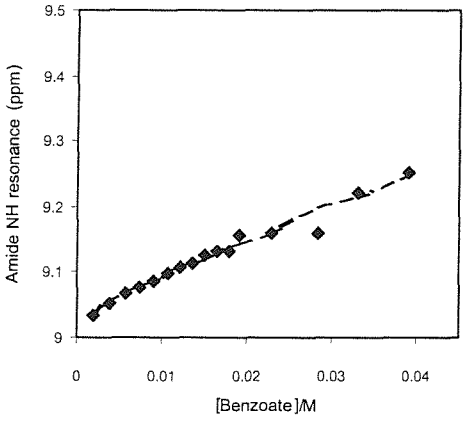

(c)

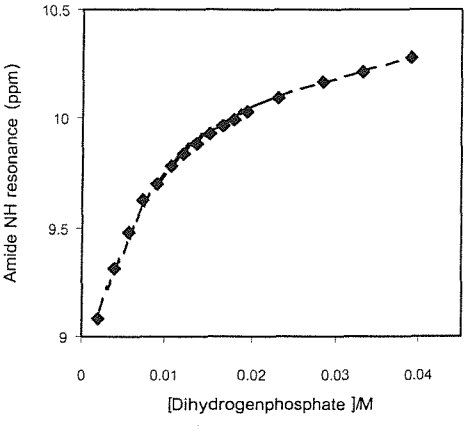

(d)

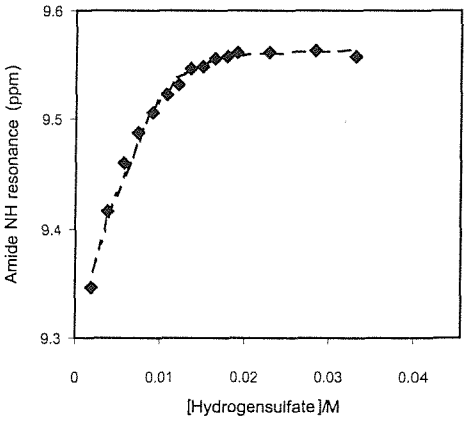

(e)

Figure A2.9: ^{1}H NMR titration curves of **57** with anions in DMSO-d_6-0.5% water at 25°C. (a) Fluoride. (b) Chloride. (c) Benzoate. (d) Dihydrogenphosphate. (e) Hydrogensulfate.

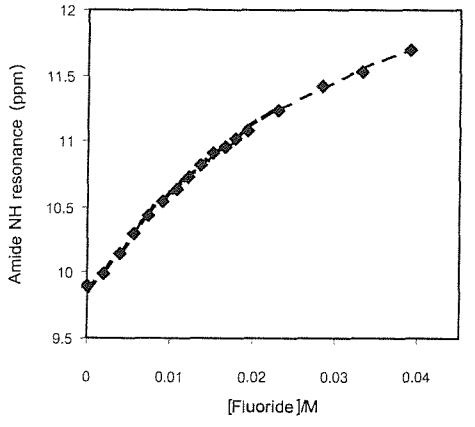

(a)

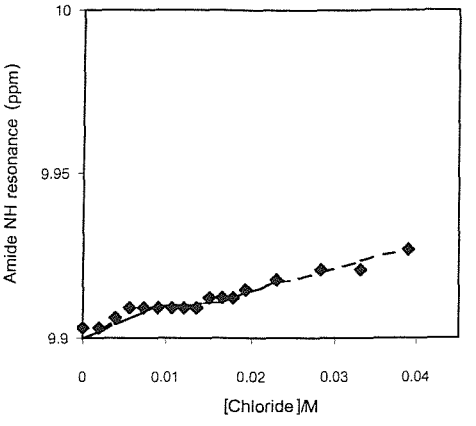

(b)

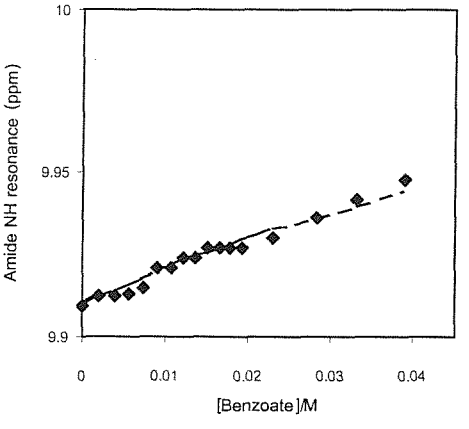

(c)

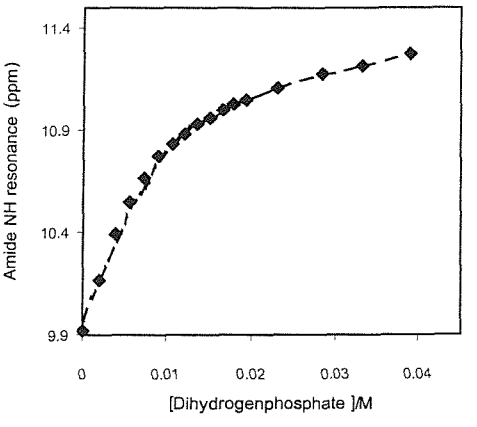

(d)

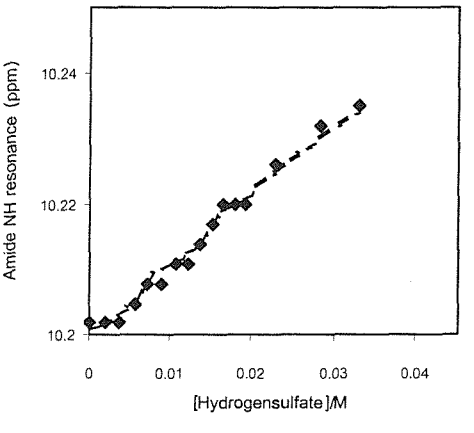

(e)

Figure A2.10: ^{1}H NMR titration curves of **58** with anions in DCM-d_2 at 25°C. (a) Fluoride. (b) Chloride. (c) Bromide. (d) Benzoate. (e) Dihydrogenphosphate. (f) Hydrogensulfate.

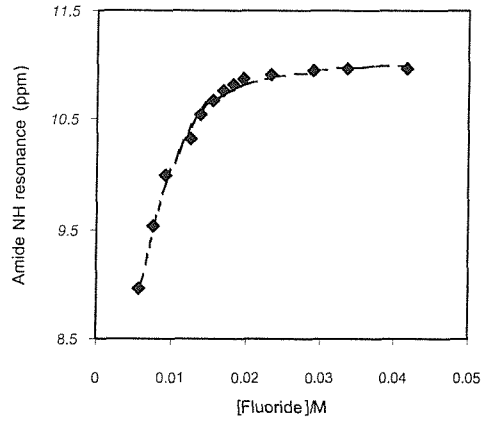

(a)

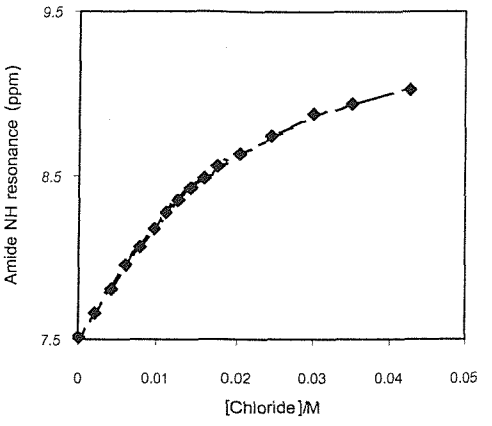

(b)

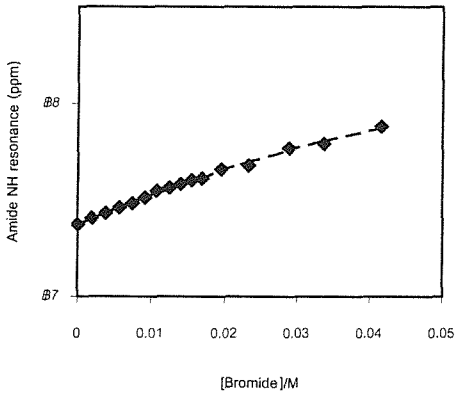

(c)

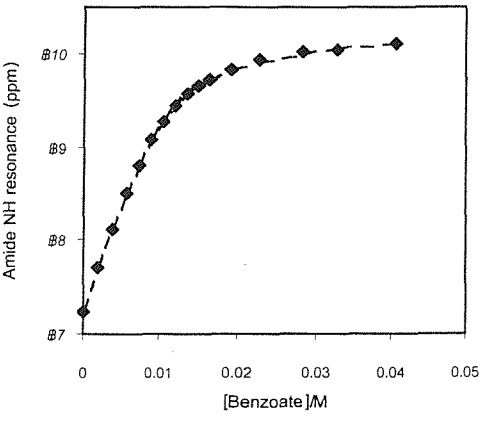

(d)

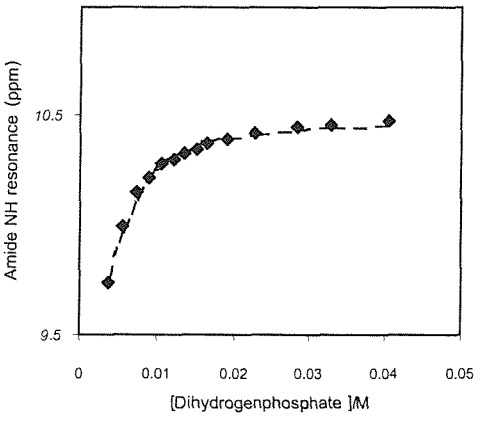

(e)

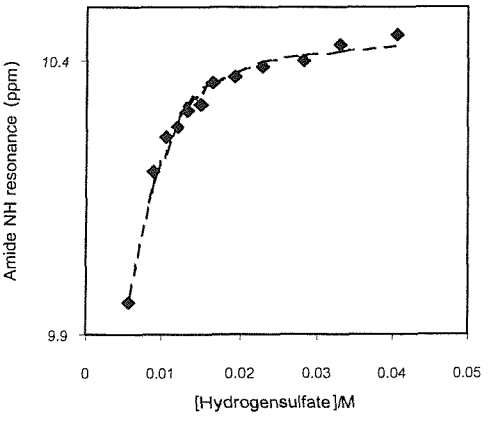

(f)

Figure A2.11: ^{1}H NMR titration curves of **59** with anions in DCM-d_2 at 25°C. (a) Fluoride. (b) Chloride. (c) Bromide. (d) Benzoate. (e) Dihydrogenphosphate. (f) Hydrogensulfate.

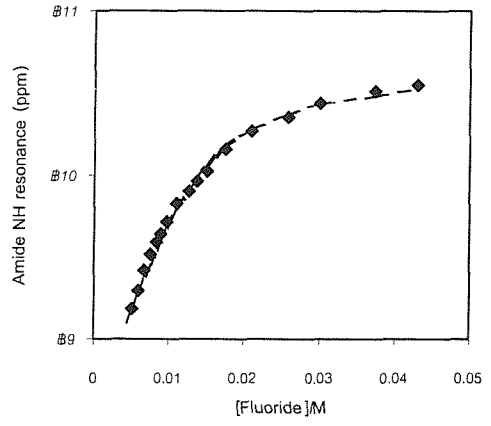

(a)

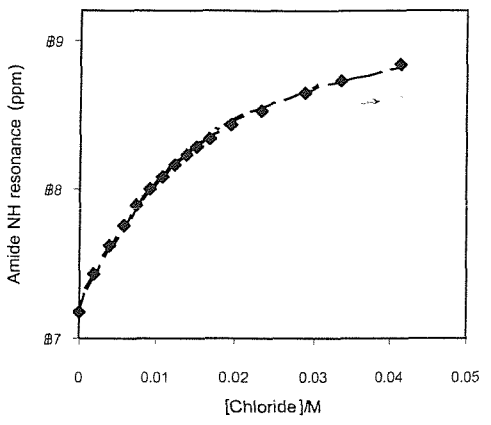

(b)

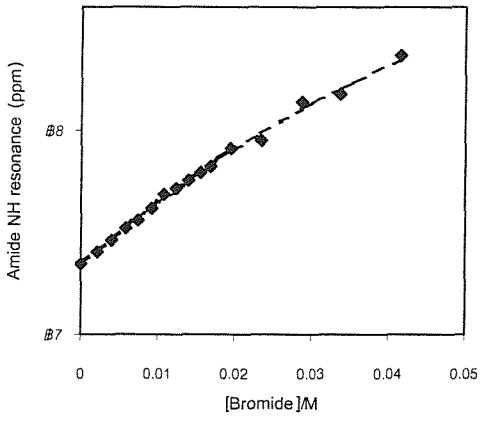

(c)

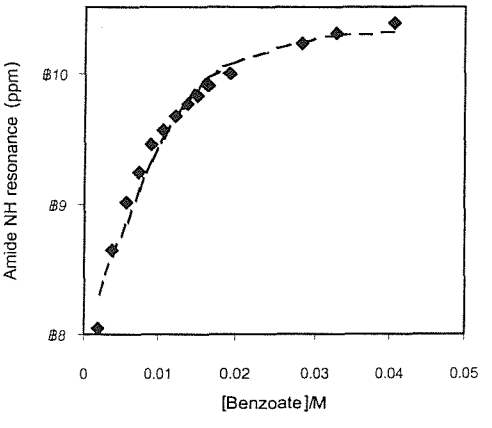

(d)

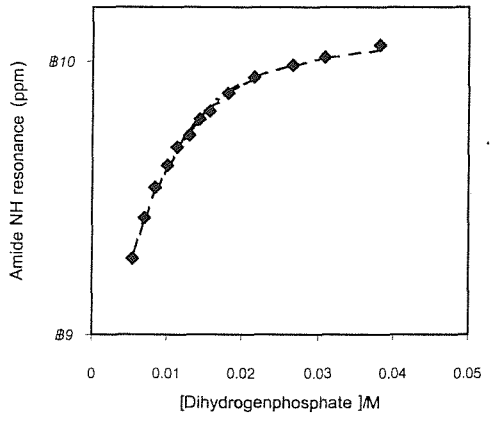

(e)

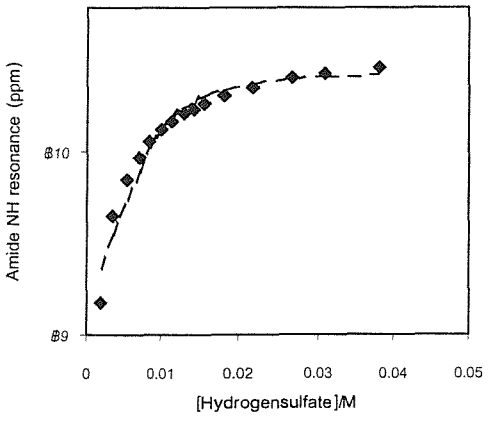

(f)

Figure A2.12: ^{1}H NMR titration curves of prodigiosin mimics with tetrabutyammonium chloride in acetronitrile-d_3 at 25°C. (a) **53**. (b) **55**. (c) **58**. (d) **59**.

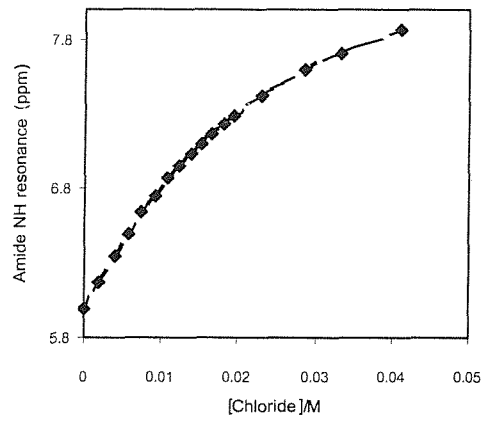

(a)

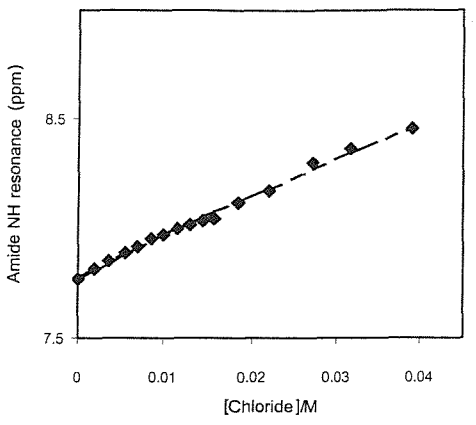

(b)

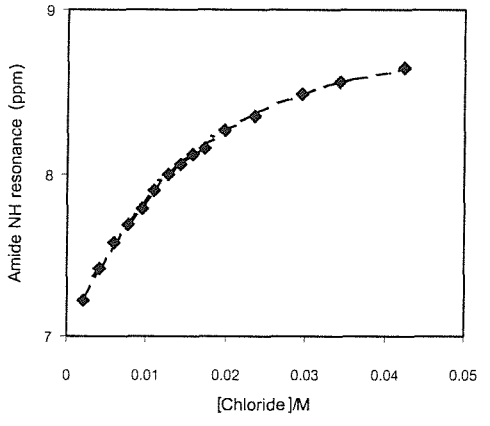

(c)

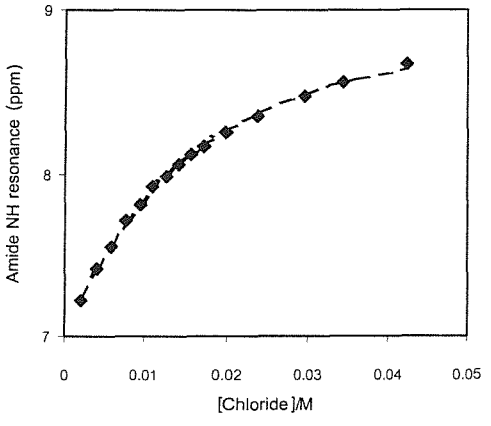

(d)

Figure A2.13: ^{1}H NMR titration curves of prodigiosin mimics with tetrabutyammonium chloride in acetronitrile-d_3 at 25°C. (a) **52**·**2HPF$_6$**. (b) **53**·**HPF$_6$**. (c) **55**·**HPF$_6$**.

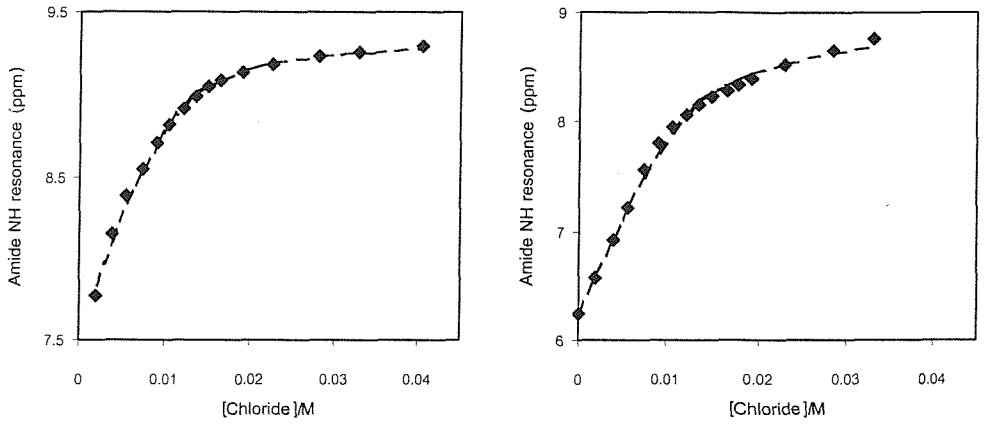

(a) **(b)**

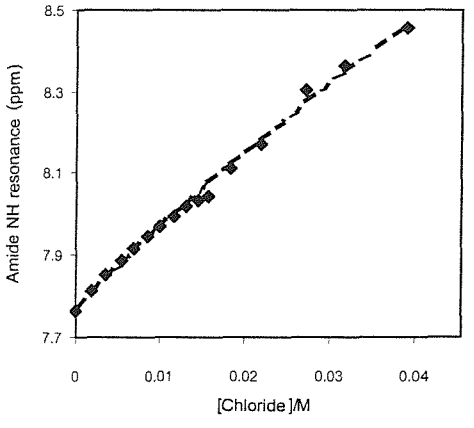

(c)

A3.4 ^{1}H NMR Titration curves in chapter 5

Figure A2.14: ^{1}H NMR titration curves of dimers compounds with TBAF in DMSO-d_6-0.5%water at 25°C. (a) **101**. (b) **102**. (c) **103**. (d) **104**. (e) **105**. (f) **106**.

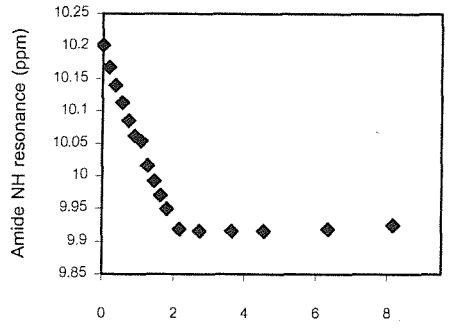

(a)

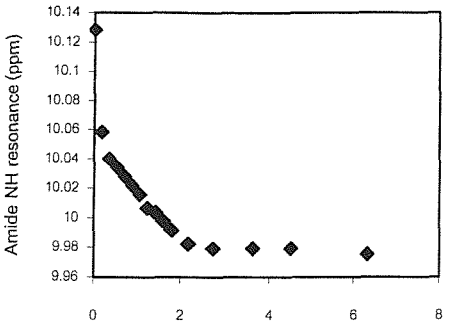

(b)

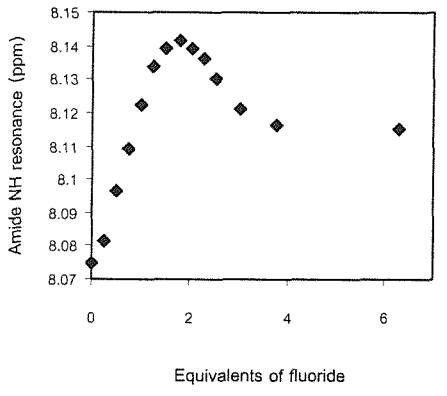

(c)

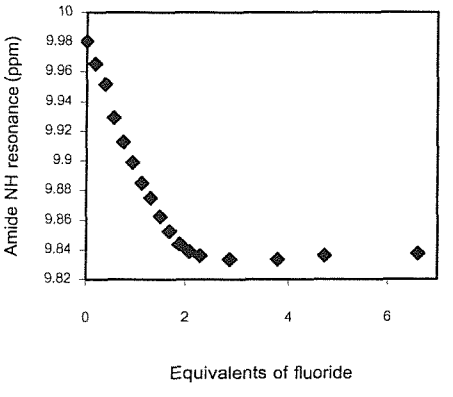

(d)

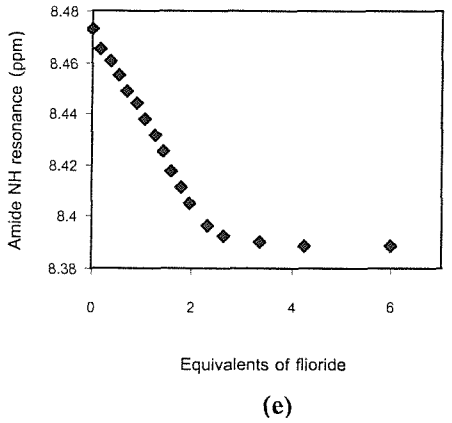

(e)

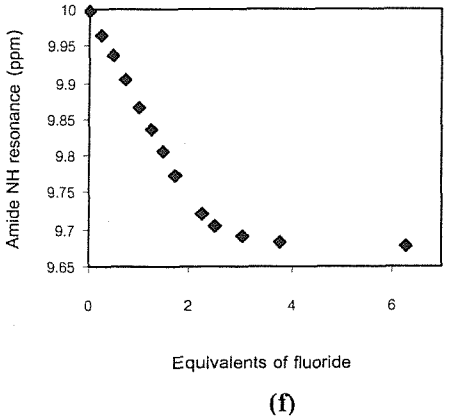

(f)

Figure A2.15: ^1H NMR titration curves of trimers compounds with TBAF in DMSO-d_6-0.5%water at 25°C. (a) **107**. (b) **108**.

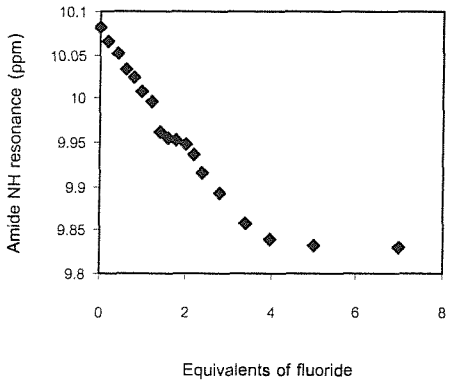

(a)

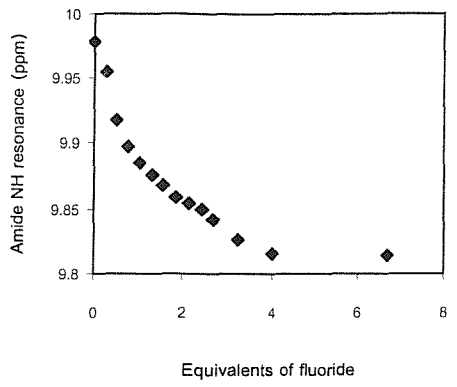

(b)

Appendix 3: HCl transport assay

A3.1 Introduction

The HCl transport properties investigation of the prodigiosin mimics shown in chapter 3 were carried out by Professor Bradley D. Smith and graduate student Beth McNally at the University of Notre Dame, Indiana. The methods of the studies are described in this appendix.

A3.2 Experimental methods

A3.2.1 Preparation of unilamellar vesicles

1-Palmitoyl-2-oleoyl-*sn*-glycerol-3-phosphocholine and cholesterol dissolved in chloroform were combined in a 10 ml round bottom flask. The chloroform was removed using a rotary evaporator and the lipid/cholesterol film was placed on a high vacuum system for over one hour. A one milliliter volume of inside solution (500 mM NaCl or 500 mM NaCl and 5 mM citric acid, pH 4 or 7.2) and a glass bead were added to the flask which was vortexed to resolvate the lipid/cholesterol film. The solution was freeze thawed nine times and extruded twenty-nine times using a 200 nm PC membrane. The vesicles were dialyzed against outside solution (500 mM $NaNO_3$ or 500 mM $NaNO_3$ and 5 mM citric acid, pH 4 or 7) for 10 hours.

A3.2.2 Chloride transport assay

Unilamellar vesicles composed of POPC/cholesterol (70:30 POPC:cholesterol), 200 nm mean diameter, and 500 mM NaCl at an initial concentration of 10 mM were diluted to a 5 ml final volume with 500 mM $NaNO_3$ to have a final concentration of 1 mM. 10 μl Of the 5 mM prodigiosin mimics were added to the 5 ml volume vesicle solution for a final 10 μM compound concentration. Chloride release was monitored using a chloride selective electrode for 20 minutes and lysed with polyoxyethylene 8 lauryl ether detergent.

A3.2.3 pH 4 Chloride transport assay

Similar to chloride transport assay except the inside solution was 500 mM NaCl, 5 mM citric acid, pH 4. The 10 mM vesicles are dialyzed against outside solution of 500 mM $NaNO_3$, 5 mM citric acid, pH 4 solution. The dilution (dispersion of vesicles in 500 mM $NaNO_3$, 5 mM citric acid, pH 7.2 solution) of 10 mM to 1 mM vesicles occurred just prior to the addition of prodigiosin mimics.

A3.2.4 pH 7.2 Chloride transport assay

Similar to pH 4 transport assay except the inside solution was 500 mM NaCl, 5 mM citric acid, pH 7.2. The 10 mM vesicles are dialyzed against outside solution of 500 mM $NaNO_3$, 5 mM citric acid, pH 7.2 solution. The dilution (dispersion of vesicles in 500 mM $NaNO_3$, 5 mM citric acid, pH 7.2 solution) of 10 mM to 1 mM vesicles occurred just prior to the addition of prodigiosin mimics.

A3.2.5 pH Gradient chloride transport assay

Similar to pH 4 chloride transport assay except the inside solution was 500 mM NaCl, 5 mM citric acid, pH 4. The 10 mM vesicles are dialyzed against outside

solution of 500 mM $NaNO_3$, 5 mM citric acid, pH 4 solution. The dilution (dispersion of vesicles in 500 mM $NaNO_3$, 5 mM Na_2HPO_4, pH 7.2 solution) of 10 mM to 1 mM vesicles occurred just prior to the addition of prodigiosin mimics.

The chloride transport results of **52** and **53**, **54** and **55** and **56** and **57** are shown in Figure A3.1, Figure A3.2 and Figure A3.3 respectively.

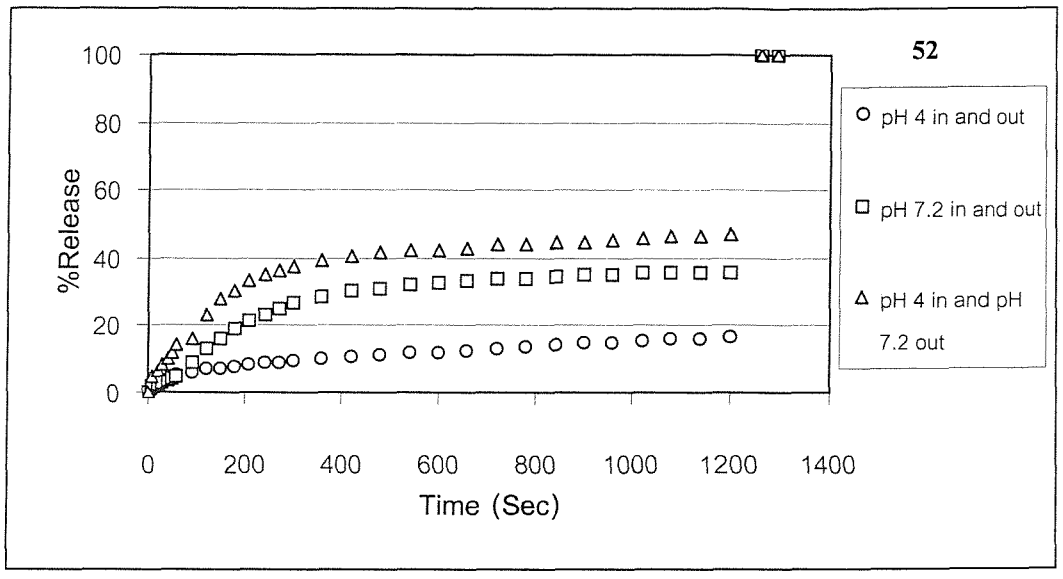

(a)

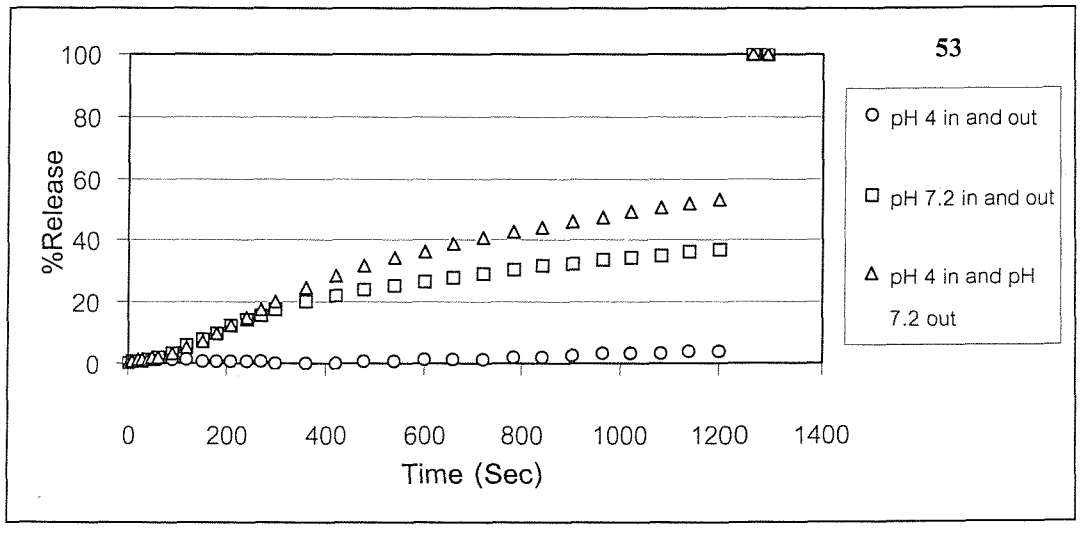

(b)

Figure A3.1: Percent of chloride efflux after addition of the prodigiosin mimic to unilamellar vesicles in pH 4 inside and outside, pH 7.2 inside and outside and pH 4 inside and pH 7.2 outside. (a) **52**. (b) **53**.

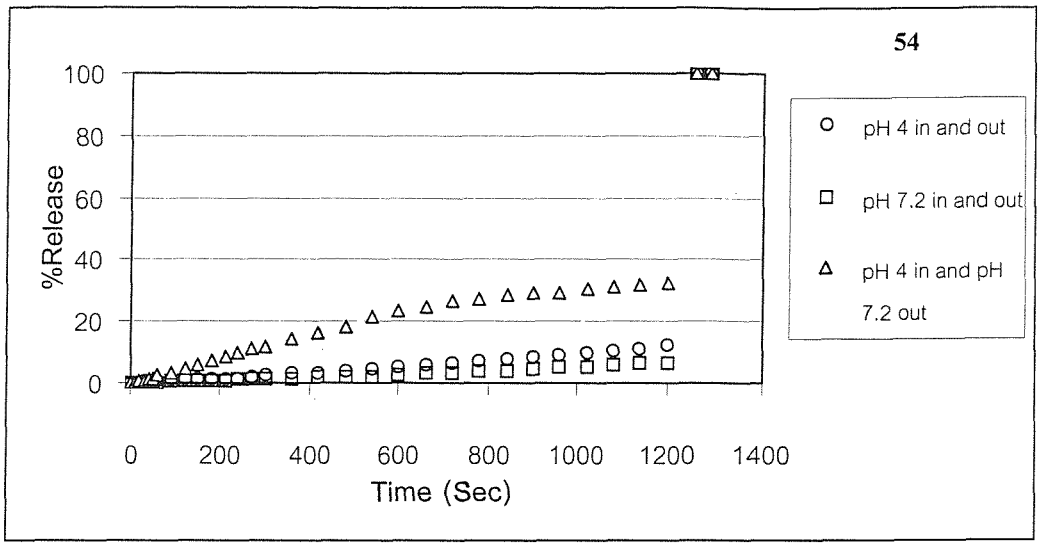

(a)

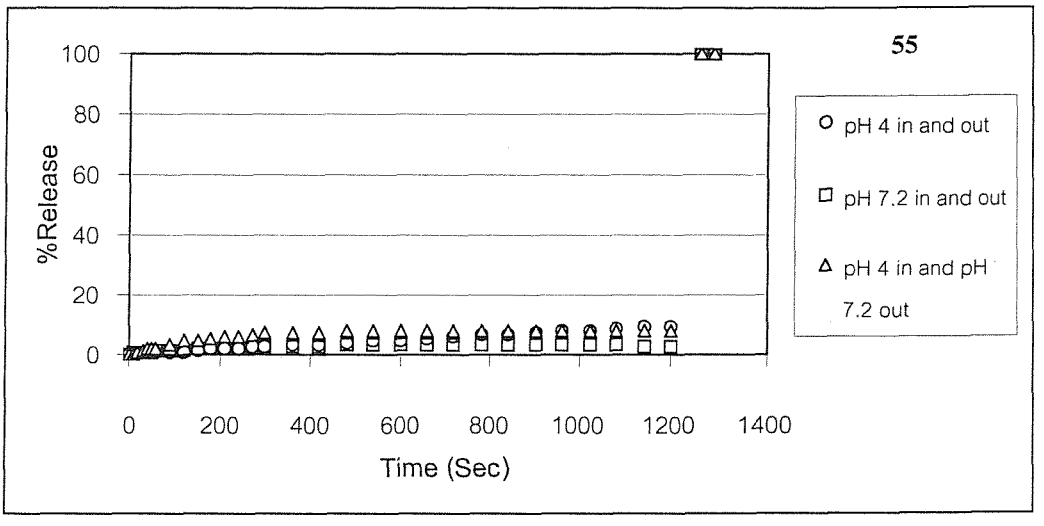

(b)

Figure A3.2: Percent of chloride efflux after addition of the prodigiosin mimic to unilamellar vesicles in pH 4 inside and outside, pH 7.2 inside and outside and pH 4 inside and pH 7.2 outside. (a) **54**. (b) **55**.

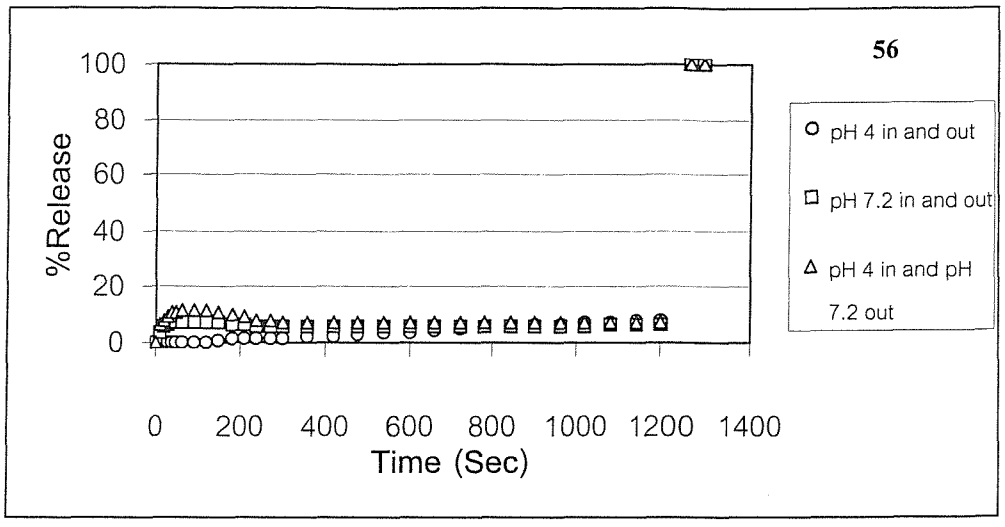

(a)

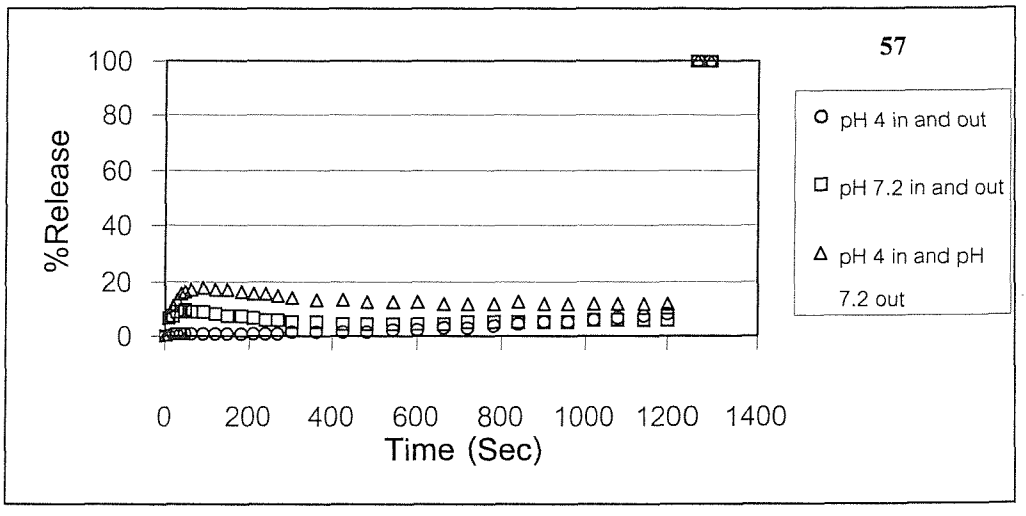

(b)

Figure A3.3: Percent of chloride efflux after addition of the prodigiosin mimic to unilamellar vesicles in pH 4 inside and outside, pH 7.2 inside and outside and pH 4 inside and pH 7.2 outside. (a) **56**. (b) **57**.

A3.2.6 pH Control experiments

Using 0, 1, 3, 5, 7, and 9 mM NaCl and 5 mM citric acid solutions, a standard curve at pH's 4, 5, and 7 was made using the chloride selective electrode. The pH change upon dilution of 30 mM and 10 mM to 1 mM vesicles was determined using the pH electrode and the inside and outside solutions.

A3.2.7 pH Sensitive assay

Unilamellar vesicles (10 mM) composed of POPC/cholesterol (70/30 POPC:cholesterol), 200 nm mean diameter, and one ml of 500 mM NaCl and 5 mM citric acid, pH 4. Vesicles containing 10 μM Oregon green were prepared by adding 40 μl of 250 μM Oregon Green solution into 960 μl of 500 mM NaCl and 5 mM citric acid, pH 4. Vesicles containing 1.5 μM Oregon green were prepared by adding 6 μl of 250 μM Oregon green solution into 994 μl of 500 mM NaCl and 5 mM citric acid, pH 4. Vesicles were dialyzed for three hours and then placed in new buffer for eleven hours. Vesicles were diluted to 550 μM concentration by adding 165 μl of vesicles into 2.835 ml of 500 mM $NaNO_3$ and 5 mM Na_2HPO_4, pH 7.2. The Perkin Elmer luminescence spectrometer was used to measure the emission of Oregon green at 555 nm with an excitation of 510 nm. The intensity baseline was established for 200 seconds whereupon 5.25 μl of a 5 mM prodigiosin mimic was added into the cuvette. Intensity was measured until 500 or 1000 seconds depending on the Oregon Green concentration, whereupon the vesicles were lysed with the addition of 20 μl of polyoxyethylene 8 lauryl ether detergent. The results are shown in Figure A3.4.

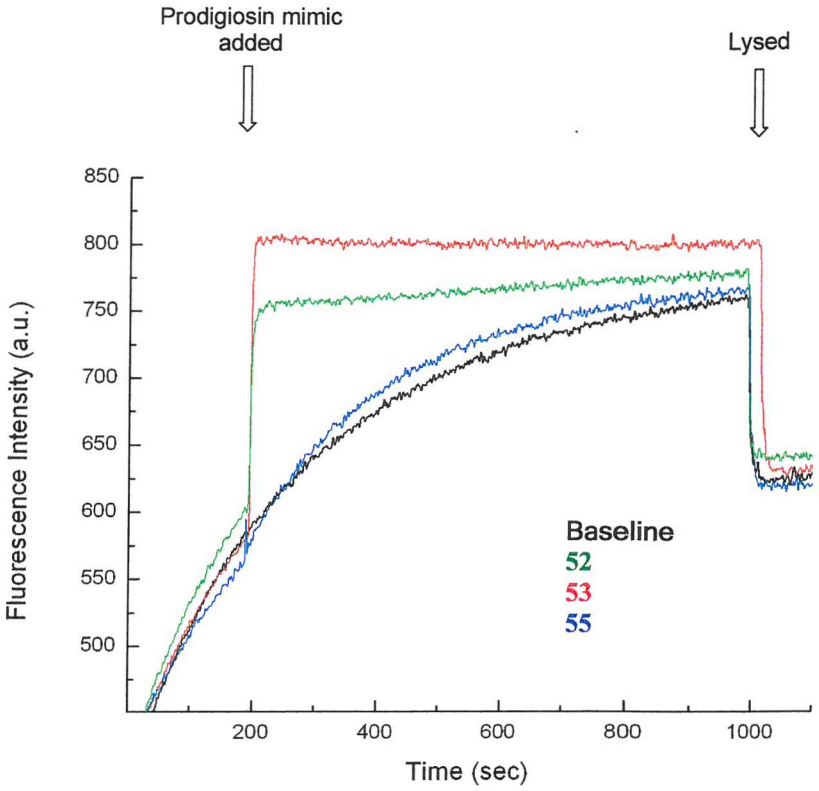

Figure A3.4: Fluorescence Intensity of proton efflux with pH gradient upon addition of the prodigiosin mimic **52**, **53** and **55** to unilamellar vesicles in pH 4 inside and pH 7.2 outside.